FERROCENES OF SUBSTITUTED INDENYL LIGANDS

A thesis
submitted in partial fulfillment
of the requirements for the Degree
of
Doctor of Philosophy in Chemistry
in the
University of Canterbury
by
Glen Matthew Fern

University of Canterbury

2005

Abstract

FERROCENES OF SUBSTITUTED
INDENYL LIGANDS

by

Glen Matthew Fern

This thesis describes the preparation and characterization of a variety of methyl-, trimethylsilyl-, and diphenylphosphino-substituted indenes. The indenes were then used in the preparation of bis(indenyl)iron(II) complexes. The bis(indenyl)iron(II) complexes were characterized by ^{1}H, ^{13}C, and ^{31}P-NMR, UV/visible spectroscopy, cyclic voltammetry, and mass spectrometry. The cyclic voltammetry shows an approximately linear relationship between the oxidation potential and the type of substituent and its ring position, but with increasing substitution leads to lower than expected oxidation potentials. The UV/visible spectra show two absorption bands in the visible region. The position of the bands are essentially unaffected by methyl-substitution, but the low energy band red-shifts with trimethylsilyl- and diphenylphosphino-substitution. Di(2-methylindenyl)iron(II), bis(4,7-dimethyl-indenyl)iron(II), bis(1,3-bis(trimethylsilyl)indenyl)iron(II), *rac*-bis(1-diphenyl-phosphinoindenyl)iron(II), *rac*-bis(1-diphenylphosphino-3-methylindenyl)iron(II), and *rac*-bis(1-diphenylphosphino-2,3-dimethylindenyl)iron(II) were characterized by X-ray crystallography.

The planar chiral ferrocenylphosphine bis(1-diphenylphosphinoindenyl)iron(II) is observed to undergo a facile ring-flipping isomerization from the *meso* isomer to the *racemic* isomer in THF at ambient temperature. The isomerization is slowed by the addition of the noncoordinating solvent chloroform, but is accelerated by the addition of LiCl. Rate and activation parameters for the isomerization have been determined to be: $k_{obs} = 1.6 \times 10^{-5}$ s^{-1} at 23 °C, $\Delta H^{\ddagger} = 58 \pm 4$ kJ mol^{-1}, $\Delta S^{\ddagger} = -140 \pm 15$ J mol^{-1} K^{-1}. Deuterium labeling of bis(1-diphenylphosphinoindenyl)iron(II) in the 3- and 3′-

position ruled out the isomerization proceeding by [1,5]-proton shifts or dissociative mechanisms. The proposed mechanism for the isomerization proceeds via coordination of two THF ligands with ring-slippage of one of the indenyl ligands until it is coordinated through the phosphine. Coordination of the indenyl ligand by the other face leads to the formation of the other isomer.

The heterobimetallic complexes (bis(1-diphenylphosphinoindenyl)iron(II))-*cis*-dichloropalladium(II), (bis(1-diphenylphosphinoindenyl)iron(II))-*cis*-dichloro-platinum(II), and [(cyclooctadiene)(*rac*-bis(1-diphenylphosphinoindenyl)iron(II))-rhodium(I)] tetraphenylborate were prepared. Attempts to prepare dichloro(bis(1-diphenylphosphinoindenyl)iron(II))nickel(II) lead to the formation of *trans*-dichloro(bis(1-diphenylphosphinoindene))nickel(II). The complex (bis(1-diphenyl-phosphinoindenyl)iron(II))-*cis*-dichloropalladium(II) is able to catalyze the cross-coupling of bromobenzene with *n*-/*sec*-butylmagnesium chloride. However. the reaction is not selective with isomerization of the alkyl group and reduction of the halide occurring via a β-hydride elimination mechanism.

Acknowledgements

The many staff and students of the Chemistry Department at the University of Canterbury are to be thanked for their help and support during my time in the department. The following people deserve a special mention:

My supervisor, Dr Owen Curnow for his patience, support, and advice throughout this journey (of two halves).

Professor Ward Robinson, Dr Jan Wikaira, Professor Peter Steel, and all the past and present members of the "Men of Steel" are to be thanked for their help with the black art that is X-ray crystallography.

Dr John Blunt and Rewi Thompson for their assistance with the UNITY 300 NMR spectrometer.

Dr's Alison Downard and Paula Brooksby for showing me the ropes in the electrochemical lab.

Bruce Clark for his ability to obtain meaningful mass spectra from my "difficult" compounds.

Rob McGregor and Dave McDonald for their extraordinary glass-blowing skills and keeping me fully stocked with Schlenk flasks.

Dr Paul Wilson for accompanying me on "Anger Management Courses".

I would also like to thank all my coworkers in the Curnow group over the years: James Butchard, Julian Adams, Kerryann Murphy, Dr Dave Berry, Gabriella Henry, Dominik "The German" Wöll, Heather Kitto, Elizabeth Jenkins, and Michelle Hamilton.

To my parents, Ann and Keith, my step-parents Alison and Noel, and my brother and sister (in law) Rochelle, for providing me with love and support over the past decade.

Finally, to my wife Linda. Thank you for putting up with me over these last few years. You were always there for me and your love and support was greatly appreciated.

Table of Contents

List of Abbreviations

n-BuLi	$CH_3CH_2CH_2CH_2Li$
Cp	Cyclopentadienyl, C_5H_5
EI-MS	Electron-Impact Mass Spectroscopy
IR	Infrared
UV	Ultra-violet
Ph	Phenyl, C_6H_5
THF	Tetrahydrofuran
Dppf	1,1'-bis(diphenylphosphino)ferrocene
NMR	Nuclear Magnetic Resonance
Dppe	1,2-bis(diphenylphosphino)ethane
Dppp	1,3-bis(diphenylphosphino)propane
PTSA	*p*-Toluenesulfonic acid

Chapter 1

Chapter 1: Introduction

Since the discovery of ferrocene, the cyclopentadienyl ligand has been amongst the most important ligands in organometallic chemistry. The success of the cyclopentadienyl ligand has been attributed to its ability to coordinate to a wide variety of different metals, stabilize multiple oxidation states, and the ease with which the steric and electronic properties can be tuned by substitution on the ring.[1] The fusion of one or more six-membered aromatic rings to the cyclopentadienyl ligand has been shown to significantly change the reactivity, stability, and catalytic activity of the resulting complexes (Figure 1.1).[2]

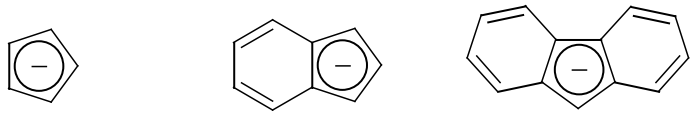

(a) (b) (c)

Figure 1.1. η^5-Carbocyclic π ligands: (a) Cyclopentadienyl, (b) Indenyl, (c) Fluorenyl.

The bonding of the cyclopentadienyl ligand to metals has been the subject of intensive investigation. O'Connor and Casey identified ten distinct bonding modes for the cyclopentadienyl ligand while a similar number are known for the indenyl ligand.[3] Of the modes known, η^5-, η^3-, η^1- bonding modes are of particular interest due to their interconversion (ring-slippage). It was initially believed that the bonding in all η^5-cyclopentadienyl transition-metal complexes involved a uniform interaction between the five carbon atoms of the C_5H_5 ring and the metal atom. However, in 1963 both Dahl and Bennett reported structural evidence for localized bonding in a number of cyclopentadienyl-metal complexes.[4] A localized allyl-ene structure was formulated in which the bonding of the cyclopentadienyl ligand was described as being $\eta^3 + \eta^2$. The indenyl ligand also exhibits a localized allyl-ene structure, though the distortion is more pronounced due to the incorporation of the ene unit into the six-membered aromatic ring.

The ring-slippage of η^5-cyclopentadienyl ligands was first proposed in 1966 by Basolo who observed that the rate of reaction between PPh_3 and the coordinatively saturated complexes $(\eta^5\text{-}C_5H_5)M(CO)_2$, (M = Rh, Co) to give $(\eta^5\text{-}C_5H_5)M(CO)PPh_3$ was unusually fast and dependent on the concentration of both metal complex and phosphine.[5] In order to explain these observations, Basolo proposed that slippage of the cyclopentadienyl ligand occurs as the phosphine coordinates to produce an intermediate that contains an η^3-cyclopentadienyl ligand. Since then, there have been numerous reports of substitution reaction resulting in the ring-slippage of cyclopentadienyl ligands. The indenyl ligand has been shown to have a pronounced effect on the rate of substitution reactions. Mawby and co-workers described the CO substitution by phosphines in $[Mo(\eta^5\text{-}C_9H_7)X(CO)_3]$ (X = Cl, Br, I) and $[Fe(\eta^5\text{-}C_9H_7)I(CO)_2]$ proceeding at a faster rate when compared with the corresponding cyclopentadienyl analogues.[6] Basolo et al. observed an 10^8 times increase in rate of substitution of CO of the indenyl complex $[Rh(\eta^5\text{-}C_9H_7)(CO)_2]$ with respect to the analogous cyclopentadienyl complex.[7] This rate enhancement, termed the indenyl effect, is attributed to the generation of the aromaticity in the fused six-membered aromatic ring upon slippage from η^5- to η^3-coordination. The reversible nature of the ring-slippage process has led the cyclopentadienyl ligand being used extensively in the formation of catalytically active species.

Metallocenes of group 4 metals (in particular zirconium) have found extensive use as co-catalysts for the polymerization of α–olefins.[2] The use of ring-substituted cyclopentadienyl ligands has been shown to affect both the activity and selectivity of the metallocene catalysts. Studies by Piccolrovazzi et al. and Lee et al. on catalysts containing unbridged indenyl ligands suggested that the presence of electron-withdrawing groups led to a decrease in catalytic activity and polymer molar mass in the polymerization of ethane and propene while Brintzinger and others have shown that the presence of methyl substituents increase the yield, tacticity, and polymer molar mass.[8] Ring substitution has also been used as a method for introducing chirality into the metallocene system.

Metallocenes containing chiral ligands are becoming increasingly important in synthetic chemistry as catalytic or stoichiometric mediators of enantioselective

reactions. The chirality in metallocenes typically arise by the coordination of chiral or prochiral ligands. In determining what type of metal complexes (achiral, enantiomeric, diastereomeric) can form from a particular cyclopentadienyl ligand, one must examine how the two π-faces of the ligand relate to each other. The π-faces of the cyclopentadienyl ligand can be related to one another, depending on the substituents, in three ways (Figure 1.2): the faces are equivalent (homotopic) if the faces can interconvert by ligand rotation or if rotation about a C_2-axis can interconvert the two faces; the faces are enantiotopic if only reflection through a mirror plane can interconvert the two faces; or the faces are diastereotopic if a rotation or symmetry operation cannot interconvert the faces. Metalation of ligands with homotopic faces produce a single isomeric complex while ligands with enantiotopic or diastereotopic faces can produce enantiomeric and diastereomeric mixtures of metallocenes.

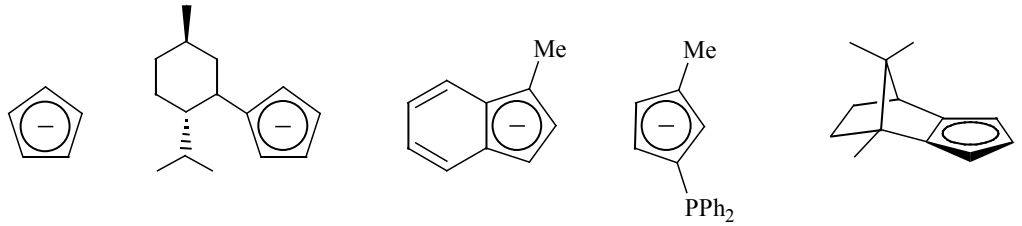

(a) (b) (c)

Figure 1.2. Examples of the different types of cyclopentadienyl ligands: (a) homotopic; (b) enantiotopic; (c) diastereotopic.

Cyclopentadienyl ligands with two (or more) different achiral substituents will have enantiotopic faces and will result in the formation of two enantiomeric metallocenes in equal amounts. The chirality in complexes of this type has been described as "planar chirality" and the π-coordination of the ligand carries an R or S stereochemical descriptor.[9] The following definition was described by Halterman as being unambiguous for the assignment R/S descriptors for planar chiral ligands:[10] *"The planar chirality in cyclopentadienylmetal or indenylmetal complexes is assigned R or S on the Cahn-Ingold-Prelog configuration of the 1-position of the ligand where the metal is treated as being individually bonded to all five of the π-atoms. The chirality can be described as (1R) or (1S) to avoid ambiguity or as (p-R) or (p-S) to emphasize that this is a description of the planar chirality based on the 1-position."*

The addition of two planar chiral cyclopentadienyl ligands to one metal results in the formation of two diastereomeric metallocenes, the C_2-symmetric racemic isomer and the C_s-symmetric meso isomer (Figure 1.3). The stereochemistry of these diastereomeric metallocene has been shown to influence the steroselectivity of asymmetric reactions.

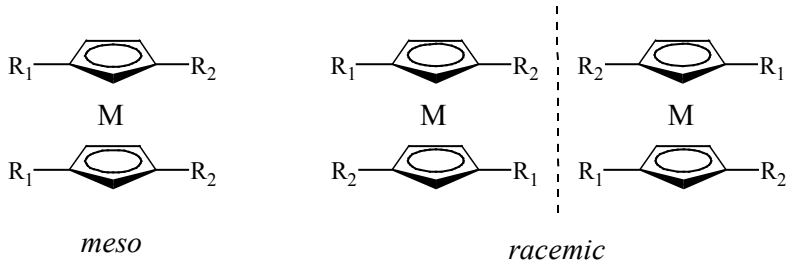

Figure 1.3. Diastereomers of bisplanar chiral metallocenes.

The chemistry of functionalized cyclopentadienyl ligands is a rapidly growing area of organometallic chemistry. The introduction of a side-chain donor group to a cyclopentadienyl group can dramatically influence the structure and reactivity of the resulting complexes through the chelate effect and differing steric properties. Bifunctional ligands in which the coordination properties of the individual components differ markedly is a common means for the preparation of heterobimetallic complexes. Neutral two-electron donating groups such as PR_2, NR_2, and OR are commonly used in conjunction with the cyclopentadienyl ligand.[11]

Ferrocenylphosphines are widely employed in the formation of polymetallic complexes, with 1,1'-bis(diphenylphosphino)ferrocene (dppf) being the subject of intensive studies.[12] The considerable growth in research directed towards dppf (and its analogues) is attributed to: the various coordination modes that dppf displays towards metal atoms; the possible catalytic activity of many of the bimetallic complexes; and the redox chemistry of the complexes.

Bimetallic complexes of ferrocenylphosphines have been shown to catalyze a wide variety of organic transformations.[13] Palladium and nickel complexes of ferrocenylphosphines are effective catalysts for the cross-coupling of organic moieties, while rhodium, ruthenium, and palladium complexes have found uses as

catalysts for the hydrogenation of olefins. Derivatives of dppf containing chiral functionalities have found use in asymmetric catalysis.[14]

An asymmetric catalyst has been described as an "ensemble of a metal ion and an optically active ligand whose combined action promotes the transfer of chiral information from the catalyst to the substrate."[14b] Ferrocenylphosphines have found widespread use as asymmetric catalysts due to: the stability of the ferrocenyl core; the eas with which steric and electronic effects can be changed by simple modifications; and the ability of the phosphine to form complexes with a variety of transition metals in a variety of coordination geometries and oxidation states. The introduction of chirality to ferrocenylphosphines may be achieved via two different methods: the addition of a chiral side chain (central chirality); or the generation of planar chirality. Many ferrocenylphosphines utilize both central and planar chirality. Several reports have shown that planar chirality has a significant effect on the enantioselectivity of asymmetric reactions.[15]

This thesis describes the synthesis of a variety of methyl-, trimethylsilyl-, and diphenylphosphino-substituted indene ligands, and subsequent use in the formation of bis(indenyl)iron(II) complexes. The phosphine substituted bis(indenyl)iron(II) complexes are of particular interest as potentially chiral analogues of dppf. The electrochemistry and the electronic absorption spectra of the ferrocenes will be discussed in terms of substituent effects.

References

1. (a) Jutzi, P.; Burford, N. *Chem. Rev*. **1999**, *99*, 969. (b) Cuenca, T.; Royo, P. *Coord*. *Chem. Rev*. **1999**, *193-195*, 447.
2. Togni, A.; Halterman, R.C. (Eds), Metallocenes: Synthesis, Reactivity, Applications, Wiley-VCH, Weinheim, Volumes 1 & 2, **1998**
3. (a) O'Connor, J.M.; Casey, C.P. *Chem. Rev*. **1987**, *87*, 307. (b) Cadierno, V.; Diez, J.; Gamasa, M.P.; Gimeno, J.; Lastra, E. *Coord*. *Chem. Rev*. **1999**, *193-195*, 147.

4. (a) Dahl, L.F.; Wei, C.H. *Inorg. Chem*. **1963**, *2*, 713. (b) Bennett, M.J.; Churchill, M.R.; Gerloch, M.; Mason, R. *Nature* (London) **1964**, *201*, 1318.
5. Schuster-Woldan, H.G.; Basolo, F. *J. Amer. Chem. Soc*. **1966**, *88*, 1657.
6. (a) Hart-Davis, A.J.; White, C.; Mawby, R.J. *Inorg. Chim. Acta*. **1970**, *4*, 441. (b) Jones, D.J.; Mawby, R.J. *Inorg. Chim. Acta*. **1972**, *6*, 157.
7. Rerek, M.E.; Ji, L.-N.; Basolo, F. *J. Chem. Soc. Chem. Commun*. **1983**, 1208.
8. (a) Piccolrovazzi, N.; Pino, P.; Consiglio, G.; Sironi, A.; Moret, M. *Organometallics* **1990**, *9*, 3098. (b) Lee, I.-M.; Gaythier, W.J.; Ball, J.M.; Iyengar, B.; Collins, S. *Organometallics* **1992**, *11*, 2115.
9. Schogel, K.J. *Topics Steroechem*. **1967**, *1*, 39.
10. Halterman, R.L. In *Metallocenes: Synthesis, Reactivity, Applications*, Wiley-VCH, Weinheim **1998**, Volume 1, Chapter 8, pp 455.
11. Butenschon, H. *Chem. Rev*. **2000**, *100*, 1527.
12. Bandoli, G.; Dolmella, A. *Coord. Chem. Rev*. **2000**, *209*, 161.
13. Gan, K.-S.; Hor, T.S.A. In *Ferrocenes*; Togni, A., Hayashi, T., Eds.; VCH: New York **1995**; Chapter 1, pp 3-104.
14. (a) Colacot, T.J. *Chem. Rev*. **2003**, *103*, 3101. (b) Barbaro, P.; Bianchini, C.; Giambastiani, G.; Parisel, S.L. *Coord. Chem. Rev*. **2004**, *248*, 2131.
15. (a) You, S.L.; Hou, X.L.; Dai, Y.H.; Xia, W. *J. Org. Chem*. **2002**, *67*, 4648. (b) Donde, Y.; Overman, L.E. *J. Amer. Chem. Soc*. **1999**, *121*, 1933. (c) Richards, C.J.; Hibbs, D.E.; Hurthose, M.B. *Tetrahedron Lett*. **1995**, *36*, 3745.

Chapter 2

Chapter 2: Experimental

General Considerations.

All manipulations and reactions were carried out under an inert atmosphere (Ar or N_2) by use of standard Schlenk line techniques. Reagent grade solvents were dried and distilled prior to use: diethyl ether, tetrahydrofuran and toluene from Na/benzophenone; dichloromethane and petroleum ether (50-70°C fraction) from CaH_2. 1-Methylindene,[1] 1,3-dimethylindene,[2] 4,7-dimethylindene,[3] 1-trimethylsilylindene,[4] and 3-diphenylphosphinoindene[5] were prepared by published procedures. 2-(Trimethylsilyl)indene, 1,2-bis(trimethylsilyl)indene, and 1,3-bis(trimethylsilyl)indene were provided by Professor Heinrich Lang and used as received.[6] 1,1-Dideutero-3-(diphenylphosphino)indene, 3-diphenylphosphino-4,7-dimethylindene, and 3-diphenylphosphino-2-methylindene were obtained from Michelle Hamilton and used as received.[7] All other reagents were purchased from Aldrich or Sigma Chemical Companies. ^{1}H-, ^{13}C{^{1}H}-, and ^{31}P{^{1}H}-NMR spectroscopy data were collected either on a Varian Unity-300 or Varian XL-300 spectrometer operating at 300, 75, and 121 MHz, respectively. 2D NMR experiments were performed on a Varian INOVA-500 spectrometer operating at 500 and 125 MHz for ^{1}H and ^{13}C respectively. Unless otherwise stated, spectra were measured at ambient temperature with residue solvent peaks as internal standards for ^{1}H- and ^{13}C{^{1}H}-NMR spectroscopy. ^{31}P{^{1}H}-NMR spectroscopy chemical shifts were reported relative to external 85% H_3PO_4, positive representing desheilding. EI mass spectra were collected on a Kratos MS80RFA mass spectrometer. Magnetic susceptibilities were measured on a Gouy balance at ambient temperature. Elemental analyses were carried out by Campbell Microanalytical Services, University of Otago, Dunedin. Infrared spectra were obtained on a Shimadzu FTIR-8201PC spectrophotometer. UV/Vis spectra were obtained on a Hewlett Packard 8452A Diode Array (2 nm resolution) spectrometer using 1 cm cuvets. Cyclic voltammetry was performed using a PAR 173 Potentiostat coupled to a PAR 175 Universal Programmer and a Graphtec WX 1200 chart recorder. All electrochemical measurements were made using a three-electrode cell comprosing of a platinum-disk working electrode (1 mm diameter), a platinum-wire auxiliary electrode, and a

Ag/Ag^+ (0.01 M $AgNO_3$, 0.1 M $[Bu_4N]PF_6$-CH_2Cl_2) reference electrode. All potentials are reported vs the ferrocene/ferrocenium (Fc/Fc^+) couple after referencing to *in situ* ferrocene. Before use, the electrodes were polished with 1μm diamond paste and cleaned with acetone and distilled water. Electrochemical measurements were made at ambient temperature under an inert atmosphere.

CHAPTER 3

Synthesis of 1,2-dimethylindene (3.4).

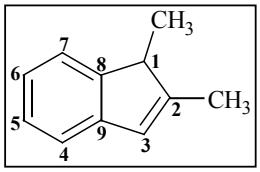

To a solution of 2-methylindene (**3.3**) (2 mL, 15 mmol) in diethyl ether (40 mL) at –80°C was added a solution of *n*-BuLi (9.32 mL, 1.6 M, 15 mmol). The solution was allowed to warm to ambient temperature and stirred for 4 h. The resulting yellow solution was then added dropwise via cannula to a solution of iodomethane (3.72 mL, 60 mmol) in diethyl ether (30 mL) at –80°C. The solution was stirred overnight at ambient temperature and the reaction quenched by the addition of 50 mL of a saturated aqueous NH_4Cl solution. The organic material was extracted with diethyl ether (4 x 20 mL), dried over $MgSO_4$, filtered and the solvent removed with a rotary-evaporator. The resulting yellow oil was distilled at reduced pressure to give 1.405 g (65%) of **3.4** as a colourless oil. ^{1}H- and ^{13}C{^{1}H}-NMR spectra are consistent with literature.[2,8]

Synthesis of 1,4,7-trimethylindene (3.7).

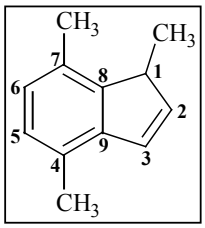

To a solution of 4,7-dimethylindene (**3.6**) (5.125 g, 36 mmol) in diethyl ether (50 mL) at –80°C was added a solution of *n*-BuLi (22.21 mL, 1.6 M, 36 mmol). The solution was allowed to warm to ambient temperature and stirred for 4 h over which time a white precipitate forms. The suspension was then added via cannula to a solution of iodomethane (8.85 mL, 140 mmol) in diethyl ether (50 mL) at –80°C. The solution was stirred overnight at ambient temperature and the reaction quenched by the addition of 50 mL of a saturated aqueous NH_4Cl solution. The organic material was extracted with diethyl ether (4 x 50 mL), dried over $MgSO_4$, filtered and the solvent removed with a rotary-evaporator. The resulting yellow oil was distilled at reduced pressure to give 3.921 g (70%) of **3.7** as a colourless oil.

^{1}H-NMR ($CDCl_3$): δ 7.03 (d, $^3J_{HH}$ = 7.8 Hz, 1H, H6), 6.94 (d, $^3J_{HH}$ = 7.8 Hz, 1H, H5), 6.89 (dd, $^3J_{HH}$ = 5.4 Hz, $^4J_{HH}$ = 1.8 Hz, 1H, H3), 6.50 (dd, $^3J_{HH}$ = 5.4 Hz, $^3J_{HH}$ = 1.2 Hz, 1H, H2), 3.60 (m, $^3J_{HH}$ = 7.8 Hz, $^4J_{HH}$ = 1.8 Hz, 1H, H1), 2.45 (br s, 6H, C4-CH_3 & C7-CH_3), 1.37 (d, $^3J_{HH}$ = 7.8 Hz, 3H, C1-CH_3). ^{13}C{^{1}H}-NMR ($CDCl_3$): δ 146.7

(C8), 142.6 (C9), 141.1 (C2), 130.2 (C7), 128.0 (C3), 127.8 (C5), 127.7 (C4), 126.6 (C6), 45.0 (C1), 18.6 (C4-*CH*$_3$), 18.2 (C7-*CH*$_3$), 14.7 (C1-*CH*$_3$). Mass spectrum: (EI, *m/z* (%)): 158 (54, M^+), 143 (31, $C_9H_5Me_2^+$), 128 (100, $C_9H_5Me^+$), 113 (22, $C_9H_5^+$). HR-MS: M^+ Calc., 158.10955; Found, 158.11038.

Synthesis of 1,3,4,7-tetramethylindene (3.8).

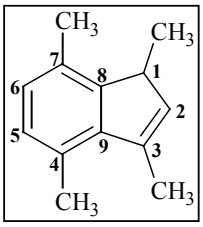

To a solution of 1,4,7-dimethylindene (**3.7**) (1.464 g, 9.3 mmol) in diethyl ether (30 mL) at –80°C was added a solution of *n*-BuLi (5.78 mL, 1.6 M, 9.3 mmol). The solution was allowed to warm to ambient temperature and stirred for 4 h over which time a white precipitate forms. The suspension was added via cannula to a solution of iodomethane (2.30 mL, 370 mmol) in diethyl ether (30 mL) at –80°C. The solution was stirred overnight at ambient temperature and the reaction quenched by the addition of 50 mL of a saturated aqueous NH_4Cl solution. The organic material was extracted with diethyl ether (4 x 30 mL), dried over $MgSO_4$, filtered and the solvent removed with a rotary-evaporator. The resulting yellow oil was distilled at reduced pressure to give 1.012 g (63%) of **3.8** as a colourless oil. ^{1}H-NMR spectrum is consistent with literature.[2]

$^{13}C\{^1H\}$-NMR ($CDCl_3$): δ 148.5 (C8), 142.3 (C9), 139.2 (C3), 137.6 (C2), 130.5 (C7), 129.4 (C5), 128.5 (C4), 126.6 (C6), 42.4 (C1), 19.5 (C4-*CH*$_3$), 18.5 (C7-*CH*$_3$), 17.5 (C3-*CH*$_3$), 15.1 (C1-*CH*$_3$).

Synthesis of 1-diphenylphosphino-3-methylindene (3.15).

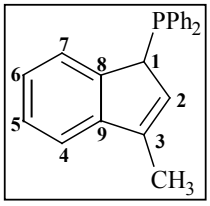

To a solution of 1-methylindene (**3.2**) (0.745 g, 5.7 mmol) in 40 mL diethyl ether at –80°C was added a solution of *n*-BuLi (3.57 mL, 1.6 M, 5.7 mmol). The solution was allowed to warm to ambient temperature and stirred for 2 h, in which time a white precipitate forms. The mixture was cooled to –80°C, and chlorodiphenylphosphine (0.892 mL, 5.7 mmol) was added dropwise. The mixture was allowed to warm to ambient temperature and

stirred for 2 h. The reaction mixture was filtered through alumina, and the solvent was removed *in vacuo* to yield 1.61 g (90%) of **3.15** as a white, air-sensitive powder.

^{1}H-NMR ($CDCl_3$): δ 7.67-6.85 (m, 14H, aromatic), 6.12 (s, 1H, H2), 4.48 (s, 1H, H1), 2.11 (s, 3H, CH_3). $^{13}C\{^{1}H\}$-NMR ($CDCl_3$): δ 145.7 (s, C9), 144.5 (d, $^{2}J_{PC}$ = 9 Hz, C8), 140.7 (d, $^{3}J_{PC}$ = 6 Hz, C3), 137.7 (d, $^{1}J_{PC}$ = 19 Hz, *ipso*-Ph), 137.2 (d, $^{1}J_{PC}$ = 18 Hz, *ipso*-Ph), 133.7 (d, $^{2}J_{PC}$ = 20 Hz, *o*-Ph), 133.1 (d, $^{2}J_{PC}$ = 20 Hz, *o*-Ph), 129.1 (s, *p*-Ph), 129.8 (d, $^{2}J_{PC}$ = 4 Hz, C2), 128.8 (s, *p*-Ph), 128.4 (d, $^{3}J_{PC}$ = 7 Hz, *m*-Ph), 128.1 (d, $^{3}J_{PC}$ = 7 Hz, *m*-Ph), 126.5 (s, C5), 124.5 (s, C6), 123.9 (d, $^{3}J_{PC}$ = 5 Hz, C7), 119.3 (s, C4), 47.1 (d, $^{1}J_{PC}$ = 20 Hz, C1), 13.0 (s, CH_3). $^{31}P\{^{1}H\}$-NMR ($CDCl_3$): δ –4.98. Mass spectrum: (EI, *m/z* (%)): 314 (82, M^+), 185 (100, Ph_2P^+), 128 (30, $C_9H_5Me^+$), 108 (6, PhP^+), 77 (8, Ph^+). HR-MS: M^+ Calc., 314.12244; Found, 314.12295.

Synthesis of 1-diphenylphosphino-2,3-dimethylindene (3.16).

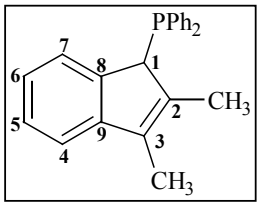

To a solution of 1,2-dimethylindene (**3.4**) (0.717 g, 5.0 mmol) in 40 mL diethyl ether at –80°C was added a solution of *n*-BuLi (3.11 mL, 1.6 M, 5.0 mmol). The solution was allowed to warm to ambient temperature and stirred for 2 h, in which time a white precipitate forms. The mixture was cooled to –80°C, and chlorodiphenylphosphine (0.892 mL, 5.0 mmol) was added dropwise. The mixture was allowed to warm to ambient temperature and stirred for 2 h. The reaction mixture was filtered through alumina, and the solvent removed *in vacuo* to leave a colourless oil, which solidifies over a period of 1 h, under vacuum to yield 1.48 g (91%) of **3.16** as a white, air-sensitive powder.

^{1}H-NMR ($CDCl_3$): δ 7.57-6.64 (m, 14H, H4-7 and Ph), 4.33 (s, 1H, H1), 1.98 (s, 3H, C2-CH_3), 1.89 (s, 3H, C3-CH_3). $^{13}C\{^{1}H\}$-NMR ($CDCl_3$): δ 146.4 (s, C9), 142.9 (s, C8), 138.2 (d, $^{3}J_{PC}$ = 6 Hz, C2) 137.0 (d, $^{1}J_{PC}$ = 18 Hz, *ipso*-Ph), 134.1 (d, $^{2}J_{PC}$ = 20 Hz, *o*-Ph), 134.0 (d, $^{1}J_{PC}$ = 18 Hz, *ipso*-Ph), 133.5 (d, $^{2}J_{PC}$ = 4 Hz, C3), 132.8 (d, $^{2}J_{PC}$ = 20 Hz, *o*-Ph), 129.1 (s, *p*-Ph), 128.4 (s, *p*-Ph), 128.2 (d, $^{3}J_{PC}$ = 6 Hz, *m*-Ph), 127.6 (d, $^{3}J_{PC}$ = 7 Hz, *m*-Ph), 126.2 (s, C5), 123.22 (s, C6), 123.16 (d, $^{3}J_{PC}$ = 3 Hz, C7),

118.1 (s, C4), 51.7 (d, $^{1}J_{PC}$ = 24 Hz, C1), 14.1 (d, $^{3}J_{PC}$ = 8 Hz, C2-*CH*$_3$), 10.1 (s, C3-*CH*$_3$). $^{31}P\{^{1}H\}$-NMR ($CDCl_3$): δ 1.76 (s). Mass spectrum: (EI, *m/z* (%)): 328 (7, M^+), 201 (100, Ph_2PO^+), 142 (17, $C_9H_4Me_2^+$), 77 (12, Ph^+). HR-MS: M^+ Calc., 328.13809; Found, 328.13708.

Synthesis of 1-diphenylphosphino-3,4,7-trimethylindene (3.17).

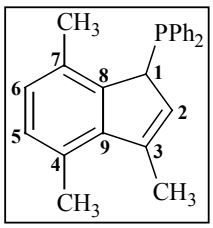

To a solution of 1,4,7-trimethylindene (**3.7**) (1.624 g, 11 mmol) in 50 mL diethyl ether at –80°C was added n-BuLi (6.41 mL, 1.6 M, 11 mmol). The solution was allowed to warm to ambient temperature and stirred for 2 h, in which time a white precipitate forms. The mixture was cooled to –80°C, and chlorodiphenylphosphine (1.84 mL, 11 mmol) was added dropwise. The mixture was allowed to warm to ambient temperature and stirred for 2 h. The reaction mixture was filtered through alumina, and the solvent was removed *in vacuo* to leave a colourless oily residue. The residue was washed with petroleum ether (2 x 25 mL) to yield 2.28 g (62%) of **3.17** as a white, air sensitive powder.

^{1}H-NMR ($CDCl_3$): δ 7.61-6.81 (m, 12H, H5,6 and Ph), 6.08 (s, 1H, H2), 4.44 (s, 1H, H1), 2.61 (s, 3H, C4-CH_3), 2.27 (s, 3H, C7-CH_3), 1.96 (s, 3H, C3-CH_3). $^{13}C\{^{1}H\}$-NMR ($CDCl_3$): δ 143.1 (d, $^{2}J_{PC}$ = 6 Hz, C8), 142.6 (d, $^{3}J_{PC}$ = 3 Hz, C3), 141.3 (s, C9), 138.3 (d, $^{1}J_{PC}$ = 20 Hz, *ipso*-Ph), 134.4 (d, $^{2}J_{PC}$ = 20 Hz, *o*-Ph) 133.4 (d, $^{1}J_{PC}$ = 19 Hz, *ipso*-Ph), 132.0 (d, $^{2}J_{PC}$ = 16 Hz, *o*-Ph), 130.8 (d, $^{3}J_{PC}$ = 4 Hz, C7), 130.3 (d, $^{2}J_{PC}$ = 5 Hz, C2), 129.1 (d, $^{4}J_{PC}$=2 Hz, C5), 128.6 (s, *p*-Ph), 128.4 (d, $^{3}J_{PC}$ = 4 Hz, *m*-Ph), 128.3 (s, C4), 127.7 (s, *p*-Ph), 126.5 (d, $^{3}J_{PC}$ = 7 Hz, *m*-Ph), 126.3 (d, $^{5}J_{PC}$=2 Hz, C6), 46.3 (d, $^{1}J_{PC}$ = 25 Hz, C1), 19.5 (d, $^{4}J_{PC}$=13 Hz, C7-*CH*$_3$), 19.3 (s, C4-*CH*$_3$), 17.0 (s, C3-*CH*$_3$). $^{31}P\{^{1}H\}$-NMR ($CDCl_3$): δ –1.71 (s). Mass spectrum: (EI, *m/z* (%)): 342 (15, M^+), 201 (100, Ph_2PO^+), 157 (39, $C_9H_4Me_3^+$), 142 (13, $C_9H_4Me_2^+$), 77 (14, Ph^+). HR-MS: M^+ Calc., 342.15374; Found, 342.15430.

Synthesis of 1-trimethylsilyl-3-diphenylphosphinoindene (3.18).

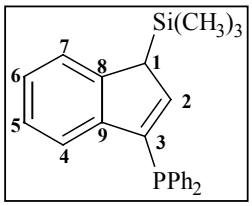

To a solution of 3-diphenylphosphinoindene (**3.13**) (1.027 g, 3.4 mmol) in 40 mL diethyl ether at –80 °C was added *n*-BuLi (2.13 mL, 1.6 M, 3.4 mmol). The solution was allowed to warm to ambient temperature and stirred for 3 h. The mixture was then cooled to –80°C, and chlorotrimethylsilane (0.43 mL, 3.4 mmol) was added dropwise. The mixture was allowed to warm to ambient temperature and stirred for 2 h. The reaction mixture was filtered through Celite, and the solvent was removed *in vacuo* to leave an orange oily residue. The residue was dissolved in petroleum ether (25 mL) and filtered to give an orange solution. Removal of solvent *in vacuo* yielded 0.97 g (76%) of **3.18** as an orange air-sensitive oil.

^{1}H-NMR ($CDCl_3$): δ 7.47-7.13 (m, 14H, H4-7 and Ph), 6.39 (dd, $^{3}J_{HH}$ = 2 Hz, $^{3}J_{PH}$ = 4 Hz 1H, H2), 3.61 (d, $^{3}J_{HH}$ = 2 Hz, 1H, H1), –0.52 (s, 9H, CH_3). $^{13}C\{^{1}H\}$-NMR ($CDCl_3$): δ 146.1 (d, $^{3}J_{PC}$ = 5 Hz, C8), 144.8 (d, $^{1}J_{PC}$ = 18 Hz, C3), 144.4 (d, $^{2}J_{PC}$ = 4 Hz, C2), 137.2 (d, $^{2}J_{PC}$ = 11 Hz, C9), 136.6 (d, $^{1}J_{PC}$ = 9 Hz, *ipso*-Ph), 136.0 (d, $^{1}J_{PC}$ = 9 Hz, *ipso*-Ph), 133.8 (d, $^{2}J_{PC}$ = 20 Hz, *o*-Ph), 133.3 (d, $^{2}J_{PC}$ = 19 Hz, *o*-Ph), 128.7 (s, *p*-Ph), 128.4 (s, *p*-Ph), 128.3 (d, $^{3}J_{PC}$ = 7 Hz, *m*-Ph), 128.2 (d, $^{3}J_{PC}$ = 7 Hz, *m*-Ph), 124.7 (s, C5), 124.0 (s, C6), 122.6 (s, C7), 121.4 (d, $^{3}J_{PC}$ = 4 Hz, C4), 47.9 (d, $^{3}J_{PC}$ = 4 Hz, C1), –2.3 (s, $Si(CH_3)_3$). $^{31}P\{^{1}H\}$-NMR ($CDCl_3$): δ –21.54 (s). Mass spectrum: (EI, *m/z* (%)): 372 (6, M^+), 300 (85, M^+-$SiMe_3$), 186 (20, $C_9H_5SiMe_3^+$), 185 (100, Ph_2P^+), 115 (15, $C_9H_7^+$), 73 (23, $SiMe_3^+$). HR-MS: M^+ Calc., 372.14632; Found, 372.14548.

Synthesis of bis(3-(diphenylphosphino)-inden-1-yl) dimethylsilane (3.19).

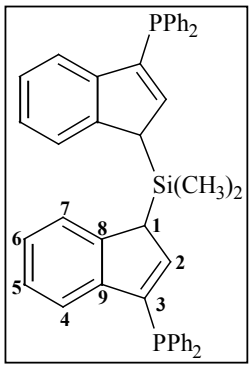

To a solution of 3-diphenylphosphinoindene (**3.13**) (1.925g, 6.4 mmol) in 40 mL diethyl ether at –80°C was added n-BuLi (4.0 mL, 1.6 M, 6.4 mmol). The solution was allowed to warm to ambient temperature and stirred for 2 h. The mixture was cooled to –80°C, and dichlorodimethylsilane (0.389 mL, 3.2 mmol) was added dropwise. The mixture was allowed to warm to ambient

temperature and stirred for 18 h. The reaction mixture was filtered through alumina, and the solvent was removed *in vacuo* to yield 1.74 g (83%) of **3.19** as a red crystalline material. Indene **3.19** was obtained as a 55:45 mixture of *meso* and *racemic* diastereomers.

***rac*-3.19**: ^{1}H-NMR ($CDCl_3$): δ 7.51-7.13 (m, 28H, H4-7 & Ph), 6.41 (dd, $^{3}J_{HH}$ = 2 Hz, $^{3}J_{PH}$ = 4 Hz, 2H, H2), 3.74 (pseudo t, $^{3}J_{HH}$ = 2 Hz, $^{4}J_{PH}$ = 1 Hz, 2H, H1), –0.32 (s, 6H, CH_3). $^{13}C\{^{1}H\}$-NMR ($CDCl_3$): δ 145.3 (d, $^{2}J_{PC}$ = 10 Hz, C9), 144.9 (s, C8), 143.2 (d, $^{2}J_{PC}$ = 10 Hz, C2), 138.7 (d, $^{1}J_{PC}$ = 12 Hz, C3), 136.3 (d, $^{1}J_{PC}$ = 8 Hz, *ipso*-Ph), 135.7 (d, $^{1}J_{PC}$ = 8 Hz, *ipso*-Ph), 134.0-133.2 (m, *o*-Ph), 128.7 (s, *p*-Ph), 128.6 (s, *p*-Ph), 128.5 (d, $^{3}J_{PC}$ = 7 Hz, *m*-Ph), 128.4 (d, $^{3}J_{PC}$ = 7 Hz, *m*-Ph), 125.2 (s, C5), 124.4 (s, C6), 122.8 (s, C7), 121.9 (d, $^{3}J_{PC}$ = 5 Hz, C4), 46.3 (d, $^{3}J_{PC}$ = 4 Hz, C1), –6.35 (s, Si-CH_3). $^{31}P\{^{1}H\}$-NMR ($CDCl_3$): δ –21.47 (s).

***meso*-3.19**: ^{1}H-NMR ($CDCl_3$): δ 7.51-7.13 (m, 28H, H4-7 & Ph), 6.24 (dd, $^{3}J_{HH}$ = 2 Hz, $^{3}J_{PH}$ = 4 Hz, 2H, H2), 3.67 (pseudo t, $^{3}J_{HH}$ = 2 Hz, $^{4}J_{PH}$ = 1 Hz,, 2H, H1), –0.07 (s, 3H, CH_3), –0.43 (s, 3H, CH_3). $^{13}C\{^{1}H\}$-NMR ($CDCl_3$): δ 145.2 (d, $^{2}J_{PC}$ = 11 Hz, C9), 144.9 (s, C8), 142.8 (d, $^{2}J_{PC}$ = 9 Hz, C2), 138.6 (d, $^{3}J_{PC}$ = 12 Hz, C3), 136.2 (d, $^{1}J_{PC}$ = 9 Hz, *ipso*-Ph), 135.7 (d, $^{1}J_{PC}$ = 8 Hz, *ipso*-Ph), 134.0-133.2 (m, *o*-Ph), 128.8 (s, *p*-Ph), 128.8 (s, *p*-Ph), 128.5 (d, $^{3}J_{PC}$ = 7 Hz, *m*-Ph), 128.4 (d, $^{3}J_{PC}$ = 7 Hz, *m*-Ph), 125.2 (s, C5), 124.4 (s, C6), 122.8 (s, C7), 121.8 (d, $^{3}J_{PC}$ = 5 Hz, C4), 46.3 (d, $^{3}J_{PC}$ = 4 Hz, C1), –5.4 (s, Si-CH_3), –6.75 (s, Si-CH_3). $^{31}P\{^{1}H\}$-NMR ($CDCl_3$): δ –21.52 (s).

Synthesis of diindenyliron(II) (3.20).

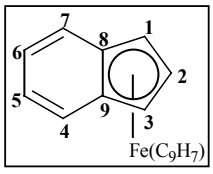

To a solution of indene (**3.1**) (1.992 g, 17 mmol) in tetrahydrofuran (95 mL) at –80°C was added a solution of *n*-BuLi (10.71 mL, 1.6 M, 17 mmol). After warming to ambient temperature and stirring for 4 h, the reaction mixture was cooled to –80°C and $FeCl_2$ (1.086 g, 8.6 mmol) was added. The reaction mixture was stirred for a further 18 h. The solvent was removed *in vacuo* and the residue was dissolved in dichloromethane (40 mL) and filtered through Celite. The Celite was washed with a further 35 mL

dichloromethane and the solvent was removed *in vacuo* to yield 1.706 g (70%) of **3.20** as a black solid. Ferrocene **3.20** was further purified by vacuum sublimation.

^{1}H-NMR (C_6D_6): δ 6.80 (m, 8H, H4-7), 4.48 (s, 4H, H1/3), 3.89 (s, 2H, H2). ^{13}C{^{1}H}-NMR (C_6D_6): δ 125.5 (C4/7), 122.8 (C5/6), 87.0 (C8/9), 69.9 (C2), 61.9 (C1/3). UV-vis (CH_2Cl_2, ε): λ_{max} 422 nm (654), 560 (332).

Synthesis of di(1-methylindenyl)iron(II) (3.21).

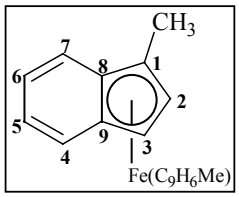

To a solution of 1-methylindene (**3.2**) (0.893 g, 6.9 mmol) in tetrahydrofuran (40 mL) at –80°C was added a solution of *n*-BuLi (4.29 mL, 1.6 M, 6.9 mmol). After warming to ambient temperature and stirring for 2 h, $FeCl_2$ (0.435 g, 3.4 mmol) was added and the reaction mixture was stirred for a further 2 h. The solvent was removed *in vacuo* and the residue was dissolved in diethyl ether (50 mL) and filtered through Celite. Removal of the solvent *in vacuo* yielded 0.485 g (45%) of **3.21** as a black solid. The product was obtained as a 1:1 mixture of *racemic* and *meso* diastereomers and was further purified by vacuum sublimation. ^{1}H-NMR spectrum is consistent with literature.[9]

Isomer 1: ^{13}C{^{1}H}-NMR (C_6D_6): δ 127.2 (C7), 125.5 (C4), 123.0 (C6), 122.6 (C5), 87.0 (C9), 86.1 (C8), 74.3 (C1), 72.6 (C2), 60.4 (C3), 11.0 (CH_3).
Isomer 2: ^{13}C{^{1}H}-NMR (C_6D_6): δ 127.1 (C7), 125.0 (C4), 122.6 (C6), 122.4 (C5), 86.9 (C9), 86.1 (C8), 74.2 (C1), 72.2 (C2), 59.6 (C3), 10.4 (CH_3).
Isomeric mixture: UV-vis (CH_2Cl_2, ε): λ_{max} 426 nm (580), 558 (368). CV (CH_2Cl_2): $E_{1/2}$ = –375 mV, ΔE_P = 160 mV.

Synthesis of di(2-methylindenyl)iron(II) (3.22).

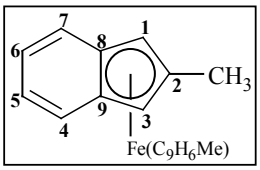

To a solution of 2-methylindene (**3.3**) (0.55 mL, 3.9 mmol) in tetrahydrofuran (50 mL) at –80°C was added a solution of *n*-BuLi (2.40 mL, 1.6 M, 3.9 mmol). After warming to ambient temperature and stirring for 4 h, $FeCl_2$ (0.244 g, 1.9 mmol) was added and the reaction mixture was stirred for a further 16 h. The solvent was removed *in vacuo* and the residue was dissolved in diethyl ether (25 mL) and filtered through Celite. Removal of the solvent *in vacuo* followed by recrystallisation from diethyl ether yielded 0.219 g (36%) of **3.22** as black crystals.

^{1}H-NMR (C_6D_6): δ 7.00 (m, 4H, H4/7), 6.85 (m, 4H, H5/6), 4.22 (s, 4H, H1/3), 1.73 (s, 6H, CH_3). $^{13}C\{^1H\}$-NMR (C_6D_6): δ 127.45 (s, C4/7), 122.99 (s, C5/6), 86.77 (s, C8/9), 85.57 (s, C2), 63.27 (s, C1/3), 13.54 (s, CH_3). Mass spectrum: (EI, *m/z* (%)): 314 (2, M^+), 258 (31, $C_{20}H_{18}^+$), 129 (100, $C_{10}H_9^+$). UV-vis (CH_2Cl_2, ε): λ_{max} 418 nm (530), 552 (304). CV (CH_2Cl_2): $E_{1/2}$ = –355 mV, ΔE_P = 145 mV. Anal. Calc. for $C_{20}H_{18}Fe$: C, 76.55; H, 5.78. Found: C, 75.80; H, 5.69.

Synthesis of bis(1,2-dimethylindenyl)iron(II) (3.23).

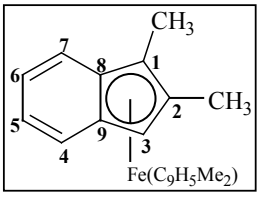

To a solution of 1,2-dimethylindene (**3.4**) (0.541 g, 3.8 mmol) in tetrahydrofuran (35 mL) at –80°C was added a solution of *n*-BuLi (2.34 mL, 1.6 M, 3.8 mmol). After warming to ambient temperature and stirring for 2 h, $FeCl_2$ (0.238 g, 1.9 mmol) was added and the reaction mixture was stirred for a further 2 h. The solvent was removed *in vacuo* and the residue was dissolved in diethyl ether (30 mL) and filtered through Celite. Removal of the solvent *in vacuo* yielded 0.433 g (67%) of **3.23** as a dark green solid. The product was obtained as a 1:1 mixture of *racemic* and *meso* diastereomers.

Isomeric mixture: ^{1}H-NMR ($CDCl_3$): δ 7.17-6.96 (m, 16H, H4-7), 4.29 (s, 2H, H3), 3.96 (s, 2H, H3), 1.95 (s, 6H, C1-CH_3), 1.79 (s, 6H, C2-CH_3), 1.77 (s, 6H, C1-CH_3), 1.68 (s, 6H, C2-CH_3). $^{13}C\{^1H\}$-NMR ($CDCl_3$): δ 127.2 (C7), 127.1 (C7), 126.1 (C4), 125.9 (C4), 123.1 (C6), 122.7 (C6), 122.4 (C5), 122.3 (C5), 85.7-84.7 (m, C2, C8,

C9), 72.6 (C1), 72.3 (C1), 62.7 (C3), 62.0 (C3), 11.7 (C2-*CH*$_3$), 11.5 (C2-*CH*$_3$), 8.7 (C1-*CH*$_3$), 7.8 (C1-*CH*$_3$). Mass spectrum: (EI, *m/z* (%)): 342 (32, M^+), 286 (88, $C_{22}H_{22}^+$), 143 (100, $Me_2C_9H_5^+$), 128 (89, $C_{10}H_8^+$). UV-vis (CH_2Cl_2, ε): λ_{max} 420 nm (484), 550 (359). CV (CH_2Cl_2): $E_{1/2}$ = –450 mV, ΔE_P = 105 mV. Anal. Calc. for $C_{22}H_{22}Fe$: C, 77.20; H, 6.48. Found: C, 77.32; H, 5.98.

Synthesis of bis(1,3-dimethylindenyl)iron(II) (3.24).

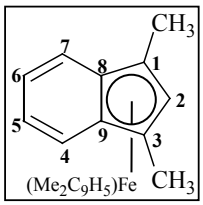

To a solution of 1,3-dimethylindene (**3.5**) (0.512 g, 3.6 mmol) in tetrahydrofuran (35 mL) at –80°C was added a solution of *n*-BuLi (2.23 mL, 1.6 M, 3.6 mmol). After warming to ambient temperature and stirring for 2 h, $FeCl_2$ (0.224 g, 1.8 mmol) was added and the reaction mixture was stirred for a further 2 h. The solvent was removed *in vacuo* and the residue was dissolved in diethyl ether (30 mL) and filtered through Celite. Removal of the solvent *in vacuo* yielded 0.359 g (59%) of **3.24** as a dark green solid. ^{1}H-NMR spectrum is consistent with literature.[10]

$^{13}C\{^1H\}$-NMR (C_6D_6): δ 128.7 (C4/7), 123.9 (C5/6), 84.9 (C8/9), 82.1 (C2), 74.4 (C1/3), 11.7 (CH_3). UV-vis (CH_2Cl_2, ε): λ_{max} 422 nm (516), 548 (342). CV (CH_2Cl_2): $E_{1/2}$ = –472 mV, ΔE_P = 125 mV.

Synthesis of bis(4,7-dimethylindenyl)iron(II) (3.25).

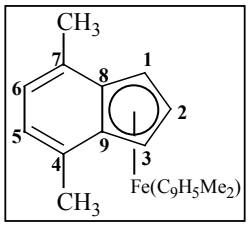

To a solution of 4,7-dimethylindene (**3.6**) (2.09 g, 14 mmol) in tetrahydrofuran (95 mL) at –80°C was added a solution of *n*-BuLi (9.05 mL, 1.6 M, 14 mmol). After warming to ambient temperature and stirring for 4 h, $FeCl_2$ (0.919 g, 7.3 mmol) was added and the reaction mixture was stirred for a further 16 h. The solvent was removed *in vacuo* and the residue was dissolved in diethyl ether (50 mL) and filtered through Celite. Removal of the solvent *in vacuo* yielded 1.86 g (75%) of **3.25** as a dark purple solid. Recrystallization from diethyl ether afforded purple-pink crystals.

^{1}H-NMR (C_6D_6): δ 6.57 (s, 4H, H5/6), 4.42 (s, 4H, H1/3), 4.02 (2, 2H, H2), 2.13 (s, 12H, CH_3). $^{13}C\{^{1}H\}$-NMR (C_6D_6): δ 133.17 (s, C4/7), 121.83 (s, C5/6), 88.95 (s, C8/9), 69.36 (s, C2), 60.05 (s, C1/3), 19.52 (s, CH_3). Mass spectrum: (EI, *m/z* (%)): 342 (18, M^+), 286 (7, $C_{22}H_{22}^+$), 145 (100, $Me_2C_9H_5^+$), 143 (27, $Me_2C_9H_3^+$). HR-MS: M^+ Calc., 342.10705; Found, 342.10595. UV-vis (CH_2Cl_2, ε): λ_{max} 416 nm (827), 556 (430). CV (CH_2Cl_2): $E_{1/2}$ = –343 mV, ΔE_P = 150 mV. Anal. Calc. for $C_{22}H_{22}Fe$: C, 77.20; H, 6.48. Found: C, 76.90; H, 6.40.

Synthesis of bis(1,4,7-trimethylindenyl)iron(II) (3.26).

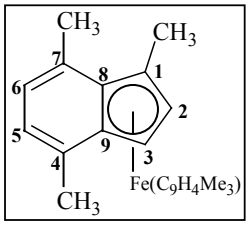

To a solution of 1,4,7-trimethylindene (**3.7**) (0.647 g, 4.1 mmol) in tetrahydrofuran (35 mL) at –80°C was added a solution of *n*-BuLi (2.55 mL, 1.6 M, 4.1 mmol). After warming to ambient temperature and stirring for 2 h, $FeCl_2$ (0.26 g, 2.0 mmol) was added and the reaction mixture was stirred for a further 2 h. The solvent was removed *in vacuo* and the residue was dissolved in dichloromethane (20 mL) and filtered through Celite. Removal of the solvent *in vacuo* yielded 0.536 g (71%) of **3.26** as a dark purple solid. The product was obtained as a 1:1 mixture of *racemic* and *meso* diastereomers.

Isomer 1: $^{13}C\{^{1}H\}$-NMR (C_6D_6): δ 136.0 (C7), 133.0 (C4), 123.0 (C6), 121.2 (C5), 90.3 (C9), 86.0 (C8), 74.6 (C1), 74.4 (C2), 58.8 (C3), 21.2 (C7-*CH*$_3$), 19.3 (C4-*CH*$_3$), 13.8 (C1-*CH*$_3$).

Isomer 2: $^{13}C\{^{1}H\}$-NMR (C_6D_6): δ 134.8 (C7), 134.6 (C4), 122.6 (C6), 121.8 (C5), 89.5 (C9), 85.6 (C8), 74.1 (C1), 72.9 (C2), 56.7 (C3), 21.4 (C7-*CH*$_3$), 19.1 (C4-*CH*$_3$), 11.6 (C1-*CH*$_3$).

Isomeric mixture: ^{1}H-NMR ($CDCl_3$): δ 6.76-6.61 (m, 8H, H5 & H6), 4.42 (s, 2H, H3), 4.16 (s, 2H, H3), 4.03 (s, 2H, H2), 3.97 (s, 2H, H2), 2.43(s, 6H, C7-CH_3), 2.33 (s, 6H, C7-CH_3), 2.30 (s, 6H, C4-CH_3), 2.23 (br s, 12H, C4-CH_3 & C1-CH_3), 1.83 (s, 6H, C1-CH_3). Mass spectrum: (EI, *m/z* (%)): 370 (66, M^+), 355 (8, $[M–CH_3]^+$), 314 (11, $C_{24}H_{26}^+$), 157 (100, $Me_3C_9H_4^+$), 141 (46, $Me_2C_9H_3^+$). HR-MS: M^+ Calc., 370.13835; Found, 370.13892. UV-vis (CH_2Cl_2, ε): λ_{max} 420 nm (658), 560 (568). CV (CH_2Cl_2):

$E_{1/2}$ = –451 mV, ΔE_P = 157 mV. Anal. Calc. for $C_{24}H_{26}Fe$: C, 77.84; H, 7.08. Found: C, 70.11; H, 6.46.

Synthesis of bis(1,3,4,7-tetramethylindenyl)iron(II) (3.27).

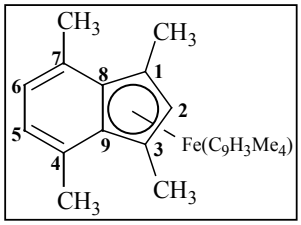

To a solution of 1,3,4,7-tetramethylindene (**3.8**) (0.789 g, 4.6 mmol) in tetrahydrofuran (40 mL) at –80°C was added a solution of *n*-BuLi (2.87 mL, 1.6 M, 4.6 mmol). After warming to ambient temperature and stirring for 2 h, $FeCl_2$ (0.290 g, 2.3 mmol) was added and the reaction mixture was stirred for a further 2 h. The solvent was removed *in vacuo* and the residue was dissolved in dichloromethane (20 mL) and filtered through Celite. Removal of the solvent *in vacuo* yielded 0.648 g (71%) of **3.27** as a dark purple solid.

^{1}H-NMR (C_6D_6): δ 6.60 (s, 4H, H5/6), 3.44 (s, 2H, H2), 2.30 (s, 12H, C4/7-CH_3), 1.94 (s, 12H, C1/3-CH_3). $^{13}C\{^1H\}$-NMR (C_6D_6): δ 135.6 (C4/7), 122.9 (C5/6), 86.8 (C8/9), 81.1 (C2), 72.5 (C1/3), 21.4 (C4/7-*CH*$_3$), 13.3 (C1/3-*CH*$_3$). Mass spectrum: (EI, *m/z* (%)): 398 (100, M+), 383 (16, $[M–CH_3]^+$), 226 (18, $Me_4C_9H_4Fe^+$), 171 (23, $Me_4C_9H_3^+$), 155 (33, $C_{12}H_{11}^+$). HR-MS: M^+ Calc., 398.16965; Found, 398.16937. UV-vis (CH_2Cl_2, ε): λ_{max} 422 nm (536), 550 (628). CV (CH_2Cl_2): $E_{1/2}$ = –568 mV, ΔE_P = 130 mV. Anal. Calc. for $C_{26}H_{30}Fe$: C, 78.39; H, 7.59. Found: C, 77.64; H, 7.49.

Synthesis of bis(1-(trimethylsilyl)indenyl)iron(II) (3.28).

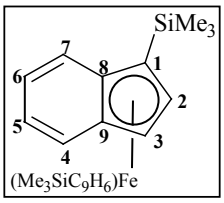

To a solution of 1-(trimethylsilyl)indene (**3.9**) (1.208 g, 6.4 mmol) in tetrahydrofuran (50 mL) at –80°C was added a solution of *n*-BuLi (4.00 mL, 1.6 M, 6.4 mmol). After stirring the reaction mixture at ambient temperature for 2 h, $FeCl_2$ (0.410 g, 3.2 mmol) was added and the reaction mixture stirred for a further 3 h at ambient temperature. The solvent was removed *in vacuo* and to leave a dark green oily residue, which was dissolved in diethyl ether and filtered through Celite. Removal of solvent *in vacuo* yielded 1.03 g

(74%) of **3.28** as a dark green oily solid. The product obtained was a mixture of *racemic* and *meso* diastereomers in a 1.6:1 ratio

Major isomer: ^{1}H-NMR ($CDCl_3$): δ 7.60-6.51 (m, 8H, H4-7), 4.94 (s, 2H, H3), 3.99 (s, 2H, H2)), 0.49 (s, 18H, $Si(CH_3)_3$). $^{13}C\{^{1}H\}$-NMR (C_6D_6): δ 127.02 (C7), 124.36 (C4) 122.35, 122.19 (C5&6), 90.41, 90.20 (C8&9), 74.07 (C2), 65.19 (C3), 62.92 (C1), 0.35 ($Si(CH_3)_3$).
Minor isomer: ^{1}H-NMR ($CDCl_3$): δ 7.60-6.51 (m, 8H, H4-7), 4.68 (s, 2H, H3), 3.24 (s, 2H, H2)), 0.39 (s, 18H, $Si(CH_3)_3$). $^{13}C\{^{1}H\}$-NMR (C_6D_6): δ 130.55, 129.73 (C4&7), 124.27, 123.94 (C5&6), 90.09, 89.96 (C8&9), 78.04 (C2), 65.60 (C3), 62.79 (C1), 0.44 ($Si(CH_3)_3$).
Mass spectrum: (EI, *m/z* (%)): 430 (33, M^+), 241 (25, $C_9H_4(SiMe_3)Fe^+$), 187 (45, $C_9H_6SiMe_3^+$), 112 (46, $C_9H_4^+$), 73 (100, $SiMe_3^+$). HR-MS: M^+ Calc., 430.12345; Found 430.12247. UV-vis (CH_2Cl_2, ε): λ_{max} 416 nm (568), 578 (239). CV (CH_2Cl_2): $E_{1/2}$ = –275 mV, ΔE_P = 125 mV.

Synthesis of bis(2-(trimethylsilyl)indenyl)iron(II) (3.29).

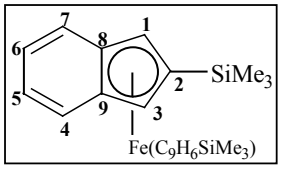

To a solution of 2-(trimethylsilyl)indene (**3.10**) (1.266 g, 6.7 mmol) in tetrahydrofuran (50 mL) at –80°C was added a solution of *n*-BuLi (4.20 mL, 1.6 M, 6.7 mmol). After stirring the reaction mixture at ambient temperature for 6 h, $FeCl_2$ (0.852 g, 3.4 mmol) was added and the reaction mixture stirred a further 16 h at ambient temperature. The solvent was removed *in vacuo* and to leave a dark green oily residue, which was dissolved in petroleum ether and filtered through Celite. Removal of solvent *in vacuo* yielded 0.92 g (63%) of **3.29** as a dark blue oily solid.

^{1}H-NMR (C_6D_6): δ 7.41 (AA'BB', 4H, H4/7), 7.00 (AA'BB', $^{3}J_{4-5}$ = 3 Hz, $^{4}J_{4-6}$ = 9 Hz, $^{3}J_{5-6}$ = 3 Hz, 4H, H5/6), 3.86 (s, 4H, H1/3), 0.36 (s, 18H, $Si(CH_3)_3$). $^{13}C\{^{1}H\}$-NMR (C_6D_6): δ 129.86 (C4/7), 124.05 (C5/6), 90.88 (C8/9), 77.21 (C2), 66.76 (C1/3), 0.35 ($Si(CH_3)_3$). Mass spectrum: (EI, *m/z* (%)): 430 (100, M^+), 358 (26, HM^+-$SiMe_3$), 172 (14, $C_9H_6SiMe_2^+$), 115 (25, $C_9H_7^+$), 73 (47, $SiMe_3^+$). HR-MS: M^+ Calc.,

430.12345; Found 430.12257. UV-vis (CH_2Cl_2, ε): λ_{max} 434 nm (316), 578 (340). CV (CH_2Cl_2): $E_{1/2}$ = –270 mV, ΔE_P = 145 mV.

Synthesis of bis(1,2-bis(trimethylsilyl)indenyl)iron(II) (3.30).

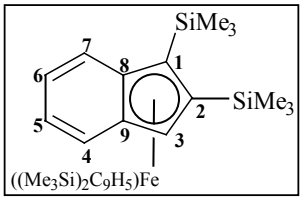

To a solution of 1,2-bis(trimethylsilyl)indene (**3.11**) (1.096 g, 4.2 mmol) in tetrahydrofuran (45 mL) at –80°C was added a solution of *n*-BuLi (2.63 mL, 1.6 M, 4.2 mmol). After stirring the reaction mixture at ambient temperature for 7 h, $FeCl_2$ (0.267 g, 2.1 mmol) was added, and the reaction mixture stirred for a further 6 h at ambient temperature. The solvent was removed *in vacuo* and to leave a green oily residue. Chromatography on silica gel with petroleum ether gave 0.41 g (35%) of **3.30** as a green solid.

^{1}H-NMR (C_6D_6): δ 7.83 (s, 2H, H4 or 7), 7.63 (s, 2H, H4 or 7), 6.95 (br s, 4H, H5&6), 5.15 (s, 2H, H3), 0.62 (s, 18H, Si(CH_3)$_3$), 0.09 (s, 18H, Si(CH_3)$_3$). ^{13}C{^{1}H}-NMR (C_6D_6): δ 131.1, 130.6 (C4&7), 125.7, 125.5 (C5&6), 95.6 (C8), 91.5 (C9), 81.9 (C2), 73.7 (C3), 68.8 (C1), 3.1 (Si(*CH*$_3$)$_3$), 2.3 (Si(*CH*$_3$)$_3$). Mass spectrum: (EI, *m/z* (%)): 574 (20, M^+), 259 (51, $C_9H_5(SiMe_3)_2^+$), 229 (9, $C_9H_5(SiMe_2)_2^+$), 172 (47, $C_9H_5SiMe_2^+$), 100 (65, $SiMe_3^+$). HR-MS: M^+ Calc., 574.20260; Found, 574.20480. UV-vis (CH_2Cl_2, ε): λ_{max} 600 (256). CV (CH_2Cl_2): $E_{1/2}$ = –291 mV, ΔE_P = 112 mV.

Synthesis of bis(1,3-bis(trimethylsilyl)indenyl)iron(II) (3.31).

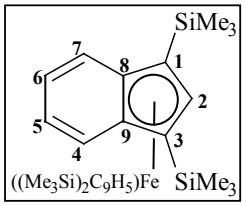

To a solution of 1,3-bis(trimethylsilyl)indene (**3.12**) (1.055 g, 4.1 mmol) in tetrahydrofuran (50 mL) at –80°C was added a solution of *n*-BuLi (2.53 mL, 1.6 M, 4.1 mmol). After stirring the reaction mixture at ambient temperature for 12 h, $FeCl_2$ (0.260 g, 2.0 mmol) was added, and the reaction mixture stirred for a further 6 h at ambient temperature. The solvent was removed *in vacuo* and to leave a green/blue oily residue. Chromatography on silica gel with petroleum ether gave 0.45 g (39%) of **3.31** as a green oily solid, which was recrystallised from petroleum ether.

^{1}H-NMR (C_6D_6): δ 7.57 (AA'BB', 4H, H4/7), 7.03 (AA'BB', $^{3}J_{4\text{-}5}$ = 3 Hz, $^{4}J_{4\text{-}6}$ = 9 Hz, $^{3}J_{5\text{-}6}$ = 3 Hz, 4H, H5/6), 4.46 (s, 2H, H2), 0.37 (s, 36H, $Si(CH_3)_3$). $^{13}C\{^{1}H\}$-NMR (C_6D_6): δ 130.94 (C4/7), 124.87 (C5/6), 95.78 (C8/9), 82.21 (C2), 64.92 (C1/3), 0.94 ($Si(CH_3)_3$). Mass spectrum: (EI, *m/z* (%)): 574 (83, M^+), 501 (7, M^+–$SiMe_3$), 259 (17, $C_9H_5(SiMe_3)_2^+$), 244 (17, $C_9H_5(SiMe_3)(SiMe_2)^+$), 229 (24, $C_9H_5(SiMe_2)_2^+$), 187 (38, $C_9H_6SiMe_3^+$), 172 (100, $C_9H_5SiMe_2^+$), 73 (65, $SiMe_3^+$). HR-MS: M^+ Calc., 574.20260; Found, 574.20464. UV-vis (CH_2Cl_2, ε): λ_{max} 464 nm (287), 622 (260). CV (CH_2Cl_2): $E_{1/2}$ = –358 mV, ΔE_P = 70 mV. Anal. Calc. for $C_{30}H_{46}FeSi_4$: C, 62.68; H, 8.07. Found: C, 63.01; H, 7.93.

Synthesis of bis(1-diphenylphosphinoindenyl)iron(II) (3.32).

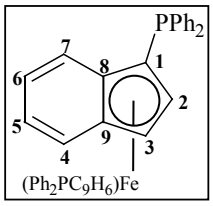

To a solution of 3-(diphenylphosphino)indene (**3.13**) (1.8 g, 6.0 mmol) in tetrahydrofuran (50 mL) at –80°C was added a solution of *n*-BuLi (3.75 mL, 1.6 M, 6.0 mmol). After 2 h, $FeCl_2$ (0.38 g, 3 mmol) was added and the reaction mixture stirred for 2 h at ambient temperature. The solvent was removed *in vacuo* and the residue was loaded onto a Celite column and washed with diethyl ether (to remove unreacted **3.13**). Subsequent washing with dichloromethane yielded 1.26 g (64%) of **3.32** as a dark green/blue solid. The product was obtained as a 55:45 mixture of *racemic* and *meso* diastereomers.

***meso*-3.32**: ^{1}H-NMR ($CDCl_3$): δ 7.53-6.88 (m, 28H, H4-7 and Ph), 3.81 (s, 2H, H3), 3.48 (s, 2H, H2). $^{13}C\{^{1}H\}$-NMR ($CDCl_3$): δ 139.1 (d, $^{1}J_{PC}$ = 14 Hz, *ipso*-Ph), 137.4 (d, $^{1}J_{PC}$ = 11 Hz, *ipso*-Ph), 135.4 (d, $^{2}J_{PC}$ = 21 Hz, *o*-Ph), 132.4 (d, $^{2}J_{PC}$ = 20 Hz, *o*-Ph), 129.0 (s, *p*-Ph), 128.2 (d, $^{3}J_{PC}$ = 8 Hz, *m*-Ph), 128.1 (d, $^{3}J_{PC}$ = 10 Hz, C7), 128.0 (d, $^{3}J_{PC}$ = 3 Hz, *m*-Ph), 127.9 (s, C4), 127.7 (s, *p*-Ph), 124.9 (s, C6), 124.3 (s, C5), 91.6 (d, $^{2}J_{PC}$ = 22 Hz, C8), 90.3 (s, C9), 74.5 (s, C2), 66.9 (d, $^{1}J_{PC}$ = 13 Hz, C1), 64.4 (s, C3). $^{31}P\{^{1}H\}$-NMR ($CDCl_3$): δ –26.53 (s). UV-vis (CH_2Cl_2, ε): λ_{max} 418 nm (869), 566 (265). CV (CH_2Cl_2): $E_{1/2}$ = –140 mV, ΔE_P = 90 mV.

Isolation of *rac*-bis(1-diphenylphosphinoindenyl)iron(II) (*rac*-3.32).

As above, except after the addition of $FeCl_2$, the reaction mixture is stirred for 12 h at ambient temperature. ^{1}H-, ^{13}C{^{1}H}-, and ^{31}P{^{1}H}-NMR are consistent with literature.[11] Dark blue crystallographic-quality crystals were obtained by recrystallisation from CH_2Cl_2/diethyl ether.

Synthesis of bis(1-diphenylphosphino-2-methyl indenyl)iron(II) (3.33).

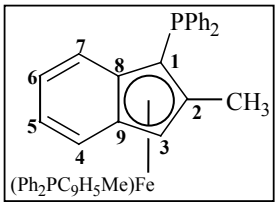

To a solution of 2-methyl-3-diphenylphosphinoindene (**3.14**) (0.73 g, 2.3 mmol) in tetrahydrofuran (40 mL) at –80°C was added a solution of *n*-BuLi (1.45 mL, 1.6 M, 2.3 mmol). After 2 h, $FeCl_2$ (0.147 g, 1.2 mmol) was added and the reaction mixture stirred for 1 h at ambient temperature. The solvent was removed *in vacuo* and the residue was loaded onto a Celite column and washed with dichloromethane. The solvent was removed in vacuo to yield 0.60 g (54%) of **3.33**. The product was obtained as a 58:42 mixture of *meso* and *racemic* diastereomers.

***meso*-3.33**: ^{1}H-NMR ($CDCl_3$): δ 7.80-6.41 (m, 28H, H4-7 and Ph), 4.84 (s, 2H, H3), 0.77 (s, 6H, CH_3). ^{13}C{^{1}H}-NMR ($CDCl_3$): δ 137.2 (d, $^1J_{PC}$ = 11Hz, *ipso*-Ph), 137.1 (d, $^1J_{PC}$ = 11 Hz, *ipso*-Ph), 135.0 (d, $^2J_{PC}$ = 20 Hz, *o*-Ph), 133.4 (d, $^2J_{PC}$ = 20 Hz, *o*-Ph), 128.9 (s, *p*-Ph), 128.5-128.0 (m, *m*-Ph, *p*-Ph, C4&7), 124.6 (s, C6), 124.2 (s, C5), 90.2 (d, $^2J_{PC}$ = 22 Hz, C8), 88.5 (s, C9), 87.4 (s, C2), 66.4 (s, C3), 65.5 (d, $^1J_{PC}$ = 15 Hz, C1), 9.4 (d, $^3J_{PC}$ = 11 Hz). ^{31}P{^{1}H}-NMR ($CDCl_3$): δ –20.04 (s).

***rac*-3.33**: ^{1}H-NMR ($CDCl_3$): δ 5.08 (s, 2H, H3), 1.86 (s, 6H, CH_3). ^{13}C{^{1}H}-NMR ($CDCl_3$): δ 134.7 (d, $^2J_{PC}$ = 20 Hz, *o*-Ph), 133.7 (d, $^2J_{PC}$ = 20 Hz, *o*-Ph), 128.8 (s, C4), 121.7 (s, C6), 121.2 (s, C5), 87.9 (s, C9), 86.9 (s, C2), 68.6 (s, C3), 13.3 (d, $^3J_{PC}$ = 10 Hz). Signals for C1, C7, C8, *ipso*-Ph, *para*-Ph and *meta*-Ph were not resolved from those of the major isomer. ^{31}P{^{1}H}-NMR ($CDCl_3$): δ –17.60 (s).

Mass spectrum: (EI, *m/z* (%)): 682 (40, M^+), 314 (100, $MeC_9H_6PPh_2^+$), 185 (83, Ph_2P^+), 128 (25, $MeC_9H_6^+$), 108 (15, PhP^+). HR-MS: M^+ Calc., 682.16413; Found,

682.16475. Anal. Calc. for $C_{44}H_{36}P_2Fe$: C, 77.43; H, 5.32. Found: C, 76.19; H, 5.33. UV-vis (CH_2Cl_2, ε): λ_{max} 414 nm (1151), 572 (196).

Synthesis of bis(1-diphenylphosphino-3-methyl-indenyl)iron(II) (3.34).

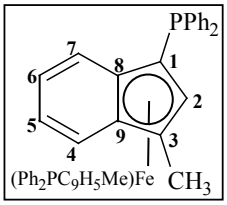

To a solution of 1-diphenylphosphino-3-methylindene (**3.15**) (0.352 g, 1.1 mmol) in tetrahydrofuran (40 mL) at –80°C was added a solution of *n*-BuLi (0.70 mL, 1.6M, 1.1 mmol). After 3 h at ambient temperature, $FeCl_2$ (0.07 g, 0.6 mmol) was added and the reaction mixture stirred for 2 h. The solvent was removed *in vacuo* and the residue was loaded onto a Celite column and washed with dichloromethane. Removal of the solvent *in vacuo* yielded a dark green powder, which was recrystallised from diethyl ether to give 0.16 g (43%) of **3.34** as dark green crystals.

***rac*-3.34**: ^{1}H-NMR ($CDCl_3$): δ 7.44-6.38 (m, 28H, H4-7 and Ph), 3.61 (s, 2H, H2), 2.38 (s, 6H, CH_3). $^{13}C\{^1H\}$-NMR ($CDCl_3$): δ 139.2 (d, $^1J_{PC}$ = 12 Hz, *ipso*-Ph), 136.7 (d, $^1J_{PC}$ = 10 Hz, *ipso*-Ph), 134.9 (d, $^2J_{PC}$ = 21 Hz, *o*-Ph), 132.5 (d, $^2J_{PC}$ = 19 Hz, *o*-Ph), 129.1 (s, *p*-Ph), 128.2 (d, $^3J_{PC}$ = 8 Hz, *m*-Ph), 127.9 (d, $^3J_{PC}$ = 6 Hz, *m*-Ph), 127.7 (s, *p*-Ph), 127.1 (d, $^3J_{PC}$ = 7 Hz, C7), 123.4 (s, C4), 123.1 (s, C6), 121.2 (s, C5), 89.3 (d, $^2J_{PC}$ = 19 Hz, C8), 89.1 (d, $^3J_{PC}$ = 4 Hz, C9), 78.1 (s, C3), 74.5 (s, C2), 65.7 (d, $^1J_{PC}$ = 11 Hz, C1), 11.8 (d, $^4J_{PC}$ = 9 Hz, CH_3). $^{31}P\{^1H\}$-NMR ($CDCl_3$): δ –24.69 (s). Anal. Calcd for $C_{44}H_{36}P_2Fe$: C 77.42; H 5.32. Found: C 75.65; H 5.55. Mass spectrum: (EI, *m/z* (%)): 682 (27, M+), 312 (100, $MeC_9H_6PPh_2^+$), 185 (64, Ph_2P^+), 128 (18, $MeC_9H_6^+$), 108 (19, PhP^+). HR-MS: M^+ Calc., 682.16413; Found, 682.16511. UV-vis (CH_2Cl_2, ε): λ_{max} 422 nm (1196), 600 (324). CV (CH_2Cl_2): $E_{1/2}$ = –233 mV, ΔE_P = 90 mV.

Synthesis of bis(1-diphenylphosphino-2,3-dimethyl-indenyl) iron(II) (3.35).

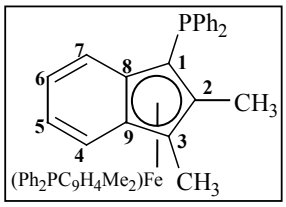

To a solution of 1-diphenylphosphino-2,3-dimethylindene (**3.16**) (0.867 g, 2.6 mmol) in tetrahydrofuran (40 mL) at –80°C was added a solution of *n*-BuLi (1.65 mL, 1.6 M, 2.6 mmol). After warming to ambient temperature and stirring for 2 h, $FeCl_2$ (0.167 g, 1.3 mmol) was added and the reaction mixture was stirred for a further 2 h. The solvent was removed *in vacuo* and the residue was loaded onto a Celite column and washed with petroleum ether (to remove unreacted 1-diphenylphosphino-2,3-dimethylindene). Washing of the column with dichloromethane and removal of solvent *in vacuo* yielded 0.392 g (42%) of **3.35** as a green powder. The product was obtained as a 5:2 mixture of diastereomers.

Major isomer: ^{1}H-NMR ($CDCl_3$): δ 7.68-6.38 (m, 28H, H4-7 and Ph), 1.96 (s, 6H, C3-CH_3), 1.50 (s, 6H, C2-CH_3). $^{13}C\{^{1}H\}$-NMR (C_6D_6): δ 138.5 (d, $^{1}J_{PC}$ = 12 Hz, *ipso*-Ph), 137.1 (d, $^{1}J_{PC}$ = 11 Hz, *ipso*-Ph), 135.9 (d, $^{2}J_{PC}$ = 21 Hz, *o*-Ph), 134.0 (d, $^{2}J_{PC}$ = 19 Hz, *o*-Ph), 129.0-127.2 (m, C7, *m*-Ph & *p*-Ph), 125.6 (s, C4), 123.5 (s, C6), 122.8 (s, C5), 88.8-88.1 (m, C8 & C9), 86.0 (s, C2), 75.6 (s, C3), 67.2 (d, $^{1}J_{PC}$ = 12 Hz, C1), 11.2 (s, C3-*CH_3*), 8.5 (s, C2-*CH_3*). $^{31}P\{^{1}H\}$-NMR ($CDCl_3$): δ –23.81 (s).

Minor isomer: ^{1}H-NMR ($CDCl_3$): δ 2.16 (s, 6H, C3-CH_3), 1.34 (s, 6H, C2-CH_3). $^{31}P\{^{1}H\}$-NMR ($CDCl_3$): δ –23.21 (s).

Mass spectrum: (EI, *m/z* (%)): 710 (10, M^+), 525 (5, $[M–PPh_2]^+$), 326 (100, $Me_2C_9H_4PPh_2^+$). HR-MS: M^+ Calc., 710.19546; Found, 710.19602. CV (CH_2Cl_2): $E_{1/2}$ = –348 mV, ΔE_P = 110 mV.

Attempted synthesis of bis(1-diphenylphosphino-3,4,7-trimethylindenyl)iron(II) (3.36).

To a solution of 1-diphenylphosphino-3,4,7-trimethylindene (**3.17**) (0.194 g, 0.57 mmol) in tetrahydrofuran (30 mL) at –80°C was added a solution of *n*-BuLi (0.35 mL, 1.6 M, 0.57 mmol). After warming to ambient temperature and stirring for 3 h, $FeCl_2$ (0.036 g, 0.28 mmol) was added and the reaction mixture was stirred for a further 3 h.

^{31}P- NMR spectrum of the reaction mixture shows predominantly unreacted ligand (**3.29**) at –2 ppm, with some minor peaks in the region of –20 ppm.

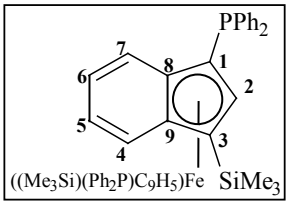

Synthesis of bis(1-diphenylphosphino-3-trimethylsilyl-indenyl)iron(II) (3.37).

To a solution of 1-trimethylsilyl-3-diphenylphosphinoindene (**3.18**) (0.803 g, 2.2 mmol) in tetrahydrofuran (35 mL) at –80°C was added a solution of *n*-BuLi (1.35 mL, 1.6 M, 2.2 mmol). After warming to ambient temperature and stirring for 5 h, $FeCl_2$ (0.137 g, 1.1 mmol) was added and the reaction mixture stirred for a further 2 h. The solvent was removed *in vacuo* and the green, oily residue loaded onto an alumina column. Elution, in the first instance with petroleum ether, followed by subsequent elution with 1:1 dichloromethane/petroleum ether yielded a green oily residue, which contains both **3.37** and 3-diphenylphosphinoindene. The residue was dissolved in petroleum ether, filtered, and the solvent removed in vacuo to yield 0.23 g (31%) of **3.37** as a green powder. The product was too unstable for microanalysis or mass spectrometry.

^{1}H-NMR ($CDCl_3$): δ 7.54-6.77 (m, 28H, H4-7 & Ph), 3.84 (s, 2H, H2), 0.23 (s, 18H, $Si(CH_3)_3$). $^{13}C\{^{1}H\}$-NMR (C_6D_6): δ 138.9 (d, $^{1}J_{PC}$ = 15 Hz, *ipso*-Ph), 137.5 (d, $^{1}J_{PC}$ = 14 Hz, *ipso*-Ph), 135.4 (d, $^{2}J_{PC}$ = 20 Hz, *o*-Ph), 132.9 (d, $^{2}J_{PC}$ = 21 Hz, *o*-Ph), 129.3 (s, *p*-Ph), 128.9-127.5 (m, C7, *m*-Ph & *p*-Ph), 124.8 (s, C4), 124.2 (s, C6), 123.8 (s, C5), 94.1 (s, C9), 92.7 (d, $^{2}J_{PC}$ = 16 Hz, C8), 78.7 (s, C2), 70.8 (d, $^{1}J_{PC}$ = 13 Hz, C1), 64.6 (s, C3), 0.8 (s, CH_3). $^{31}P\{^{1}H\}$-NMR ($CDCl_3$): δ –28.49 (br s). UV-vis (CH_2Cl_2, ε): λ_{max} 591 (212). CV (CH_2Cl_2): $E_{1/2}$ = –220 mV, ΔE_P = 118 mV.

Attempted synthesis of (bis(1-diphenylphosphinoinden-3-yl)dimethylsilane) iron(II) (3.38).

To a solution of bis(3-(diphenylphosphino)-inden-1-yl)dimethylsilane (**3.19**) (1.297 g, 2.0 mmol) in tetrahydrofuran (50 mL) at –80°C was added a solution of *n*-BuLi (2.46 mL, 1.6 M, 4.0 mmol). After warming to ambient temperature and stirring for 2 h,

$FeCl_2$ (0.25 g, 2.0 mmol) was added and the reaction mixture stirred for a further 18 h at ambient temperature to give a dark green solution. The solvent was removed *in vacuo* and the residue chromatographed on Silica gel using 5:1 cyclohexane/ethylacetate. Analysis of the $^{31}P\{^1H\}$-NMR spectrum obtained from the single band eluted off the column shows multiple signals in the region of –4 and –21ppm. It was not possible to unambiguously assign these signals to particular compounds.

Attempted synthesis of bis(1-(diphenylphosphino)tetrahydroindenyl)iron(II) (3.39).

Typical procedure: To a two-necked flask was added bis(1-diphenylphosphinoindenyl)iron(II) (**3.32**) (0.11 g, 0.16 mmol) and PtO_2 (100 mg). The flask was evacuated, charged with hydrogen gas and left to sit for 1h. The flask was cooled to –80°C and tetrahydrofuran (40 mL) introduced. The resulting suspension was warmed to ambient temperature and stirred for 2-18 h under an atmosphere of hydrogen gas. The mixture was filtered, and the solvent was removed *in vacuo*. Analysis of the resulting material generally indicated that either no reaction had occurred or **3.32** had decomposed to give 3-(diphenylphosphineoxide)indene (**3.39**) by unknown means. Reaction of diindenyliron(II) (**3.20**) under identical conditions produced, in good yield, bis(tetrahydroindenyl)iron(II).

Synthesis of 3-(diphenylphosphineoxide)indene (3.40).

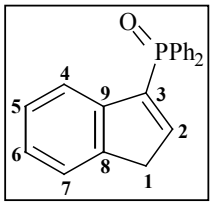

To a solution of 3-diphenylphosphinoindene (**3.13**) (2.53 g, 8.4 mmol) in toluene (50 mL) was added an excess of aqueous hydrogen peroxide (2 mL, 50% w/w). The reaction mixture was stirred at ambient temperature for 12 h. After filtering, the solvent was removed *in vacuo* to leave a yellow oily residue. Recrystallisation from diethyl ether yielded 0.93 g (35%) of **3.40** as a yellow powder.

^1H-NMR ($CDCl_3$): δ 7.79-6.82 (m, 15H, H2, H4-7 and Ph), 3.57 (s, 2H, H1). $^{13}C\{^1H\}$-NMR ($CDCl_3$): δ 148.8 (d, $^2J_{PC}$ = 10 Hz, C2), 143.8 (d, $^3J_{PC}$ = 10 Hz, C8),

142.4 (d, $^{2}J_{PC}$ = 12 Hz, C9), 138.2 (d, $^{1}J_{PC}$ = 106 Hz, C3), 132.0 (d, $^{4}J_{PC}$ = 3 Hz, *p*-Ph), 131.7 (d, $^{1}J_{PC}$ = 106 Hz, *ipso*-Ph), 131.6 (d, $^{2}J_{PC}$ = 10 Hz, *o*-Ph), 128.5 (d, $^{3}J_{PC}$ = 12 Hz, *m*-Ph), 126.6 (s, C5), 125.6 (s, C6), 123.8 (s, C7), 122.6 (s, C4), 40.1 (d, $^{3}J_{PC}$ = 14 Hz, C1). $^{31}P\{^{1}H\}$-NMR ($CDCl_3$): δ 23.85 (s). Mass Spectra (EI, *m/z* (%)): 316 (47, M^+), 201 (100, M^+ - C_9H_7), 115 (26, $C_9H_7^+$), 77 (30, $C_6H_5^+$). HR-MS: M^+ Calc., 316.10170; Found, 316.10186.

Synthesis of 3-(diphenylphosphineselenide)indene (3.41).

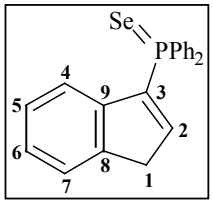

To a solution of 3-diphenylphosphinoindene (**3.13**) (0.40 g, 1.3 mmol) in tetrahydrofuran (30 mL) was added selenium powder (0.16 g, 2.0 mmol). The reaction mixture was stirred at ambient temperature for 16 h. After filtering, the solvent was removed *in vacuo* to yield 0.47 g (93%) of **3.41** as a white powder.

^{1}H-NMR ($CDCl_3$): δ 7.91-6.61 (m, 15H, H2, H4-7 and Ph), 3.58 (s, 2H, H1). $^{13}C\{^{1}H\}$-NMR ($CDCl_3$): δ 147.0 (d, $^{2}J_{PC}$ = 9 Hz, C2), 144.2 (d, $^{3}J_{PC}$ = 10 Hz, C8), 141.7 (d, $^{2}J_{PC}$ = 13 Hz, C9), 136.8 (d, $^{1}J_{PC}$ = 78 Hz, C3), 132.4 (d, $^{2}J_{PC}$ = 11 Hz, *o*-Ph), 131.7 (d, $^{4}J_{PC}$ = 3 Hz, *p*-Ph), 130.3 (d, $^{1}J_{PC}$ = 77 Hz, *ipso*-Ph), 128.6 (d, $^{3}J_{PC}$ = 12 Hz, *m*-Ph), 126.3 (s, C5), 125.6 (s, C6), 123.9 (s, C7), 123.2 (s, C4), 39.8 (d, $^{3}J_{PC}$ = 13 Hz, C1). $^{31}P\{^{1}H\}$-NMR ($CDCl_3$): δ 20.79 (t, $^{1}J_{PSe}$ = 721 Hz). Mass Spectrum (EI, *m/z* (%)): 380 (20, M^+), 300 (77, M^+-Se), 265 (53, $M^+ - C_9H_7$), 185 (100, Ph_2P^+), 115 (24, $C_9H_7^+$), 77 (9, $C_6H_5^+$). HR-MS: M^+ Calc., 380.02329; Found, 380.02262.

CHAPTER 4

Isomerization Studies –General Considerations.

Under an argon atmosphere, a 5 mm NMR tube was charged with 5.0 mg of a 55:45 mixture of *rac*- and *meso*-bis(1-diphenylphosphinoindenyl)iron(II) (**4.2**). Tetrahydrofuran (0.4 mL) was introduced and an external D_2O lock standard was inserted. The sample was immediately inserted into the thermostated probe of a

Varian Unity-300, and an initial $^{31}P\{^{1}H\}$-NMR spectrum was recorded. The ^{31}P 90° pulse width was 13 μs, and a sweep width of approximately 2400 Hz was used. A relaxation time of 3 s was applied with 130 transients being collected. Using these parameters, a single experiment takes approximately 10 minutes. For each isomerization study, up to 40 spectra were collected over a period of 14 h. The integrals of each signal were obtained, and the corresponding plots of integrals vs. time were analyzed with a single exponential function. The plot of $\ln[(X_{t=0})/(X_{t=t})]$, where X is the mole fraction of ***meso*-4.2** at time t, versus time, afforded k from the slope.

Isomerization Studies-Presence of salts.

Under an argon atmosphere, a 5 mm NMR tube was charged with 5.0 mg of a 55:45 mixture of ***rac*-** and ***meso*-4.2**. To this was added n molar equivalents of LiCl (n = 0, 2, 4) or $LiClO_4$ (n = 2). Tetrahydrofuran (0.4 mL) was introduced and an external D_2O lock standard was inserted. The sample was immediately inserted into the thermostated probe of a Varian Unity-300 at 30 °C. Experiment and analysis are as described above.

Isomerisation Studies-Mixed THF/$CDCl_3$ Solvent.

Under an argon atmosphere, a 5 mm NMR tube was charged with 5.0 mg of a 55:45 mixture of ***rac*-** and ***meso*-4.2**. To this was added a mixed-solvent system containing varying ratios of tetrahydrofuran and $CDCl_3$ (total volume of 0.4 mL). An external D_2O lock standard was inserted, and the sample was immediately inserted into the thermostated probe of a Varian Unity-300 at 30 °C. Experiment and analysis are as described above.

Synthesis of bis(1-diphenylphosphino-3-deuterioindenyl)iron(II) (4.2-*d_2*).

To a solution of 3-diphenylphosphinoindene-d_2 (**4.1-*d_2***) (1.0 g, 3.31 mmol) in tetrahydrofuran (30 mL) at –80 °C was added a solution of *n*-BuLi (2.07 mL, 1.6 M, 3.31 mmol). After 2 h, $FeCl_2$ (0.21 g, 1.66 mmol) was added and the reaction mixture

stirred for 2 h at ambient temperature. The solvent was removed *in vacuo* and the residue was loaded onto a Celite column and washed with diethyl ether. Subsequent washing with dichloromethane yielded 0.66 g (61%) of **4.2-*d*$_2$** as a 60:40 mixture of *rac* and *meso* diastereomers. Stirring of the reaction mixture for a period of 12 h after the addition of the $FeCl_2$ produces exclusively the *racemic* isomer. Analysis of the isotope pattern from EI-MS and the integrals from ^{1}H-NMR indicates the product contains 85% **4.2-*d*$_2$** and 15% **4.2-*d*$_1$**.

***rac*-4.2-*d*$_2$**: ^{1}H-NMR ($CDCl_3$): δ 7.54-6.48 (m, 28H, H4-7 and Ph), 3.17 (s, 2H, H2). ^{13}C{^{1}H}-NMR ($CDCl_3$): δ 139.8 (d, $^1J_{PC}$ = 10 Hz, *ipso*-Ph), 136.7 (d, $^1J_{PC}$ = 7 Hz, *ipso*-Ph), 135.2 (d, $^2J_{PC}$ = 22 Hz, *o*-Ph), 131.7 (d, $^2J_{PC}$ = 18 Hz, *o*-Ph), 129.3 (s, *p*-Ph), 128.3 (d, $^3J_{PC}$ = 8 Hz, *m*-Ph), 128.0 (d, $^3J_{PC}$ = 5 Hz, *m*-Ph), 127.6 (s, *p*-Ph), 124.2 (d, $^3J_{PC}$ = 8 Hz, C7), 123.6 (s, C4), 122.9 (s, C5), 122.4 (s, C6), 90.9 (d, $^2J_{PC}$ = 25 Hz, C8), 89.6 (d, $^3J_{PC}$ = 5 Hz, C9), 72.0 (s, C2), 68.1 (d, $^1J_{PC}$ = 9 Hz, C1), 66.1 (m, C3). ^{31}P{^{1}H}-NMR ($CDCl_3$): δ –22.59 (s). ^{2}H-NMR ($CHCl_3$): δ 5.07 (s).
***meso*-4.2-*d*$_2$**: ^{1}H-NMR ($CDCl_3$): δ 7.56-6.84 (m, 28H, H4-7 and Ph), 3.82 (s, 2H, H2). ^{31}P{^{1}H}-NMR ($CDCl_3$): δ –26.51 (s). ^{2}H-NMR ($CHCl_3$): δ 3.83 (s).

Attempted Crossover Experiment of 4.2 with 4.2-*d*$_2$.

To a solution containing a 55:45 mixture of ***rac*-** and ***meso*-4.2** (0.075 g, 0.115 mmol) in tetrahydrofuran (25 mL) was added a 60:40 mixture of ***rac*-** and ***meso*-4.2-*d*$_2$** (0.075 g, 0.115 mmol, d_2: d_1: d_0 ratio = 85:15:0). After stirring for 3 days at ambient temperature, the solvent was removed *in vacuo* and the residue dissolved in dichloromethane (15 mL). After filtering through Celite, the solvent was removed *in vacuo* to yield a green powder (0.141 g, 94%). Analysis of the isotope pattern from EI-MS indicates the product contains 49% **4.2**, 12% **4.2-*d*$_1$**, and 39% **4.2-*d*$_2$** (expected 50% **4.2**, 7.5% **4.2-*d*$_1$**, and 42.5% **4.2-*d*$_2$** if crossover not occurring). Analysis of the integrals from ^{1}H-NMR indicates the product contains 50% **4.2**, 10% **4.2-*d*$_1$**, and 40% **4.2-*d*$_2$**.

Isomerization of 4.2 in the presence of 1-diphenylphosphinoindenide-d_1.

To a solution of 3-diphenylphosphinoindene-d_2 (**4.1-*d*$_2$**) (0.05 g, 0.166 mmol) in tetrahydrofuran (20 mL) at –80°C was added a solution of *n*-BuLi (0.1 mL, 1.6 M, 0.166 mmol). After stirring at ambient temperature for 2 h, a 55:45 mixture of ***rac-*** and ***meso*-4.2** (0.108 g, 0.166 mmol) was added and the solution stirred for 3 days. The solvent was removed *in vacuo* and residue dissolved in dichloromethane (20 mL). After filtering through Celite, the solvent was removed *in vacuo* to yield a green powder. Analysis of the isotope pattern from EI-MS and the integrals from ^{1}H NMR indicates the product contains only **4.2**.

Synthesis of (1-diphenylphosphinoindenyl)(4,7-dimethyl-1-diphenylphosphino indenyl)iron(II) (4.8).

To a solution of 3-diphenylphosphinoindene (**4.1**) (0.335 g, 1.12 mmol) and 3-diphenylphosphino-4,7-dimethylindene (**4.7**) (0.366 g, 1.12 mmol) in tetrahydrofuran (35 mL) at –80°C was added a solution of *n*-BuLi (1.40 mL, 1.6 M, 2.24 mmol). After 2 h, $FeCl_2$ (0.142 g, 1.12 mmol) was added and the reaction mixture stirred for 2 h at ambient temperature. $^{31}P\{^1H\}$-NMR indicates the presence of ten unique phosphorous environments (2 peaks corresponding to the free ligands in addition to the eight signals arising from the ferrocenes). The solution was stirred for a further 24 h, before the solvent was removed *in vacuo*. The residue was dissolved in dichloromethane (20 mL) and filtered through Celite. Removal of the solvent *in vacuo* yielded 0.64 g of a black powder, which was shown to contain, by $^{31}P\{^1H\}$-NMR, ***rac-*** and ***meso*-4.8**, ***rac-*** and ***meso*-4.4**, and ***rac*-4.2** in a ratio of 3.7: 3: 1.3: 1.8: 1. There was no significant variation in these ratios with a further 24 h stirring of the mixture in tetrahydrofuran.

***meso*-4.8**: ^{1}H-NMR ($CDCl_3$): δ 4.07 (s, 1H, H3(**4.7**)), 3.90 (s, 1H, H2(**4.7**)), 3.85 (s, 1H, H3(**4.1**)), 3.55 (s, 1H, H2(**4.1**)). $^{31}P\{^1H\}$-NMR ($CDCl_3$): δ –23.9 (s, **4.7**), –25.61 (s, **4.1**).

***rac*-4.8**: ^{1}H-NMR ($CDCl_3$): δ 5.34 (s, 1H, H3(**4.7**)), 4.98 (s, 1H, H3(**4.1**)), 3.27 (s, 1H, H2(**4.7**)), 3.11 (s, 1H, H2(**4.1**)). $^{31}P\{^{1}H\}$-NMR ($CDCl_3$): δ –16.81 (s, **4.7**), –22.20 (s, **4.1**).

Mass spectrum: (EI, *m/z* (%)): 682 (51, M^+), 327 (31, $Me_2C_9H_4PPh_2^+$), 300 (36, $C_9H_7PPh_2^+$), 185 (100, Ph_2P^+). HR-MS: M^+ Calc., 682.16416; Found, 682.16576. CV (CH_2Cl_2): $E_{1/2}$ = –188 mV, ΔE_P = 200 mV.

Synthesis of dicarbonyl(η^5-cyclopentadienyl)(η^1-1-diphenylphosphinoindenyllithium)iron(II) iodide (4.9).

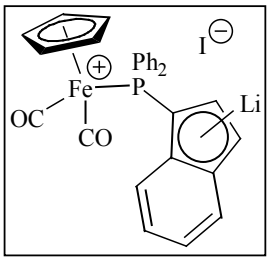

To a solution of 3-diphenylphosphinoindene (**4.1**) (0.91 g, 3.03 mmol) in tetrahydrofuran (25 mL) at –80 °C was added a solution of *n*-BuLi (1.91 mL, 1.6 M, 3.03 mmol). The solution was allowed to warm to ambient temperature and the reaction mixture was stirred for 2 h. To this was added a solution of $CpFe(CO)_2I$ (0.92 g, 3.03 mmol) in tetrahydrofuran (25 mL). The addition resulted in an instant change in colour to dark blue, with a small amount of yellow precipitate. ^{31}P-NMR (D_2O) spectroscopy shows single peak at 34 ppm. The solution was filtered and the solvent removed *in vacuo* to leave a dark blue powder.

^{1}H-NMR ($CDCl_3$): δ 7.65-6.40 (m, 16H, H2-7 & Ph), 4.88 (s, 5H, C_5H_5). $^{13}C\{^{1}H\}$-NMR (THF, D_2O insert): δ 213.5 (d, $^{2}J_{PC}$ = 23 Hz, CO), 137.9 (d, $^{1}J_{PC}$ = 55 Hz, *ipso*-Ph), 133.0 (d, $^{2}J_{PC}$ = 10 Hz, *o*-Ph), 130.1 (s, *p*-Ph), 129.0-127.9 (m, C1, C8, C9 & *m*-Ph), 127.1 (d, $^{2}J_{PC}$ = 15 Hz, C2), 119.8 (C7), 118.6 (C4), 116.1 (C5), 115.8 (C6), 104.2 (d, $^{3}J_{PC}$ = 13 Hz, C3), 88.7 (s, Cp). $^{31}P\{^{1}H\}$-NMR ($CDCl_3$): δ 34.2 (s). IR (KBr, cm^{-1}): υ_{CO} 2038, 1992. Anal. Calc. for $C_{28}H_{21}FeLiIO_2P$: C, 55.12; H, 3.47. Found: C, 51.29; H, 4.22.

Synthesis of dicarbonyl(η^5-cyclopentadienyl)(η^1-3-diphenylphosphinoindene)iron(II) iodide (4.10).

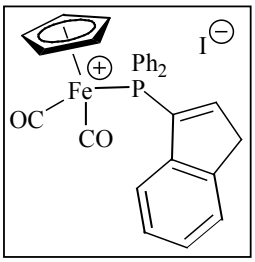

To a mixture of 3-diphenylphosphinoindene (**4.1**) (0.77 g, 2.57 mmol), $CpFe(CO)_2I$ (0.78 g, 2.57 mmol), and $[CpFe(CO)_2]_2$ (0.03 g, 0.077 mmol) was added diethyl ether (50 mL) to give a brown coloured solution. The solution was stirred at ambient temperature for 2 h, in which time a yellow precipitate formed. The mixture was filtered to yield 1.27 g (87%) of **4.10** as a yellow powder.

^{1}H-NMR ($CDCl_3$): δ 7.55 – 7.09 (m, 14H, aromatic), 6.72 (d, $^3J_{HH}$ = 7.2 Hz, 1H, H2), 5.47 (s, 5H, C_5H_5), 3.94 (s, 2H, H1). $^{13}C\{^1H\}$-NMR ($CDCl_3$): δ 209.4 (d, $^2J_{PC}$ = 24.2 Hz, CO), 154.0 (d, $^2J_{PC}$ = 10.9 Hz, C2), 144.6 (d, $^3J_{PC}$ = 8.3 Hz, C8), 141.5 (d, $^2J_{PC}$ = 8.8 Hz, C9), 134.7 (d, $^1J_{PC}$ = 51.1 Hz, C3), 132.2 (d, $^2J_{PC}$ = 10.3 Hz, *o*-Ph), 132.2 (d, $^4J_{PC}$ = 3.1 Hz, *p*-Ph), 129.9 (d, $^3J_{PC}$ = 10.8 Hz, *m*-Ph), 129.8 (d, $^1J_{PC}$ = 53.6 Hz, *ipso*-Ph), 126.6 (s, C5), 126.4 (s, C6), 124.9 (s, C7), 122.2 (s, C4), 88.8 (s, Cp), 41.3 (d, $^3J_{PC}$ = 12.4 Hz, C1). $^{31}P\{^1H\}$-NMR ($CDCl_3$): δ 45.5 (s). IR (KBr, cm^{-1}): υ_{CO} 2044, 1998.

Synthesis of carbonyl(η^5-cyclopentadienyl)iodo(η^1-3-diphenyphosphinoindene)iron(II) (4.11).

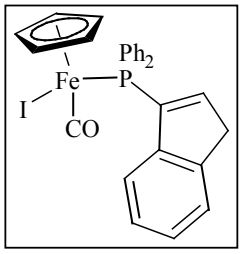

To a solution of 3-diphenylphosphinoindene (**4.1**) (1.70 g, 5.66 mmol) in tetrahydrofuran (200 mL) was added $CpFe(CO)_2I$ (1.80 g, 5.66 mmol). The solution was stirred at ambient temperature for 7 days to yield a green coloured solution. The solvent was removed in vacuo to leave green powder that was shown to contain, by ^{31}P-NMR spectroscopy, both **4.1** and **4.11**. The residue was loaded onto a Celite column and washed with methanol. Removal of the solvent *in vacuo* yielded 1.68 g (52%) of **4.11** as a green solid.

^{1}H-NMR ($CDCl_3$): δ 7.77-7.12 (m, 14H, H4-7 & Ph-H), 6.75 (d, 1H, H2), 4.48 (s, 5H, C_5H_5), 3.63 (s, 2H, H1). $^{13}C\{^1H\}$-NMR ($CDCl_3$): δ 220.7 (d, $^2J_{PC}$ = 30 Hz, CO), 147.1

(d, $^{2}J_{PC}$ = 9 Hz, C2), 144.1 (d, $^{3}J_{PC}$ = 7 Hz, C8), 141.4 (d, $^{2}J_{PC}$ = 8 Hz, C9), 134.1 (d, $^{1}J_{PC}$ = 47 Hz, C3), 133.8 (d, $^{2}J_{PC}$ = 10 Hz, *o*-Ph), 133.3 (d, $^{2}J_{PC}$ = 9 Hz, *o*-Ph), 130.3 (d, $^{4}J_{PC}$ = 2 Hz, *p*-Ph), 130.2 (d, $^{4}J_{PC}$ = 2 Hz, *p*-Ph), 128.4 (d, $^{1}J_{PC}$ = 49 Hz, *ipso*-Ph), 128.2 (d, $^{3}J_{PC}$ = 10 Hz, *m*-Ph), 128.1 (d, $^{3}J_{PC}$ = 10 Hz, *m*-Ph), 126.3 (C5), 125.4 (C6), 124.0 (C7), 123.6 (C4), 82.7 (d, $^{2}J_{PC}$ = 1 Hz, Cp), 39.7 (d, $^{3}J_{PC}$ = 11 Hz, C1). $^{31}P\{^{1}H\}$-NMR ($CDCl_3$): δ 51.5 (s). IR (KBr, cm^{-1}): υ_{CO} 1952.

Synthesis of dicarbonyl(η^5-cyclopentadienyl)(η^1-1-diphenylphosphinoindenylthallium)iron(II) iodide (4.12).

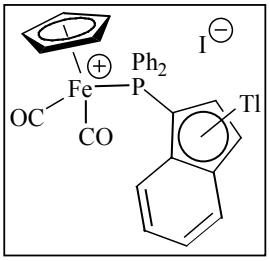

To a solution of 3-diphenylphosphinoindene (**4.1**) (0.459 g, 1.53 mmol) in tetrahydrofuran (25 mL) at –80 °C was added thallium ethoxide (0.11 mL). The solution was allowed to warm to ambient temperature and the reaction mixture was stirred for 2 h. To this mixture was added a solution of $CpFe(CO)_2I$ (0.465 g, 1.53 mmol) in tetrahydrofuran (15 mL). The resulting blue solution was stirred for 1 h. The solution was filtered and the solvent removed in vacuo to leave a dark brown powder.

^{1}H-NMR (C_6D_6): δ 8.18 – 6.57 (m, 16H, H2-7 & Ph), 3.88 (s, 5H, C_5H_5). $^{31}P\{^{1}H\}$-NMR (C_6D_6): δ 34.22. IR (KBr, cm^{-1}): υ_{CO} 2032, 1990. Anal. Calc. for $C_{28}H_{21}FeIO_2PTl$: C, 41.64; H, 2.62. Found: C, 41.32; H, 2.50.

CHAPTER 5

Synthesis of *rac*-bis(1-diphenyphosphinoindenyl)iron(II) diborane (5.2).

To a solution of *rac*-bis(1-diphenylphosphinoindenyl)iron(II) (**5.1**) (0.51 g, 0.81 mmol) in tetrahydrofuran (30 mL) was added a solution of borane dimethylsulfide complex (1.1 mL, 2 M diethyl ether, 2.2 mmol). The reaction mixture was stirred at ambient temperature for 12 h. The mixture was filtered through Celite and the solvent removed *in vacuo* to leave a brown residue. Chromatography of the residue on Silica gel yielded 0.46 g (83%) of **5.2** as a brown powder.

^{1}H-NMR ($CDCl_3$): δ 7.64-6.42 (m, 28H, H4-7 and Ph), 5.81 (d, $^{3}J_{HH}$ = 2.4 Hz, 2H, H3), 3.42 (t, $^{3}J_{HH}$ = 2.4 Hz, 2H, H2), 1.65 (br s, 6H, BH_3). $^{13}C\{^{1}H\}$-NMR ($CDCl_3$): δ 135.4 (d, $^{2}J_{PC}$ = 21 Hz, *o*-Ph), 132.4 (d, $^{2}J_{PC}$ = 20 Hz, *o*-Ph), 131.2 (d, $^{4}J_{PC}$ = 2 Hz, *p*-Ph), 131.0 (d, $^{1}J_{PC}$ = 58 Hz, *ipso*-Ph), 130.8 (d, $^{4}J_{PC}$ = 3 Hz, *p*-Ph), 129.9 (d, $^{1}J_{PC}$ = 60 Hz, *ipso*-Ph), 128.5 (d, $^{3}J_{PC}$ = 6 Hz, *m*-Ph), 128.4 (d, $^{3}J_{PC}$ = 6 Hz, *m*-Ph), 125.7 (s, C7), 124.0 (s, C4), 123.3 (s, C5), 123.2 (s, C6), 91.0 (d, $^{3}J_{PC}$ = 7 Hz, C9), 89.3 (d, $^{2}J_{PC}$ = 13 Hz, C8), 73.5 (d, $^{2}J_{PC}$ = 4 Hz, C2), 68.3 (d, $^{3}J_{PC}$ = 5 Hz, C3), 62.0 (d, $^{1}J_{PC}$ = 64 Hz, C1). $^{31}P\{^{1}H\}$-NMR ($CDCl_3$): δ 16.53 (br s). Anal. Calcd. For $C_{42}H_{38}B_2P_2Fe$: C, 73.95; H, 5.62. Found: C, 72.00; H, 5.64.

Synthesis of *rac*-bis(1-diphenylphosphinoindenyl)iron(II)(*cis*-dichloro-palladium(II)) (5.3).

To a solution of *rac*-bis(1-diphenylphosphinoindenyl)iron(II) (**5.1**) (0.191 g, 0.29 mmol) in tetrahydrofuran (50 mL) was added bis(benzonitrile)dichloropalladium(II) (0.122 g, 0.29 mmol). After stirring at ambient temperature for 4 h, the solvent was removed *in vacuo*. The resulting brown residue was dissolved in dichloromethane (30 mL) and filtered through Celite. The Celite was washed with a further 20 mL of dichloromethane. The volume was reduced to 15 mL, and 25 mL of diethyl ether was added. The flask was placed in a freezer, and the crystals that grew were collected by filtration to yield 0.177 g (73%) of **5.3** as brown crystals.

^{1}H-NMR ($CDCl_3$): δ 8.12-6.75 (m, 28H, H4-7 & Ph), 4.70 (s, 2H, H3), 2.53 (s, 2H, H2). $^{13}C\{^{1}H\}$-NMR ($CDCl_3$): δ 135.8 (t, $^{1}J_{PC}$ = 6 Hz, *ipso*-Ph), 135.3 (t, $^{1}J_{PC}$ = 5 Hz, *ipso*-Ph), 132.6 (s, *o*-Ph), 131.2 (s, *o*-Ph), 129.4-127.9 (m, C4, C7, *m*-Ph & *p*-Ph), 126.5 (s, C5), 124.9 (s, C6), 90.2 (s, C9), 86.9 (t, $^{2}J_{PC}$ = 5 Hz, C8), 80.4 (s, C2), 70.7 (d, $^{1}J_{PC}$ = 8 Hz, C1), 66.7 (s, C3). $^{31}P\{^{1}H\}$-NMR ($CDCl_3$): δ 35.79. Mass spectrum (EI, *m/z* (%)): 831 (4, M^+), 705 (81, $[(PPh_2C_9H_7)_2Pd]^+$). Anal. Calc. for $C_{42}H_{32}Cl_2P_2FePd$: C, 60.64; H, 3.88. Found: C, 59.12; H, 4.35.

Synthesis of *rac*-bis(1-diphenylphosphinoindenyl)iron(II)(*cis*-dichloro-platinum(II)) (5.4).

To a solution of *rac*-bis(1-diphenylphosphinoindenyl)iron(II) (**5.1**) (0.196 g, 0.30 mmol) in tetrahydrofuran (50 mL) was added bis(benzonitrile)dichloroplatinum(II) (0.141 g, 0.30 mmol). After stirring overnight at ambient temperature, the solvent was removed *in vacuo*. The resulting brown residue was dissolved in dichloromethane (10 mL) and filtered through a Celite column. Washing of the Celite with a further 30 mL of dichloromethane produced a light brown solution that was reduced in volume to 10 mL. To this solution was added 20 mL of diethyl ether to induce precipitation. The flask was then placed in a freezer and left overnight to ensure maximum yield. The brown precipitate that formed was filtered to yield 0.217 g (79%) of **5.4**. Crystals suitable for X-ray structural analysis were grown by vapour diffusion of diethyl ether into a dichloromethane solution of **5.4**.

^{1}H-NMR ($CDCl_3$): δ 8.04 (m, 4H, *o*-Ph), 7.65 (d, $^{3}J_{HH}$ = 8 Hz, 2H, H7), 7.57 (d, $^{3}J_{HH}$ = 8 Hz, 2H, H4), 7.53 (m, 4H, *o*-Ph), 7.37 (t, $^{3}J_{HH}$ = 7 Hz, 2H, *p*-Ph), 7.32 (t, $^{3}J_{HH}$ = 7 Hz, 2H, *p*-Ph), 7.26-7.21 (m, 8H, *m*-Ph), 6.94 (t, $^{3}J_{HH}$ = 8 Hz, 2H, H6), 6.65 (t, $^{3}J_{HH}$ = 8 Hz, 2H, H5), 4.62 (d, $^{3}J_{HH}$ = 2 Hz, 2H, H3), 2.42 (d, $^{3}J_{HH}$ = 2 Hz, 2H, H2). ^{13}C{^{1}H}-NMR ($CDCl_3$): δ 135.7 (t, $^{1}J_{PC}$ = 6 Hz, *ipso*-Ph), 135.0 (t, $^{1}J_{PC}$ = 5 Hz, *ipso*-Ph), 131.3 (s, *o*-Ph), 130.9 (s, *o*-Ph), 129.8 (s, C7), 128.2 (s, C4), 127.9-127.5 (m, *m*-Ph & *p*-Ph), 126.2 (s, C5), 124.9 (s, C6), 89.9 (s, C9), 86.2 (t, $^{2}J_{PC}$ = 5 Hz, C8), 81.4 (s, C2), 71.1 (d, $^{1}J_{PC}$ = 68 Hz, C1), 66.3 (s, C3). ^{31}P{^{1}H}-NMR ($CDCl_3$): δ 12.65 (J_{PtP} =3818 Hz). CV (CH_2Cl_2): $E_{1/2}$ = 248 mV, ΔE_P = 75 mV. Mass spectrum (EI, *m/z* (%)): 884 (100, $[(PPh_2C_9H_6)_2FePtCl]^+$), 830 (54, $[(PPh_2C_9H_7)_2PtCl]^+$). Anal. Calc. for $C_{42}H_{32}Cl_2P_2FePt$: C, 54.80; H, 3.50. Found: C, 54.24; H, 3.52.

Synthesis of [bis(diphenylphosphinoindenyl)iron(II)(cyclooctadiene)rhodium(I)] tetraphenylborate (5.5).

To a solution of *rac*-bis(1-diphenylphosphinoindenyl)iron(II) (**5.1**) (0.477 g, 0.73 mmol) in dichloromethane (25 mL) was added a solution of $[Rh(COD)_2]BF_4$ (0.148 g, 0.36 mmol) in dichloromethane (15 mL). The resulting solution was stirred at ambient temperature for 3 h. The solvent was removed *in vacuo* to leave a brown powder. The

crude product was dissolved in dichloromethane (5 mL) and to this was added a solution of $NaBPh_4$ (0.137 g, 0.40 mmol) in dichloromethane. Diethyl ether was added to induce precipitation. The yellow precipitate was collected by filtration to yield 0.529 g (84%) of **5.5**.

^{1}H-NMR ($CDCl_3$): δ 7.73-6.80 (m, 48H, H4-7 & Ph), 4.96 (s, 2H, H3), 4.37 (m, 4H, COD-*CH*), 2.81 (s, 2H, H2), 2.56 (m, 8H, COD-CH_2). ^{13}C{^{1}H}-NMR (Acetone-d_6): δ 134.2 (m, *ipso*-Ph), 132.7 (m, *ipso*-Ph), 130.7 (s, *o*-Ph), 130.2 (s, *o*-Ph), 128.2 (s, *p*-Ph), 127.8-127.1 (m, C4&7, *m*-Ph and COD-*CH*), 124.9 (s, C5 or 6), 124.3 (s, C5 or 6), 102.4 (m, C8 or 9), 97.5 (m, C8 or 9), 90.7 (d, $^1J_{PC}$ = 3 Hz, C1), 80.1 (s, C2), 67.4 (t, $^3J_{PC}$ = 3 Hz, C3), 30.1 (s, COD-CH_2). ^{31}P{^{1}H}-NMR ($CDCl_3$): δ 29.1 (d, $^1J_{PRh}$ = 150 Hz). Mass spectrum (EI, *m/z* (%)): 865 (100, M^+), 511 (20, $[(PPh_2C_9H_7)Rh(COD)]^+$). Anal. Calc. for $C_{74}H_{64}P_2BFeRh$: C, 75.02; H, 5.44. Found: C, 74.40; H, 5.70.

Attempted synthesis of *rac*-bis(1-diphenylphosphinoindenyl)iron(II) dichloronickel(II) (5.6).

To a solution of *rac*-bis(1-diphenylphosphinoindenyl)iron(II) (**5.1**) (0.284 g, 0.43 mmol) in THF (50 mL) was added bis(triphenylphosphine)dichloronickel(II) (0.284 g, 0.43 mmol). After stirring overnight at ambient temperature, the solvent was removed *in vacuo*. The resulting red residue was dissolved in dichloromethane (10 mL) and filtered through a Celite column. Washing of the Celite with a further 30 mL of dichloromethane produced a brown solution, which was reduced in volume to 10 mL. To this solution was added 20 mL of diethyl ether. The flask was then placed in a freezer, and the brown precipitate that formed was filtered. Due to the presence of paramagnetic material, it was not possible to obtain an assignable NMR spectrum of the brown powder. Mass spectrometry did not conclusively show the presence of **5.6**. Crystals suitable for X-ray structural analysis were grown by vapour diffusion of diethyl ether into a dichloromethane solution of the brown powder. The crystals analysed to be bis(1-diphenylphosphinoindene)(*trans*-dichloronickel(II)) (**5.7**), and not **5.6**.

Synthesis of bis(3-diphenylphosphinoindene)dichloronickel(II) (5.8).

To a hot solution of 3-diphenylphosphinoindene (1.27 g, 4.2 mmol) in tetrahydrofuran (50 mL) was added anhydrous nickel chloride (0.27 g, 2.1 mmol). The resulting mixture was stirred for 1 h, in which time a red precipitate formed. The precipitate was filtered to yield 1.14 g (74%) of **5.8**. **5.8** is insoluble in all common solvents tried. IR (KBr, cm^{-1}) 1433, 1379, 1271, 1097, 777, 764, 721, 696, 556, 511, 490, 347, 322, 316, 305, 289, 246, 237. Anal. Calc. for $C_{42}H_{34}Cl_2P_2Ni$: C, 69.08; H, 4.69. Found: C, 70.06; H, 4.93. Solid-state magnetic moment (Gouy method): μ_{eff} = 3.01 B.M.

Cross-coupling of *n-/sec*-butylmagnesium chloride with bromobenzene in the presence of 5.3.

Grignard Preparation: To a suspension of activated magnesium turnings (1.28 g) in tetrahydrofuran (30 mL) was added, dropwise, a solution of chlorobutane (5.50 mL, 52.7 mmol) in tetrahydrofuran (60 mL). After initiation, the mixture was refluxed until the magnesium was consumed. The solution was cooled to ambient temperature and the concentration verified by titration.

Cross-Coupling: To a solution of bromobenzene (4 mmol) and Pd catalyst (0.5-5 mol%) in tetrahydrofuran (50 mL) at –80°C was added *n*-butylmagnesium chloride (8 mmol). The reaction mixture was allowed to warm to ambient temperature and stirred for a given period of time (1-18 h). The reaction mixture was quenched with 10% HCl, and an appropriate internal standard was added to the organic layer, which was analysed by GC. The organic layer and aqueous phase washings were combined, washed with saturated $NaHCO_3$ solution, water, and then dried over $MgSO_4$. The solvent was evaporated and the resulting oil analysed by ^{1}H- and $^{13}C\{^{1}H\}$-NMR spectroscopy. Results are summarized in Table 2.1.

Table 2.1. Cross-Coupling of (*n*-/*sec*-)Butylmagnesium Chloride with Bromobenzene in tetrahydrofuran.

				Yields, %[a]		
catalyst	conc.[b]	chloride	time, h	*sec*-BuPh	*n*-BuPh	other[c]
$(Ph_3P)_2PdCl_2$	1	*n*-BuCl	16	34	49	5
5.3	0.5	*n*-BuCl	18	24	34	24
5.3	1	*n*-BuCl	17	27	45	7
5.3	0.5	*sec*-BuCl	1	11	4	81
5.3	1	*sec*-BuCl	1	18	7	63
5.3	5	*sec*-BuCl	2	48	26	5
5.3	1	*sec*-BuCl	18	47	28	8

[a] Yield determined by GC using an internal standard. [b] Concentration in mol% of Pd. [c] Recovered bromobenzene. When the yields of the coupled products were low compared with consumed bromobenzene, benzene was detected by GC.

Attempted synthesis of 1-indenyl-2,6-diphenylbenzene (5.9) via Stille Coupling.

To a solution of iodo-2,6-diphenylbenzene (1.42 g, 4.0 mmol) and tributyl(indenyl)tin (2.5 g, 6.2 mmol) in tetrahydrofuran (50 mL) was added $Pd(PhCN)_2Cl_2$ (76.7 mg, 0.2 mmol), copper(I) iodide (0.305 g, 1.6 mmol), and triphenylarsine (0.245 g, 0.8 mmol). The resulting brown solution was heated to reflux for 41 h. The solution was poured onto water and extracted with petroleum ether (2 x 50 mL). The organic layer was washed with water (2 x 50 mL), dried over $MgSO_4$, filtered, and the solvent removed *in vacuo* to leave an orange oily residue. Analysis of the ^{1}H-NMR spectrum shows predominantly iodo-2,6-diphenylbenzene, with trace amounts of unidentified products.

Attempted Synthesis of 1-indenyl-2,6-diphenylbenzene (5.9) via a Zn mediated reaction.

To a solution of indene (0.79 mL, 6.8 mmol) in tetrahydrofuran (50 mL) at –80°C was added a solution of *n*-BuLi (4.23 mL, 1.6 M, 6.8 mmol). The solution was allowed to warm to ambient temperature and stirred for 1 h. The solution was then added dropwise to a suspension of anhydrous $ZnCl_2$ (0.924 g, 6.8 mmol) in tetrahydrofuran

(40 mL) at 0°C, and the resulting solution stirred for 1 h at ambient temperature. To this solution was added dropwise a solution of iodo-2,6-diphenylbenzene (2.41 g, 6.8 mmol) and $Pd(PPh_3)_4$ (94 mg, 0.08 mmol, 1.2 mol%) in tetrahydrofuran (70 mL). The reaction vessel was heated to 95°C for 33 h. The mixture was cooled to ambient temperature and the reaction was quenched with saturated aqueous NH_4Cl (100 mL). The mixture was extracted with petroleum ether (3 x 75 mL), dried with $MgSO_4$, and concentrated to a red-brown oil. Analysis of the ^{1}H-NMR spectrum shows predominantly iodo-2,6-diphenylbenzene, with trace amounts of unidentified products.

Synthesis of 1- and 3-phenylindene (5.10).

To a solution of iodobenzene (1.43 g, 7 mmol) and tributyl(indenyl)tin (4.28 g, 11 mmol) in tetrahydrofuran (50 mL) was added $Pd(PhCN)_2Cl_2$ (0.125 g, 0.35 mmol), copper(I) iodide (0.525 g, 2.8 mmol), and triphenylarsine (0.425 g, 1.4 mmol). The resulting brown solution was heated to reflux for 46 h. The solution was poured onto water and extracted with petroleum ether (2 x 40 mL). The organic layer was washed with water (2 x 60 mL), dried over $MgSO_4$, filtered, and the solvent removed in vacuo to leave an orange oily residue. The crude product was chromatographed (silica, petroleum ether) to yield 0.52 g (39%) of **5.10** as a mixture of double bond isomers. ^{1}H-NMR spectrum consistent with literature.[12]

Synthesis of 2-(indenyl)biphenyl (5.11).

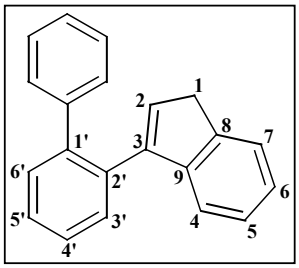

To a solution of 2-iodobiphenyl (2.652 g, 9.5 mmol) and tributyl(indenyl)tin (4.86 g, 12 mmol) in tetrahydrofuran (50 mL) was added $Pd(PhCN)_2Cl_2$ (170 mg, 0.50 mmol), copper(I) iodide (1.5 g, 8 mmol), and triphenylarsine (1.2 g, 4.0 mmol). The resulting brown solution was heated to reflux for 38 h. The solution was poured onto water and extracted with petroleum ether (2 x 60 mL). The organic layer was washed with water (2 x 50 mL), dried over $MgSO_4$, filtered, and the solvent removed *in vacuo* to leave an orange oily residue. The crude product was

chromatographed (silica, petroleum ether) to yield 1.292 g (51%) of **5.11** as a 2:1 mixture of 2-(inden-3-yl)biphenyl and 2-(inden-1-yl)biphenyl.

2-(Inden-3-yl)biphenyl: ^{1}H-NMR ($CDCl_3$): δ 7.49-7.15 (m, 13H, aromatic), 6.82 (t, $^{3}J_{HH}$ = 2 Hz, H2), 3.55 (d, $^{3}J_{HH}$ = 2 Hz, H1). ^{13}C-NMR ($CDCl_3$): δ 145.0 (C9), 144.5 (C8), 143.9, 141.6, 141.3 (C1', C2', *ipso*-Ph), 133.7 (C3), 133.0 (C2,), 129.1 (*o*-Ph), 127.7 (*m*-Ph), 126.6 (*p*-Ph), 125.6 (C5), 124.4 (C6), 123.6 (C7), 120.5 (C4), 38.3 (C1). Unassigned resonances at 130.4, 129.9, 128.6, 127.1 correspond to C3', C4', C5', & C6'.

2-(Inden-1-yl)biphenyl: ^{1}H-NMR ($CDCl_3$): δ 7.49-7.15 (m, 13H, aromatic), 6.86 (m, 1H, H3), 6.54 (m, 1H, H2), 4.22 (1H, H1).

Mass spectrum: (EI, *m/z* (%)): 268 (79, M^+), 152 (28, $C_{12}H_8^+$), 115 (7, $C_9H_7^+$), 77 (16, $C_6H_5^+$). HR-MS: M^+ Calc., 268.12520; Found, 268.12508.

References

1. Grimmer, N.E.; Coville, N.J.; de Koning, C.B.; Smith, J.M.; Cook L.M. *J. Organomet. Chem*. **2000**, *616*, 112.
2. Ready, T.E.; Chien, J.C.W.; Rausch, M.D. *J. Organomet. Chem*. **1999**, *583*, 11.
3. Halterman, R.L.; Fahey, D.R.; Bailly, E.F.; Dockter, D.W.; Stenzel, O.; Shipman, J.L.; Khan, M.A.; Dechert, S.; Schumann, H. *Organometallics* **2000**, *19*, 5464.
4. Ready, T.E.; Chien, J.C.W.; Rausch, M.D. *J. Organomet. Chem*. **1996**, *519*, 21.
5. Fallis, K.A.; Anderson, G.K.; Rath, N.P. *Organometallics* **1992**, *11*, 885.
6. (a) Rerek, M.E.; Ji, L.; Basolo, F. *J. Chem. Soc., Chem, Commun*. **1983**, 1208. (b) Rakita, P.E.; Davison, A. *J. Organomet. Chem*. **1970**, *23*, 407.
7. (a) Curnow, O.J.; Fern, G.M.; Hamilton, M.L.; Zahl, A.; van Eldik, R. *Organometallics* **2004**, *23*, 906. (b) Curnow, O.J.; Fern, G.M.; Hamilton, M.L.; Jenkins, E.M. *J. Organomet. Chem*. **2004**, *689*, 1897.
8. Edlund, U. *Org. Magn. Reson*. **1978**, *11*, 516.
9. Treichel, P.M.; Johnson, J.W.; Wagner, K.P. *J. Organomet. Chem*. **1975**, *88*, 227.

10. Treichel, P.M.; Johnson, J.W.; Calabrese, J.C. *J. Organomet. Chem*. **1975**, *88*, 215.
11. Adams, J.J.; Berry, D.E.; Browning, J.; Burth, D.; Curnow, O.J. *J. Organomet. Chem*. **1999**, *580*, 245.
12. Greifenstein, L.G.; Lambert, J.B.; Nienhuis, R.J.; Fried, H.E.; Paganini, G.A. *J. Org. Chem*. **1981**, *46*, 5125.

Chapter 3

Chapter 3: Ferrocenes containing substituted indenyl ligands

3.1. Introduction

The synthesis of ferrocene in 1951 heralded a new era in organometallic chemistry.[1] Since this initial synthesis, extensive studies have been carried out on the use of cyclopentadienyl ligands in the preparation of ferrocenes.[2] In contrast, the use of the indenyl anion as a six electron donor ligand in the formation of ferrocenes has attracted considerably less attention, despite diindenyliron(II) being first synthesised just two years after ferrocene.[3] In recent years, however, the use of the indenyl ligand as an alternative to the cyclopentadienyl ligand has increased due to the recognition of enhanced reactivity of the $[(C_9H_7)M]$ fragment when compared with the $[(C_5H_5)M]$ fragment in substitution reactions.[4]

The enhanced reactivity of indenyl-metal complexes has been demonstrated most convincingly in ligand exchange reactions.[5] The driving force responsible for these processes is the ability of the indenyl group to undergo a slippage from the η^5- to η^3-coordination that is favoured by the generation of the aromaticity in the fused benzene ring. For bis(indenyl)iron(II) complexes, the presence of a six-membered aromatic ring enables them to undergo reactions not observed for ferrocene. Sutherland et al. demonstrated that diindenyliron(II) undergoes an intramolecular ligand exchange reaction upon treatment with $BF_3{\cdot}Et_2O$ to yield the cationic arene complex $[(\eta^5$-indenyl)$(\eta^6$-indene)Fe$]PF_6$.[6] Similarly, $[(\eta^5$-indenyl)$(\eta^6$-indene)Fe$]PF_6$ was prepared by the stereospecific protonation of diindenyliron(II).[7] The haptotropic shift responsible for this rearrangement is believed to pass through an η^3 intermediate (Figure 3.1).[8] The six-membered aromatic ring has also been shown to exhibit butadiene-like characteristics, with Wang and co-workers reporting the Diels-Alder addition of benzyne to the six-membered rings of substituted bis(indenyl)iron(II) complexes.[9]

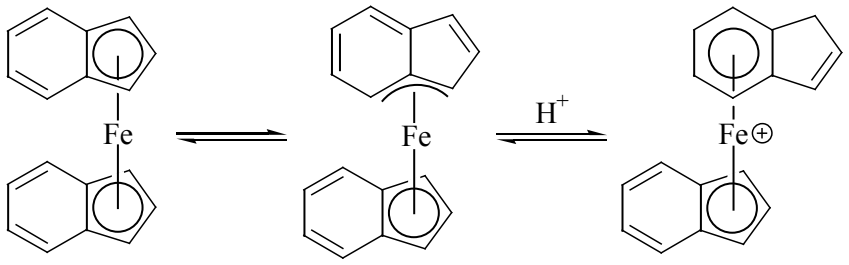

Figure 3.1. Haptotropic rearrangement of diindenyliron(II).

The success of the cyclopentadienyl ligand in organometallic chemistry arises from its ability to stabilize a range of metal oxidation states and the relative ease with which both steric and electronic properties can be altered by the introduction of substituents. For ferrocenes, the effects of substitution on the cyclopentadienyl ligand can be observed at the iron centre using electrochemistry and UV/Visible spectroscopy. While the influence of different substituents on the electrochemistry of cyclopentadienyl-based ferrocenes has been extensively studied,[10] few reports have been made concerning bis(indenyl)iron(II) complexes.[11]

This chapter describes the preparation of a variety of substituted indene ligands, and the use of these ligands in the preparation of bis(indenyl)iron(II) complexes. The electrochemistry and electronic absorption spectroscopy of the complexes will be discussed.

3.2. Indene Synthesis

The synthesis of multi-substituted indenes may be approached via several synthetic routes. Many of these reactions involve the formation of the five-membered ring as a last step from a substituted benzene precursor, followed by reduction to form the indene (Scheme 3.1). Mono-substitution of indenes at the 1- or 3- position is easily accomplished by salt elimination/metathesis reactions.

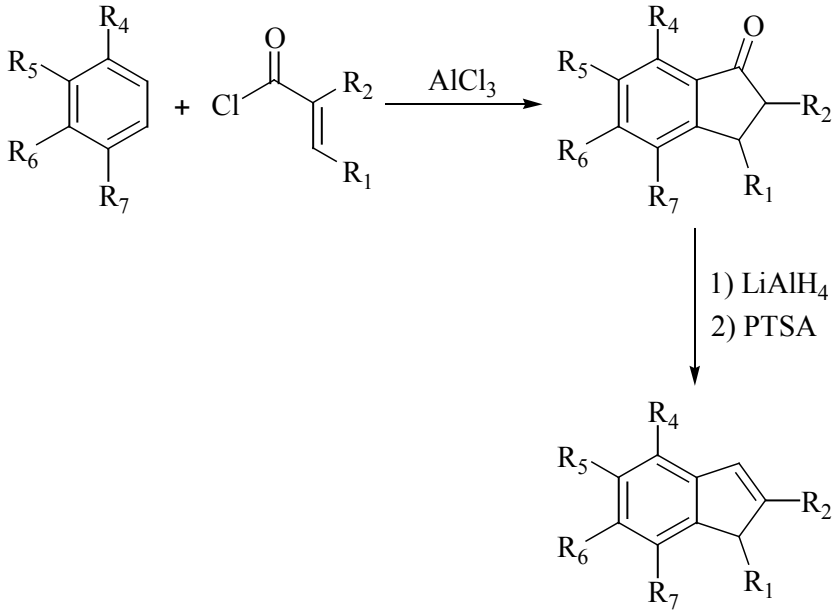

Scheme 3.1. Synthesis of multi-substituted indenes.

Potential indenyl ligand precursors **3.2**, **3.4** – **3.9**, **3.13**, and **3.15** – **3.18** were synthesised by modifications of literature procedures. Indenes **3.10** – **3.12** and **3.14** were prepared elsewhere and used as received.[12,13] Figure 3.2 illustrates the indenes used in this thesis.

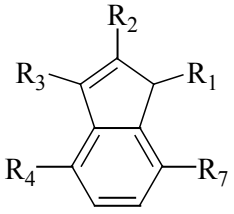

	R_1	R_2	R_3	$R_{4/7}$		R_1	R_2	R_3	$R_{4/7}$
3.1	H	H	H	H	**3.10**	H	$SiMe_3$	H	H
3.2	Me	H	H	H	**3.11**	$SiMe_3$	$SiMe_3$	H	H
3.3	H	Me	H	H	**3.12**	$SiMe_3$	H	$SiMe_3$	H
3.4	Me	Me	H	H	**3.13**	H	H	PPh_2	H
3.5	Me	H	Me	H	**3.14**	H	Me	PPh_2	H
3.6	H	H	H	Me	**3.15**	PPh_2	H	Me	H
3.7	Me	H	H	Me	**3.16**	PPh_2	Me	Me	H
3.8	Me	H	Me	Me	**3.17**	PPh_2	Me	Me	Me
3.9	$SiMe_3$	H	H	H	**3.18**	$SiMe_3$	H	PPh_2	H

Figure 3.2. Substituted-indenes used in this thesis.

1-Methylindene (**3.2**) was synthesised by the reaction of indenyllithium with iodomethane in diethyl ether, as shown in Scheme 3.2, following the method of Coville et al.[14] The indene was isolated as the allylic isomer in good yield (78%) as a colourless oil. The choice of solvent used in these substitution reactions has been found to dictate which isomer is isolated. The use of diethyl ether (or hexane) as the solvent favours the formation of the allylic isomer whereas the use of THF favours the formation of the vinylic isomer due to the solvent stabilization of the transition state ion-pair.[15]

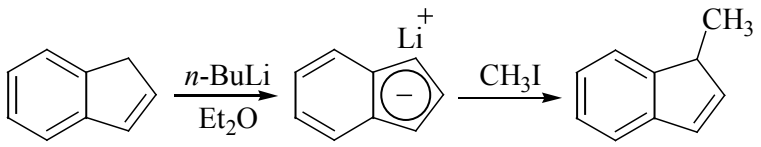

3.1 **3.2**

Scheme 3.2. Synthesis of 3.2.

1,2-Dimethylindene (**3.4**) has previously been synthesised by the reduction of 2,3-dimethylindan-1-one to 2,3-dimethylindan-1-ol, with subsequent dehydration using *p*-toluenesulfonic acid.[16] Using this procedure, **3.4** was isolated in a yield of 57%. A one-pot synthesis of **3.4** was carried out by the reaction of 2-methylindenyllithium with iodomethane in diethyl ether, as shown in Scheme 3.3. Indene **3.4** was isolated in moderate yield (65%) as a colourless oil. The vinylic isomer, 2,3-dimethylindene, has been prepared by Yarboro et al. by the reaction of 2-methylindan-1-one with MeMgI, with subsequent dehydration by oxalic acid.[17]

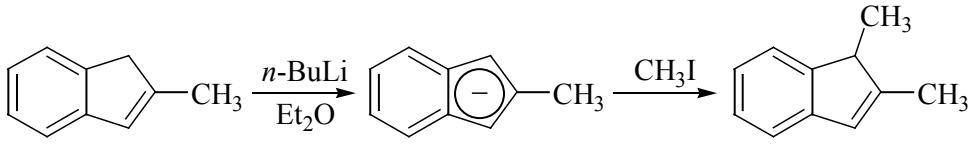

3.3 **3.4**

Scheme 3.3. Synthesis of 3.4.

1,3-Dimethylindene (**3.5**) has previously been prepared by two published procedures: Rausch et al. prepared **3.5** by the reaction of 3-methylindan-1-one with methyllithium, with subsequent dehydration of the resulting 1,3-dimethylindan-1-ol.[16] Alternatively, **3.5** was synthesised by the reaction of 1-methylindenyllithium with iodomethane in diethyl ether, as shown in Scheme 3.4.[18] The indene was prepared via the latter method and was isolated in moderate yield (69%) as a colourless oil.

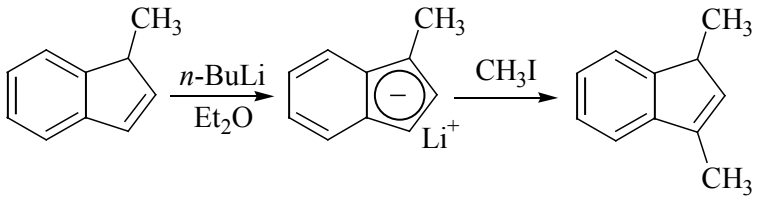

3.5

Scheme 3.4. Synthesis of 3.5.

4,7-Dimethylindene (**3.6**) was synthesised using the procedure of Halterman et al., which involves the base-catalysed cyclocondensation of cyclopentadienylsodium with 2,5-hexanedione in methanol, as shown in Scheme 3.5.[19] The indene was isolated in moderate yield (63%) as a colourless oil.

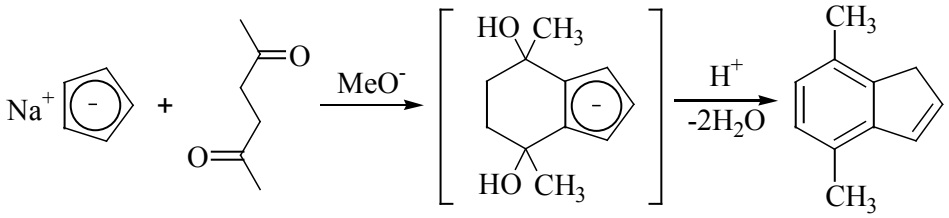

3.6

Scheme 3.5. Synthesis of 3.6.

1,4,7-Trimethylindene (**3.7**) was synthesised by the reaction of 4,7-dimethylindenyllithium with iodomethane in diethyl ether, as shown in Scheme 3.6. The indene was isolated in moderate yield (65%) as a colourless oil. The ^{1}H-NMR of **3.7** is consistent with the formation of the allylic isomer illustrated, with a multiplet observed at 3.60 ppm corresponding to H1 in addition to two doublet of doublets at 6.50 and 6.89 ppm for H2 and H3, respectively. The resonances for the methyl

protons are observed at 1.37 and 2.45 ppm for C1-CH_3 and C4/7-CH_3, respectively. The synthesis of 3,4,7-trimethylindene has previously been reported.[20]

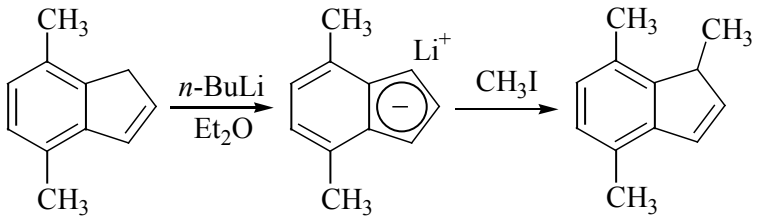

3.7

Scheme 3.6. Synthesis of 3.7.

1,3,4,7-Tetramethylindene (**3.8**) has previously been synthesised by the reaction of 3,4,7-trimethylindan-1-one with methyl lithium, with subsequent dehydration using *p*-toluenesulfonic acid.[16] Using this procedure, Rausch et al. isolated **3.8** in a yield of 56%. Indene **3.8** was instead synthesised by the reaction of 1,4,7-trimethylindenyllithium with iodomethane in diethyl ether, as shown in Scheme 3.7, and isolated in moderate yield (63%) as a colourless oil.

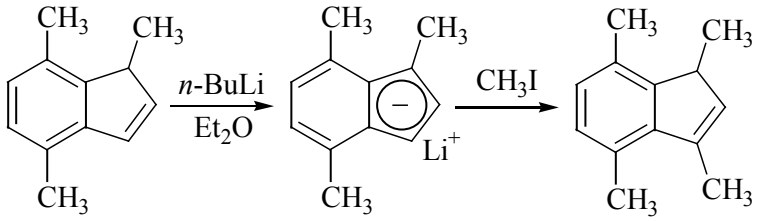

3.8

Scheme 3.7. Synthesis of 3.8.

1-Trimethylsilylindene (**3.9**) was synthesised by the reaction of indenyllithium with chlorotrimethylsilane in diethyl ether, as shown in Scheme 3.8, following the method of Rausch et al.[21] The indene was isolated in good yield (78%) as a colourless oil. As with indene **3.2**, the allylic isomer of **3.9** was produced.

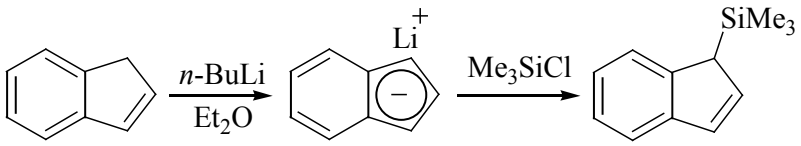

3.9

Scheme 3.8. Synthesis of 3.9.

3-Diphenylphosphinoindene (**3.13**) was synthesised by the reaction of chlorodiphenylphosphine with indenyllithium as shown in Scheme 3.9, following the method of Anderson et al..[22] The passage of the reaction mixture through a column of alumina ensured the thermodynamically favoured vinylic isomer of **3.13** was isolated. The product was isolated in excellent yield (92%) as a white powder. The different isomers are readily distinguished from one another by their ^{31}P-NMR chemical shift: The allylic and vinylic isomers of **3.13** resonate at –4.30 and –22.26 ppm, respectively.

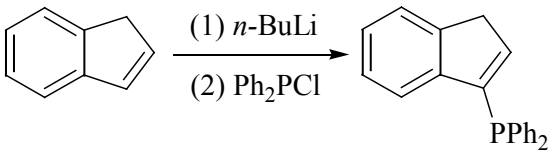

3.13

Scheme 3.9. Synthesis of 3.13.

1-Diphenylphosphino-3-methylindene (**3.15**) can potentially be synthesised by two methods, which differ only in the order with which the two substituents are added to the indenyl fragment. The addition of iodomethane to a diethyl ether solution of 1-diphenylphosphinoindenyllithium produced a complex mixture of products. In contrast, the addition of chlorodiphenylphosphine to 1-methylindenyllithium produced **3.15** in excellent yield (90%) as a white, air-sensitive powder. Interestingly, the passage of a diethyl ether solution of **3.15** through a column of alumina did not result in isomerization from the allylic to the vinylic isomer. The ^{1}H-NMR spectrum of **3.15** consists of an aromatic multiplet centred at 7.26 ppm and three singlets at 2.11, 4.48, and 6.12 ppm for the methyl group protons, H1, and H2 respectively. The resonances for H1 and H2 are upfield of those observed for the allylic isomer of **3.13**,

due to the shielding influence of the methyl group. The $^{31}P\{^{1}H\}$-NMR spectrum of **3.15** consists of a singlet at –4.98 ppm.

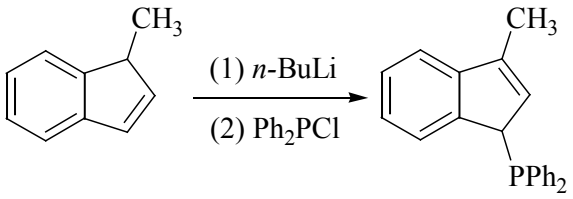

3.15

Scheme 3.10. Synthesis of 3.15.

1-Diphenylphosphino-2,3-dimethylindene (**3.16**) was synthesised by the reaction of 1,2-dimethylindenyllithium with chlorodiphenylphosphine in diethyl ether, as shown in Scheme 3.11. The product, **3.16**, was isolated in excellent yield (91%) as an air-sensitive white powder. As with **3.15**, the isomer containing the allylic phosphine was isolated, with no isomerization to the vinylic phosphine observed. The ^{1}H-NMR spectrum of **3.16** consists of an aromatic multiplet centred at 7.10 ppm, and singlets at 1.89, 1.98, and 4.33 ppm corresponding to the two methyl groups and H1, respectively. The downfield of the methyl resonances is assigned to C2-CH_3 on the basis of previous studies.[16] The resonance for H1 is upfield of those observed for allylic **3.13** and **3.15**. The $^{31}P\{^{1}H\}$-NMR spectrum of **3.16** consists of a singlet at 1.76 ppm, downfield of the resonances observed for **3.15** and allylic **3.13**.

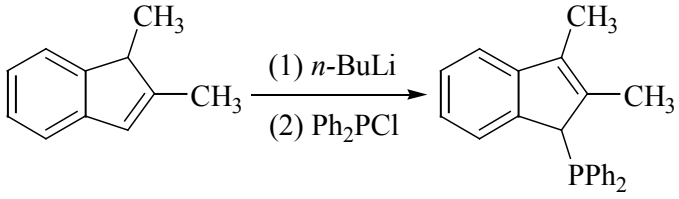

3.16

Scheme 3.11. Synthesis of 3.16.

1-Diphenylphosphino-3,4,7-trimethylindene (**3.17**) was synthesised by the reaction of 1,4,7-trimethylindenyllithium with chlorodiphenylphosphine in diethyl ether, as shown in Scheme 3.12. The indene was isolated in moderate yield (62%) as a

white, air-sensitive powder. The ^{1}H-NMR spectrum is consistent with the formation of the isomer containing the allylic phosphine, with an aromatic multiplet centred at 7.21 ppm and two singlets at 4.44 and 6.08 ppm corresponding to H1 and H2 respectively. The methyl groups resonate at 1.96, 2.27, and 2.61 ppm, corresponding to C3-CH_3, C7-CH_3, and C4-CH_3 respectively. The $^{31}P\{^{1}H\}$-NMR spectrum consists of a singlet at –1.71 ppm.

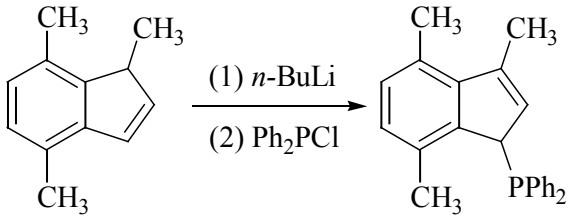

3.17

Scheme 3.12. Synthesis of 3.17.

1-Trimethysilyl-3-diphenylphosphinoindene (**3.18**) was synthesised by the reaction of 1-diphenylphosphinoindenyllithium with chlorotrimethylsilane in diethyl ether as shown in Scheme 3.13. The indene was isolated in good yield (76%) as a white powder. The ^{1}H-NMR of **3.18** is consistent with the formation of the isomer containing the vinylic phosphine. An aromatic multiplet is observed at 7.30 ppm in addition to resonances at 3.61 and 6.39 ppm corresponding to H1 and H2, respectively. The resonance for H2 is upfield of that observed in **3.9**, a result of the shielding influence of the phosphine. The protons of the trimethylsilyl group resonate at –0.52 ppm. The $^{31}P\{^{1}H\}$-NMR spectrum of **3.18** consists of a singlet at –21.54 ppm.

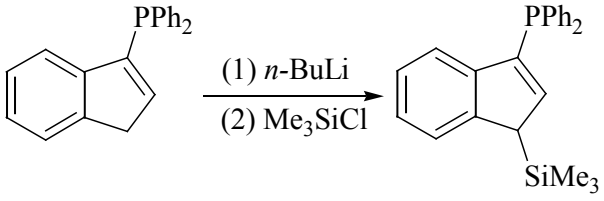

3.18

Scheme 3.13. Synthesis of 3.18.

Bis(3-(diphenylphosphino)-inden-1-yl)dimethylsilane (**3.19**) was synthesised by the reaction of two equivalents of 1-diphenylphosphinoindenyllithium with dichlorodimethylsilane in diethyl ether as shown in Scheme 3.14. The indene was isolated in good yield (83%) as a red/orange powder. The product was obtained as a mixture of *meso* and *racemic* diastereomers. The diastereomers of **3.19** are readily distinguished from one another upon examination of their ^{1}H-NMR spectrum. The *meso* isomer contains a single mirror plane and exhibits C_s symmetry. This symmetry renders the methyl groups bonded to the silicon non-equivalent and gives rise to two singlets in the ^{1}H-NMR spectrum at –0.07 and –0.43ppm. In contrast, the *racemic* isomer exhibits C_2 symmetry that renders the methyl groups equivalent. A single CH_3 resonance is observed for ***rac*-3.19** in the ^{1}H-NMR spectrum at –0.32ppm. The resonances for the H1 protons of ***meso-*** and ***rac*-3.19** occur at 3.67 and 3.74 ppm respectively, with the H2 protons resonating at 6.24 and 6.41 ppm. The $^{31}P\{^{1}H\}$-NMR spectrum of **3.19** consists two singlets at –21.47 and –21.52 ppm corresponding to ***rac*-3.19** and ***meso*-3.19** respectively.

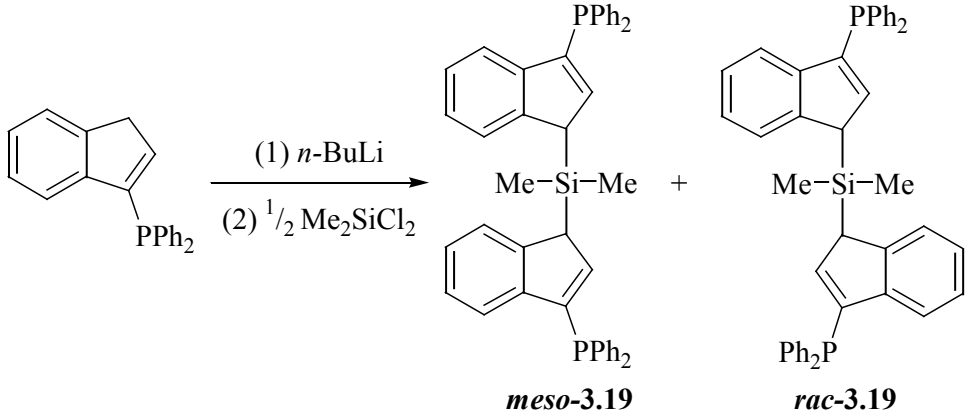

Scheme 3.14. Synthesis of 3.19.

3.3. Ferrocenes of methyl-substituted indenyl ligands

3.3.1. Diindenyliron(II) (3.20)

In 1953, Fischer and Seus reported the synthesis of diindenyliron(II) (**3.20**) by the reaction of ferric chloride with indenylmagnesium bromide.[3a] An alternative synthesis using indenyllithium and ferric chloride was reported soon afterwards by Pauson and Wilkinson.[3b] In both instances, an excess of the organometallic reagent was used to facilitate the reduction of the Fe(III). An improved synthesis was developed by King et al. in which indenylsodium was treated with ferrous chloride.[23] The rigorous exclusion of oxygen was seen as the key to obtaining high yields due to the ease with which **3.20** is oxidised in polar solvents.[24] Instead of using these procedures, **3.20** was synthesised by the reaction of indenyllithium (readily prepared *in situ* by the treatment of indene with *n*-BuLi) with anhydrous ferrous chloride in tetrahydrofuran as shown in Scheme 3.15. The ferrocene **3.20** was produced in good yield (70%) as a black powder and was purified by vacuum sublimation. The ^{1}H-NMR spectrum of **3.20** is consistent with that previously reported, a broad singlet at 6.80 ppm corresponding to the protons of the benzo-ring and two singlets at 3.89 and 4.48 ppm corresponding to H2 and H1/3, respectively.

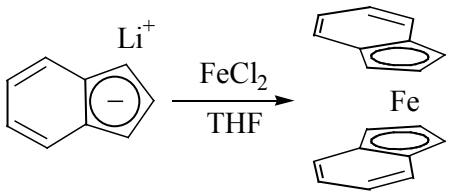

3.20

Scheme 3.15. Synthesis of 3.20.

3.3.2. Di(1-methylindenyl)iron(II) (3.21)

Di(1-methylindenyl)iron(II) (**3.21**) has previously been synthesised by the reaction of 1-methylindenyllithium with ferrous chloride (formed *in situ* by the treatment of ferric chloride with iron powder).[11a] In an analogous manner, 1-methylindenyllithium reacts with anhydrous ferrous chloride in tetrahydrofuran to form **3.21** in modest yield (45%) as a dark blue solid (Scheme 3.16). The ferrocene **3.21** was isolated as a 1:1 mixture of *racemic* and *meso* diastereomers.

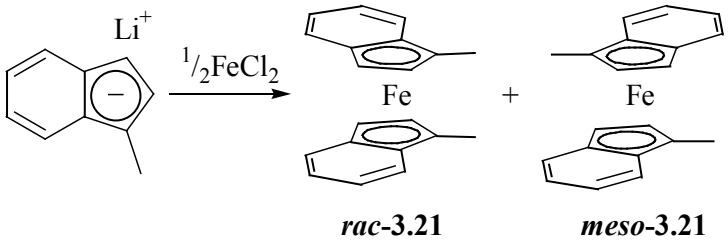

***rac*-3.21** ***meso*-3.21**

Scheme 3.16. Synthesis of 3.21.

The presence of the diastereomers is readily observed upon examination of the NMR spectra of **3.21**. The ^{1}H-NMR spectrum of **3.21** contains four resonances in the region associated with the cyclopentadienyl protons. The resonances for the H2 protons appear as overlapping singlets at 3.74 and 3.77 ppm while the H3 protons resonate at 4.25 and 4.31 ppm. While the observation of these four resonances establishes the presence of *racemic* and *meso* diastereomers, it is not possible to unambiguously assign individual signals to a particular diastereomer. The addition of a methyl group to the 1-position of the indenyl ligands induces an upfield in the resonances of both H2 and H3 relative to **3.20**. However, the magnitude of these shifts is dependent on the particular diastereomer formed. This observed difference in shielding indicates both the relative orientation of the indenyl ligands and inter-ring shielding effects are influencing the chemical shifts of H2 and H3. Schumann et al. have demonstrated that protons lying in a position over top of the benzo-ring of an indenyl ligand are shielded to a greater degree than those orientated away from the indenyl ligand.[19,25] This phenomenon has previously been observed in the related (1-$MeC_9H_6)_2ZrCl_2$, with significant differences observed in the H2 and H3 resonances of *racemic* and *meso* diastereomers.[14] The relatively minor difference observed in the chemical shifts of the diastereotopic H2 protons are an indication that the small size of the methyl group is not overtly influencing the relative orientation of the indenyl ligands, with the indenyl ligands of both diastereomers most likely adopting a π-offset conformation similar to that observed for **3.20**. The methyl group protons of the two diastereomers resonate at 1.81 and 1.97 ppm.

3.3.3. Di(2-methylindenyl)iron(II) (3.22)

Di(2-methylindenyl)iron(II) (**3.22**) was synthesised by the reaction of 2-methylindenyllithium with anhydrous ferrous chloride in tetrahydrofuran as shown in Scheme 3.17. The ferrocene was isolated in a modest yield (36%) as a dark red crystalline solid. The homotopic nature of the 2-methylindenyl ligand precludes the formation of *racemic* and *meso* diastereomers.

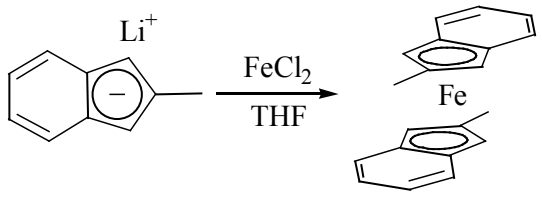

3.22

Scheme 3.17. Synthesis of 3.22.

The C_{2v}-symmetry of the ferrocene greatly simplifies the ^{1}H-NMR spectrum of **3.22**: The protons of the benzo-ring appear as two multiplets centred at 6.85 and 7.00 ppm for H5/6 and H4/7, respectively, whereas H1/3 resonates at 4.22 ppm. The shielding effect of the methyl group is clearly evidenced in **3.22**, with an upfield shift in the resonance of H1/3 when compared with **3.20**. The methyl group protons of **3.22** resonate at 1.73 ppm, upfield of the methyl resonances observed for both diastereomers of **3.21**. The assignment of the ^{1}H-NMR spectrum of **3.22** is in agreement with that recently published by Wang et al..[9]

Crystals of **3.22** suitable for single crystal X-ray structure analysis were obtained from a diethyl ether solution of **3.22**. The molecular structure of **3.22** is shown in Figure 3.3. Selected bond lengths (Å) and angles (°) are listed in Table 3.1.

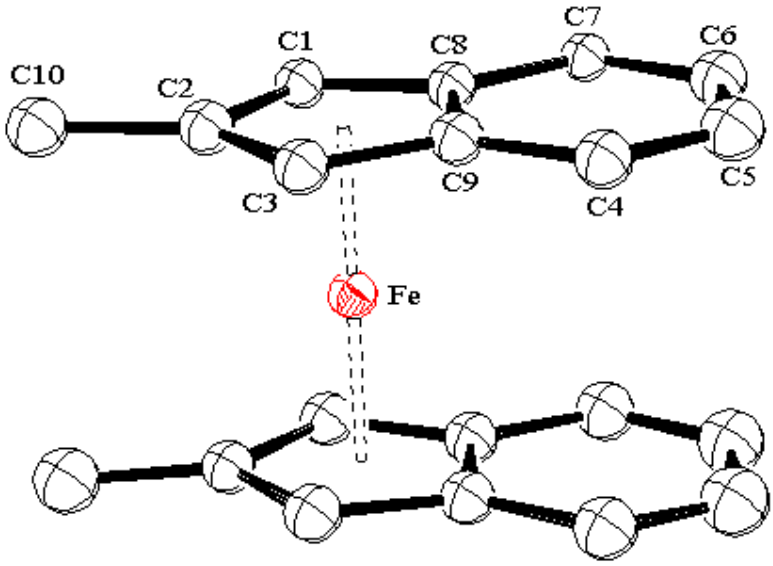

Figure 3.3. ORTEP of 3.22 indicating the numbering of the atoms. The thermal ellipsoids have been drawn at 50% probability.

Table 3.1. Selected bond lengths [Å] and angles [°] 3.22.

Fe-C1	2.050(4)	C1A-C8A	1.442(5)	C1-C2-C3	108.4(3)
Fe-C1A	2.069(4)	C2-C3	1.434(5)	C1A-C2A-C3A	108.0(3)
Fe-C2	2.063(4)	C2A-C3A	1.438(5)	C2-C3-C9	108.5(3)
Fe-C2A	2.061(3)	C3-C9	1.425(5)	C2A-C3A-C9A	108.4(3)
Fe-C3	2.066(4)	C3A-C9A	1.428(5)	C1-C8-C9	107.2(3)
Fe-C3A	2.042(4)	C8-C9	1.456(5)	C1A-C8A-C9A	107.6(3)
Fe-C8	2.092(3)	C8A-C9A	1.449(5)	C3-C9-C8	107.6(3)
Fe-C8A	2.112(4)	C2-C10	1.508(5)	C3A-C9A-C8A	107.7(3)
Fe-C9	2.103(4)	C2A-C10A	1.504(5)	C1-C2-C10	125.8(3)
Fe-C9A	2.101(4)	C10-C2-Fe	129.4(3)	C1A-C2A-C10A	125.9(4)
C1-C2	1.421(5)	C10A-C2A-Fe	130.0(3)	C3-C2-C10	125.6(3)
C1A-C2A	1.427(5)	C2-C1-C8	108.1(3)	C3A-C2A-C10A	125.9(4)
C1-C8	1.446(5)	C2A-C1A-C8A	108.2(3)		

Complex **3.22** crystallises in the tetragonal space group $P4_32_12$, with one complete molecule being in the asymmetric unit. The indenyl ligands are coordinated to the iron atom via their five-membered rings in a distorted η^5-fashion. The ten Fe-carbon bond lengths fall between 2.042 and 2.112 Å, with the distances between the iron atom and the bridgehead carbons (C8 and C9) being, on average, 0.043 Å longer than those of the other carbon atoms in the five-membered rings. The average carbon-carbon bond length within the five-membered rings is 1.437 Å. The methyl groups are bonded to C2 and C2A at a distance of 1.508 and 1.504 Å respectively. The benzo rings of the indenyl ligands lie over top of one another in an eclipsed fashion. The methyl groups adopt, with respect to each other, a synperiplanar conformation with a C2-CNT-CNT'-C2' torsion angle of 3.3°. The eclipsed nature of the 2-methylindenyl ligands indicates that there are minimal steric interactions between the methyl groups, with C10 and C10A being displaced out of the C_5 ring planes by only 0.130 and 0.157 Å respectively. The related (+)-bis(2-menthylindenyl)iron(II), which has the same substitution pattern but with bulkier substituents, adopts an "anticlinical staggered" conformation (C2-CNT-CNT'-C2' torsion angle of 134°) due to intramolecular steric interactions of the terpene moieties with the indenyl ring.[25] Examination of the extended packing diagram of **3.22** reveals the presence of CH–π hydrogen bonding interactions between the methyl group (C10A) and the six-membered benzo ring of an adjacent molecule (Figure 3.4). The carbon C10A is situated over the centre of the benzo ring, with an intermolecular distance of 3.900 Å between C10A and the benzo ring centroid. Short contacts between C–H and π systems have been observed in a large number of organic crystals, with such interactions believed to be a crucial driving force for crystal packing.[26] Studies have shown the interaction of the π–face of benzene and hydrocarbons is generally weak, with the calculated interaction energy of the benzene–methane complex being approximately 30% of the hydrogen bonding energy of the water dimer.[27] A detailed discussion of the solid-state structure of **3.22** and the parameters used to describe the slip-fold distortion of the indenyl ligands upon coordination will be included later in the chapter, along with the other complexes studied by X-ray crystallography.

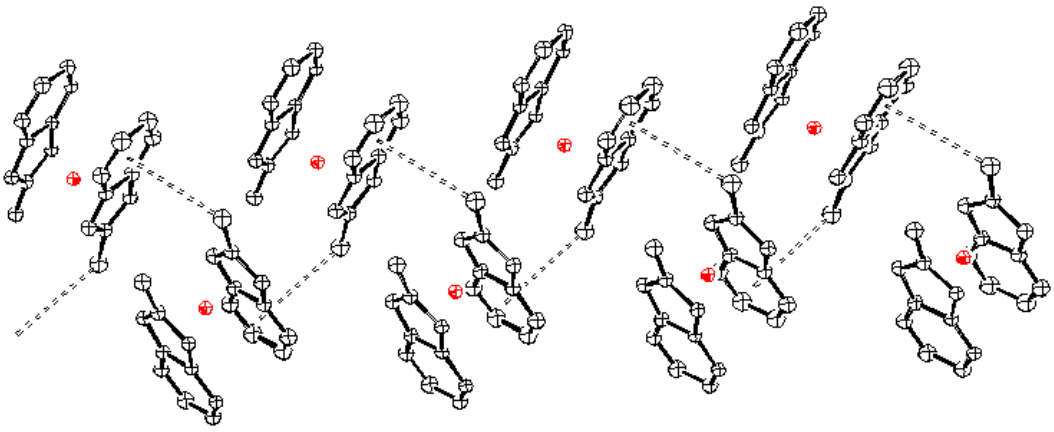

Figure 3.4. Packing diagram of 3.22 showing CH–π hydrogen bonding.

3.3.4. Bis(1,2-dimethylindenyl)iron(II) (3.23)

Bis(1,2-dimethylindenyl)iron(II) (**3.23**) was synthesised by the reaction of 1,2-dimethylindenyllithium with anhydrous ferrous chloride in tetrahydrofuran (Scheme 3.18). The ferrocene **3.23** was isolated in moderate yield (67%) as a green powder and as a 1:1 mixture of *racemic* and *meso* diastereomers.

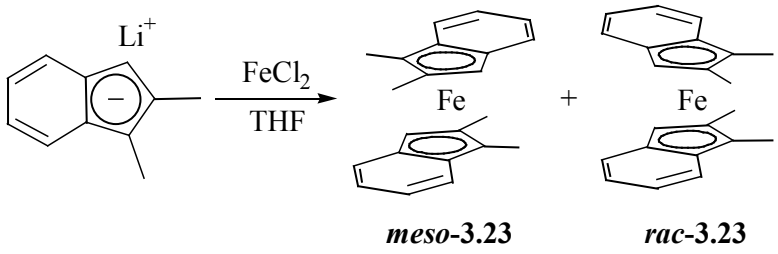

Scheme 3.18. Synthesis of 3.23.

The ^{1}H–NMR spectrum of **3.23** clearly shows the presence of both diastereomers. The H3 protons of the *racemic* and *meso* diastereomers of **3.23** resonate at 3.96 and 4.29 ppm, though it is not possible to unambiguously assign a resonance to a particular diastereomer. Both resonances for the diastereotopic H3 protons are upfield of those observed in **3.20** due to the shielding influence of the methyl groups. However, the separation of the resonances for the H3 protons is considerably greater than that observed for the equivalent protons in **3.21**. This suggests that the relative orientations of the indenyl ligands for the two diastereomers of **3.23** differ more than

the diastereomers of **3.21**. The highly-shielded nature of the H3 proton at 3.96 ppm indicates a conformation in which H3 is positioned close to the benzo ring of the other ligand. The methyl groups of the diastereomers of **3.23** resonate at 1.68, 1.78, 1.79, and 1.95 ppm, with the downfield resonances assigned to the methyl groups in the 1-position of the indenyl ligands.

3.3.5. Bis(1,3-dimethylindenyl)iron(II) (3.24)

Bis(1,3-dimethylindenyl)iron(II) (**3.24**) has previously been synthesised by Treichel et al. by the reaction of 1,3-dimethylindenyllithium with ferrous chloride (formed *in situ* by the reaction of ferric chloride and iron metal).[28] The product was obtained in a yield of 55%. In a similar fashion, the reaction of 1,3-dimethylindenyllithium with anhydrous ferrous chloride in tetrahydrofuran produced **3.24** in moderate yield (59%) as a dark green powder. The homotopic nature of the 1,3-dimethylindenyl ligand precludes the formation of *racemic* and *meso* diastereomers.

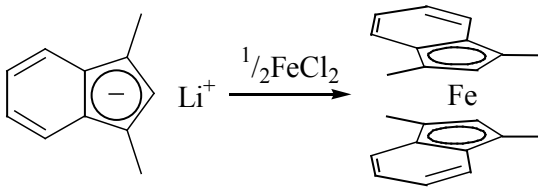

3.24

Scheme 3.19. Synthesis of 3.24.

The ^{1}H–NMR spectrum of **3.24** is consistent with that previously reported. The resonances for the protons of the benzo-ring protons appear at 6.89 ppm while the H2 proton resonates at 3.43 ppm. The presence of the methyl groups in both the 1- and 3-position of the indenyl ligand greatly influences the shielding experienced by H2, with a large upfield shift observed in the chemical shift of H2 relative to both **3.20** and **3.21**. The protons of the methyl groups resonate at 1.94 ppm, similar to the resonances observed for the methyl groups in **3.21**.

3.3.6. Bis(4,7-dimethylindenyl)iron(II) (3.25)

Bis(4,7-dimethylindenyl)iron(II) (**3.25**) was synthesised by the reaction of 4,7-dimethylindenyllithium with anhydrous ferrous chloride in tetrahydrofuran. The ferrocene **3.25** was isolated in good yield (75%) as a purple powder and was purified by recrystallization from diethyl ether. The symmetrical nature of the 4,7-dimethylindenyl ligand precludes the formation of *racemic* and *meso* diastereomers.

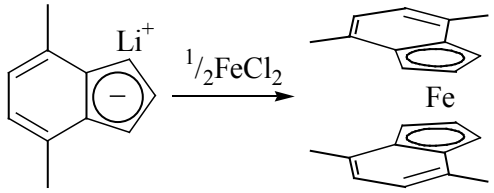

3.25

Scheme 3.20. Synthesis of 3.25.

The ^{1}H–NMR spectrum of **3.25** consists of singlets at 2.13, 4.02, 4.42, and 6.57 ppm corresponding the protons of the methyl groups, H2, H1/3, and H5/6, respectively. The presence of the methyl groups in the 4- and 7-position of the indenyl ligands induces an upfield shift in the resonances of H5/6 with respect to **3.20**. A small upfield shift is also observed for the resonance of H1/3, while there is a downfield shift in the resonance for H2 when compared with **3.20**. The protons of the methyl groups resonate downfield of those previously discussed above.

Crystals of **3.25** suitable for single crystal X-ray structure analysis were obtained from a diethyl ether solution of **3.25**. The molecular structure of **3.25** is shown in Figure 3.5. Selected bond lengths (Å) and angles (°) are listed in Table 3.2.

Table 3.2. Selected bond lengths [Å] and angles [°] for 3.25.

Fe1-C1	2.0510(19)	C7A-C11A	1.507(3)	C1B-C8B	1.421(6)
Fe1-C1A	2.0429(19)	C2-C1-C8	107.87(16)	C1C-C8C	1.447(7)
Fe1-C2	2.039(2)	C2A-C1A-C8A	108.07(18)	C2B-C3B	1.429(6)
Fe1-C2A	2.038(2)	C1-C2-C3	108.67(16)	C2C-C3C	1.432(10)
Fe1-C3	2.048(2)	C1A-C2A-C3A	108.96(18)	C3B-C9B	1.433(7)
Fe1-C3A	2.054(2)	C2-C3-C9	107.91(16)	C3C-C9C	1.426(6)
Fe1-C8	2.090(2)	C2A-C3A-C9A	107.68(18)	C8B-C9B	1.467(9)
Fe1-C8A	2.092(2)	C1-C8-C9	107.93(16)	C8C-C9C	1.478(8)
Fe1-C9	2.0957(18)	C1A-C8A-C9A	107.53(17)	C4B-C10B	1.526(8)
Fe1-C9A	2.0914(19)	C3-C9-C8	107.58(16)	C4C-C20C	1.502(7)
C1-C2	1.428(3)	C3A-C9A-C8A	107.73(17)	C7B-C20B	1.554(7)
C1A-C2A	1.422(3)	Fe2-C1B	2.052(6)	C7C-C11C	1.523(8)
C1-C8	1.429(3)	Fe2-C1C	2.048(4)	C2B-C1B-C8B	108.2(5)
C1A-C8A	1.427(3)	Fe2-C2B	2.039(4)	C2C-C1C-C8C	108.8(4)
C2-C3	1.425(3)	Fe2-C2C	2.041(4)	C1B-C2B-C3B	108.3(4)
C2A-C3A	1.414(3)	Fe2-C3B	2.044(4)	C1C-C2C-C3C	109.1(4)
C3-C9	1.435(2)	Fe2-C3C	2.051(9)	C2B-C3B-C9B	108.7(5)
C3A-C9A	1.437(3)	Fe2-C8B	2.101(4)	C2C-C3C-C9C	107.4(7)
C8-C9	1.444(2)	Fe2-C8C	2.108(7)	C1B-C8B-C9B	108.1(6)
C8A-C9A	1.441(3)	Fe2-C9B	2.110(8)	C1C-C8C-C9C	105.5(5)
C4-C10	1.503(3)	Fe2-C9C	2.097(4)	C3B-C9B-C8B	106.7(6)
C4A-C10A	1.495(3)	C1B-C2B	1.434(7)	C3C-C9C-C8C	109.1(7)
C7-C11	1.504(3)	C1C-C2C	1.429(6)		

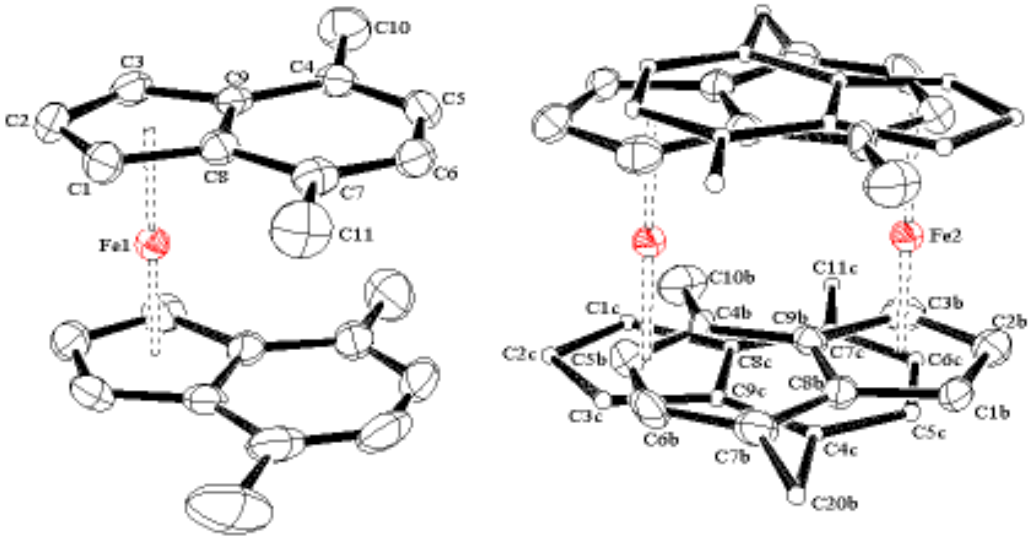

Figure 3.5. ORTEP of 3.25 indicating the numbering of the atoms. The thermal ellipsoids have been drawn at 50% probability.

Ferrocene **3.25** crystallises in the orthorhombic space group Pbca, with one and a half molecules in the asymmetric unit. The half molecule lies on a crystallographic centre of inversion such that the molecule is disordered over this position (Figure 3.5). The two independent molecules are quite similar with respect to molecular dimensions and geometry. The indenyl ligands are coordinated to their respective iron atoms via their five-membered rings in distorted η^5- fashions. The Fe-carbon bond distances vary between 2.038 and 2.110 Å, with the Fe–C8/9 bond lengths being, on average, 0.052 Å longer than those to the remaining carbons of the five-membered rings. For both independent molecules, the benzo rings of the indenyl ligands lie over one another in a π-offset arrangement to maximize π–π-stacking interactions.[29] The C1-CNT-CNT'-C1' torsion angles for the two molecules are 14.5 and 18.3°. The methyl groups are bonded to their respective carbons at an average distance of 1.514 Å and are, on average, displaced out of the plane of the indenyl ligand by 0.081 Å. A comparison of the solid-state structure of **3.25** with other structurally-characterized bis(indenyl)iron(II) complexes will be discussed later in this chapter.

3.3.7. Bis(1,4,7-trimethylindenyl)iron(II) (3.26)

Bis(1,4,7-trimethylindenyl)iron(II) (**3.26**) was synthesised as a 1:1 mixture of *racemic* and *meso* diastereomers by the reaction of 1,4,7-trimethylindenyllithium with anhydrous ferrous chloride in tetrahydrofuran (Scheme 3.21). The ferrocene **3.26** was isolated in good yield (71%) as a purple powder.

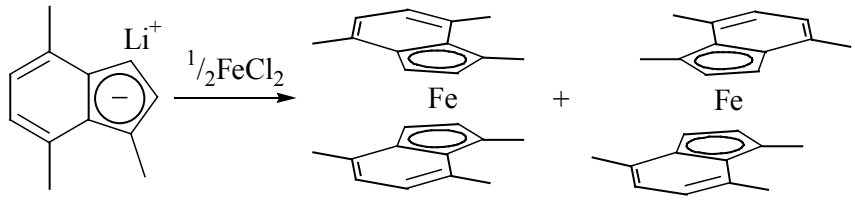

***rac*-3.26** ***meso*-3.26**

Scheme 3.21. Synthesis of 3.26.

The ^{1}H–NMR spectrum of **3.26** is consistent with the formation of *racemic* and *meso* diastereomers. In addition to the aromatic multiplet centred at 6.69 ppm, resonances for the H2 protons occur at 3.97 and 4.03 ppm with the H3 protons resonating at 4.16 and 4.42 ppm. The protons of the methyl groups resonate between 1.83 and 2.43 ppm, with the downfield resonances corresponding to the methyl groups bonded to the benzo ring. The H2 protons resonate in similar positions to those in **3.25**, but are deshielded with respect to **3.20**. The H3 resonance at 4.16 ppm is upfield of the equivalent resonances for **3.20** and **3.25**.

3.3.8. Bis(1,3,4,7-tetramethylindenyl)iron(II) (3.27)

Bis(1,3,4,7-tetramethylindenyl)iron(II) (**3.27**) was synthesised by the reaction of 1,3,4,7-tetramethylindenyllithium with anhydrous ferrous chloride in tetrahydrofuran (Scheme 3.22). The ferrocene **3.27** was isolated in good yield (71%) as a purple powder. The homotopic nature of the 1,3,4,7-tetramethylindenyl ligand precludes the formation of *racemic* and *meso* diastereomers.

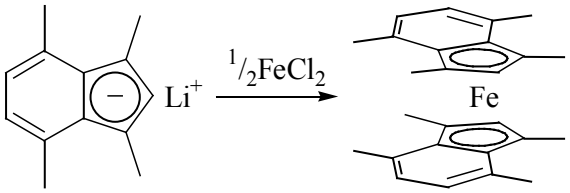

3.27

Scheme 3.22. Synthesis of 3.27.

The ^{1}H-NMR spectrum of **3.27** is greatly simplified due to the symmetrical nature of the ligand, with four resonances observed at 1.94, 2.30, 3.44, and 6.60 ppm corresponding to C1/3-CH_3, C4/7-CH_3, H2, and H5/6, respectively. The resonances for C1/3-CH_3 and H2 are relatively unchanged compared with **3.24**, while the resonance for C4/7-CH_3 is shifted downfield of that observed for **3.25**.

3.4. Ferrocenes of trimethylsilyl-substituted indenyl ligands

3.4.1. Bis(1-trimethylsilylindenyl)iron(II) (3.28)

Bis(1-trimethylsilylindenyl)iron(II) (**3.28**) was synthesised by the reaction of 1-trimethylsilylindenyllithium with anhydrous ferrous chloride in tetrahydrofuran (Scheme 3.23). The ferrocene **3.28** was isolated in good yield (74%) as a dark green oily solid. The product was produced as a mixture of *racemic* and *meso* diastereomers. Unlike the methyl-substituted bis(indenyl)iron(II) complexes previously discussed, the diastereomers of **3.28** were not produced in equal amounts, with a ratio of 1.6:1 observed. The non-statistical distribution of the diastereomers suggests that steric interactions are influencing product formation. Non-statistical distributions of this type have previously been observed in menthyl-functionalised bis(indenyl) complexes of iron and zirconium.[25]

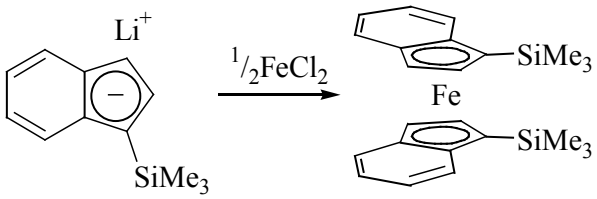

3.28

Scheme 3.23. Synthesis of 3.28.

The ^{1}H-NMR spectrum of **3.28** is consistent with the formation of *racemic* and *meso* diastereomers. The resonances for the H2 and H3 protons of the major isomer occur at 3.99 and 4.94 ppm, respectively, while the equivalent resonances for the minor isomer appear at 3.24 and 4.68 ppm, respectively. The protons of the trimethylsilyl groups resonate at 0.49 and 0.39 ppm for the major and minor isomers, respectively. For the major isomer, a downfield shift is observed for the resonances of both H2 and H3 relative to **3.20**, whereas for the minor isomer, the resonances for H2 and H3 are shifted upfield and downfield, respectively. The upfield shift in the resonance of H2 for the minor isomer of **3.28** indicates that the proton is uniquely positioned compared with the other cyclopentadienyl protons of the diastereomers. The highly-shielded environment of the H2 proton is most probably due to the enforced rotation of the indenyl ligands away from an eclipsed geometry to alleviate adverse steric interactions. A rotation of this magnitude is more likely to occur with the *meso* diastereomer as an eclipsed conformation of the indenyl ligands would bring the bulky trimethylsilyl groups into a sterically-constrained position. The *racemic* diastereomer would not suffer such constraints as the trimethylsilyl groups would be positioned on opposite sides of the molecule, thus minimising steric interactions while maintaining any π–π-stacking interactions (Figure 3.6). The observation of an NOE from the H3 resonance for the major isomer at 4.94 ppm to the trimethylsilyl protons resonance at 0.49 ppm indicates the close proximity of these protons to each other. No such NOE is observed for the H3 resonance at 4.68 ppm. This suggests that the major isomer of **3.28** is in fact the *racemic* diastereomer since the expected eclipsed conformation would bring the H3 protons close in space to the trimethylsilyl group of the other ligand. For the *meso* diastereomer, the H3 protons should be separated to a greater degree from the trimethylsilyl groups. The assignment of the major isomer as ***rac*-3.28** is, however, by no means unambiguous.

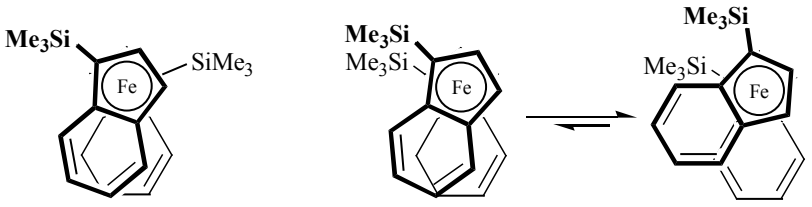

***rac*-3.28** ***meso*-3.28**

Figure 3.6. Likely orientation of indenyl ligands in 3.28.

3.4.2. Bis(2-trimethylsilylindenyl)iron(II) (3.29)

Bis(2-trimethylsilylindenyl)iron(II) (**3.29**) was synthesised by the reaction of 2-trimethylsilylindenyllithium with anhydrous ferrous chloride in tetrahydrofuran (Scheme 3.24). The ferrocene **3.29** was isolated in moderate yield (63%) as a dark blue oily solid. The homotopic nature of the 2-trimethylsilylindenyl ligand precludes the formation of *racemic* and *meso* diastereomers.

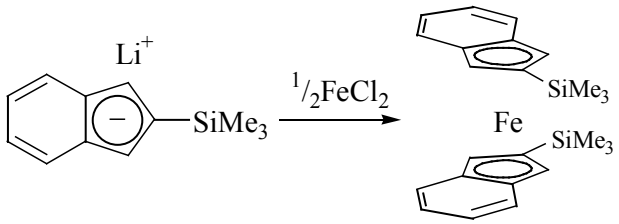

3.29

Scheme 3.24. Synthesis of 3.29.

The ^{1}H-NMR spectrum of **3.29** consists of two multiplets centred at 7.00 and 7.41 ppm for H5/6 and H4/7, respectively, with singlets at 0.36 and 3.89 ppm for the methyl groups and H1/3, respectively. The protons of the benzo rings exhibit an AA'BB' coupling pattern, with three and four bond-coupling of 3 and 9 Hz, respectively. The resonance for H1/3 occurs in an upfield position when compared with the equivalent signals for **3.20** and **3.22**. This increase in shielding being, most probably, a consequence of the rotation of the indenyl ligands away from the eclipsed conformation, with its favourable π–π-stacking interactions, to a conformation in which protons H1/3 are positioned close to the benzo ring of the other ligand (Figure 3.7). This rotation would be necessary to alleviate any steric interactions experienced

by the bulky trimethylsilyl groups. The protons of the trimethylsilyl groups resonate at 0.36 ppm, similar to those observed for the diastereomers of **3.28**.

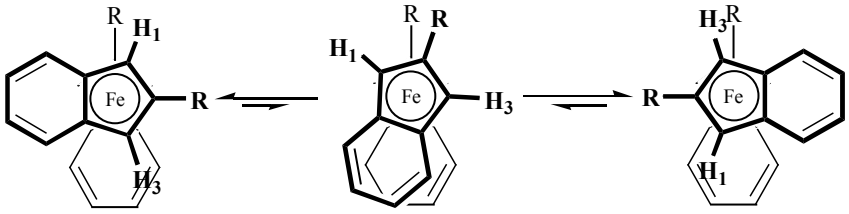

Figure 3.7. Enforced rotation of 3.29.

3.4.3. Bis(1,2-bis(trimethylsilyl)indenyl)iron(II) (3.30)

Bis(1,2-bis(trimethylsilyl)indenyl)iron(II) (**3.30**) was synthesised by the reaction of 1,2-bis(trimethylsilyl)indenyllithium with anhydrous ferrous chloride in tetrahydrofuran (Scheme 3.25). The ferrocene **3.30** was isolated in modest yield (35%) as a green powder. The prochiral nature of the 1,2-bis(trimethylsilyl)indenyl ligand gives rise to the possibility for the formation of *racemic* and *meso* diastereomers. However, in practise only one diastereomer is observed by NMR spectroscopy. The identity of the diastereomer produced is not conclusively known, but due to expected steric interactions, formation of the *meso* isomer is expected to be disfavoured. This suggests that it is the *racemic* diastereomer of **3.30** produced, but this is not without ambiguity.

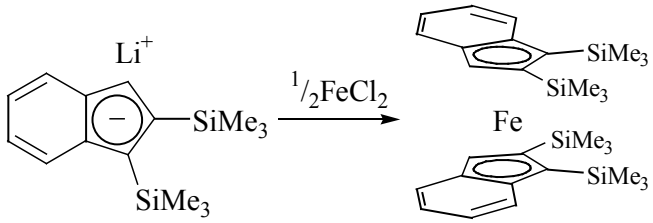

***rac*-3.30**

Scheme 3.25. Synthesis of 3.30.

The ^{1}H-NMR spectrum of **3.30** consists of, in addition to the resonances for the benzo ring protons, singlets at 0.09, 0.62, and 5.15 ppm corresponding to the protons of the trimethylsilyl groups and H3, respectively. The resonance for H3 is downfield

of those previously observed in **3.28** and **3.29**, as is the resonances for one of the trimethylsilyl groups. The resonance for the other trimethylsilyl group is upfield of those previously discussed.

3.4.4. Bis(1,3-bis(trimethylsilyl)indenyl)iron(II) (3.31)

Bis(1,3-bis(trimethylsilyl)indenyl)iron(II) (**3.31**) was synthesised by the reaction of 1,3-bis(trimethylsilyl)indenyllithium with anhydrous ferrous chloride in tetrahydrofuran (Scheme 3.26). The ferrocene **3.31** was isolated in modest yield (39%) as a green oily solid. The homotopic nature of the 1,3-bis(trimethylsilyl)indenyl ligand precludes the formation of *racemic* and *meso* diastereomers.

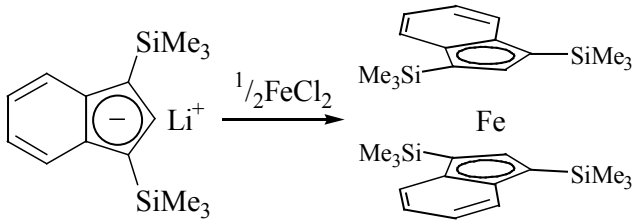

3.31

Scheme 3.26. Synthesis of 3.31.

The ^{1}H-NMR spectrum of **3.31** consists of two multiplets centred at 7.03 and 7.57 ppm corresponding to H5/6 and H4/7 respectively, with singlets at 0.37 and 4.46 ppm for the protons of the trimethylsilyl group and H2, respectively. The benzo ring protons exhibit a similar coupling pattern to that observed in **3.29**; an AA'BB' system with three and four bond couplings of 3 and 9 Hz, respectively. The resonance for H2 is downfield of those previously observed for **3.20** and **3.28**.

Crystals of **3.31** suitable for single crystal X-ray structure analysis were obtained from a petroleum ether solution of **3.31**. The molecular structure of **3.31** is shown in Figure 3.8. Selected bond lengths (Å) and angles (°) are listed in Table 3.3.

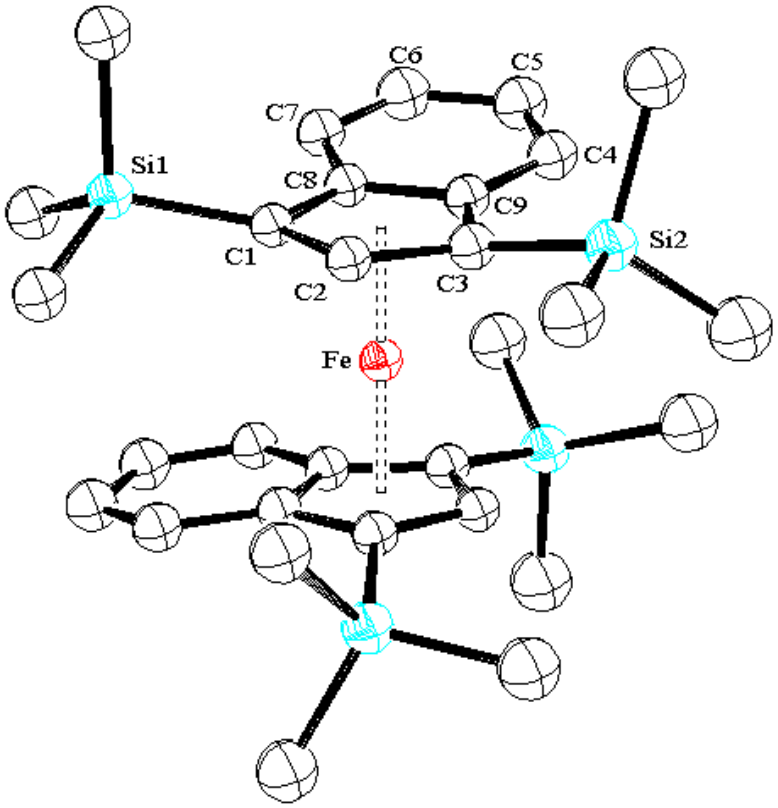

Figure 3.8. ORTEP of 3.31 indicating the numbering of the atoms. The thermal ellipsoids have been drawn at 50% probability.

Table 3.3. Selected bond lengths [Å] and angles [°] for 3.31.

Fe-C1	2.075(3)	Si2A-C3A	1.860(4)	Si2-C3-Fe	139.28(18)
Fe-C1A	2.074(3)	C1-C2	1.435(5)	Si2A-C3A-Fe	136.23(18)
Fe-C2	2.043(3)	C1A-C2A	1.431(5)	C2-C1-C8	105.1(3)
Fe-C2A	2.045(3)	C1-C8	1.449(5)	C2A-C1A-C8A	104.7(3)
Fe-C3	2.080(3)	C1A-C8A	1.462(5)	C1-C2-C3	112.2(3)
Fe-C3A	2.091(3)	C2-C3	1.424(5)	C1A-C2A-C3A	112.3(3)
Fe-C8	2.130(3)	C2A-C3A	1.436(5)	C2-C3-C9	105.0(3)
Fe-C8A	2.123(3)	C3-C9	1.458(5)	C2A-C3A-C9A	105.0(3)
Fe-C9	2.125(3)	C3A-C9A	1.439(5)	C1-C8-C9	108.9(3)
Fe-C9A	2.121(3)	C8-C9	1.434(5)	C1A-C8A-C9A	108.4(3)
Si1-C1	1.859(4)	C8A-C9A	1.438(5)	C3-C9-C8	108.8(3)
Si1A-C1A	1.863(4)	Si1-C1-Fe	139.18(18)	C3A-C9A-C8A	109.6(3)
Si2-C3	1.867(4)	Si1A-C1A-Fe	138.34(18)		

Ferrocene **3.31** crystallizes in the monoclinic space group $P2_1/c$, with one complete molecule being present in the asymmetric unit. The indenyl ligands are coordinated to the iron atom via their five-membered rings in a distorted η^5- fashion. The Fe-carbon bond lengths are generally longer than those previously discussed for **3.22** and **3.25**, with a range of 2.043 – 2.130 Å. The Fe-C2 bond distances are the shortest at an average of 2.044 Å, with the distances between Fe and C1/3 being, on average, 2.080 Å. The Fe-C8/9 bond distances are the longest, with an average bond length of 2.125 Å. The increase in the average Fe-C bond length is a result of the steric interference caused by the bulky trimethylsilyl groups with the benzo rings of the indenyl ligands. In order to accommodate the four bulky substituents, the indenyl rings must rotate away from the favoured π-stacked conformation to one in which a trimethylsilyl group of each ligand is situated over top of the benzo ring of the other ligand (C1-CNT-CNT'-C1' torsion angle of 94.7°). This causes significant steric interactions between the substituent and the benzo ring, resulting in the displacement of both the trimethylsilyl group and benzo ring out of the plane of the C_5 ring. The trimethylsilyl groups are displaced from the C_5 ring plane by an average of 0.38 Å, with a maximum value of 0.41 Å. The conformation seen here for **3.31** is similar to that observed for the related chromium complex $(1,3\text{-}(SiMe_3)_2C_9H_5)_2Cr$:[53] with long Cr-C8/9 bond lengths, a C1-CNT-CNT'-C1' torsion angle of 86.5°, and the trimethylsilyl groups displaced from the C_5 ring plane by an average of 0.31 Å. A comparison of the solid-state structure of **3.31** with other structurally-characterized bis(indenyl)iron(II) complexes will be discussed later in this chapter.

3.5. Ferrocenes of phosphine-substituted indenyl ligands

3.5.1. Bis(1-diphenylphosphinoindenyl)iron(II) (3.32)

Bis(1-diphenylphosphinoindenyl)iron(II) (**3.32**) has previously been synthesized by the reaction of 1-diphenylphosphinoindenyllithium with anhydrous ferrous chloride in tetrahydrofuran (Scheme 3.27).[30] Purification of the crude product by column chromatography (silica gel, cyclohexane/ethylacetate) followed by recrystallisation from toluene produced **3.32** in a modest yield (40%). With the bisplanar chiral nature of the ferrocene, the possibility exists for the formation of

racemic and *meso* diastereomers, though the previous study did not fully comprehend the exact nature of the isomeric mixture.

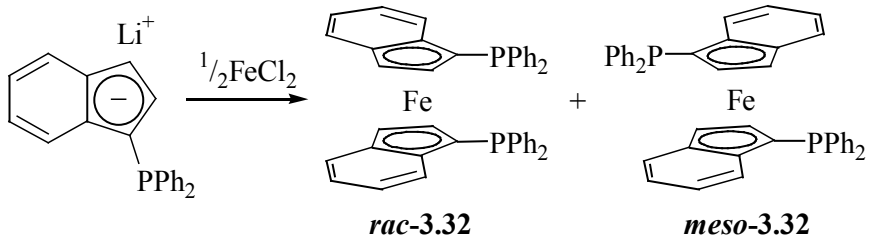

Scheme 3.27. Synthesis of 3.32.

The synthesis of bis(1-diphenylphosphinoindenyl)iron(II) (**3.32**) was performed in a manner analogous to that previously reported. Purification, however, was achieved by loading the crude product onto a Celite column and washing with diethyl ether to remove any unreacted **3.13**. Subsequent washing with dichloromethane produced **3.32** in good yield (64%) as a dark green solid. The isomeric composition of **3.32** was found to be dependent on the length of time with which the reaction is allowed to proceed. The reaction of 1-diphenylphosphinoindenyllithium with ferrous chloride initially produces a 1:1 mixture of two phosphorus-containing compounds as evidenced by peaks in the $^{31}P\{^{1}H\}$-NMR spectrum at –22.26 and –26.53 ppm. If the reaction is allowed to proceed for longer than 12 h, only the compound with the peak at –22.26 ppm is isolated. This compound was shown by X-ray crystallography to be ***rac*-3.32** (see below). If the reaction is terminated after 2 h, the two compounds initially produced can be isolated as a mixture. The identical nature of an elemental analysis performed on the mixture of compounds and a separate analysis performed on ***rac*-3.32** strongly suggests that the second compound is ***meso*-3.32**. The invariance of yield with reaction time suggests a process must be occurring by which ***meso*-3.32** is converting to ***rac*-3.32**. An isomerization of this type would require one of the indenyl ligands of ***meso*-3.32** to flip over and coordinate to the iron atom by the other face (Figure 3.9). The kinetics and mechanism of this isomerization process will be discussed fully in Chapter 4.

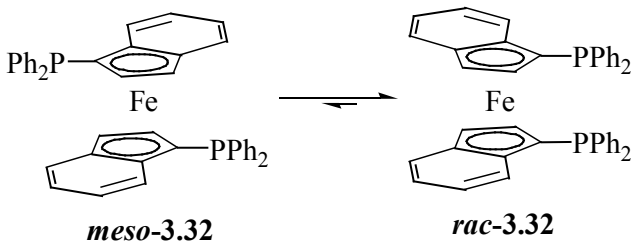

Figure 3.9. Isomerization of *meso*-3.32 to *rac*-3.32.

The ^{1}H-NMR spectrum of ***rac*-3.32** is consistent with that previously reported, with resonances observed for H2 and H3 at 3.07 and 4.92 ppm, respectively. For ***meso*-3.32**, the equivalent resonances occur at 3.48 and 3.81 ppm, respectively. The observed differences in chemical shifts between the diastereomers are a consequence of the differing spatial arrangements of the indenyl ligands. The highly shielded nature of H2 in ***rac*-3.32** indicates the close proximity of the proton to either the benzo or phenyl rings. Similarly, the shielding of H3 in ***meso*-3.32** indicates the ring currents of the benzo or phenyl rings are also affecting this proton.

Crystals of ***rac*-3.32** suitable for single crystal X-ray structure analysis were obtained by vapour diffusion of diethyl ether into a dichloromethane solution of ***rac*-3.32**. The molecular structure of ***rac*-3.32** is shown in Figure 3.10. Selected bond lengths (Å) and angles (°) are listed in Table 3.4.

Table 3.4. Selected bond lengths [Å] and angles [°] for *rac*-3.32.

Fe-C1	2.062(3)	P-C20	1.833(3)	P-C1-Fe	123.18(17)
Fe-C2	2.045(3)	C1-C2	1.446(4)	C2-C1-C8	105.9(3)
Fe-C3	2.067(3)	C1-C8	1.448(4)	C3-C2-C1	110.1(3)
Fe-C8	2.090(3)	C2-C3	1.425(4)	C2-C3-C9	107.4(3)
Fe-C9	2.104(3)	C3-C9	1.432(4)	C1-C8-C9	108.5(3)
P-C1	1.829(3)	C8-C9	1.447(4)	C3-C9-C8	108.2(3)
P-C10	1.850(3)				

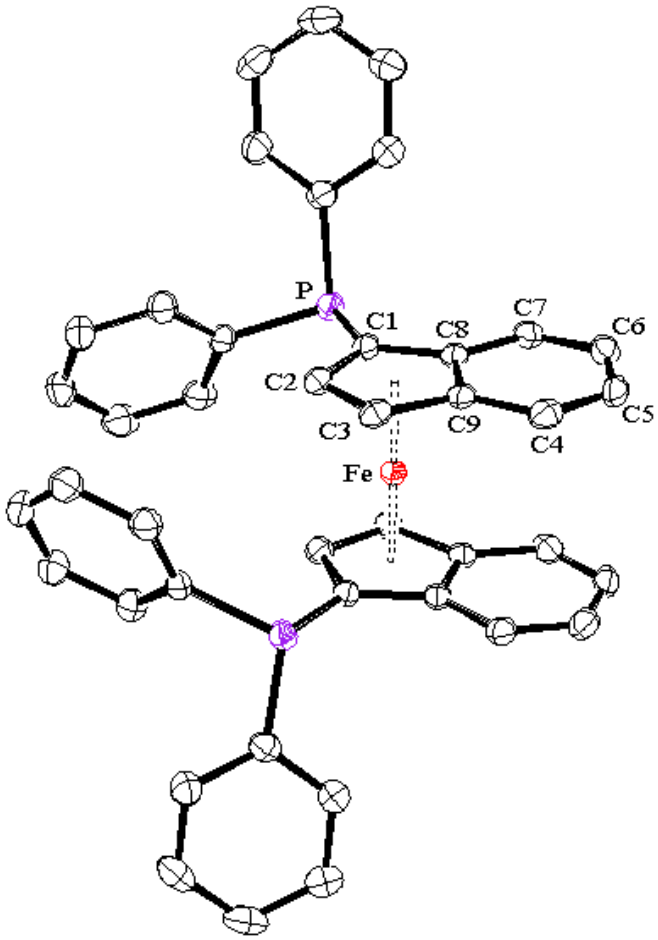

Figure 3.10. ORTEP of *rac*-3.32 indicating the numbering of the atoms. The thermal ellipsoids have been drawn at 50% probability.

Complex ***rac*-3.32** crystallizes in the orthorhombic space group Pbcn, with one half molecule being in the asymmetric unit. Coordination of the indenyl ligands to the iron atom is via their five-membered rings in a η^5- fashion. As with most ferrocenes of this type, the carbons of five-membered ring are not bonded to the iron with equivalent bond lengths. The average bond length between Fe and C1-3 is 2.058 Å whereas the equivalent average bond length for C8 and C9 is 2.097 Å. The benzo rings of the indenyl ligands lie approximately over top of one another in a π-offset arrangement to maximize π–π-stacking interactions.[29] The diphenylphosphino moieties adopt, with respect to each other, an "anticlinical staggered" arrangement with a C1-CNT-CNT'-C1' torsion angle of 123.1°. The conformation of the diphenylphosphino moieties in dppf is antiperiplanar, with the equivalent torsion

angle being 180°.[31] The phenyl rings of the ligands can be seen to sandwich the H2-protons, accounting for the large upfield shift observed for the resonances of H2 in the ^{1}H-NMR spectrum. If the benzo rings of ***rac*-3.32** were π-offset in the other direction by an equal amount, the diphenylphosphino groups would be further apart form each other without increasing the steric interactions between the phenyl groups and the benzo ring of the other ligand. Thus, the conformation of ***rac*-3.32** may be, in part, due to edge-type CH–π hydrogen bonding interactions between the phenyl rings and H2 atoms, with three C···H distances of less than 3.0 Å: two to a phenyl group on the same ligand (C20 and C25) and one to C21 on the other ligand (2.90, 2.69, and 2.98 Å respectively). The geometry around the phosphorus atoms is approximately tetrahedral (the lone pair of electrons counting as the fourth substituent), with angles of 100.87, 101.53, and 102.38° for C1-P-C20, C1-P-C10, and C10-P-C20 respectively. The carbon-phosphorus bond lengths are 1.829, 1.833, and 1.849 Å for C1, C20, and C10 respectively. The phenyl ring containing C10 is positioned above the plane of the indenyl ligand, with an angle between the C_5 ring plane and the plane defined by C1-P-C10 of 91.6°. The other phenyl ring is below the plane of the indenyl ligand, with the C_5 ring plane and C1-P-C20 plane bisecting at an angle of 13.9° (Figure 3.11). A comparison of the solid-state structure of ***rac*-3.32** with other structurally-characterized bis(indenyl)iron(II) complexes will be discussed later in this chapter.

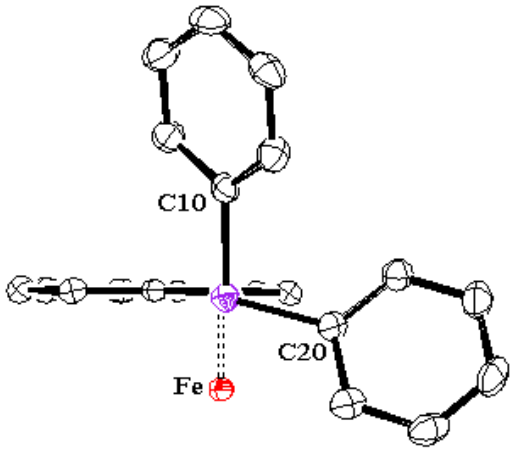

Figure 3.11. Views down P–C1 axes of *rac*-3.32 showing orientation of phenyl rings.

3.5.2. Bis(1-diphenylphosphino-2-methylindenyl)iron(II) (3.33)

Bis(1-diphenylphosphino-2-methylindenyl)iron(II) (**3.33**) was synthesised by the reaction of 1-diphenylphosphino-2-methylindenyllithium with anhydrous ferrous chloride in tetrahydrofuran as shown in Scheme 3.28. The ferrocene was isolated in moderate yield (54%) as a green powder. The reaction produced the two diastereomers in a ratio of 58:42, as evidenced by peaks in the $^{31}P\{^{1}H\}$-NMR spectrum at –20.04 and –17.60 ppm. The ^{1}H-NMR resonances for the H3 protons of the two isomers occur at 4.84 and 5.08 ppm, with the former belonging to the major isomer. The methyl groups resonate at 0.77 and 1.86 ppm, again, with the former corresponding to the major isomer. The methyl group of the major isomer is highly shielded when compared with the equivalent resonances for **3.22** and **3.23**, an indication that the conformation of the major isomer is quite different from that previously observed for **3.22**. The identity of the major isomer is unknown, but comparison of the NMR spectra of **3.33** with **3.32**, **3.34**, and bis(1-diphenylphosphino-4,7-dimethylindenyl)iron(II)[32] suggests that the major isomer is in fact ***meso*-3.33**. The phosphorus nuclei of the *meso* diastereomers of **3.32**, **3.34**, and bis(1-diphenylphosphino-4,7-dimethylindenyl)iron(II) occur upfield of the equivalent resonances for their *racemic* counterparts. The phosphorus nucleus of the major isomer of **3.33** is upfield of the resonance for the minor isomer. A similar situation is observed in the ^{1}H-NMR spectra of **3.32** and bis(1-diphenylphosphino-4,7-dimethylindenyl)iron(II), with the resonances of the H3 protons occurring upfield of the H3 protons of the *racemic* diastereomers. The resonance of H3 for the major isomer of **3.33** appears in a position upfield of the H3 proton for the minor isomer. These trends are consistent with the major isomer of **3.33** being the *meso* diastereomer, although this assignment is not unambiguous.

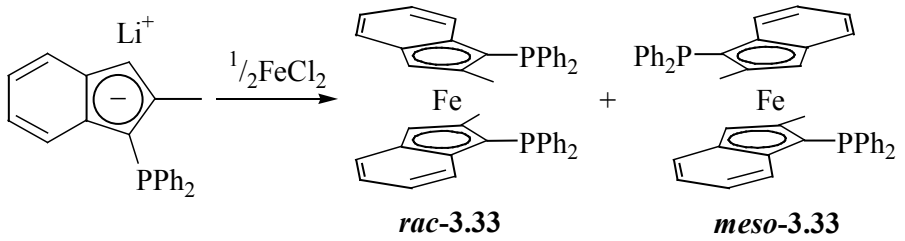

Scheme 3.28. Synthesis of 3.33.

3.5.3. Bis(1-diphenylphosphino-3-methylindenyl)iron(II) (3.34)

Bis(1-diphenylphosphino-3-methylindenyl)iron(II) (**3.34**) was synthesised by the reaction of 1-diphenylphosphino-3-methylindenyllithium with anhydrous ferrous chloride in tetrahydrofuran (Scheme 3.29). The ferrocene was isolated in modest yield (43%) as a dark green powder. The reaction produced two compounds in a 3:1 ratio as evidenced by peaks in the $^{31}P\{^{1}H\}$-NMR spectrum at –24.69 and –26.35 ppm. The major isomer, with the downfield chemical shift, was identified by X-ray crystallography to be ***rac*-3.34** (see below). The ^{1}H-NMR spectrum of ***rac*-3.34** consists of an aromatic multiplet centred at 6.91 ppm, with singlets at 2.38 and 3.61 ppm corresponding to the methyl group and H2, respectively. The resonance for H2 is downfield of the equivalent proton in ***rac*-3.32**, suggesting the shielding of the proton by the phenyl rings is not as great as previously observed. The methyl resonance is also downfield of the equivalent protons in **3.21**.

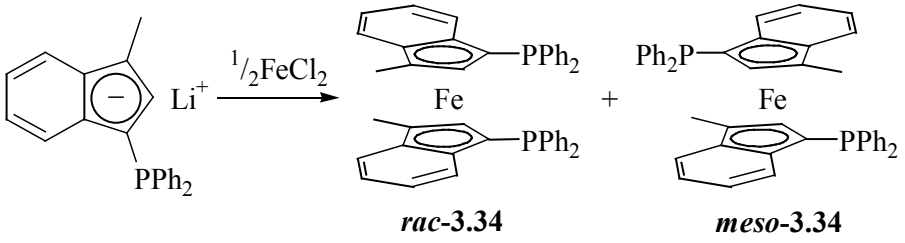

Scheme 3.29. Synthesis of 3.34.

Crystals of ***rac*-3.34** suitable for single crystal X-ray structure analysis were obtained from vapour diffusion of diethyl ether into a dichloromethane solution of ***rac*-3.34**. The molecular structure of ***rac*-3.34** is shown in Figure 3.12. Selected bond lengths (Å) and angles (°) are listed in Table 3.5.

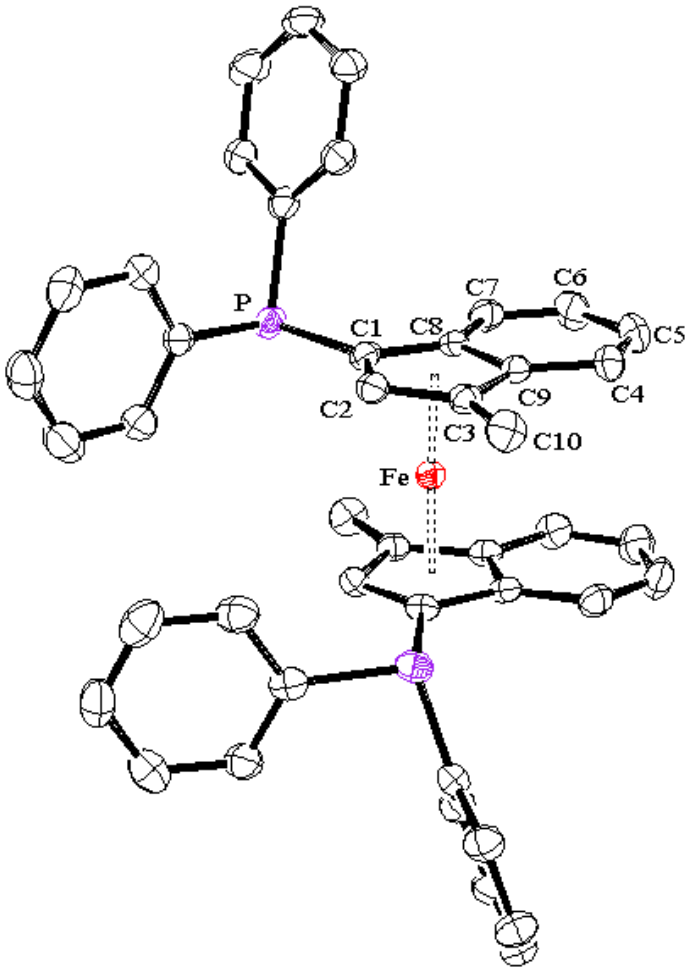

Figure 3.12. ORTEP of *rac*-3.34 indicating the numbering of the atoms. The thermal ellipsoids have been drawn at 50% probability.

Table 3.5. Selected bond lengths [Å] and angles [°] for *rac*-3.34.

Fe-C1	2.064(3)	P-C21	1.854(3)	P-C1-Fe	130.06(13)
Fe-C2	2.065(3)	C1-C2	1.445(4)	C10-C3-Fe	128.65(17)
Fe-C3	2.089(3)	C1-C8	1.447(4)	C2-C1-C8	106.6(2)
Fe-C8	2.094(3)	C2-C3	1.429(3)	C3-C2-C1	110.2(2)
Fe-C9	2.113(3)	C3-C9	1.445(3)	C2-C3-C9	106.8(2)
P-C1	1.830(3)	C8-C9	1.453(4)	C1-C8-C9	107.9(2)
P-C11	1.846(3)	C3-C10	1.509(4)	C3-C9-C8	108.5(2)

Complex ***rac*-3.34** crystallizes in the monoclinic space group C2/c, with one half molecule being in the asymmetric unit. The indenyl ligands are coordinated to the iron atom via their five-membered rings in a distorted η^5-fashion. The carbon-Fe bond lengths are similar to those observed in ***rac*-3.32** with the exception of Fe-C3, which is considerably longer at 2.089 Å. The presence of the methyl group causes changes in the relative orientation of the diphenylphosphino moieties. While the conformation remains "anticlinical staggered", the C1-CNT-CNT'-C1' torsion angle has increased slightly to 130.06°. The phenyl rings are now both above the plane of the indenyl ligand, with the planes through C1-P-C11 and C1-P-C21 bisecting the C_5 ring plane of the indenyl ligand at angles of 109.1° and 6.5°, respectively. This rotation about the P-C1 bond occurs to eliminate any potential steric interactions between the methyl group and phenyl ring of the other ligand. A consequence of the rotation of the diphenylphosphino moiety is that the H2 protons are no longer sandwiched by the phenyl rings, reducing the amount of shielding that the proton is experiences. There is now only one C···H distance of less than 3.0 Å, with the distance between C21 and H2 (of the same ligand) being 2.888 Å. All other C···H distances are greater than 3.25 Å. The phosphorus atoms adopt a tetrahedral geometry, with angles of 99.86, 101.09, and 101.95° for C1-P-C11, C1-P-21, and C11-P-C21, respectively. The phosphorus-carbon bond lengths for C1, C11, and C21 are 1.830, 1.846, 1.854 Å, respectively. A comparison of the solid-state structure of ***rac*-3.34** with other structurally-characterized bis(indenyl)iron(II) complexes will be discussed later in this chapter.

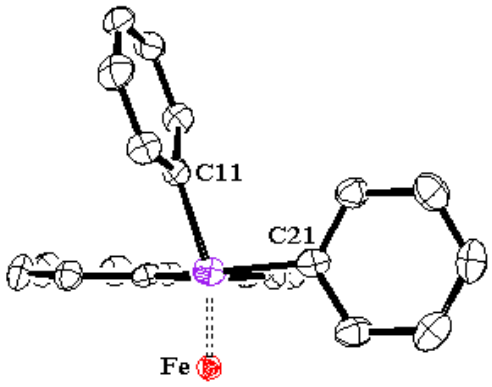

Figure 3.13. Views down P–C1 axes of *rac*-3.34 showing orientation of phenyl rings.

3.5.4. Bis(1-diphenylphosphino-2,3-dimethylindenyl)iron(II) (3.35)

Bis(1-diphenylphosphino-2,3-dimethylindenyl)iron(II) (**3.35**) was synthesised by the reaction of 1-diphenylphosphino-2,3-dimethylindenyllithium with anhydrous ferrous chloride in tetrahydrofuran, as shown in Scheme 3.30. The ferrocene, **3.35**, was isolated in modest yield (42%) as a green powder. The product was obtained as a 5:2 mixture of diastereomers as evidenced by peaks in the $^{31}P\{^{1}H\}$-NMR spectrum at –23.81 and –23.21 ppm. The ^{1}H-NMR spectrum of **3.35** clearly shows the two diastereomers, with the methyl groups of the major isomer resonating at 1.50 and 1.96 ppm, and the minor isomer methyl groups resonating at 1.34 and 2.16 ppm. The downfield resonance for each isomer corresponds to the methyl groups bonded to C3. Solutions of **3.35** were found to be very sensitive, with decomposition occurring readily at ambient temperature. This sensitivity meant that it was not possible to unambiguously assign the major diastereomer, although a few crystals of ***rac*-3.35** were obtained (see below).

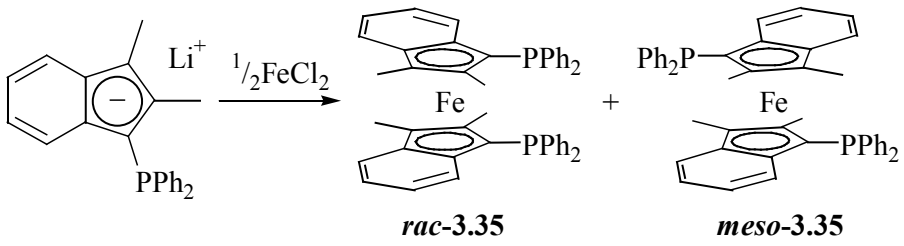

Scheme 3.30. Synthesis of 3.35.

Crystals of ***rac*-3.35** suitable for single crystal X-ray structure analysis were obtained from a diethyl ether solution of ***rac*-3.35**. The molecular structure of ***rac*-3.35** is shown in Figure 3.14. Selected bond lengths (Å) and angles (°) are listed in Table 3.6.

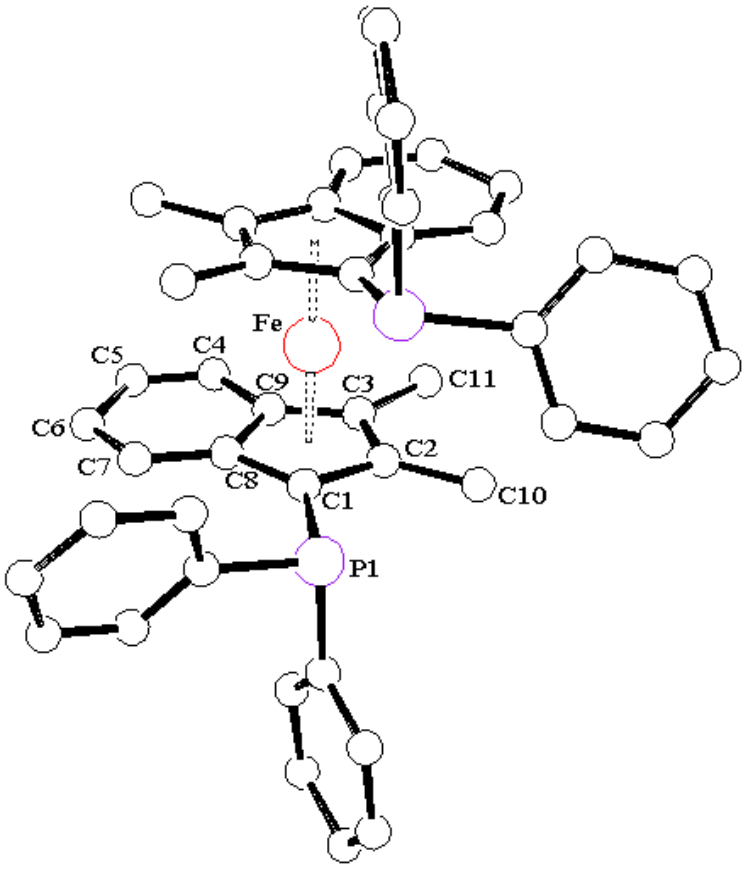

Figure 3.14. PLUTO of *rac*-3.35 indicating the numbering of the atoms. The atoms have been drawn at 40% probability.

Table 3.6. Selected bond lengths [Å] and angles [°] for *rac*-3.35.

Fe-C1	2.063(9)	C1-C8	1.430(13)	C10-C2-Fe	129.2(6)
Fe-C1A	2.083(9)	C1A-C8A	1.451(13)	C10A-C2A-Fe	130.9(7)
Fe-C2	2.102(11)	C2-C3	1.447(14)	C11-C3-Fe	126.7(7)
Fe-C2A	2.085(12)	C2A-C3A	1.414(15)	C11A-C3A-Fe	128.6(7)
Fe-C3	2.087(11)	C3-C9	1.392(15)	C2-C1-C8	108.9(8)
Fe-C3A	2.073(12)	C3A-C9A	1.363(18)	C2A-C1A-C8A	106.7(8)
Fe-C8	2.112(9)	C8-C9	1.512(13)	C1-C2-C3	107.7(9)
Fe-C8A	2.101(9)	C8A-C9A	1.492(14)	C1A-C2A-C3A	109.6(11)
Fe-C9	2.148(10)	C2-C10	1.489(14)	C2-C3-C9	109.4(9)
Fe-C9A	2.091(10)	C2A-C10A	1.521(16)	C2A-C3A-C9A	108.4(10)
P-C1	1.852(9)	C3-C11	1.550(14)	C1-C8-C9	106.1(9)
PA-C1A	1.837(8)	C3A-C11A	1.591(16)	C1A-C8A-C9A	105.0(9)
C1-C2	1.440(13)	P-C1-Fe	131.1(5)	C3-C9-C8	107.6(8)
C1A-C2A	1.451(14)	PA-C1A-Fe	131.2(4)	C3A-C9A-C8A	110.3(9)

Complex ***rac*-3.35** crystallizes in the triclinic space group P-1, with one complete molecule being in the asymmetric unit. Coordination of the indenyl ligands to the iron atom is via their five-membered rings in a η^5-fashion. While the conformation observed for ***rac*-3.35** is unambiguous, the poor refinement (R = 11.0%) obtained during the crystallographic analysis means that a direct comparison of bond lengths and angles with the previous complexes is not reasonable. The π-offset stacking observed in ***rac*-3.32** and ***rac*-3.34** is not present in ***rac*-3.35**. The diphenylphosphino moieties adopt a synclinical (or gauche) conformation, with a C1-CNT-CNT'-C1' torsion angle of 30°. The methyl group in the 2 position of the indenyl ligand causes a rotation of the diphenylphosphino moiety such that one of the phenyl rings is now orientated back towards the benzo ring (Figure 3.15), with the C_5 ring plane and C1-P-C31 plane bisecting at an angle of 11°. The other phenyl group is positioned above the C_5 ring plane, with the plane defined by C1-P-C21 bisecting the C_5 ring plane at an angle of 95°. The geometry of the phosphorus atoms is approximately tetrahedral, with average bond angles of 101, 101, and 106° for C21-P-C31, C1-P-C21, and C1-P-C31, respectively. The large value observed for the C1-P-C31 bond angle is a result of steric interactions due to the phenyl ring now orientating towards the benzo ring. This orientation places C7 at a distance of just 3.36 Å from C31 and C36, and a smaller C1-P-C31 bond angle would only serve to increase steric interactions. A comparison of the solid-state structure of ***rac*-3.35** with other structurally-characterized bis(indenyl)iron(II) complexes will be discussed later in this chapter.

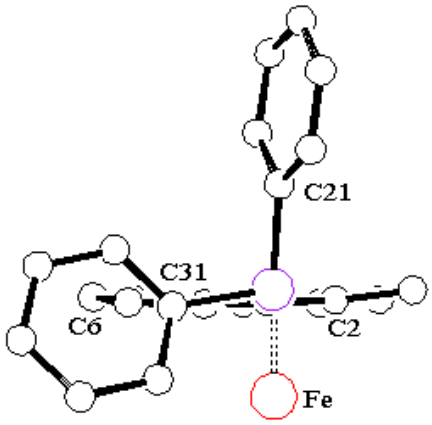

Figure 3.15. Views down P–C1 axes of *rac*-3.35 showing orientation of phenyl rings.

3.5.5. Bis(1-diphenylphosphino-3,4,7-trimethylindenyl)iron(II) (3.36)

The synthesis of bis(1-diphenylphosphino-3,4,7-trimethylindenyl)iron(II) (**3.36**) was attempted by the reaction of 1-diphenylphosphinoindenyllithium with anhydrous ferrous chloride in tetrahydrofuran as shown in Scheme 3.31. Unfortunately, the reaction was unsuccessful, with the $^{31}P\{^{1}H\}$-NMR spectrum of the resulting brown solution showing predominantly free indene (**3.17**) at –2 ppm, with only minor peaks in the region of –20 ppm. The compounds associated with the peaks in the region of –20 ppm may include the ferrocenes as well as the vinylic isomer of the **3.17**, but this is by no means certain. As seen with **3.35**, the increase in substitution of the indenyl ligands increases the reactivity (and conversely decreases stability) of the ferrocenes. In particular, methyl-substitution of indenyl ligands has been shown to increase the ease of ferrocene oxidation.[11] Steric crowding from the heavily-substituted indenyl ligand may also be a factor preventing formation of the ferrocene.

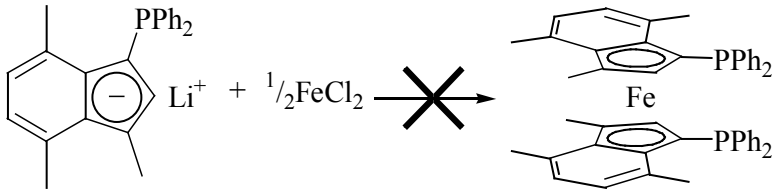

3.36

Scheme 3.31. Attempted synthesis of 3.36.

3.5.6. Bis(1-diphenylphosphino-3-trimethylsilylindenyl)iron(II) (3.37)

Bis(1-diphenylphosphino-3-trimethylsilylindenyl)iron(II) (**3.37**) was synthesised by the reaction of 1-diphenylphosphino-3-trimethylsilylindenyllithium with anhydrous ferrous chloride in tetrahydrofuran as shown in Scheme 3.32. The ferrocene was isolated in modest yield (31%) as a green powder. Initially, two products are formed in a ratio of 3:2 as evidenced by peaks in the $^{31}P\{^{1}H\}$-NMR spectrum at –27.3 and –25.3 ppm. The material produced is very air-sensitive, presumably due to the steric demands of the ligands, so upon work-up only the compound with the upfield chemical shift was isolated. The identity of the isolated diastereomer is unknown. The ^{1}H-NMR spectrum of **3.37** consists of an aromatic multiplet centred at 7.16 ppm, with singlets at 0.23 and 3.84 ppm corresponding to the

trimethylsilyl and H2 protons respectively. The $^{31}P\{^{1}H\}$-NMR spectrum of **3.37** consists of a singlet at –28.49 ppm.

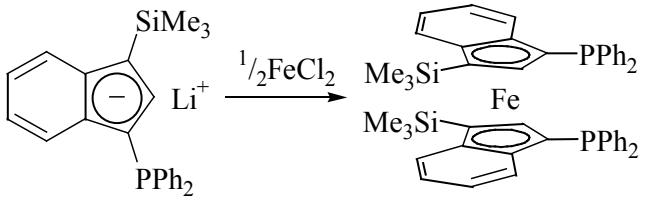

3.37

Scheme 3.32. Synthesis of 3.37.

3.5.7. (Bis(1-diphenylphosphinoinden-3-yl)dimethylsilane)iron(II) (3.38)

The synthesis of (bis(1-diphenylphosphinoinden-3-yl)dimethylsilane)iron(II) (**3.38**) was attempted by the reaction of bis(1-diphenylphosphinoinden-3-yllithium)dimethylsilane with anhydrous ferrous chloride in tetrahydrofuran as shown in Scheme 3.33. Unfortunately, the reaction was unsuccessful, with the $^{31}P\{^{1}H\}$-NMR spectrum of the reaction mixture showing multiple signals in the regions of –4 and –21 ppm. It was not possible to assign the resonances to particular compounds, but the downfield resonances are most probably due to the isomerisation of **3.19** to the isomer containing an allylic phosphine. As part of a study on ring-tilted ferroceneophanes, Manners et al. have reported the synthesis of the *ansa*-bridged bis(indenyl)iron(II) complex $Fe(C_9Me_6)_2SiMe_2$.[11c] The low yield obtained for $Fe(C_9Me_6)_2SiMe_2$ (20%) suggests that the increased steric crowding of **3.19** may be further hindering formation of the desired ferrocene.

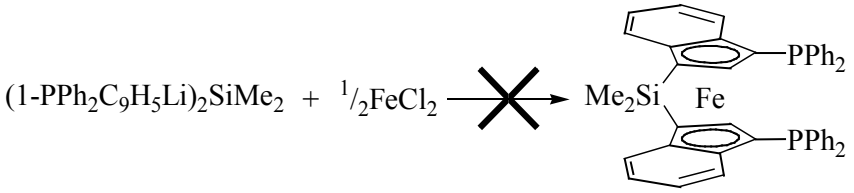

3.38

Scheme 3.33. Attempted synthesis of 3.38.

3.5.8. Bis(1-(diphenylphosphino)tetrahydroindenyl)iron(II) (3.39)

The hydrogenation of indenyl complexes has been shown to produce compounds that, in addition to having a higher stability, are also more catalytically active. Hydrogenation usually occurs quantitatively and under mild reaction conditions.[23,24] The synthesis of bis(1-(diphenylphosphino)tetrahydroindenyl)iron(II) (**3.39**) was attempted by the reaction of hydrogen with **3.32**in the presence of PtO_2 (Scheme 3.34). Unfortunately, the reaction was unsuccessful with either decomposition of **3.32** to 3-(diphenylphosphineoxide)indene (**3.40**) or no reaction occurring. It is unclear as to why the presence of the diphenylphosphino moieties is preventing the hydrogenation of the benzo rings. Reetz et al. have previously reported the synthesis of **3.39** by the phosphorylation of bis(tetrahydroindenyl)iron(II), albeit in low yield (3%).[33]

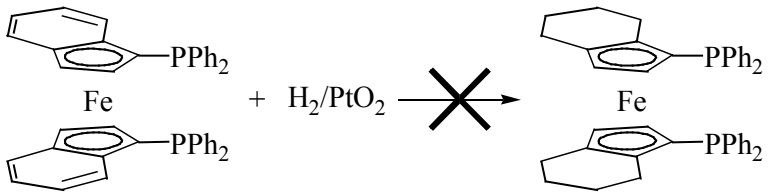

***rac*-3.39**

Scheme 3.34. Attempted Synthesis of 3.39.

The identity of the major decomposition product (**3.40**) was confirmed by the independent synthesis. The reaction of **3.13** with hydrogen peroxide gave **3.40** in modest yield (35%) as a yellow powder (Scheme 3.35). In a similar fashion, 3-(diphenylphosphineselenide)indene (**3.41**) was synthesized by the reaction of **3.13** with selenium. The indene **3.41** was isolated in excellent yield (93%) as a white powder.

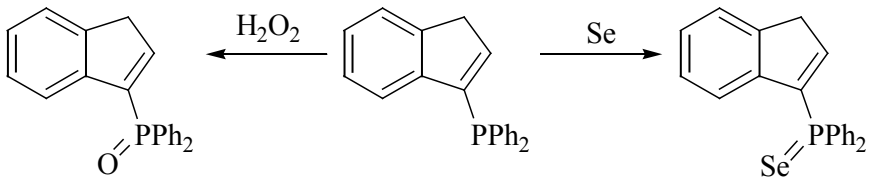

3.40 **3.41**

Scheme 3.35. Synthesis of 3.40 and 3.41.

3.6. $^{13}C\{^1H\}$-NMR spectroscopy of ligands and ferrocenes

The $^{13}C\{^1H\}$-NMR spectra of indene and simple methyl-substituted indenes has previously been assigned using selective and off-resonance decoupling methods.[34] For most cases described, the shielding fluctuations observed for the carbon atoms on the addition of a substituent are additive, allowing for the accurate prediction of chemical shifts for multi-substituted indenes. However, significant deviations between the actual and predicted chemical shifts were observed when the molecules contained sterically-congested methyl groups. The introduction of a methyl group to C1 or C3 of indene was seen to induce shielding fluctuations for carbons within two bonds of the site of substitution. With the introduction of a methyl to C2, the shielding effects were more widespread with significant fluctuations observed for C6 (five bonds from the point of substitution) due to resonance/conjugation effects.

Table 3.7. $^{13}C\{^1H\}$-NMR spectroscopy data for substituted indenes[a]

Indene substituent(s)		C1	C2	C3	C4	C5	C6	C7	C8	C9
C_9H_8[b]	**3.1**	39.0	133.8	132.1	120.9	126.1	124.5	123.6	143.5	144.7
1-Me	**3.2**	45.0	141.1	130.1	121.0	126.3	124.7	122.5	149.1	143.9
2-Me[b]	**3.3**	42.6	145.9	127.2	119.7	126.1	123.2	123.4	143.3	145.7
3-Me[b]		37.6	128.6	139.9	118.8	126.0	124.5	123.5	144.3	146.1
1,2-Me_2	**3.4**	47.2	150.8	125.6	119.7	126.3	123.6	122.4	148.9	144.3
1,3-Me_2	**3.5**	43.6	136.0	138.0	118.8	126.2	124.6	122.4	149.7	145.2
4,7-Me_2	**3.6**	38.3	133.2	130.5	127.7	127.6	125.8	130.1	142.1	143.2
1,4,7-Me_3	**3.7**	45.0	141.1	128.0	127.7	127.8	126.6	130.2	146.7	142.6
1,3,4,7-Me_4	**3.8**	42.4	137.6	139.2	128.5	129.4	126.6	130.5	148.5	142.3
1-$SiMe_3$	**3.9**	46.5	135.7	128.8	121.0	124.7	123.6	122.6	145.3	144.1
3-PPh_2	**3.13**	$40.2^{(6)}$	$142.0^{(6)}$	$141.9^{(13)}$	$121.5^{(5)}$	126.4	125.3	124.1	$144.8^{(5)}$	$145.9^{(20)}$
1-PPh_2[c]		$48.6^{(34)}$	$135.0^{(5)}$	$132.1^{(4)}$	121.5	126.6	124.6	$124.0^{(5)}$	$144.0^{(9)}$	$144.6^{(2)}$
1-PPh_2-3-Me	**3.15**	$47.1^{(20)}$	$129.8^{(4)}$	$140.7^{(6)}$	119.3	126.5	124.5	$123.9^{(5)}$	$144.5^{(9)}$	145.7
1-PPh_2-2,3-Me_2	**3.16**	$51.7^{(24)}$	$138.2^{(6)}$	$133.5^{(4)}$	118.1	126.2	123.2	$123.2^{(3)}$	142.9	146.4
1-PPh_2-3,4,7-Me_3	**3.17**	$46.3^{(25)}$	$130.3^{(5)}$	$142.6^{(3)}$	128.3	129.1	126.3	$130.8^{(4)}$	$141.3^{(6)}$	142.6
1-$SiMe_3$-3-PPh_2	**3.18**	$47.9^{(4)}$	$144.4^{(4)}$	$137.2^{(11)}$	$121.4^{(4)}$	124.7	124.0	122.6	$146.1^{(5)}$	$144.8^{(18)}$

[a] Spectra recorded in $CDCl_3$. Chemical shifts are in ppm, relative to internal TMS. Coupling constants, J_{PC} (Hz), are given in parentheses. [b] Data taken from Ref. 34. c Data taken from Ref. 22.

Table 3.7 summarises the $^{13}C\{^{1}H\}$-NMR spectroscopy data for the substituted indenes prepared in this thesis (along with pertinent literature examples). The addition of a methyl group can be seen to induce a downfield shift in the resonance for the carbon at the site of substitution. The magnitude of the shift is dependent on the position at which substitution occurs, with shifts of 6-8 ppm for methyl substitution at C1, C3, C4, and C7 while shifts of 10-12 ppm are observed for substitution at C2. A similar effect is observed upon the introduction of a diphenylphosphino or trimethylsilyl substituent, with downfield shifts of 9-10 ppm and 7-8 ppm observed, respectively, for the carbon atom at the point of substitution. In addition, significant shifts are also observed for the resonances of the carbon atoms adjacent to the site of substitution, with the magnitude and direction of the shift dependent on both the substituent and the site of substitution. As previously seen for simple methyl-substituted indenes, the shielding fluctuations observed for indenes upon substitution are additive, allowing for predictions of chemical shifts for the nine indenes with multiple substituents. The accuracy of the predicted values decreases with increasing substitution, with a difference of 3.7 ppm observed between the predicted and actual values of the chemical shift for C2 in **3.16**. For indenes **3.15** and **3.18**, where the substituents are sterically non-interacting, the experimentally determined values for the chemical shifts and those predicted using additivity are in agreement, within 0.5 ppm, for all carbons.

The assignment of the resonances for the diphenylphosphino-substituted indenes was aided by the observation of coupling between the phosphorus and carbon nuclei of the indene ring. For the indenes containing allylic phosphines (**3.15**–**3.17**), the magnitude of the coupling is greatest for the carbons directly bonded to the phosphorus (C1). The magnitude of the coupling decreases rapidly for the indenes containing the allylic phosphines, with three-bond couplings of 2–6 Hz observed for C3, C7, and C9 of **3.15**–**3.17**. The situation is different for the indenes containing the vinylic phosphines (**3.13** and **3.18**), with $^{2}J_{PC}$ between P and C9 being larger than the $^{1}J_{PC}$ between P and C3 (average couplings of 19 and 12 Hz, respectively). This is typical of phenyl-phosphine compounds, with the magnitude of $^{2}J_{PC}$ being greater than $^{1}J_{PC}$ and $^{3}J_{PC}$.[35]

Table 3.8. $^{13}C\{^1H\}$-NMR spectroscopy data for bis(indenyl)iron(II) complexes[a]

Indenyl substituent(s)		C1	C2	C3	C4	C5	C6	C7	C8	C9
C_9H_7	**3.20**	61.9	69.9		125.5	122.8			87.0	
1-Me	**3.21**	74.3	72.6	60.4	125.5	122.6	123.0	127.2	86.1	87.0
	3.21	74.2	72.2	59.6	125.0	122.4	122.6	127.1	86.1	86.9
2-Me	**3.22**	63.3	85.6		127.5	123.0			86.8	
1,3-Me_2	**3.24**	74.4	82.1		128.7	123.9			84.9	
4,7-Me_2	**3.25**	60.1	69.4		133.2	121.8			89.0	
1,4,7-Me_3	**3.26**	74.6	74.4	58.3	133.0	121.2	123.0	136.0	86.0	90.3
	3.26	74.1	72.9	56.7	134.6	121.8	122.6	134.8	85.6	89.5
1,3,4,7-Me_4	**3.27**	72.5	81.1		135.6	122.9			86.8	
1-$SiMe_3$[b]	**3.28-major**	62.9	74.1	65.2	124.4	122.2	122.4	127.0	90.4	90.2
	3.28-minor	62.8	78.0	65.6	129.7	123.9	124.3	130.6	90.1	90.0
2-$SiMe_3$	**3.29**	66.8	77.2		129.9	124.1			90.1	
1,2-$(SiMe_3)_2$	**3.30**	68.8	81.9	73.7	130.6	125.5	125.7	131.1	95.6	91.5
1,3-$(SiMe_3)_2$	**3.31**	64.9	82.2		130.9	124.9			95.8	
1-PPh_2[b]	***rac*-3.32**	68.1$^{(9)}$	72.0$^{(4)}$	66.1$^{(4)}$	123.6	122.5	122.9	124.1$^{(9)}$	91.0$^{(25)}$	90.3$^{(4)}$
	***meso*-3.32**	66.9$^{(13)}$	74.5	64.4	127.9	124.3	124.9	128.1$^{(10)}$	91.6$^{(22)}$	90.3
1-PPh_2-2-Me[b]	**3.33-major**	65.5$^{(15)}$	87.4	66.4	128.1	124.2	124.6	128.4	90.2$^{(22)}$	88.5
	3.33-minor	[c]	86.9	68.6	[c]	121.2	121.7	[c]	[c]	87.9
1-PPh_2-3-Me[b]	***rac*-3.34**	65.7$^{(11)}$	74.5	78.1	123.4	121.2	123.1	127.1$^{(7)}$	89.3$^{(19)}$	89.1$^{(4)}$
1-PPh_2-2,3-Me_2[b]	**3.35**	67.2$^{(12)}$	86.0	75.6	125.6	122.5	123.5	127.2	88.6	88.3
1-PPh_2-3-$SiMe_3$[b]	**3.37**	70.8$^{(13)}$	78.7	64.6	124.8	123.8	124.2	127.6	92.7$^{(16)}$	94.1

[a] Spectra recorded in C_6D_6. Chemical shifts in ppm, relative to internal TMS. Coupling constants, J_{PC} (Hz), are given in parentheses. [b] Spectra recorded in $CDCl_3$. [c] Resonances could not be resolved from that of the major isomer.

Table 3.8 summarises the $^{13}C\{^1H\}$-NMR spectroscopy data for the substituted bis(indenyl)iron(II) complexes studied in this thesis. The chemical shifts of the carbon atoms for the complexes can be seen to vary in a similar fashion to the indenes upon the introduction of a substituent. The addition of a diphenylphosphino substituent induces a similar downfield shift for the resonance of the carbon at the site of substitution, though the magnitude of the shift is generally smaller at 2-6 ppm. The introduction of a methyl group induces a downfield shift of 9-15 ppm in the resonance for the carbon at the point of substitution. As seen in the ^1H-NMR spectra of bis(indenyl)iron(II) complexes, the magnitude of the downfield shifts for the resonances are also dependent on the particular diastereomer formed. This

dependence makes predictions of chemical shifts based on shielding fluctuations less accurate than was possible with the substituted indenes, though the general trends are still visible.

The resonances for the carbon nuclei of the indenyl ligands generally occur in fairly narrow bands. The C1, C2, and C3 nuclei typically resonate in the range of 58-75 ppm, though the addition of substituents can shift the resonances outside of this band. The bridgehead carbons, C8 and C9, resonate further downfield at 85-96 ppm, reflecting the decreased bonding of these nuclei to the metal.[36] The remaining nuclei of the benzo ring resonate further downfield between 121 and 136 ppm, with the resonances for C4 and C7 being downfield of those for C5 and C6. For complexes containing planar chiral indenyl ligands, two resonances were observed for each carbon nuclei, one for each diastereomer. Interestingly, for both **3.32** and bis(1-diphenylphosphino-4,7-dimethylindenyl)iron(II),[32] on going from the *racemic* to the *meso* diastereomer there is a consistent downfield shift of 2 ppm for the resonances of both C5 and C6 and 4–5 ppm for both C4 and C7. Similar trends can be seen in the $^{13}C\{^{1}H\}$-NMR spectra of **3.28** and **3.33**, with the resonances for the C4-C7 nuclei of one of the diastereomers being downfield of those for the second. This trend suggests that ***rac*-3.28** and ***meso*-3.33** are the major isomers formed for these particular complexes. This assignment is consistent with the trends already discussed for the ^{31}P- and ^{1}H-NMR spectra of **3.33** and the shielding and NOE information obtained from the ^{1}H-NMR spectrum of **3.28**. The diastereomers of **3.21** and **3.26** cannot be elucidated in a similar manner due to relatively minor differences in chemical shifts for the nuclei of the benzo ring.

3.7. X-ray crystallography of bis(indenyl)iron(II) complexes

The coordination chemistry of the indenyl ligand has been found to be structurally diverse due to the variety of modes with which coordination can occur. A recent review identified a total of ten coordination modes that have been described for the indenyl ligand,[37] with modes ranging from simple mononuclear (η^5, η^3, η^1) to complex polynuclear (μ_3-η^5:η^2:η^2). By far, the most common coordination mode is η^5, with relatively few examples of the others reported to date. Currently, [PPN][(η^3-

$C_9H_7)Fe(CO)_3]$, $(\eta^5\text{-}C_5H_5)Fe(\eta^1\text{-}C_9H_7)(CO)_2$, and an η^1-indenyl-iron derivative of 2,2'-biindene are the only examples of tri- and monohapto indenyl complexes isolated for iron.[38,39]

The most important structural feature of η^5-indenyl complexes is the distortion from η^5- to η^3-coordination. While distortions of this type have been observed for η^5-cyclopentadienyl complexes,[40] the ability of the indenyl ligand to stabilize the allyl-ene structure by aromatisation of the benzo ring makes the distortion more pronounced in the indenyl complexes.

Different parameters have been used to describe the slip-fold distortion observed in indenyl complexes. Based on the $^{13}C\{^1H\}$-NMR spectra of $(C_9H_7)_2M$ (M = Fe, Co^+, Ni) and indene, Köhler proposed a correlation between the $^{13}C\{^1H\}$-NMR chemical shifts of the bridgehead carbons and the hapticity of the coordinated indenyl ligand.[36a] Baker and Tulip selected sodium indenide as a more appropriate reference, with slip-fold distortions observed in the solid-state of indenyl complexes correlating well with the $^{13}C\{^1H\}$-NMR chemical shifts.[36b] However, these correlations are only applicable when the complex contains the unsubstituted indenyl ligand, as the addition of substituents can affect the chemical shifts of the bridgehead carbons. In the solid-state, Taylor and Marder have chosen the slip parameter, hinge angle, and fold angle to describe the slip-fold distortion in indenyl complexes (Figure 3.16).[41] The slip parameter (Δ) is defined as the difference in the average bond lengths of the metal to the bridgehead carbons (C8, C9) and the metal to the adjacent carbon atoms of the five-membered ring (C1, C3): Δ = avg. d[M-C8,C9] – avg. d[M-C1,C3]. The hinge angle (HA) has been defined as the angle between the planes defined by [C1, C2, C3] and [C1, C3, C8, C9] and represents the bending of the indenyl ligand at C1, C3. The fold angle (FA) has been defined as the angle between the planes defined by [C1, C2, C3] and [C4, C5, C6, C7, C8, C9] and represents the bending of the indenyl ligand at C8, C9. For sandwich complexes, an additional parameter was deemed necessary to describe the relative orientation of the two indenyl rings. The rotation angle (RA) was defined as the angle formed by the intersection of the two lines determined by the centroids of the five- and six-membered rings. An RA of 0° would indicate a

completely eclipsed geometry whereas an RA of 180° corresponds to the fully staggered arrangement of the two rings.

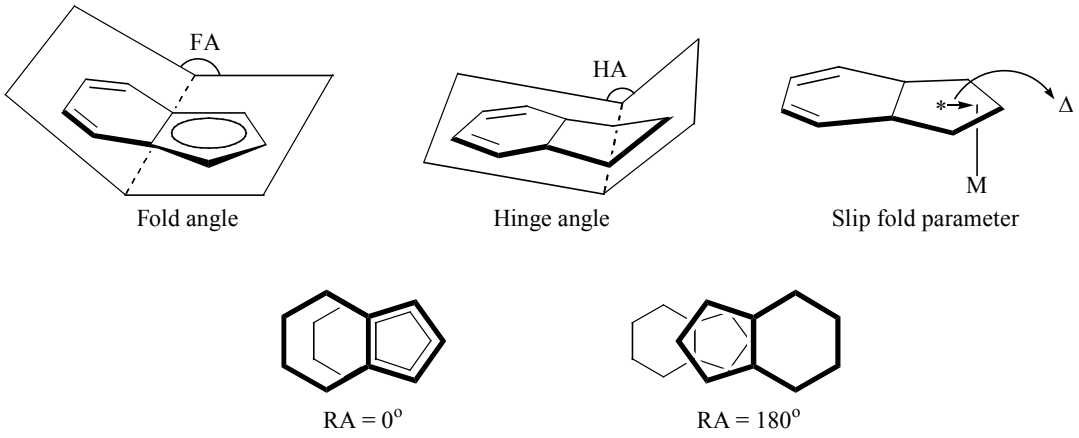

Figure 3.16. Slip-fold distortion parameters.

In general, indenyl complexes are considered to exhibit η^5-coordination if their values of HA and Δ are less than 10° and 0.25 Å, respectively. In contrast, HA and Δ values between 20-30° and 0.69-0.80 Å are considered to indicate η^3-coordination. Near perfect η^5-coordination has previously been reported for $(C_9H_7)_2Ru$, with values for HA and Δ of 0° and 0.03 Å, respectively.[42] Complexes $[PPN][(\eta^3\text{-}C_9H_7)Fe(CO)_3]$ and $[Ir(\eta^3\text{-}C_9H_7)(PMe_2Ph)_3]$ are considered to be true examples of η^3-indenyl coordination, with Δ values of 0.69 and 0.79 Å, respectively.[38,43]

Table 3.9 summarises the slip-fold distortion parameters for the complexes studied in this thesis, along with a variety of those reported in the literature. For bis(indenyl)iron(II) complexes, the distance between the iron atom and the centroids of the five-membered rings range between 1.668 and 1.717 Å. The indenyl ligands are orientated almost parallel to one another, with the angle between the iron and the centroids of the five-membered rings ranging between 175.4 and 179.6°. The larger values of Fe-C^* (C^* = centroid of C_5 ring) observed in **3.31**, ***rac*-3.34**, and ***rac*-3.35** are an indication of the increased steric interactions experienced by the heavily substituted ligands. The Fe- C^* distance of 1.695 Å for **3.31** is currently the longest observed for a bis(indenyl)iron(II) complex, though the equivalent distance for oxidised bis(indenyl)iron complexes are slightly longer.

Table 3.9. Comparison of solid-state structural data for indenyl complexes[a]

Compound	M-C*[b]	C*-Fe-C*	Δ (Å)[c]	HA (°)[d]	FA (°)[e]	RA (°)[f]	Ref.
$(C_9H_7)_2Fe$ **3.20**	1.675[g]	–	0.04[h]	2.2[h]	0.8[h]	6.0,13.0[i]	41,44
$(2\text{-}MeC_9H_6)_2Fe$ **3.22**	1.678	178.6	0.05	2.6	1.4	3.4	[k]
$(+)\text{-}(2\text{-}menthylC_9H_6)_2Fe$	1.676	177.8	0.06	3.2	5.1	134.0	25
$[(1,3\text{-}Me_2C_9H_5)_2Fe][PF_6]$	1.716	177.7	0.07	–	–	93.5	28
$(4,7\text{-}Me_2C_9H_5)_2Fe$ **3.25**	1.668	179.3	0.05	1.8	1.1	14.7	[k]
	1.668[j]	178.8[j]	0.06[j]	2.5[j]	0.8[j]	17.9[j]	[k]
$(C_9Me_7)_2Fe$	–	–	0.03	2.5	4.4	151.3	41
$[(C_9Me_7)_2Fe][TCNQ]$	1.717	–	0.07	3.5	1.5	85.0	45
$(1,3\text{-}(SiMe_3)_2C_9H_5)_2Fe$ **3.31**	1.695	178.0	0.05	3.5	8.2	94.7	[k]
$(1\text{-}PPh_2C_9H_6)_2Fe$ ***rac*-3.32**	1.674	179.6	0.03	2.1	0.9	20.8	[k]
$(1\text{-}PPh_2\text{-}3\text{-}Me\text{-}C_9H_5)_2Fe$ ***rac*-3.34**	1.685	177.0	0.03	2.4	2.5	28.7	[k]
$(1\text{-}PPh_2\text{-}2,3\text{-}Me_2C_9H_4)_2Fe$ ***rac*-3.35**	1.70	175.8	0.04	4.0	5.6	118.8	[k]
rac-$(1\text{-}PPh_2\text{-}4,7\text{-}Me_2C_9H_4)_2Fe$	1.668	178.8	0.05	2.4	1.9	12.1	32
meso-$(1\text{-}PPh_2\text{-}4,7\text{-}Me_2C_9H_4)_2Fe$	1.681	175.4	0.04	2.3	1.1	40.5	32
$(C_9H_7)_2Ru$	1.822	–	0.03	0.0	0.0	0.2	42
$(C_9H_7)_2Co$	–	–	0.12	7.6	6.0	10.7	41
$(C_9H_7)_2Ni$	–	–	0.42	13.9	13.1	175.0	41
$[PPN][(\eta^3\text{-}C_9H_7)Fe(CO)_3]$	–	–	0.69	–	22	–	38

[a] Average values from both ligands are given for bis(indenyl)metal complexes. [b] C* = centroids of C1, C2, C3, C8, C9. [c] Δ = avg. d[M-C8, C9] – avg. d[M-C1, C3]. [d] HA = angle defined by [C1, C2, C3] and [C1, C3, C8, C9]. [e] FA = angle defined by [C1, C2, C3] and [C4, C5, C6, C7, C8, C9]. [f] RA = angle formed by the intersection of two lines determined by the centroids of the five- and six-membered rings. [g] Value estimated from average Fe-C bond lengths. [h] Average value of the two independent molecules in the asymmetric unit. [i] Values given for the two independent molecules in the asymmetric unit. [j] Value refers to second independent molecule in the asymmetric unit of **3.25**. [k] This work.

Most bis(indenyl)iron(II) complexes show small distortions towards η^3-coordination, with the slip-fold distortion parameter ranging between 0.03–0.07 Å and HA between 1.8–4.0°. Diindenyliron(II) (**3.20**), with Δ and HA values of 0.04 Å and 2.2°, respectively, is considered to be a good example of η^5-coordination; similar values for the slip-fold distortion parameters are obtained for ***rac*-3.32** and **3.25**. The steric demands of the heavily-substituted ligands in **3.31** and ***rac*-3.35** are reflected in the relatively large HA values of these complexes: 3.5 and 4.0°, respectively. The larger values for HA in **3.31** and ***rac*-3.35** are mirrored by an increase in FA (5.6 and

8.1°, respectively). Although large for bis(indenyl)iron(II) complexes, these distortions are relatively minor when compared with other indenyl-metal complexes. Increased slip-fold distortion towards η^3-coordination has been found to be a function of d-electron count, with values of 2.2, 7.6, and 13.9° for the HA of **3.20**, $(C_9H_7)_2Co$ and $(C_9H_7)_2Ni$, respectively.[41]

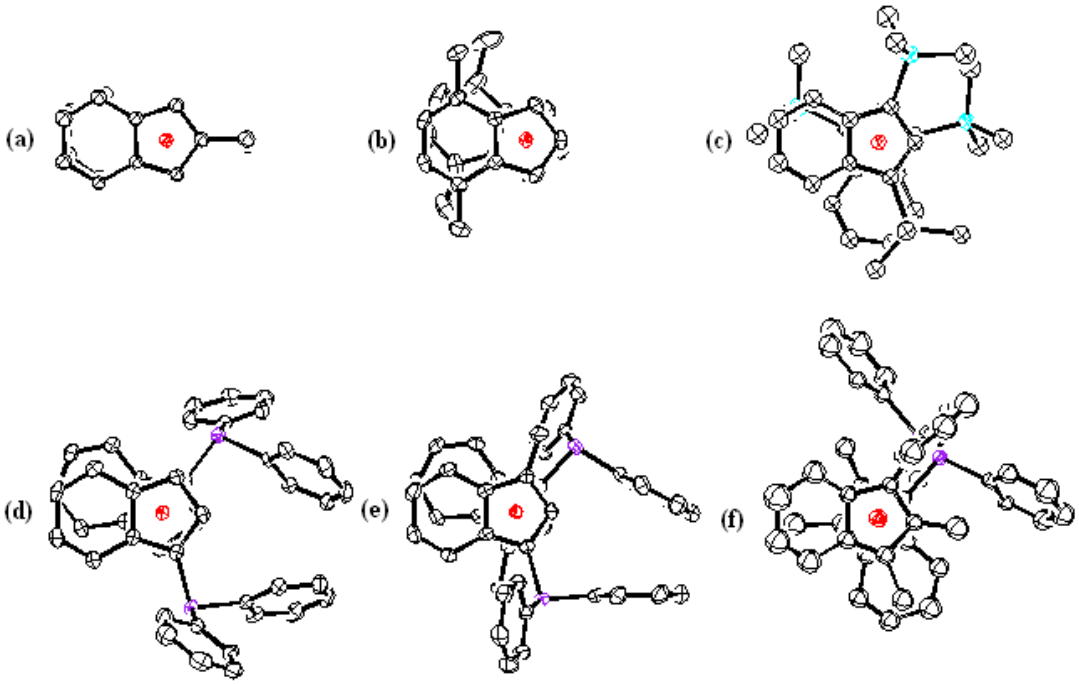

Figure 3.17. Views down the CNT-CNT axes: (a) 3.22, (b) 3.25, (c) 3.31, (d) *rac*-3.32, (e) *rac*-3.34, and (f) *rac*-3.35.

The rotation angle of bis(indenyl)iron(II) complexes is highly variable. The RA values observed for the independent molecules of **3.20** are significantly different, indicating a relatively soft energy surface for ring rotation of this complex. Permethylation of the indenyl ligand leads to an significant increase in rotation angle, with a RA of 151.3° found for $(C_9Me_7)_2Fe$.[41] It was believed that steric interactions between the methyl groups were not a factor in determining the solid state structure of $(C_9Me_7)_2Fe$. Figure 3.17 shows the six bis(indenyl)iron(II) complexes characterised in this thesis by x-ray crystallography viewed down their centroid-centroid axes. Ferrocene **3.22** has the smallest RA currently observed for a bis(indenyl)iron(II) complex at 3.4°. Clearly, there are minimal steric interactions between the two methyl

groups. The indenyl ligands of **3.25**, ***rac*-3.32**, and ***rac*-3.34** adopt π-offset conformations, with rotation angles of 14.7, 20.8, and 28.7° respectively. These conformations are believed to maximize π–π-stacking interactions between the benzo rings. For the heavily substituted **3.31** and ***rac*-3.35**, the rotation angles increase to values greater than 90° in order to accommodate all the substituents. The *rac* and *meso* isomers of bis(1-diphenylphosphino-4,7-dimethylindenyl)iron(II) have both been characterized by x-ray crystallography. The indenyl ligands of the *rac* isomer adopt a similar π-offset conformation to that of **3.32**, with a RA of 12.1°. In contrast, the *meso* isomer has a rotation angle of 40.5° due to steric interactions between the bulky diphenylphosphino groups.[32]

3.8. Electrochemistry of bis(indenyl)iron(II) complexes

One of the best known properties of ferrocene molecules is their ability to lose an electron at potentials that are a function of the electron-donating ability of the substituents attached to the cyclopentadienyl rings.[46] Electron-donating substituents facilitate the ease of oxidation, while electron-withdrawing substituents impede the process. Good correlations for the oxidation potentials of ferrocene derivatives with substituent constants σ_p and σ_m have been reported.[10c,47]

Table 3.10. Electrochemical data for bis(indenyl)iron(II) complexes[a]

Indenyl substituent(s)		$E_{1/2}$	Indenyl substituent(s)		$E_{1/2}$
C_9H_7	**3.20**	–278	2-$SiMe_3$	**3.29**	–270
1-Me	**3.21**	–375	1,2-$(SiMe_3)_2$	**3.30**	–291
2-Me	**3.22**	–355	1,3-$(SiMe_3)_2$	**3.31**	–358
1,2-Me_2	**3.23**	–450	1-PPh_2	**3.32**	–140
1,3-Me_2	**3.24**	–472	1-PPh_2-2-Me	**3.33**	–230
4,7-Me_2	**3.25**	–343	1-PPh_2-3-Me	**3.34**	–233
1,4,7-Me_3	**3.26**	–451	1-PPh_2-2,3-Me_2	**3.35**	–348
1,3,4,7-Me_4	**3.27**	–568	1-PPh_2-3-$SiMe_3$	**3.37**	–220
1-$SiMe_3$	**3.28**	–275	1-PPh_2-4,7-Me_2		–230

[a] Potentials measured in mV vs. Fc^+/Fc. Solutions in CH_2Cl_2 ($5x10^{-3}$ M) with [*n*-Bu_4N]PF_6 (0.1 M). Scan rate = 200 mV sec^{-1}. Error associated with measurements is ± 10 mV.

The electrochemistry of the bis(indenyl)iron(II) complexes studied here was investigated by cyclic voltammetry. The results are summarised in Table 3.10. Figure 3.18 shows typical cyclic voltammograms for complex **3.26**. The oxidation potentials for **3.20**, **3.21**, and **3.24** are consistent with those previously reported. All complexes studied exhibit single one-electron reversible oxidations. The differences in peak potentials indicate a slow redox process is occurring for all bis(indenyl)iron(II) complexes.

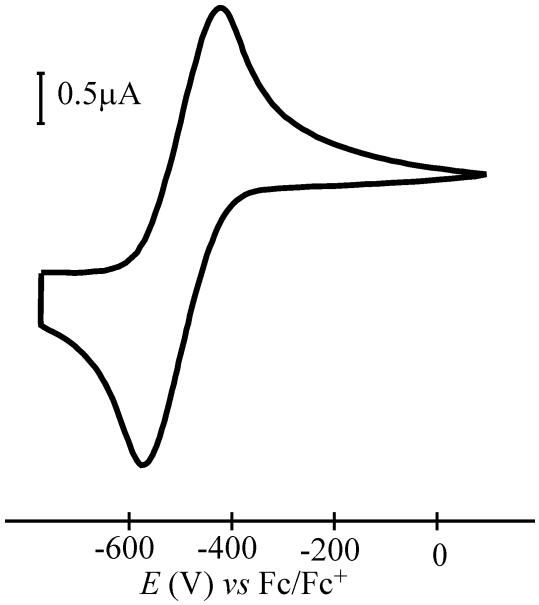

Figure 3.18. Cyclic voltammograms of 3.26.

3.8.1. Methyl-substituted bis(indenyl)iron(II) complexes

The introduction of a methyl group to the indenyl ligand can be seen to decrease the potential at which oxidation of the bis(indenyl)iron(II) complexes occur. However, unlike the cyclopentadienyl ligand the magnitude of the drop in potential is dependent on the position at which the substitution occurs. The introduction of a methyl group to the 1-position (**3.21**) gives a decrease in oxidation potential of 49 mV per methyl group from **3.20** whereas substitution at the 2- (**3.22**) and 4/7-positions (**3.25**) gives decreases in oxidation potential of 39 and 16 mV per methyl group, respectively. These differences in the drop of oxidation potentials can be rationalised in terms of the bonding interactions between the π orbitals of the indenyl ligands and

the *d* orbitals of the iron. The main bonding interactions present in diindenyliron(II) has been the subject of molecular orbital calculations and photoelectron spectroscopic studies.[48,49] The HOMO of the indenyl anion was shown to be of appropriate energy (and symmetry) to interact with the d_{xz} and d_{zy} orbitals of the iron. Unlike the HOMO of the cyclopentadienyl anion, the electron density is not distributed evenly between the atoms of the five-membered ring, with the electron density predominately situated on C1 and C3. Consequently, the introduction of a substituent to the 1/3-position will have a greater effect on the oxidation potential than substitution at other positions.

As observed for bis(cyclopentadienyl)iron complexes,[50] the addition of multiple methyl groups to **3.20** has an additive effect on the decrease in oxidation potential. This allows for predictions to be made for the oxidation potential of multi-substituted bis(indenyl)iron(II) complexes. Using the decreases in oxidation potential observed for **3.21**, **3.22**, and **3.25**, the calculated value for the oxidation potential of **3.23** is –452 mV (observed –450 mV); –472 mV for **3.24** (observed –472 mV); –440 mV for **3.26** (observed –451 mV); and –537 for **3.27** (observed –568 mV). The accuracy of the calculations decreases with increasing substitution, indicating that steric effects are becoming a factor. It should be noted that $(1,2,4,5,6,7\text{-}Me_6C_9H)_2Fe$ and $(C_9Me_7)_2Fe$ have been reported to have oxidation potentials of –690 and –730 mV, respectively.[11b,c]

3.8.2. Trimethylsilyl-substituted bis(indenyl)iron(II) complexes

The introduction of trimethylsilyl substituents to the indenyl ligand can be seen to have a variable effect on the oxidation potential of the resulting bis(indenyl)iron(II) complexes. The addition of a single trimethylsilyl group to either the 1- or 2-position of the indenyl ligand causes a minor increase in the oxidation potential of the resultant ferrocenes (**3.28** and **3.29**) relative to **3.20**. However, disubstitution produces a significant decrease for the oxidation potentials of **3.30** and **3.31** (18 and 80 mV, respectively) relative to **3.20**. The electronic effect of the trimethylsilyl group is considered to have a strong π-acceptor (*–M*) effect compared to the σ-donor (*+I*) effect.[51] The electron-withdrawing nature should make ferrocenes containing the trimethylsilyl group harder to oxidise than the corresponding unsubstituted

complexes. This is indeed the case, with oxidation potentials of 0, 20, and 33 mV reported for $(C_5H_5)_2Fe$, $(1\text{-}SiMe_3C_5H_4)_2Fe$, and $(1,3\text{-}(SiMe_3)_2C_5H_3)_2Fe$, respectively.[52] However, the oxidation potential of $(1,2,4\text{-}(SiMe_3)_3C_5H_2)_2Fe$ was found to be unexpectedly low at –104 mV versus Fc^+/Fc.[52] The cathodic shift observed for the oxidation potential of $(1,2,4\text{-}(SiMe_3)_3C_5H_2)_2Fe$ was attributed to the relief of steric constraints upon oxidation of the sterically-hindered ferrocene. The corresponding ferrocenium cation $[(1,2,4\text{-}(SiMe_3)_3C_5H_2)_2Fe]BF_4$ was found to be less sterically hindered due to longer metal-ligand bond distances. A similar argument may be applicable to the trimethylsilyl-substituted bis(indenyl)iron(II) complexes, with **3.30** and **3.31** expected to suffer from considerable steric hindrance. In an independent study, Chirik et al. observed the same cathodic shift in the oxidation potential of **3.31** and other tetrasilylated bis(indenyl)iron(II) complexes.[54]

3.8.3. Diphenylphosphino-substituted bis(indenyl)iron(II) complexes

The electrochemistry of phosphine-substituted ferrocenes has been the subject of extensive studies,[55] with particular interest focussing on the incorporation of the redox-active ferrocenyl moiety into transition metal complexes.[56] Coordinated ferrocenylphosphines usually exhibit a reversible one-electron oxidation of the ferrocene. In contrast, free ferrocenylphosphines typically display complex electrochemistry due to the involvement of the phosphorus lone pair electrons. It has been proposed that for dppf, the ferrocene-based oxidation is followed by a fast chemical reaction involving intramolecular electron transfer and radical-substrate coupling to produce phosphine dimers of the type $(R_3P–PR_3)^+$.[57]

The introduction of a diphenylphosphino group to the indenyl ligand has a significant effect on the oxidation potential. The electron-withdrawing nature of the phosphine substituent is clearly evident, with an oxidation potential of –140 mV for **3.32** (an increase of 138 mV when compared with **3.20**). A cumulative effect is observed upon the introduction of multiple substituents, with the addition of a methyl group having the expected effect of decreasing the oxidation potential of the ferrocene (relative to **3.32**). Using the methodology employed for predicting the oxidation potentials of methyl-substituted bis(indenyl)iron(II) complexes, an oxidation potential

of –217 mV is calculated for **3.33** (observed –230 mV); –237 mV for **3.34** (observed –233 mV); and –314 for **3.35** (observed –348 mV). As previously observed, the calculations tend to underestimate the potential at which the oxidation occurs for the sterically-congested **3.33** and **3.35**. The addition of a trimethylsilyl to **3.32** decreases the potential at which the oxidation of the resultant ferrocene (**3.37**) occurs. The magnitude of the decrease in oxidation potential is similar to that observed on going from **3.21** to **3.24**, an indication that the relief of steric constraints may again be a factor in this cathodic shift.

3.9. UV/visible spectroscopy of bis(indenyl)iron(II) complexes

The electronic absorption spectra of metallocenes and many of their derivatives have been the subject of intensive investigations.[58] Absorption spectroscopy, in conjunction with molecular orbital calculations and magnetic susceptibility studies, has been used as a means to locate excited states and as verification of bonding theories for metallocenes. Substitution of the metallocenes allows for the identification of ligand-metal (LMCT) and metal-ligand (MLCT) charge transfer bands.[58c]

3.9.1 Molecular orbitals

The π orbitals of the cyclopentadienyl and indenyl anions have been the subjects of numerous studies and are shown in Figure 3.19, projected down onto the *xy* plane.[59] The cyclopentadienyl anion possesses five π orbitals, three of which are filled. The orbitals that make up the degenerate e_1 HOMO of the cyclopentadienyl anion are of appropriate symmetry to interact with the d_{xz} and d_{yz} orbitals of a metal, possessing a single nodal plane through the C_5 ring. The situation is quite different for the indenyl anion, with nine π orbitals of which five are filled. The presence of the six-membered ring removes the degeneracy previously seen for the orbitals of the cyclopentadienyl anion. The three highest-lying filled π orbitals of the indenyl anion, π_3, π_4, and π_5 possess a nodal plane through the C_5 ring, and like the e_1 HOMO of the cyclopentadienyl anion are of appropriate symmetry to interact with the d_{xz} and d_{yz} orbitals of a metal. As the orbital π_5 is localized more on the C_5 ring than π_3, it is believed that π_5 will have a greater overlap with the metal orbitals.

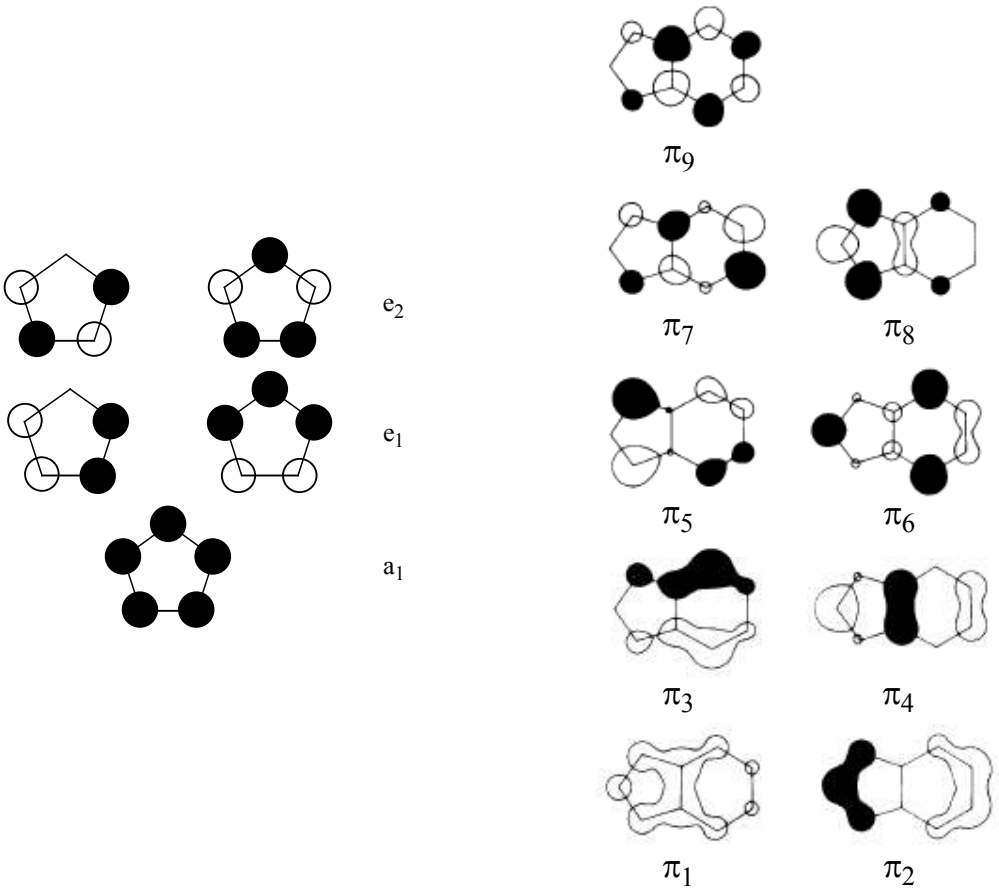

Figure 3.19. Projection onto the xy plane of the π-orbitals of the cyclopentadienyl and indenyl anions.

The main bonding interaction in bis(cyclopentadienyl) and bis(indenyl) complexes has been described as electron donation from the filled π orbitals of the ligands to the empty *d* orbitals of the metal, with back donation being negligble. The π orbitals of the two ligand fragments have been shown to combine in an antisymmetric fashion (with respect to the *xy* plane) with the metal d_{xz} and d_{yz} orbitals. Molecular orbital energy level diagrams have been reported for both $(C_5H_5)_2Fe$ and $(C_9H_7)_2Fe$ (**3.20**), and are shown in Figure 3.20.[58a,49] Calculations have predicted that, like ferrocene, the three highest occupied molecular orbitals of **3.20** are primarily non-bonding metal-based orbitals (d_{xy}, $d_{x^2-y^2}$, d_{z^2}). These predictions were confirmed by photoelectron and EPR spectroscopy.[11b]

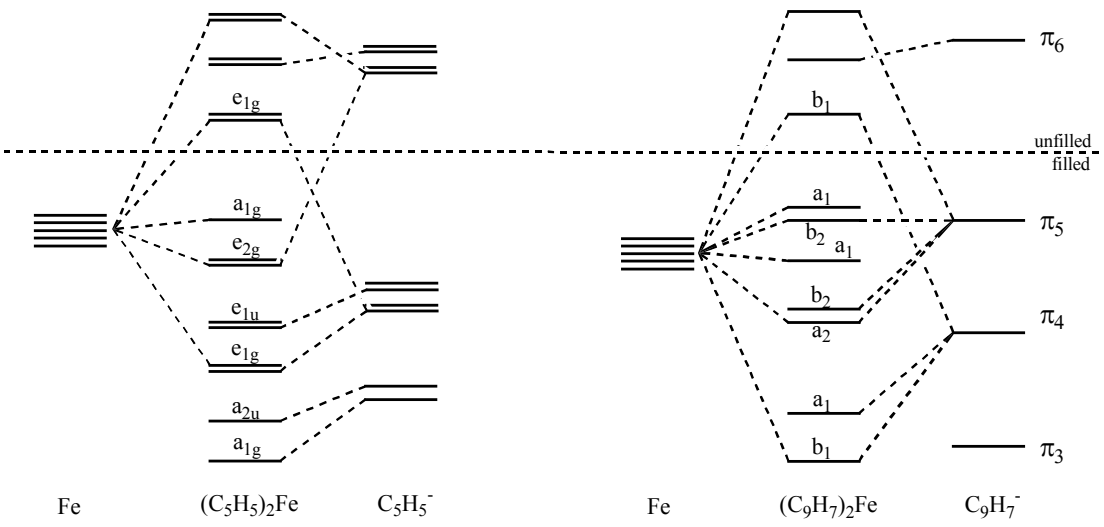

Figure 3.20. Qualitative MO diagrams of: (a) ferrocene (b) 3.20.

3.9.2 Uv/visible spectroscopy

The UV/visible spectrum of ferrocene consists of two low-intensity bands in the visible region centred at 324 and 438 nm.[58a] These bands have been assigned as d-d transitions. Strong-field theory predicts three spin-allowed d-d transitions (two $^1A_{1g} \rightarrow {}^1E_{1g}$ and one $^1A_{1g} \rightarrow {}^1E_{2g}$). There was considerable controversy as to the location of these three transitions, though it was shown conclusively, by low-temperature single-crystal absorption spectroscopy, that the band centred at 438 nm actually consists of two absorptions (at 417 and 458 nm). The ultraviolet region of the absorption spectra of ferrocene consists of a strong band at 200nm and two shoulders at 265 and 240 nm. The addition of methyl groups to ferrocene induces a red shift in the position of these charge transfer bands, indicative of them being MLCT transitions.

Table 3.11. UV/Visible spectroscopic data for bis(indenyl)iron(II) complexes[a]

Indenyl substituent(s)		λ_{max} (ε)	Indenyl substituent(s)		λ_{max} (ε)
C_9H_7	**3.20**	422 (654), 560 (332)	1-$SiMe_3$	**3.28**	416 (568), 578 (239)
1-Me	**3.21**	426 (580), 558 (368)	2-$SiMe_3$	**3.29**	434 (316), 578 (340)
2-Me	**3.22**	418 (530), 552 (304)	1,2-$(SiMe_3)_2$	**3.30**	600 (256)
1,2-Me_2	**3.23**	420 (484), 550 (359)	1,3-$(SiMe_3)_2$	**3.31**	464 (287), 622 (260)
1,3-Me_2	**3.24**	422 (516), 548 (342)	1-PPh_2	**3.32**	418 (869), 566 (265)
4,7-Me_2	**3.25**	416 (827), 556 (430)	1-PPh_2-2-Me	**3.33**	414 (1151), 572 (196)
1,4,7-Me_3	**3.26**	420 (658), 560 (568)	1-PPh_2-3-Me	**3.34**	422 (1196), 600 (324)
1,3,4,7-Me_4	**3.27**	422 (536), 550 (628)	1-PPh_2-3-$SiMe_3$	**3.37**	591 (212)

[a] Absorption maxima measured in nm. Solutions in CH_2Cl_2 (1 mM). Error associated with measurements is ± 5 nm.

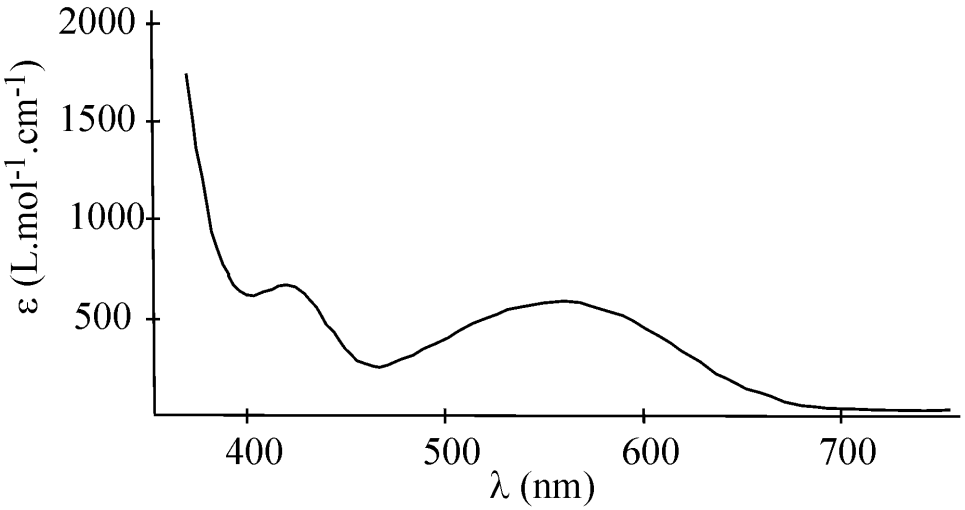

Figure 3.21. UV/visible spectra of 3.26.

The absorption spectra of the bis(indenyl)iron(II) complexes studied here was investigated between 200 and 800 nm. The results are summarized in Table 3.11. Figure 3.21 shows a typical UV/visible absorption spectra for complex **3.26**. Bis(indenyl)iron(II) complexes generally exhibit two absorption bands in the visible region of the spectrum centred at approximately 420 nm and 555 nm. The intensity of the absorptions suggests that both are d-d transitions, with the lowest energy absorption band most likely arising from a transition between the metal-based HOMO and LUMO. Group theory predicts that, under C_{2v} symmetry, **3.20** will exhibit two

spin-allowed d-d transitions (both $^1A_1 \rightarrow {}^1B_1$).[60] The same transitions are also allowed under C_2 and C_{2h} symmetry.

The introduction of methyl groups to **3.20** does not have a significant effect on the UV/visible spectrum of the resulting ferrocenes, with a variance of only 12 nm for both absorption bands. The complex bis(1,2,4,5,6,7-hexamethylindenyl)iron(II) has previously been reported to have similar absorption bands centred at 425 nm and 550 nm.[11c] The relative invariance of the absorption spectra for the methyl-substituted bis(indenyl)iron(II) complexes suggests that their metal-based molecular orbitals, including the HOMO and LUMO, are all affected to the same degree by the sigma inductive effects of the methyl groups. The effect of methylation on the molecular orbitals of **3.20** has previously been studied by photoelectron spectroscopy.[11b] Methylation of the indenyl ligand was shown to decrease the ionization energies of all the molecular orbitals, with the magnitude of the decrease being greater for the ligand-based ionizations. The metal-based ionizations all decreased by similar amounts, an indication that while methylation raises the energy of the molecular orbitals, the gap between the orbitals remains constant.

The introduction of trimethylsilyl substituents to the indenyl ligand can be seen to have a greater effect on the absorption spectra of the resulting bis(indenyl)iron(II) complexes (**3.28** – **3.31**). The addition of a single trimethylsilyl group induces shifts in the absorption bands of 6–18 nm while disubstitution red shifts both bands by 40–62 nm. A similar situation is observed for trimethylsilyl-substsituted bis(cyclopentadienyl)iron, with the absorption arising from the $^1A_{1g} \rightarrow {}^1E_{1g}$ transition shifting to lower energy with increasing substitution.[52] These shifts were attributed to the electron-withdrawing effect of the trimethylsilyl substituent, though a poor correlation was observed between λ_{max} and substituent parameters. From these results, it appears that the π-acceptor effect of the trimethylsilyl substituent destabilizes the HOMO to a greater degree than the LUMO.

The introduction of a diphenylphosphino group to **3.20** induces minor shifts in the bands of UV/visible spectrum of 4–6 nm. Similarly, ferrocene and dppf have been shown to exhibit near identical absorption and photoelectron spectra, an indication

that the HOMO and LUMO are destabilized to the same degree by the phosphine moiety.[61] The introduction of a methyl or trimethylsilyl group to **3.32** can be seen to red-shift the low energy absorption band. The magnitude of the red-shift is dependent on both the substituent and the position of the substitution. It appears that the addition of multiple substituents has a considerable effect on the molecular orbitals of the indenyl ligands.

3.10. Conclusions

The preparation of a range of methyl-, trimethylsilyl-, and diphenylphosphino-substituted indenes has been described by salt elimination/metathesis reactions. The indenes were subsequently used in the preparation of bis(indenyl)iron(II) complexes. For heterotopic indenyl ligands, the ferrocenes were obtained as mixtures of *racemic* and *meso* isomers.

Crystallographic studies on six of the bis(indenyl)iron(II) complexes were carried out. The indenyl ligands are all coordinated in an η^5-manner. The complexes prefer to adopt a conformation in which the indenyl ligands lie over top of one another in a π-offset arrangement. This conformation is believed to maximize π–π-stacking interactions between the benzo rings.

The electrochemistry of the bis(indenyl)iron(II) complexes was studied by cyclic voltammetry. The introduction of methyl substituents can be seen to decrease the potential at which oxidation occurs, while trimethylsilyl and diphenylphosphino substituents increase the oxidation potential, relative to **3.20**. The changes in oxidation potential are additive, allowing for the prediction to be made for the oxidation potential of multi-substituted bis(indenyl)iron(II) complexes. The accuracy of the calculations decreases with increasing substitution due to steric effects.

The UV/visible spectra of the bis(indenyl)iron(II) complexes were obtained and found to contain two absorption bands corresponding to spin-allowed d-d transitions. The bands are unaffected by the introduction of σ-inductive effects of methyl

substituents but are red-shifted upon the addition of the π-accepting trimethylsilyl substituent.

References

1. (a) Kealy, T.J.; Pauson, P.L. *Nature* **1951**, *168*, 1039. (b) Miller, S.A.; Tebboth, J.A.; Tremaine, J.F. *J. Chem. Soc*. **1952**, 633.
2. *Ferrocenes*; Togni, A.; Hayashi, T.; VCH: New York, **1995**.
3. (a) Fischer, E.O.; Seus, D. *Z. Naturforsch*. **1953**, *8b*, 694. (b) Pauson, P.L; Wilkinson, G. *J. Am. Chem. Soc*. **1954**, *76*, 2024.
4. O'Connor, J.M.; Casey, C.P. *Chem. Rev*. **1987**, *87*, 307.
5. (a) Hart-Davis, A.J.; Mawby, R.J. *J. Chem. Soc. (A)* **1969**, 2403. (b) Ji, L.-N.; Rerek, M.E.; Basolo, F. *Organometallics* **1984**, *3*, 740. (c) Jones, D.J.; Mawby, R.J. *Inorg. Chim. Acta* **1972**, *6*, 157.
6. Lee, C.C.; Sutherland, R.G.; Thomson, B.J. *Chem. Commun*. **1971**, 1071.
7. Treichel, P.M.; Johnson, J.W. *J. Organomet. Chem*. **1975**, *88*, 207.
8. (a) Rigby, S.S.; Decken, A.; Bain, A.D.; McGlinchey, M.J. *J. Organomet. Chem*. **2001**, *637-639*, 372. (b) Albright, T.A.; Hofmann, P.; Hoffmann, R.; Lillya, C.P.; Dobosh, P.A. *J. Am. Chem. Soc*. **1983**, *105*, 3396.
9. Wang, B.; Mu, B.; Chen, D.; Xu, S.; Zhou, X. *Organometallics* **2004**, *23*, 6225.
10. (a) Little, W.F.; Reilley, C.N.; Johnson, J.D.; Lynn, K.N.; Saunders, A.P. *J. Am. Chem. Soc*. **1964**, *86*, 1376. (b) Page, J.A.; Wilkinson, G. *J. Am. Chem. Soc*. **1952**, *74*, 6149. (c) Lu, S.; Strelets, V.V.; Ryan, M.F.; Pietro, J.; Lever, A.B.P. *Inorg. Chem*. **1996**, *35*, 1013.
11. (a) Treichel, P.M.; Johnson, J.W.; Wagner, K.P. *J. Organomet. Chem*. **1975**, *88*, 227. (b) O'Hare, D.; Green, J.C.; Marder, T.; Collins, S.; Stringer, G.; Kakkar, A.K.; Kaltsoyannis, N.; Kuhn, A.; Lewis, R.; Mehnert, C.; Scott, P.; Kurmoo, M.; Pugh, S. *Organometallics* **1992**, *11*, 48. (c) Alias, F.; Balrow, S.; Tudor, J.S.; O'Hare, D.; Perry, R.T.; Nelson, J.M.; Manners, I. *J. Organomet. Chem*. **1997**, *528*, 47.
12. (a) Rerek, M.E.; Ji, L.; Basolo, F. *J. Chem. Soc., Chem, Commun*. **1983**, 1208. (b) Rakita, P.E.; Davison, A. *J. Organomet. Chem*. **1970**, *23*, 407.

13. Curnow, O.J.; Fern, G.M.; Hamilton, M.L.; Jenkins, E.M. *J. Organomet. Chem*. **2004**, *689*, 1897.
14. Grimmer, N.E.; Coville, N.J.; de Koning, C.B.; Smith, J.M.; Cook L.M. *J. Organomet. Chem*. **2000**, *616*, 112.
15. (a) Cram, D.J.; Almy, J. *J. Am. Chem. Soc*. **1969**, *91*, 4459. (b) Greifenstein, L.G.; Lambert, J.B.; Nienhuis, R.J.; Fried, H.E.; Paganini, G.A. *J. Org. Chem*. **1981**, *46*, 5125. (c) Matsson, O. *J. Chem. Soc. Perkins Trans. II* **1985**, 221.
16. Ready, T.E.; Chien, J.C.W.; Rausch, M.D. *J. Organomet. Chem*. **1999**, *583*, 11.
17. Yarboro, T.L.; Karr, C.; Estep, P.A. *J. Chem. Eng. Data* **1961**, *6*, 421.
18. Bosch, A.; Brown, R.K. *Can. J. Chem*. **1964**, *42*, 1718.
19. Halterman, R.L.; Fahey, D.R.; Bailly, E.F.; Dockter, D.W.; Stenzel, O.; Shipman, J.L.; Khan, M.A.; Dechert, S.; Schumann, H. *Organometallics* **2000**, *19*, 5464.
20. Goffart, J.; Desreux, J.F.; Gilbert, B.P.; Delsa, J.L.; Fenkin, J.M.; Duyckaerts, G. *J. Organomet. Chem*. **1981**, *209*, 281.
21. Ready, T.E.; Chien, J.C.W.; Rausch, M.D. *J. Organomet. Chem*. **1996**, *519*, 21.
22. Fallis, K.A.; Anderson, G.K.; Rath, N.P. *Organometallics* **1992**, *11*, 885.
23. King, R.B.; Bisnette, M.B. *Inorg. Chem*. **1964**, *3*, 796.
24. Osiecki, J.H.; Hoffman, C.J.; Hollis, D.P. *J. Organomet. Chem*. **1965**, *3*, 107.
25. Stenzel, O.; Dechert, S.; Schumann, H. *Organometallics* **2001**, *20*, 1983.
26. Umezawa, Y.; Tsuboyama, S.; Honda, K.; Uzawa, J.; Nishio, M. Bull. Chem. Soc. Jpn. 1998, 71, 1207.
27. (a) Tsuzuki, S.; Honda, K.; Uchimaru, T.; Mikami, M.; Tanabe, K. *J. Am. Chem. Soc*. **2000**, *122*, 3746. (b) Tsuzuki, S.; Honda, K.; Uchimaru, T.; Mikami, M.; Tanabe, K. *J. Am. Chem. Soc*. **2000**, *122*, 11450.
28. Treichel, P.M.; Johnson, J.W.; Calabrese, J.C. *J. Organomet. Chem*. **1975**, *88*, 215.
29. Janiak, J. *J. Chem. Soc., Dalton Trans*. **2000**, 3885.
30. Adams, J.J.; Berry, D.E.; Browning, J.; Burth, D.; Curnow, O.J. *J. Organomet. Chem*. **1999**, *580*, 245.
31. Csaellato, U.; Ajo, D.; Valle, G.; Corain, B.; Longata, B.; Graziani, R. *J. Crystallogr. Spectrosc. Res*. **1988**, *18*, 583.

32. Curnow, O.J.; Fern, G.M.; Hamilton, M.L.; Jenkins, E.M. *J. Organomet. Chem*. **2004**, *689*, 1897.
33. Reetz, M.T.; Beuttenmuller, E.W.; Goddard, R.; Pasto, M. *Tetrahedron Lett*. **1999**, *40*, 4977.
34. Edlund, U. *Org. Magn. Reson*. **1978**, *11*, 516.
35. Houlton, A.; Bishop, P.T.; Roberts, R.M.G.; Silver, J.; Herberhold, M. *J. Organomet. Chem*. **1989**, *364*, 381.
36. (a) Kohler, F.H. *Chem. Ber*. **1974**, *107*, 570. (b) Baker, R.T.; Tulip, T.H. *Organometallics* **1986**, *5*, 839.
37. Cadierno, V.; Diez, J.; Gamasa, M.P.; Gimeno, J.; Lastra, E. *Coord. Chem. Rev*. **1999**, *193-195*, 147.
38. Forschner, T.C.; Cutler, A.R.; Kullnig, R.K. *Organometallics* **1987**, *6*, 889.
39. (a) Stradiotto, M.; Hughes, D.W.; Bain, A.D.; Brook, M.A.; McGlinchey, M.J. *Organometallics* **1997**, *16*, 5563. (b) Waldbaum, B.R.; Kerber, R.C. *Inorg. Chim. Acta* **1999** *291* 109.
40. (a) Faller, J.W.; Crabtree, R.H.; Habib, A. *Organometallics* **1985**, *4*, 929. (b) Calhorda, M.J.; Veiros, L.F. *Coord. Chem. Rev*. **1999**, *185-186*, 37.
41. Westcott, S.A.; Kakkar, K.; Stringer, G.; Taylor, N.J.; Marder, T.B. *J. Organomet. Chem*. **1990**, *394*, 777.
42. Webb, N.C.; Marsch, R.E. *Acta Crystallogr*. **1967**, *22*, 382.
43. Merola, J.S.; Kacmarcik, R.T.; Van Engen, D. *J. Am. Chem. Soc*. **1986**, *108*, 329.
44. Trotter, J. *Acta Crystallogr*. **1958**, *11*, 355.
45. Murphy, V.J.; O'Hare, D. *Inorg. Chem*. **1994**, *33*, 1833.
46. Little, W.F.; Reilley, C.N.; Johnson, J.D.; Saunders, A.P. *J. Am. Chem. Soc*. **1964**, *86*, 1382. (b) Fujita, E.; Gordon, B.; Hillman, M. *J. Organomet. Chem*. **1981**, *218*, 105. (c) Hoh, G.L.K.; McEwen, W.E.; Kleinberg, J. *J. Am. Chem. Soc*. **1961**, *93*, 3949. (d) Britton, W.E.; Kashyap, R.; El-Hashash, M.; El-Kady, M. *Organometallics* **1986**, *5*, 1029. (e) Hall, D.W.; Russell, C.D. *J. Am. Chem. Soc*. **1967**, *89*, 2316.
47. Gubin, S.P. *Pure Appl. Chem*. **1970**, *23*, 463.
48. Calhorda, M.J.; Veiros, L.F. *J. Organomet. Chem*. **2001**, *635*, 197.

49. Crossley, N.S.; Green, J.C.; Nagy, A.; Stringer, G. *J. Chem. Soc., Dalton Trans*. **1989**, 2139.
50. (a) Gassman, P.G.; Macomber, D.W.; Hershberger, D.W. *Organometallics* **1983**, *2*, 1471. (b) Robbins, J.L.; Edelstein, N.; Spencer, B.; Smart, J.C. *J. Am. Chem. Soc*. **1982**, *104*, 1882.
51. Bassindale, A.R.; Taylor, P.G. In *The Chemistry of Organic Silicon Compounds*; Patai, S.; Rappoport, Z., Eds.; John Wiley: New York, **1989**; p. 893.
52. Okuda, J.; Albach, R.W.; Herdtweck, E.; Wagner, F.E. *Polyhedron* **1991**, *10*, 1741.
53. Brady, E.D.; Overby, J.S.; Meredith, M.B.; Mussman, A.B.; Cohn, M.A.; Hanusa, T.P.; Yee, G.T.; Pink, M. *J. Am. Chem. Soc*. **2002**, *124*, 9556.
54. Bradley, C.A.; Flores-Torres, S.; Lobkovsky, E.; Abruna, H.D.; Chirik, P.J. *Organometallics* **2004**, *23*, 5332.
55. (a) Zanello, P.; Opromolla, G.; Giorgi, G.; Sasso, G.; Togni, A. *J. Organomet. Chem*. **1996**, *506*, 61. (b) Durfey, D.A.; Kiriss, R.U.; Frommen, C.; Feighery, W. *Inorg. Chem*. **2000**, *39*, 3506. (c) Horie, M.; Sakano, T.; Osakada, K.; Nakao, H. *Organometallics* **2004**, *23*, 18. (d) Barriere, F.; Kiriss, R.U.; Geiger, W.E. *Organometallics* **2005**, *24*, 48.
56. Zanello, P. In *Ferrocenes*; Togni, A., Hayashi, T., Eds.; VCH: New York, **1995**; Chapter 7, pp 317-430.
57. Pilloni, G.; Longato, B.; Corain, B. *J. Organomet. Chem*. **1991**, *420*, 57.
58. (a) Sohn, Y.S.; Hendrickson, D.N.; Gray, H.B. *J. Am. Chem. Soc*. **1971**, *93*, 3603. (b) Warren, K.D. *Inorg. Chem*. **1974**, *13*, 1317. (c) Warren, K.D.; Gordon, K.R. *Inorg. Chem*. **1978**, *17*, 987. (d) Nielson, D.; Boone, D.; Eyring, H. *J. Chem. Phys*. **1972**, *76*, 511.
59. Adapted from: (a) Shriver and Atkins, *Inorganic Chemistry 3rd Edition*, Oxford University Press, **1999**, Chapter 16, p. 568. (b) Reference 49.
60. Williamson, B.E. personal communication.
61. Favero, G.; Pilloni, G.; Corain, B.; Longato, B.; Ajo, D.; Russo, U.; Kreissl, F.R. *Inorg. Chim. Acta* **1989**, *157*, 259.

Chapter 4

Chapter 4: Isomerization of Ferrocenylphosphines

4.1. Introduction

Phosphine-functionalized ferrocenes continue to be intensively investigated for their utility in homogeneous catalysis, with chiral derivatives being of particular interest for asymmetric catalysis.[1] The chirality in the ferrocenes can arise from the introduction of a stereogenic side-chain, the use of cyclopentadienyl ligands with enantiotopic faces (planar chirality), or the combination of both (Figure 4.1).[2] Ferrocenes containing two planar chiral ligands may exist as *racemic* and *meso* isomers.

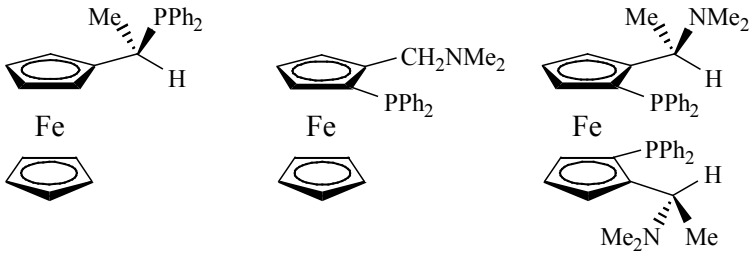

Figure 4.1. Examples of chiral ferrocenylphosphines.

The polymerization performance of planar chiral group 3 and 4 *ansa*-metallocene catalysts has been shown to be diastereomer dependent, with the *racemic* isomer producing the desired isotactic polymers.[3] These differences in performance have led to the *racemic* isomer being the more desired product from the metalation of enantiotopic cyclopentadienyl ligands. Brintzinger has suggested that the *rac*:*meso* ratio may be kinetically controlled by the face selection for the coordination of the second cyclopentadienyl ligand to the metal,[4] while the observation that some lanthanide *ansa*-metallocenes undergo *rac*/*meso* isomerization to a more stable diastereomer suggests that the ratio may be thermodynamically controlled.[5] Such an isomerization requires one of the cyclopentadienyl ligand to dissociate from the metal and recoordinate by the other face. In addition to lanthanides, this type of isomerization has been observed for metallocenes of group 3 and group 4 metals,[6,7] with a number of the group 4 examples being photochemically initiated.[8] Also of particular note, Hollis and Fu have independently described the *rac*/*meso*

isomerization of group 4 diphosphametallocenes in which a phosphole ligand flips over via an intermediate in which the ligand is coordinated by only the phosphorus atom (Figure 4.2).[9,10]

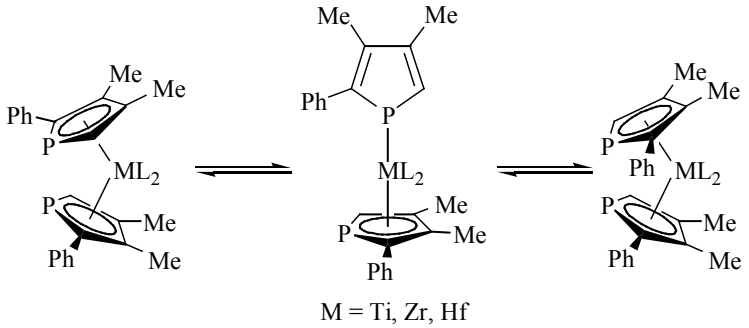

Figure 4.2. Isomerization of diphosphametallocenes.

The *rac*/*meso* isomerizations observed for these other metallocene systems is not generally seen to occur for ferrocenes, though the racemization of acylferrocenes in the presence of strong acids, such as $HClO_4$ and $AlCl_3$, has been reported.[11] However, ferrocenes have been shown to undergo intermolecular exchange processes with cyclopentadienyl ligands being transferred between metal centres. Acylferrocenes have been observed to transfer cyclopentadienyl ligands to rhenium,[12] while a redistribution reaction between ferrocene and 1,1-dimethylferrocene occurs at 250 °C after 3 days.[13] Ruthenocene has been synthesized from ferrocene and $RuCl_3$ at 250 °C.[14]

Recently, the preparation of bis(1-diphenylphosphinoindenyl)iron(II) (**4.2**) was described along with the characterization of its *rac* and *meso* isomers by X-ray crystallographic studies of their tetracarbonylmolybdenum complexes.[15] This chapter describes the facile ring-flipping isomerization of ***meso*-4.2** to ***rac*-4.2** and the mechanistic studies that were carried out to elucidate the mechanism of the process.

4.2. *Rac*/*meso* isomerization of bis(1-diphenylphosphinoindenyl)iron(II) (4.2)

The reaction of 1-diphenylphosphinoindenyllithium with anhydrous ferrous chloride in tetrahydrofuran initially produces equal amounts of two phosphorus-containing compounds as evidenced by peaks in the $^{31}P\{^{1}H\}$-NMR spectrum at –

22.26 and –26.53 ppm. If the reaction is allowed to proceed for longer than 12 h, the peak at –26.53 ppm almost disappears, leaving a single product (Scheme 4.1). This compound was shown, by X-ray crystallography, to be ***rac*-4.2**. If the reaction is terminated after 2 h by the removal of solvent, the product can be isolated as mixture of *racemic* and *meso* isomers.

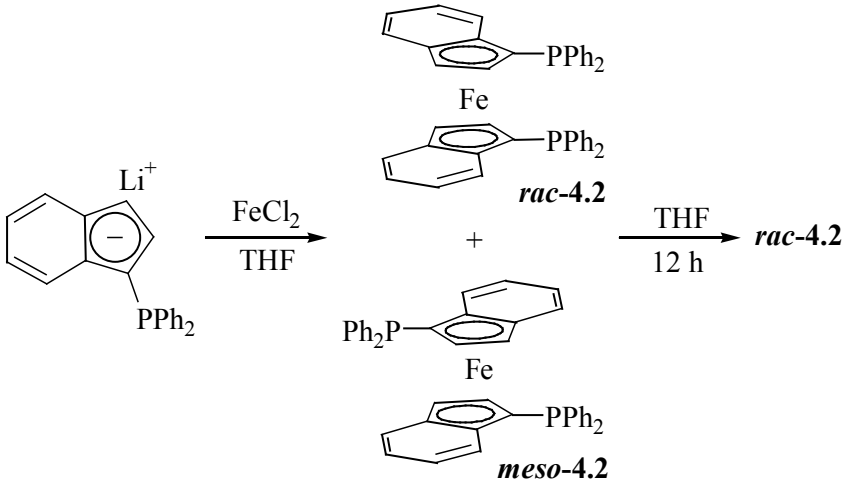

Scheme 4.1. Synthesis and Isomerization of 4.2.

The isomerization of ***meso*-4.2** to ***rac*-4.2** was followed by ^{31}P-NMR spectroscopy as a function of temperature (Figure 4.3). The isomerization does not go to completion, an indication that the reverse process of *racemic* to *meso* isomerization is also occurring. The equilibrium lies on the side of the *racemic* isomer, with an equilibrium constant of K = 13.5(9) in neat THF at 23 °C. The isomerization is first-order with respect to the concentration of ***meso*-4.2**, with plots of decreasing integral versus time being analyzed with a single-exponential function. From these plots, the observed rate constants (k_{obs}) were obtained (Table 4.1). A linear plot of $\ln(k_{obs}/T)$ versus 1/T (Figure 4.4) allowed for the determination of the activation parameters for the isomerization process, with the enthalpy and entropy of activation being $\Delta H^{\ddagger} = 58 \pm 4$ kJ mol^{-1} and $\Delta S^{\ddagger} = -140 \pm 15$ J mol^{-1} K^{-1}, respectively. The negative entropy of activation is indicative of a highly ordered transition state while the positive value for $\Delta H^{\ddagger}$ reflects the bond disruption energy required to overcome the formal charge separation between the cyclopentadienyl groups and the metal core.

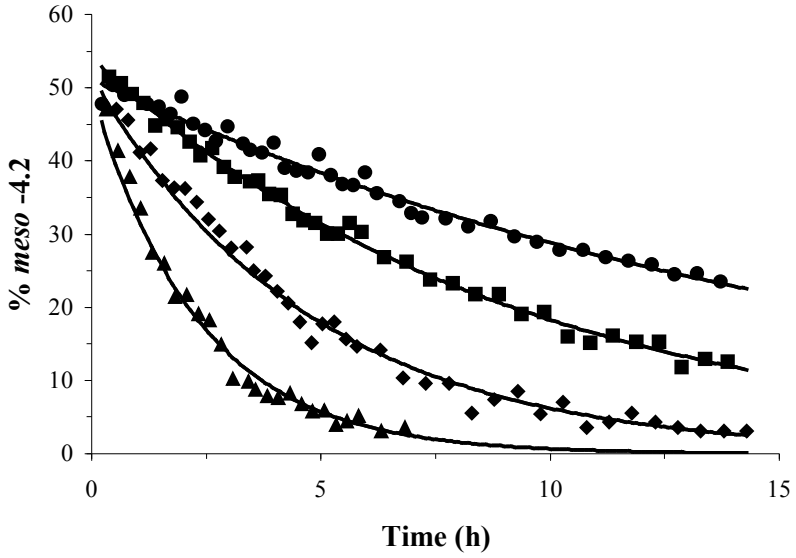

Figure 4.3. Isomerization of *meso*-4.2 to *rac*-4.2 in THF at various temperatures (top to bottom: 23, 30, 40, 50 °C).

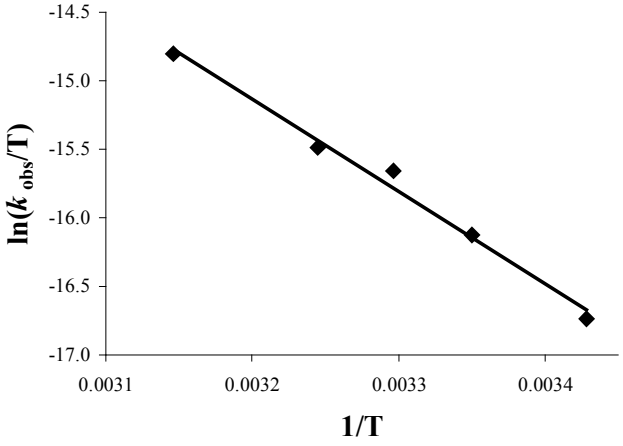

Figure 4.4. Plot of ln(k_{obs}/T) versus 1/T for the isomerization of *meso*-4.2 to *rac*-4.2.

Table 4.1. Temperature dependence on rate of isomerization.

T (K)	k_{obs} (10^{-5} s^{-1})	$t_{1/2}$ (h)	T (K)	k_{obs} (10^{-5} s^{-1})	$t_{1/2}$ (h)
296[a]	3.60(9)	5.3	308	4.89(14)	3.9
296	1.59(3)	12.1	313	5.89(16)	3.3
303	3.01(9)	6.4	323	12.0(4)	1.6

[a] Rate of isomerization during synthesis.

The rate of isomerization for **4.2** is considerably faster during the initial synthesis than for the isolated compound. During the initial synthesis ([**4.2**] = 0.0605 M, T = 23 °C) the observed rate constant is [3.60(9)] x 10^{-5} s^{-1}, while in neat THF at 23 °C, the rate was found to be [1.59(3)] x 10^{-5} s^{-1}. The increased rate observed during the synthesis of **4.2** is due to the presence of dissolved LiCl (see below). Previous studies have shown the presence of dissolved salts substantially increase the rate of *rac*/*meso* isomerization for substituted metallocenes. Marks and co-workers suggested that Li^+ assisted with the heterolysis of the M–Cp bond by the formation of the lithium cyclopentadienyl ion pair,[5a,b] while Bercaw et al. demonstrated that increasing the ionic strength of the solution was sufficient to promote the isomerization of *ansa*-scandocene derivatives.[6]

Table 4.2. Rate of Isomerisation for *meso*-4.2 to *rac*-4.2 under various conditions.

[LiCl][a] (M)	k_{obs} (10^{-5} s^{-1})	$t_{1/2}$ (h)	$CDCl_3$ in THF[b] (%)	k_{obs} (10^{-5} s^{-1})	$t_{1/2}$ (h)
0	3.01(9)	6.4	0	3.01(9)	6.4
0.019	3.58(20)	5.4	25	1.26(3)	15.3
0.038	6.83(20)	2.8	40	0.87(3)	22.1
0.076	35.9(6)	0.53	50	0.62(2)	31.1

[a] In THF at 303 K. [b] At 303 K

The effect of dissolved salts on the isomerization process was investigated by the addition of LiCl (Table 4.2). Significant increases in the rate of isomerization were obtained, with a greater than ten-fold increase in the rate when [LiCl] = 0.076 M (approximately 4 equivalents of LiCl, relative to **4.2**). This suggests that the isomerization proceeds via a charged (or highly polar) intermediate that is stabilized by the presence of the dissolved salt. The effect of the anionic component of the salt was investigated by carrying out the isomerization in the presence of $LiClO_4$. The rate

of isomerization is identical, within experimental error, to that observed for the reaction in the presence of LiCl (k_{obs} = [6.3(6)] x 10^{-5} s^{-1}, [$LiClO_4$] = 0.038 M, T = 303 K). The identical rates suggest that a coordinating anion is not necessarily a requirement for the isomerization process to occur. Similar effects have been observed by Bercaw et al., with the isomerization of *ansa*-scandocenes proceeding at identical rates in the presence of either LiCl or $LiB(C_6F_5)_4$.[6]

The diastereomers of **4.2** are configurationally stable in noncoordinating solvents such as chloroform and dichloromethane. However, isomerization occurs upon dissolution of ***meso*-4.2** in the polar coordinating solvent THF. Donor solvents have previously been shown to increase the rate of isomerization for a variety of substituted metallocenes, with the solvent believed to be stabilizing coordinatively unsaturated intermediates.[6,9a,10] The solvent dependency was investigated by carrying out the isomerization in varying ratios of THF and chloroform (Table 4.2). The rate of isomerization decreases significantly with increasing chloroform concentration, with the rate being approximately proportional to the square of the THF concentration (Figure 4.5). While this suggests that a coordinating solvent is required for the isomerization to occur, the high polarity of the THF must also be taken into account when interpreting this result.

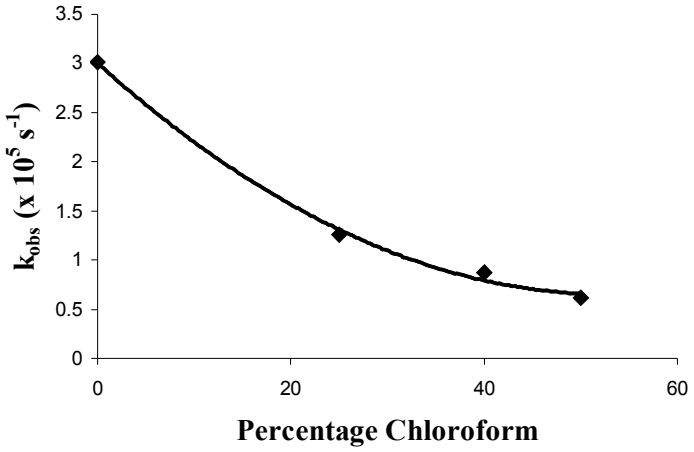

Figure 4.5. Effect of increasing the amount of chloroform on the rate of isomerization for *meso*-4.2 to *rac*-4.2 at 30 °C.

On the basis of these observations, a mechanism (Scheme 4.2) is proposed for the isomerization of ***meso*-4.2** to ***rac*-4.2** in which coordination of THF to the metal induces ring-slippage of the indenylphosphine ligand until heterolysis of the metal-indenyl bond occurs completely and the ligand is coordinated by only the phosphorus atom (intermediate **III**). Recoordination of the five-membered ring could then occur by either face, resulting in inversion or retention of configuration. The solvent-assisted heterolysis of the metal–carbon bond (**II** to **III**) is the rate-determining step. The large negative entropy of activation supports an associative rate-determining step and a solvent-stabilized intermediate while the presence of ionic species such as LiCl could stabilize the zwitterionic intermediate **III**.

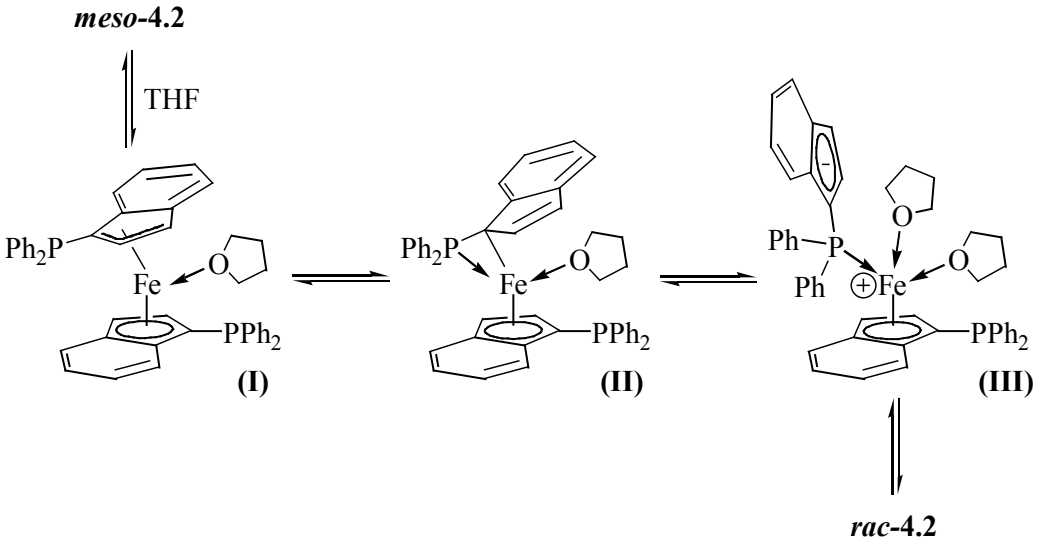

Scheme 4.2. Preferred Mechanism for the Isomerization of *meso*-4.2 to *rac*-4.2.

4.3. Mechanistic Studies

In order for the isomerization of ***meso*-4.2** to ***rac*-4.2** to take place, one of the indenyl ligands needs to flip over and coordinate to the iron atom by its other face. For this to occur, the indenyl ligand must either completely dissociate from the metal or undergo ring-slippage reactions. Both mechanisms have previously been seen in the *rac*/*meso* isomerization of substituted metallocenes.

The preferred mechanism for the isomerization is shown in Scheme 4.2. In addition to this, other mechanisms involving ring-slippage reactions were also considered (Scheme 4.3). For isomerization to occur via intermediates **IV** and **VI**, ring-slippage must be accompanied by a [1,5]-proton shift to give **V** and **VII**. Miyoshi et al. have recently isolated a compound, $[Fe(P(OMe)_3)_2(\eta^5:\eta^1\text{-}PPhS(C_5H_4)_2)]$, in which ring-slippage of one of the cyclopentadienyl ligands is followed by a [1,5]-proton shift as a result of coordination of $P(OMe)_3$ to the starting [1]ferrocenophane.[16] For this type of mechanism to be operating in the case of **4.2**, the aromatic nature of the system must be disrupted at some point (isoindene intermediates **IV** and **VII**) resulting in an increase in activation energy for the process. McGlinchey et al. demonstrated that the indene ligand in $(\eta^5\text{-}C_5H_5)Fe(CO)_2(\eta^1\text{-}C_9H_7)$ undergoes successive [1,5]-suprafacial shifts via an isoindene intermediate.[17] The activation energy of this process was reported to be 10 kcal mol^{-1} higher than what had been reported for $(\eta^5\text{-}C_5H_5)Fe(CO)_2(\eta^1\text{-}C_5H_5)$. In order to establish if the isomerization is proceeding via these isoindene intermediates, deuterium-labeling studies were carried out on **4.2**.

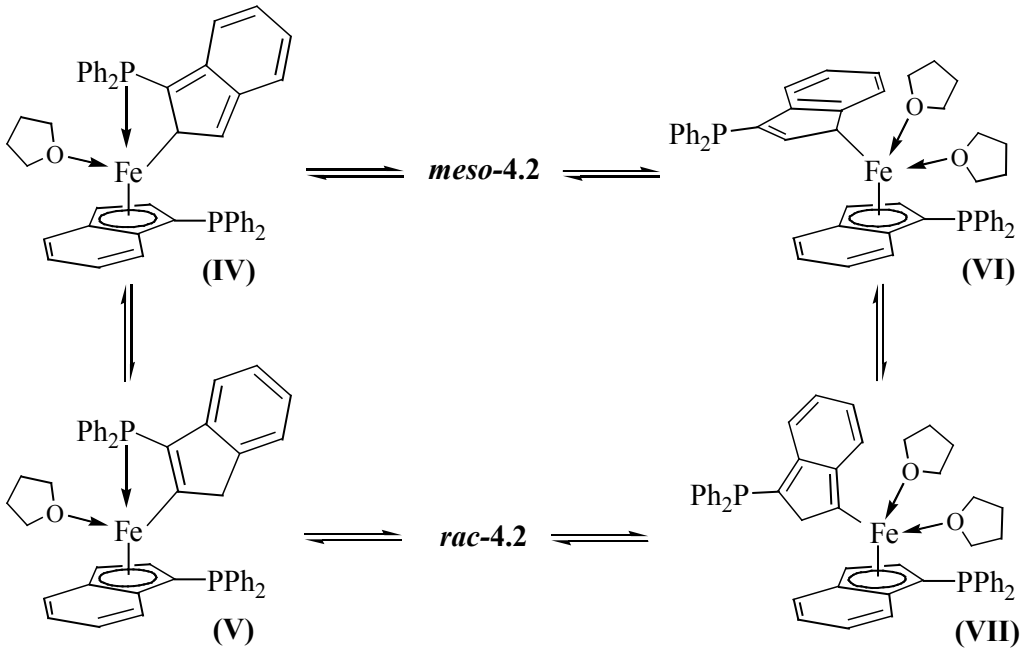

Scheme 4.3. Possible [1,5]-proton shift mechanisms.

Bis(3-deuterio-1-diphenylphosphinoindenyl)iron(II) (**4.2-*d*$_2$**) was synthesized by the reaction of 3-deutrio-1-diphenylphosphinoindenyllithium with anhydrous ferrous chloride as shown in Scheme 4.4. The ferrocene was isolated as a 60:40 mixture of *racemic* and *meso* diastereomers. Both ^{1}H and ^{2}H-NMR spectroscopy confirmed that the deuterium is present in only the 1- and 1′-positions of both diastereomers while mass spectrometry revealed the presence of both **4.2-*d*$_2$** and **4.2-*d*$_1$** in a ratio of 85:15 (a consequence of incomplete deuteration of **4.1**). The isomerization of ***meso*-4.2-*d*$_2$** to ***rac*-4.2-*d*$_2$** was carried out in an identical manner to that of the nondeuterated analogue. Analysis of the NMR spectra of the isolated *racemic* isomer showed no incorporation of deuterium into the 2- and 2′-position of the indenyl ligand. This result effectively rules out the possibility of the isomerization proceeding via isoindene intermediates as [1,5]-proton shifts would result in scrambling of the position of the deuterium.[18]

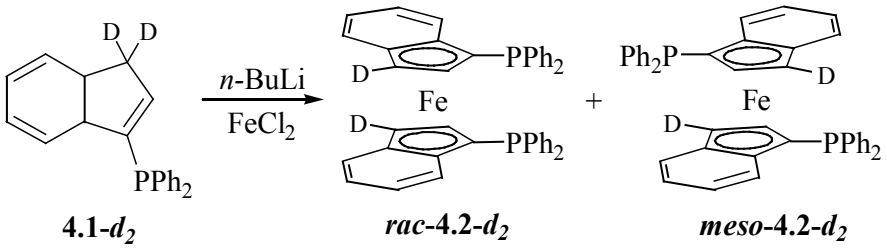

4.1-*d*$_2$ ***rac*-4.2-*d*$_2$** ***meso*-4.2-*d*$_2$**

Scheme 4.4. Synthesis of 4.2-*d*$_2$.

Mechanisms in which complete dissociation of the indenylphosphine ligand occurs may also lead to *rac*/*meso* isomerization. Complete dissociation of one of the indenyl ligands from ***meso*-4.2**, in the presence of THF, could give the monocationic piano-stool complex **VIII** (Scheme 4.5). Related complexes in which solvent molecules are coordinated to Cp–metal moieties are well known and are often used in the synthesis of mixed-ring metallocenes. Complex **VIII** could then either recoordiante an indenyl ligand by the other face to give ***rac*-4.2** or react with another molecule of ***meso*-4.2** to give the triple-decker sandwich complex **IX**. Reaction of THF at the other iron centre would lead to the formation of the ***rac*-4.2** and another molecule of **VII**. In order to eliminate these as possible mechanisms, two experiments were performed using deuterium labeled material. First, the isomerization of a ***meso*-**

and ***rac*-4.2** in the presence of 3-deuterio-1-diphenylphosphinoindenyllithium was shown to yield ***rac*-4.2** with no incorporation of deuterium (as shown by mass spectrometry and ^{1}H-NMR spectroscopy). Second, a crossover experiment was attempted by carrying out the isomerization of a 1:1 mixture of **4.2** and **4.2-*d*$_2$**. Analysis of the isotope pattern from EI-MS indicates the product contains: 49% **4.2**, 12% **4.2-*d*$_1$**, and 39% **4.2-*d*$_2$**. These values are consistent, within experimental error, with what is expected if a crossover mechanism is not occurring (50% **4.2**, 7.5% **4.2-*d*$_1$**, and 42.5% **4.2-*d*$_2$**). Both these results explicitly rule out the possibility of a dissociative mechanism for the isomerization of **4.2**.

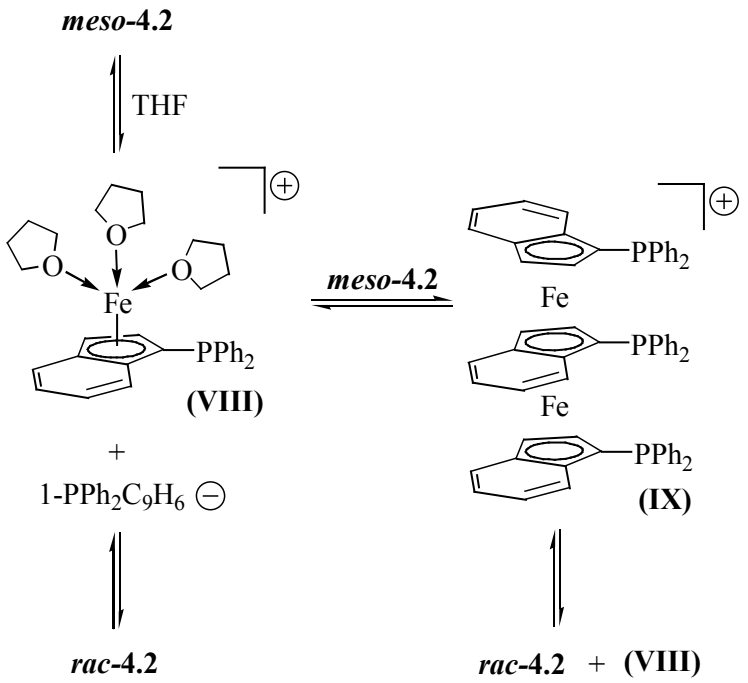

Scheme 4.5. Possible Dissociative Mechanisms.

In further support of the mechanism proposed in Scheme 4.2, the effect of pressure on the rate of isomerization was investigated in order to determine the volume of activation.[19] The rate of isomerization increases with increasing pressure, with a linear plot of RTln(k) versus pressure (Figure 4.6) allowing for the determination of the volume of activation ($\Delta V^{\ddagger} = -12.9 \pm 0.8$ cm^3 mol^{-1}). This negative volume of activation is consistent with the isomerization proceeding via an associative type mechanism.[20]

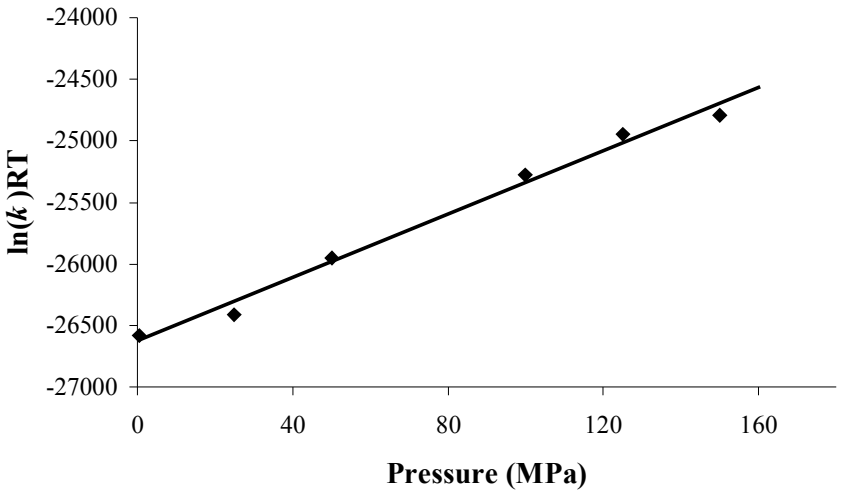

Figure 4.6. Plot of ln(*k*)RT versus pressure for the isomerization of *meso*-4.2 to *rac*-4.2 in THF.

4.4. *Rac*/*meso* isomerization behavior of other ferrocenylphosphines

The isomerization of ***meso*-4.2** to ***rac*-4.2** is the first example of an intramolecular isomerization of a planar-chiral ferrocenylphosphine system. In an attempt to further understand the factors influencing the isomerization process, a number of methyl derivatives of **4.2** (Figure 4.7) were prepared and their isomerization behaviour and structural features examined.

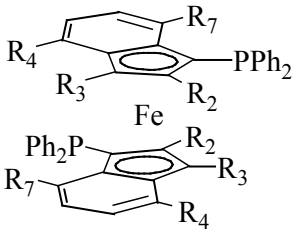

4.3 $R_2 = CH_3$; $R_{3,4,7} = H$
4.4 $R_3 = CH_3$; $R_{2,4,7} = H$
4.5 $R_{2,3} = CH_3$; $R_{4,7} = H$
4.6 $R_{4,7} = CH_3$; $R_{2,3} = H$

Figure 4.7. Methyl-substituted derivatives of 4.2.

The preparations of **4.3**–**4.5** were described in chapter 3, while **4.6** was prepared elsewhere.[21] The ferrocenes were all initially prepared as mixtures of *racemic* and *meso* diastereomers as evidenced by peaks in the ^{31}P-NMR spectrum. The amount of each diastereomer varied between the ferrocenes with isomeric ratios of 3:2 for **4.3**,

3:1 for **4.4**, 5:2 for **4.5**, and 1:1 for **4.6**. These ratios did not change with prolonged stirring at ambient (or higher) temperature. The lack of isomerization for these ferrocenes suggests that the increased steric protection of the iron atom and the electron-donating ability of the methyl groups (see Chapter 3, Electrochemistry) are preventing nucleophilic attack at the iron by the solvent THF molecules. Interestingly, bis(1-(diisopropylphosphino)indenyl)iron(II) has been shown to undergo *rac*/*meso* isomerization at rates comparable to **4.2**.[21] At 23 °C and 30 °C the observed rate constants were found to be [1.75(30)] x 10^{-5} s^{-1} and [3.05(2)] x 10^{-5} s^{-1}, respectively, while for **4.2** the equivalent rates were [1.59(3)] x 10^{-5} s^{-1} and [3.01(9)] x 10^{-5} s^{-1}, respectively. The similarity of the rates suggest that the nucleophilicity of the phosphine, diisopropyl versus diphenyl, does not have an effect on the isomerization and is consistent with the rate-determining step involving coordination THF solvent and indenyl ring-slippage.

As the *rac*/*meso* isomerization was only observed for the two systems with the least amount of steric crowding around the iron atom, the preparation of a mixed-ligand ferrocene was undertaken. (4,7-Dimethyl-1-diphenylphosphinoindenyl)(1-diphenylphosphinoindenyl)iron(II) (**4.8**) was synthesized by the reaction of ferrous chloride with a 1:1 mixture of 4,7-dimethyl-1-diphenylphosphinoindenyllithium and 1-diphenylphosphinoindenyllithium in tetrahydrofuran as shown in Scheme 4.6. The ^{31}P-NMR spectrum of the reaction mixture initially contains eight ferrocenylphosphine signals, four of which are assigned to the diastereomers of **4.2** and **4.6** while the other four correspond to the *rac* and "*meso"* isomers of **4.8**. It should be noted that "*meso"* isomer of **4.8** actually exists as a pair of enantiomers due to the absence of a mirror-plane. After stirring the reaction mixture for 24 h, all of ***meso*-4.2** had isomerized to ***rac*-4.2**, however, there was no change in the relative intensities of the other signals. From this result, it appears that the addition of two methyl groups to one of the benzo rings is enough of an increase in steric bulk to hinder the isomerization process.

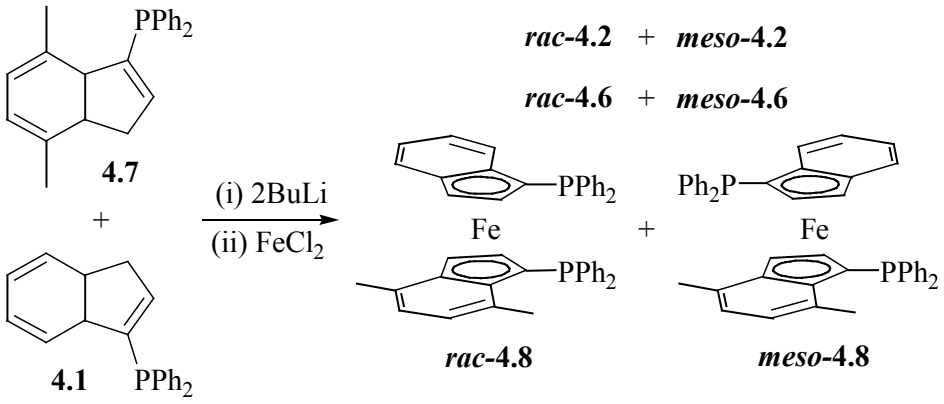

Scheme 4.6. Synthesis of 4.8.

The lack of *rac*/*meso* isomerization observed for **4.3** – **4.8** and other cyclopentadienyl-based ferrocenylphosphines suggests that the process is selective for ferrocenes containing non-sterically crowded indenylphosphine ligands. When compared with cyclopentadienyl ligands, indenyl ligands undergo more facile ring-slippage reactions due to the generation of aromaticity in the six-membered ring upon ring-slippage. In the proposed mechanism (Scheme 4.2), intermediates **I** and **II** contain aromatic six-membered rings and the intermediate **III** contains an aromatic five-membered ring. As a consequence, aromaticity is not lost at any stage. In an analogous cyclopentadienyl system, aromaticity would be lost upon formation of the analogues of **I** and **II**. This suggests that the initial ring-slippage reaction prior to dechelation of the indenyl ligand is important in facilitating the isomerization

4.5. Model studies for the *rac*/*meso* isomerization of 4.2

The proposed mechanism for the *meso*/*rac* isomerization of **4.2** outlined in Scheme 4.2 proceeds via a number of ring-slipped intermediates until complete dechelation of the indenyl ligand occurs, leaving the ligand coordinated only by the phosphorus atom. The presence of the benzo ring in the indenyl ligand stabilizes these distortions by aromatization, a feature that cannot occur in their cyclopentadienyl analogues.[22] Although relatively few η^1- and η^3-indenyl complexes of group 8 metals have been isolated,[17,23] spectroscopic evidence exists for the formation of such species during metallocene synthesis.[24]

The thermal and photochemical reactions between $CpFe(CO)_2I$ and tertiary phosphines are well documented and have been shown to yield both $CpFe(CO)(PR_3)I$ and $[CpFe(CO)_2(PR_3)]I$ in varying amounts.[25] The relative amounts of each product can be altered by variation of reaction time and temperature as well as the presence of catalytic species.[26] Dicarbonyl(η^5-cyclopentadienyl)(η^1-1-diphenylphosphinoindenyl-lithium)iron(II) iodide (**4.9**) was synthesized by the reaction of 1-diphenylphosphino-indenyllithium and $CpFe(CO)_2I$ in tetrahydrofuran as shown in Scheme 4.7. As the five-membered ring of the indenyl ligand is not coordinated to the iron, complex **4.9** is similar in structure to proposed intermediate **III** (Scheme 4.2). In chloroform, **4.9** decomposes readily to yield dicarbonyl(η^5-cyclopentadienyl)(η^1-3-diphenyl-phosphinoindene)iron(II) iodide (**4.10**) and carbonyl(η^5-cyclopentadienyl)iodo(η^1-3-diphenylphosphinoindene)iron(II) (**4.11**). This was confirmed by the independent synthesis of both **4.10** and **4.11** by modifications of literature procedures. In an attempt to reduce the sensitivity of **4.9**, dicarbonyl(η^5-cyclopentadienyl)(η^1-1-diphenyl-phosphinoindenylthallium)iron(II) iodide (**4.12**) was synthesized in an analogous manner.

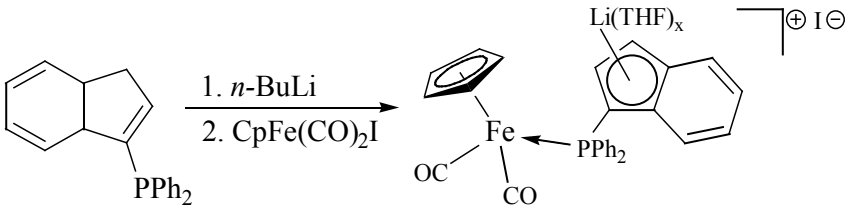

Scheme 4.7. Synthesis of 4.9.

Spectroscopic data for complexes **4.9** – **4.12** are given in Table 4.3. The electronic nature of complexes **4.9** – **4.12** can readily be determined by NMR (^{1}H and ^{31}P) and IR spectroscopy, with previous studies showing that both the chemical shift of the cyclopentadienyl protons and stretching frequencies of the carbonyl groups are sensitive to the changes in the charge density of the Fe atom. When compared with a neutral metal centre, a cationic metal centre will induce an upfield shift in the resonance of the cyclopentadienyl protons and a decrease in the carbonyl stretching frequency. Analysis of the data in Table 4.3 confirms the cationic nature of **4.10** as well as the neutrality of **4.11**. Complex **4.9** can be seen to exist between these two extremes, with both the carbonyl stretching frequency and cyclopentadienyl proton

chemical shift occurring at lower values than those in **4.10** but higher than those in **4.11**.

Table 4.3. Selected spectroscopic data for iron-phosphine complexes.

Compound	^{31}P-NMR[a]	^{1}H-NMR[b]	IR[c]
$CpFe(CO)(PPh_3)I$[d]	–	4.47	1957
$[CpFe(CO)_2PPh_3]I$[e]	67.9	5.50	2045, 2005
4.11	51.5	4.48	1946
4.10	45.5	5.47	2044, 1998
4.9	34.2	4.88	2038, 1992
4.12	34.2	3.88[f]	2032, 1990

[a] Measured in $CDCl_3$. Chemical shifts in ppm (δ) downfield from 85% H_3PO_4 (external). [b] Measured in $CDCl_3$. Chemical shifts in ppm downfield from $SiMe_4$. Resonance corresponds to the cyclopentadienyl protons. [c] υ_{CO} (cm^{-1}). Measured in KBr. [d] Data from ref 27. [e] Data from ref 26,27. [f] Measured in C_6D_6.

Attempts were made to prepare (cyclopentadienyl)(1-diphenylphosphino-indenyl)iron(II) by the thermal and photochemical decarbonylation of **4.9**. Previous studies had shown that the irradiation of $(\eta^5\text{-}C_5H_5)Fe(CO)_2(\eta^1\text{-}C_9H_7)$ and $(\eta^5\text{-}C_9H_7)Fe(CO)_2$ $(\eta^1\text{-}C_9H_7)$ with near-UV light leads to the loss of CO and the formation $(\eta^5\text{-}C_5H_5)Fe(\eta^5\text{-}C_9H_7)$ and $(\eta^5\text{-}\ C_9H_7)_2Fe$, respectively. Unfortunately, the refluxing or near-UV irradiation of a THF solution of **4.9** did not produce any conclusive results.

4.6. Conclusions

The ferrocenylphosphine **4.2** has been shown to undergo an unprecedented and facile *meso* to *rac*emic isomerization. The solvent and salt effects, along with the various activation parameters were measured and are consistent with an associative solvent-assisted ring-slipping process resulting in the dechelation of the indenyl moiety and coordination of the phosphine in the key intermediate species. Deuterium labeling of **4.2** and subsequent isomerization reactions ruled out the possibility of a dissociative intermolecular exchange process occurring. The lack of *rac*/*meso* isomerization for complexes **4.3** – **4.7** is attributed to steric effects with the methyl groups preventing nucleophilic attack at the iron by the solvent THF molecules.

While the isomerization appears to be selective for ferrocenes containing non-sterically crowded indenylphosphine ligands, one can no longer assume the stability of the phosphinoferrocenyl unit with respect to ring-flipping and racemization. In particular, nucleophillic solvents, high salt concentrations, and elevated temperatures (all common conditions in the synthesis of metallocenes) have all been shown to promote the racemization via ring-flipping processes.

References

1. Barbaro, P.; Bianchini, C.; Giambastiani, G.; Parisel, S.L. *Coord. Chem. Rev*. **2004**, *248*, 2131.
2. Colacot, T.J. *Chem. Rev*. **2003**, *103*, 3101.
3. (a) Ewen, J.A. *J. Amer. Chem. Soc*. **1984**, *106*, 6355. (b) Kaminsky, W.; Kulper, K.; Brintzinger, H.-H.; Wild, F.R.W.P. *Angew. Chem., Int. Ed. Engl*. **1985**, *24*, 507. (c) Brintzinger, H.H.; Fischer, D.; Mulhaupt, R.; Rieger, B.;Waymouth, R.N. *Angew. Chem., Int. Ed. Engl*. **1995**, *34*, 1143.
4. Wiesenfeldt, H.; Reinmuth, A.; Barsties, E.; Evertz, K.; Brintzinger, H.-H. *J. Organomet. Chem.* **1989**, *369*, 359.
5. (a) Giardello, M.A.; Conticello, V.P.; Brand, L.; Sabat, M.; Rheingold, A.L.; Stern, C.L.; Marks, T.J. *J. Am. Chem. Soc*. **1994**, *116*, 10212. (b) Haar, C.M.; Stern, C.L.; Marks, T.J. *Organometallics* **1996**, *15*, 1765. (c) Hultzsch, K.C.; Spaniol, T.P.; Okuda, J. *Organometallics* **1997**, *6*, 4845.
6. Yoder, J.C.; Day, M.W.; Bercaw, J.E. *Organometallics* **1998**, *17*, 4946.
7. (a) Diamond, G.M.; Rodewald, S.; Jordan, R.F. *Organometallics* **1995**, *14*, 5. (b) Diamond, G.M.; Jordan, R.F.; Petersen, J.L. *Organometallics* **1996**, *15*, 4030. (c) Christopher, J.N.; Diamond, G.M.; Jordan, R.F.; Petersen, J.L. *Organometallics* **1996**, *15*, 4038. (d) Diamond, G.M.; Jordan, R.J.; Petersen, J.L. *Organometallics* **1996**,*15*, 4045.
8. (a) Schmidt, K.; Reinmuth, A.; Rief, U.; Diebold, J.; Brintzinger,H.-H. *Organometallics* **1997**, *16*, 1724. (b) Kaminsky, W.; Schauwienold,A.-M.; Freidanck, F. *J. Mol. Catal. A* **1996**, *112*, 37. (c) Rheingold, A.L.; Robinson, N.P.; Whelan, J.; Bosnich, B. *Organometallics* **1992**, *11*, 1869. (d) Wild, F.R.W.P.; Zsolnai, L.; Huttner, G.; Brintzinger, H.-H. *J. Organomet. Chem.*

1982, *232*, 233. (e) Wiesenfeldt, H.; Reinmuth, A.; Barsties, E.; Evertz, K.; Brintzinger, H.-H. *J. Organomet. Chem*. **1989**, *369*, 359. (f) Collins, S.; Hong, Y.; Taylor, N. J. *Organometallics* **1990**, *9*, 2695.

9. (a) Hollis, T.K.; Wang, L.-S.; Tham, F. *J. Am. Chem. Soc*. **2000**, *122*, 11737. (b) Hollis, T.K.; Ahn, Y.-J.; Tham, F. *Organometallics* **2003**, *22*, 1432.
10. Bellemin-Laponnaz, S.; Lo, M.M.C.; Peterson, T.H.; Allen, J.M.; Fu, G.C. *Organometallics* **2001**, *20*, 3453.
11. (a) Falk, H.; Lehner, H.; Paul, J.; Wagner, U. *J. Organomet. Chem*. **1971**, *28*, 115. (b) Slocum, D.W.; Tucker, S.P.; Engelmann, T.R. *Tetrahedron Lett*. **1970**, 621.
12. Spradau, T.W.; Katzenellenbogen, J.A. *Organometallics* **1998**, *17*, 2009.
13. Allcock, H.R.; McDonnell, G.S.; Riding, G.H.; Manners, I. *Chem. Mater*. **1990**, *2*, 425.
14. Gauthier, G. *J. Chem. Soc., Chem. Commun*. **1969**, 690.
15. Adams, J.J.; Berry, D.E.; Browning, J.; Burth, D.; Curnow, O.J. *J. Organomet. Chem*. **1999**, *580*, 245.
16. Mizuta, T.; Imamura, Y.; Miyoshi, K. *J. Am. Chem. Soc*. **2003**, *125*, 2068.
17. Stradiotto, M.; Hughes, D.W.; Bain, A.D.; Brook, M.A.; McGlinchey, M.J. *Organometallics* **1997**, *16*, 5563.
18. (a) Cram, D.J.; Almy, J. *J. Am. Chem. Soc*. **1969**, *91*, 4459. (b) Cram, D.J.; Almy, J. *J. Am. Chem. Soc*. **1970**, *92*, 4316. (c) Miller, L.L.; Boyer, R.F. Cram, D.J.; Almy, J. *J. Am. Chem. Soc*. **1971**, *93*, 650.
19. Curnow, O.J.; Fern, G.M.; Hamilton, M.L.; Zahl, A.; van Eldik, R. *Organometallics* **2004**, *23*, 906.
20. (a) van Eldik, R.; Asano, T.; le Noble, W.J. *Chem. Rev*. **1989**, *89*, 549. (b) Drljaca, A.; Hubbard, C.D.; van Eldik, R.; Asano, T.; Basilevsky, M.V.; le Noble, W.J. *Chem. Rev*. **1998**, *98*, 2167.
21. Curnow, O.J.; Fern, G.M.; Hamilton, M.L.; Jenkins, E.M. *J. Organomet. Chem*. **2004**, *689*, 1897.
22. O'Conner, J.; Casey, C. *Chem. Rev*. **1987**, *87*, 307.
23. (a) Forschner, T.C.; Cutler, A.R.; Kullnig, R.K. *Organometallics* **1987**, *6*, 889. (b) Waldbaum, B.R.; Kerber, R.C. *Inorg. Chim. Acta* **1999** *291* 109.
24. Belmont, J.A.; Wrighton, M.S *Organometallics* **1986**, *5*, 1421.

25. (a) Pandey, V.N. *Inorg. Chim. Acta* **1977**, *22*, L39. (b) Zakrezewski, J. *J. Organomet. Chem*. **1991**, *412*, C23. (c) Liu, L.-K.; Eke, U.B.; Mesubi, M.A. *Organometallics* **1995**, *14*, 3958.
26. (a) Colville, N., Darling, E., Hearn, A., Johnston, P. *J. Organomet. Chem*. **1987**, *328*, 375. (b) Gipson, S., Liu, L-K., Soliz, R. *J. Organomet. Chem*. **1996**, *526*, 393.
27. Schumann, H.; Eguren, L. *J. Organomet. Chem*. **191**, *403*, 183.

Chapter 5

Chapter 5: Complexes of bis(1-diphenylphosphinoindenyl)iron(II)

5.1. Introduction

Multifunctional ligands have found widespread use in the preparation of polymetallic complexes.[1] The presence of two or more metal atoms within these complexes gives rise to the possibility of the metals behaving in a cooperative manner to effect a transformation that would not be possible through the use of either metal alone.[2] The use of a multifunctional ligand eliminates the need for metal-metal bonds to hold the metals close enough for cooperative interaction and helps maintain the integrity of the complex during its reactions. The phosphine and cyclopentadienyl moieties are commonly used in the formation of bifunctional ligands due to the ease with which steric and electronic effects can be tuned.[3]

Ferrocenylphosphines are widely employed in the formation of polymetallic complexes. Of these, 1,1'-bis(diphenylphosphino)ferrocene (dppf) is the most studied. As a ligand, dppf is capable of coordination to a variety of transition metals, with examples of group 5 metalates,[4] carbonyl complexes of group 6, 7, and 8,[5-7] and halo complexes of the late transition metals being known.[8,9] The success of dppf as a ligand has been attributed to the different ways the diphosphine can coordinate to a metal centre, with unidentate, chelate, and bridging coordination modes possible (Figure 5.1).[60] The flexibility of the ferrocenyl core along with the ability of the phosphorus atoms to deviate from coplanarity with the cyclopentadienyl rings makes dppf highly adaptable to the individual requirements of the different metals.

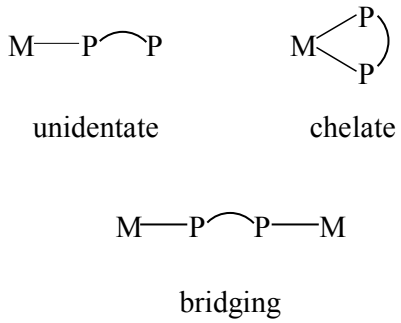

Figure 5.1. Common coordination modes of dppf.

Bimetallic complexes of dppf are known to catalyze a wide variety of organic transformations. Palladium and nickel complexes of dppf are effective catalysts for the cross-coupling of organic moieties,[10-12] while rhodium, ruthenium, and palladium complexes are efficient at the hydrogenation of olefins.[13-15] Platinum complexes of dppf have been employed as catalysts for the hydrosilylation of olefins.[16] Derivatives of dppf containing chiral functionalities have found use in asymmetric catalysis.[17-19]

Recently, the preparation of bis(1-diphenylphosphinoindenyl)iron(II) (**5.1**) was described.[20] The planar chiral nature of the substituted-indenyl ligand means that **5.1** exists in two isomeric forms: a C_2-symmetric *racemic* isomer and a C_s-symmetric *meso* isomer. The tetracarbonylmolybdenum complexes of both the *rac* and *meso* isomers of **5.1** were characterized by X-ray crystallography. The related bis(1-(diphenylphosphino)tetrahydroindenyl)iron(II) has been reported along with the characterization of molybdenum, rhodium, and iridium complexes.[21]

This chapter describes the preparation and isolation of heterobimetallic complexes of the ferrocenylphosphine **5.1**. The palladium complex of **5.1** is assessed as a catalyst for the cross-coupling of alkyl Grignard reagents with aryl bromides.

5.2. Bis(1-diphenylphosphinoindenyl)iron(II) diborane (5.2)

The ability of tertiary phosphines to strongly coordinate to a wide variety of transition metals is well documented. In addition to transition metals, phosphines have been shown to form strongly bonded acid-base adducts with Lewis acidic boranes. The reaction of two equivalents of $BH_3{\cdot}S(CH_3)_2$ with ***rac*-5.1** gave the bis(borane) complex **5.2,** as shown in Scheme 5.1. Complex **5.2** was isolated in good yield (82%) as an air-stable brown powder.

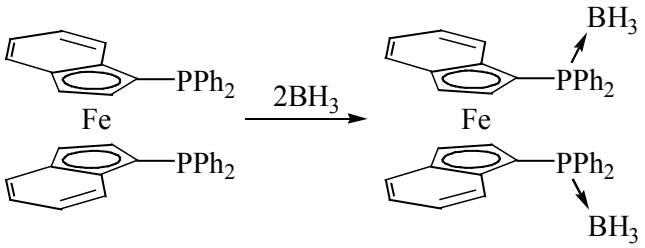

5.2

Scheme 5.1. Synthesis of 5.2.

The NMR spectra for **5.2** are consistent with the formation of the bis(borane) complex. The ^{1}H-NMR spectrum of **5.2** contains an aromatic multiplet centred at 7.00 ppm and two singlets at 3.42 and 5.81 ppm attributed to protons H2 and H3, respectively. The resonance associated with the six BH protons occurs at 1.65 ppm and is broad due to the coupling of these protons to both the phosphorus and boron nuclei. The bonding of the phosphorus lone pair to the borane effects a downfield shift in the resonances of H2 and H3 relative to **5.1**. The observed shift in the resonance of H2 is similar to those observed in dppf·$(BH_3)_2$ while a greater shift is observed for the resonance of H3, indicative of intra-ring shielding effects. The $^{13}C\{^{1}H\}$-NMR spectrum of **5.2** has the phenyl resonances occurring between 129.9 and 135.4 ppm, the benzo resonances between 123.2 and 125.7 ppm, and the five cyclopentadienyl resonances between 62.0 and 91.0 ppm. Complexation of the borane to the phosphines causes an upfield shift in the resonances of the carbons bonded directly of the phosphorus atom. The upfield shifts (5.9, 6.8, and 8.8 ppm for C1 and the two *ipso*-Ph carbons, respectively) are similar to those observed in the analogous dppf complex.[22] In addition to the differences in chemical shifts, complexation of the borane increases the magnitude of the $^{1}J_{PC}$ couplings when compared with **5.1**. This increase in coupling is consistent with the phosphine becoming four-coordinate.[59] The $^{31}P\{^{1}H\}$-NMR spectrum of **5.2** shows a single broad resonance at 16.53 ppm, consistent with complexation of both phosphines to BH_3. The chemical shift is similar to that found for dppf·$(BH_3)_2$ and $Ph_3P{\cdot}BH_3$ (16.5 and 20.7 ppm, respectively) but downfield of that observed for **5.1** (–22.3 ppm).[23]

5.3. (Bis(1-diphenylphosphinoindenyl)iron(II))-*cis*-dichloropalladium(II) (5.3)

Palladium complexes of tertiary phosphine ligands have been extensively used in the field of homogeneous catalysis. Complexes containing dppf have been found to be particularly effective in catalyzing a wide variety of organic transformations.[24] It is anticipated that palladium complexes of **5.1** would also be able to catalyze organic transformation, with the planar chiral nature of the **5.1** providing interesting possibilities in the field of asymmetric catalysis. Previous work within our group had established that the reaction of **5.1** with bis(benzonitrile)dichloropalladium(II) yielded two products in a 4:1 ratio (based on $^{31}P\{^{1}H\}$-NMR spectroscopy).[25] The major product was identified, by X-ray crystallography, to be ***meso*-5.3**. The identity of the minor product was never established.

The reaction of a 1:1 mixture of ***rac*-** and ***meso*-5.1** with bis(benzonitrile)dichloropalladium(II) in tetrahydrofuran produced the two previously observed complexes as evidenced by peaks in the $^{31}P\{^{1}H\}$-NMR spectrum at 33.9 and 35.3 ppm. A 1:1 ratio is observed for these two products, reflecting the original ratio of the isomeric starting material. Previous studies had established the upfield peak of the pair to be associated with ***meso*-5.3**, but no definitive assignment was made on the downfield peak. Repeating the reaction with ***rac*-5.1**, and not an isomeric mixture of **5.1**, a single complex was produced. The $^{31}P\{^{1}H\}$-NMR spectrum of the isolated complex consists of a singlet at 35.3 ppm. Single crystal X-ray structural analysis identified the complex to be ***rac*-5.3**.

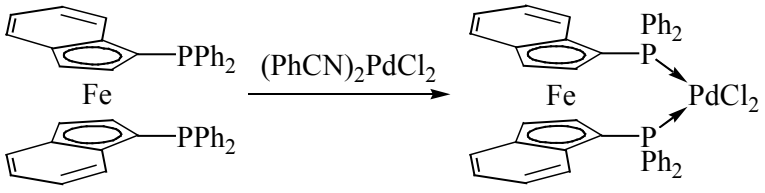

5.3

Scheme 5.2. Synthesis of *rac*-5.3.

Crystals of ***rac*-5.3** suitable for single crystal X-ray structure analysis were obtained from vapour diffusion of diethyl ether into a dichloromethane solution of ***rac*-5.3**. The molecular structure of ***rac*-5.3** is shown in Figure 5.2. Selected bond lengths (Å) and angles (°) are listed in Table 5.1.

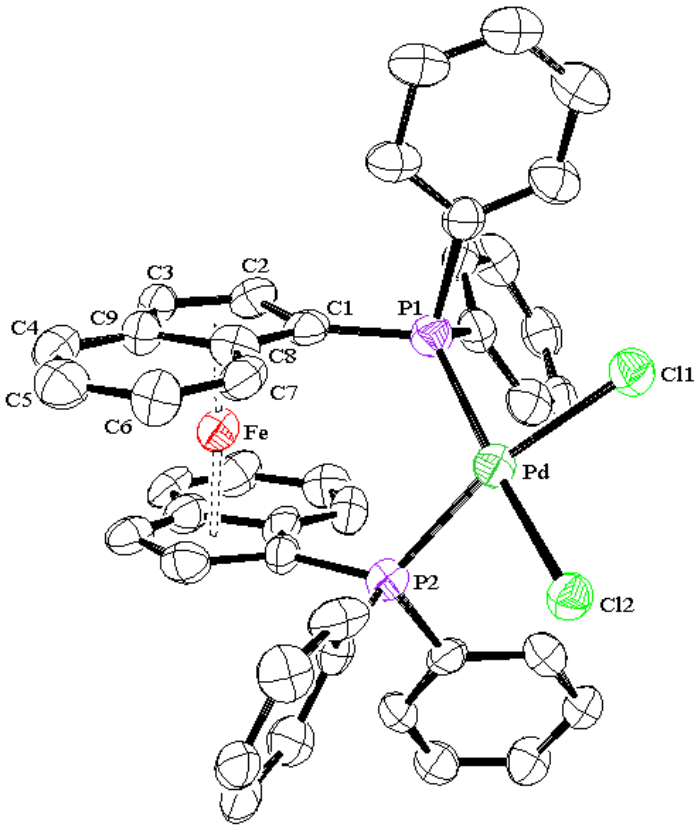

Figure 5.2. ORTEP of *rac*-5.3 indicating the numbering of the atoms. The thermal ellipsoids have been drawn at 50% probability.

Table 5.1. Selected bond lengths [Å] and angles [°] for *rac*-5.3.

Pd-P1	2.275(3)	P1-C1	1.764(11)	Cl1-Pd-Cl2	86.80(10)
Pd-P2	2.282(3)	P2-C1A	1.815(10)	P1-C1-Fe	127.4(5)
Pd-Cl1	2.317(3)	C1-C2	1.455(15)	P2-C1A-Fe	125.2(5)
Pd-Cl2	2.329(3)	C1A-C2A	1.435(15)	C2-C1-C8	104.9(9)
Fe-C1	2.021(10)	C1-C8	1.458(16)	C2A-C1A-C8A	107.9(9)
Fe-C1A	1.999(10)	C1A-C8A	1.422(16)	C1-C2-C3	108.3(10)
Fe-C2	2.036(11)	C2 C3	1.400(15)	C1A-C2A-C3A	108.1(10)
Fe-C2A	2.024(11)	C2A-C3A	1.416(16)	C2-C3-C9	110.9(10)
Fe-C3	2.019(10)	C3-C9	1.372(16)	C2A-C3A-C9A	109.5(10)
Fe-C3A	2.046(11)	C3A-C9A	1.407(17)	C1-C8-C9	108.2(9)
Fe-C8	2.031(10)	C8-C9	1.444(15)	C1A-C8A-C9A	107.4(9)
Fe-C8A	2.069(10)	C8A-C9A	1.471(15)	C3-C9-C8	107.6(10)
Fe-C9	2.029(12)	P1-Pd-P2	100.21(10)	C3A-C9A-C8A	107.0(10)
Fe-C9A	2.080(11)				

Complex ***rac*-5.3** crystallizes in the monoclinic space group $P2_1/n$, with one complete molecule being in the asymmetric unit. The indenyl ligands are coordinated to the iron atom via their five-membered rings in an η^5-fashion. There is a greater variation in the iron-carbon bond lengths of ***rac*-5.3** than previously observed for ***rac*-5.1**. The average Fe-C bond lengths for the indenyl ligands are 2.027 and 2.044 Å for C1-C9 and C1A-C9A, respectively. While these average values are similar, the spread in Fe-C bond lengths differs considerably between ligands, with differences of 0.017 and 0.081 Å between the maximum and minimum Fe-C bond lengths for C1-C9 and C1A-C9A, respectively. The Fe-C bond lengths for C8A and C9A are, on average, 0.049 Å longer than the remaining eight carbons of the five-membered rings. The increased Fe-C bond length observed for C8A and C9A appears to be the result of an unfavorable steric interaction between C7A and C21. In order for both phosphine moieties to coordinate to the palladium, the indenyl ligands of ***rac*-5.3** adopt a conformation in which the rotation angle (RA) is 172.6°, considerably greater than the π-offset conformation observed in ***rac*-5.1** (RA = 20.8°). This enforced rotation brings C21 into close proximity with C7A, with a C···C distance of 3.230 Å. As a consequence, the indenyl rings of ***rac*-5.3** are no longer parallel to one another, with an angle of 4.6° between the planes of the indenyl ligands (compared with 3.0° and

1.9° for ***rac*-5.1** and ***meso*-5.3**, respectively).[25] The slip-fold parameters of ***rac*-5.3** reflect the distortion from planarity, with values of 0.01 and 0.05 Å for C1-C9 and C1A-C9A, respectively. The CNT-Fe-CNTA bond angle of 177.2° is slightly smaller than those seen in ***rac*-5.1** and ***meso*-5.3** (179.6° and 178.7°, respectively) and the Fe-CNT distances (average of 1.634 Å) are similar to those in ***meso*-5.3** (average of 1.632 Å) but shorter than ***rac*-5.1** (1.674 Å).

The diphenylphosphino moieties of ***rac*-5.3** adopt, with respect to each other, a synclinical conformation with a C1-CNT-CNTA-C1A torsion angle of 29.5°. The phosphorus atoms are both displaced out of the C_5 ring plane, towards the Fe atom: P1 by 0.016 Å, and P2 by 0.036 Å. The geometry around the phosphorus atoms is approximately tetrahedral, with average values for C-P-C and C-P-Pd of 103.6° and 114.9°, respectively. The average dihedral angle between the C10-P-C20 and C1-P-Pd planes is 91.8°. The carbon-phosphorus bond lengths are: 1.764, 1.801, 1.798 Å for C1, C10, and C20, respectively; and 1.815, 1.812, 1.809 Å for C1A, C10A, and C20A, respectively. The phenyl rings bonded to P1 adopt orientations similar to what is observed for the phenyl rings of ***rac*-5.1**, with the planes through C1-P1-C10 and C1-P1-C20 bisecting the C_5 ring plane of the indenyl ligand at angles of 87.2° and 14.1° respectively (Figure 5.3). The phenyl rings bonded to P2, however, adopt quite different orientations. Both phenyl rings bonded to P2 are now on the same side of the C_5 ring plane of the indenyl ligand, with the planes through C1A-P2-C10A and C1A-P2-C20A bisecting the C_5 ring plane at angles of 130.0° and 17.6°, respectively (Figure 5.3). This rotation of the diphenylphosphino moiety about the P2-C1A bond forces P2 out of the $PdCl_2$ plane by 0.34 Å. P1 lies within 0.08 Å of the $PdCl_2$ plane. The deviation from the $PdCl_2$ plane is similar to that observed in other palladium-phosphine complexes, with the phosphorus atoms positioned out of the plane by: 0.02 and 0.31 Å for ***meso*-5.3**; and 0.01 and 0.21 Å for (dppf)$PdCl_2$.[26,27]

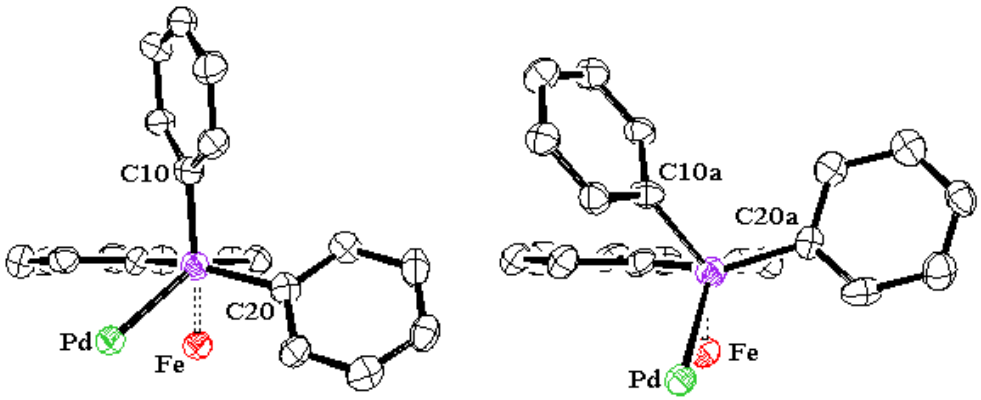

Figure 5.3. Views down P–C1 axes showing orientation of phenyl rings.

The palladium atom in ***rac*-5.3** adopts a distorted square planar geometry similar to what has been observed previously for other diphosphine-palladium complexes (Table 5.2). The average Pd-P bond distance for ***rac*-5.3** is 2.279 Å, slightly longer than those observed for ***meso*-5.3** (2.268 Å) but shorter than those in (dppf)$PdCl_2$ (2.292 Å). The steric bulk of the diphosphine ligands influences the geometry around the palladium, with the bulkier ligands giving larger values for the P-Pd-P bite angle (and conversely smaller Cl-Pd-Cl bond angles). The values of P-Pd-P and Cl-Pd-Cl bond angles have been proposed to important in the catalytic activity of palladium-phosphine complexes, with a large P-Pd-P and small Cl-Pd-Cl bond angle seen to be crucial for high selectivity and catalytic activity. For ***rac*-5.3,** the values for P-Pd-P and Cl-Pd-Cl are 100.2 and 86.8° respectively. When compared with the other diphosphine-palladium complexes (Table 5.2), ***rac*-5.3** has a relatively large P-Pd-P bond angle (second only to ***meso*-5.3**) and a small Cl-Pd-Cl bond angle.

Table 5.2. Structural data for (P–P)$PdCl_2$ complexes.

P–P	Pd-P (Å)	Pd-Cl (Å)	P-Pd-P (°)	Cl-Pd-Cl (°)
dppp[a]	2.247	2.355	90.6	90.8
dppe[b]	2.230	2.359	85.8	94.2
dppf[c]	2.292	2.348	99.1	87.8
***meso*-5.1**[d]	2.268	2.317	100.3	87.6
***rac*-5.1**	2.279	2.323	100.2	86.8

[a] 1,3-bis(diphenylphosphino)propane. Data from ref 28. [b] 1,2-bis(diphenylphosphino)ethane. Data from ref 28. [c] Data from ref 27. [d] Data from ref 25.

The ^{1}H-NMR spectrum of ***rac*-5.3** consists of an aromatic multiplet centred at 6.93 ppm and two singlets at 2.53 and 4.70 ppm for H2 and H3, respectively. For ***meso*-5.3**, protons H2 and H3 have been found to resonate at 3.95 and 4.65 ppm, respectively. These chemical shifts are markedly different from those observed for the parent ferrocenes (Table 5.3), with the resonances for H2 and H3 shifted upfield for ***rac*-5.3** and downfield for ***meso*-5.3** (relative to ***rac*-** and ***meso*-5.1** respectively). These differences in chemical shifts, which are considerably greater than observed for the analogous dppf complex, are indicative of the major conformational change that has occurred to the indenyl ligands upon coordination of the phosphorus atoms to the palladium. The increasing of the RA of the indenyl ligands from 20.8° (***rac*-5.1**) to 172.6° (***rac*-5.3**) forces H2 to adopt a position over top of the benzo ring of the other indenyl ligand, and consequently experiences increased shielding. The resonances for H3 of both ***rac*-** and ***meso*-5.3** now occur at similar chemical shifts, another consequence of the enforced rotation of the indenyl ligands.

Table 5.3. ^{1}H- and ^{31}P{^{1}H}-NMR Spectral Data for Pd complexes.[a]

Complex	H2	H3	^{31}P{^{1}H}	Complex	H2	H3	^{31}P{^{1}H}
dppf[b]	4.07	4.32	–17.2	(dppf)$PdCl_2$[b]	4.18	4.36	34.9
***rac*-5.1**	3.07	4.92	–22.3	***rac*-5.3**	2.53	4.70	35.3
***meso*-5.1**	3.48	3.81	–26.5	***meso*-5.3**	3.95	4.65	33.9

[a] Chemical shifts are in ppm (δ) downfield from Me_4Si (^{1}H) and 85% H_3PO_4 (^{31}P); spectra obtained in $CDCl_3$. [b] H2 and H3 refer to the α and β protons of the cyclopentadienyl ring respectively. Data from Ref. 27 and 29.

The ^{13}C{^{1}H}-NMR spectrum of ***rac*-5.3** is consistent with the formation of the diphosphine-palladium complex. The chemical shift assignments were made by comparison of the spectra of ***rac*-5.1** and ^{31}P–^{13}C coupling constants. Interestingly, the resonances for the *ipso*-Ph and C8 nuclei appear as apparent triplets, instead of the doublets normally associated with the phenylphosphine moieties. These triplets are a result of long-range coupling of the carbon nuclei with the second phosphorus, via the palladium atom, and are common for *cis*-palladium-phosphine complexes.[30,31] As the second phosphorus nucleus is mostly bound to ^{12}C atoms, the system approximates to an AA'X combination where A and A' are the isotopomeric phosphorus nuclei and X

is the ^{13}C nucleus. The AA'X system often yields simple triplets due to the overlap of the inner lines of the multiplet.

The electrochemistry of ***meso*-5.3** has previously been studied using cyclic voltammetry.[25] The complex was shown to undergo a reversible one-electron oxidation of the ferrocenyl fragment centred at 260 mV and an irreversible two-electron reduction of the Pd at –1240 mV versus Fc/Fc^+. The electrochemistry of ***rac*-5.3** is identical to that observed for the ***meso*-5.3**, with a reversible a one-electron oxidation centred at 260 mV. The oxidation of the ferrocenyl moiety of **5.3** occurs at a potential 320 mV less positive than $(dppf)PdCl_2$ in keeping with the electron-rich character of the indenyl ligand when compared with the cyclopentadienyl ligand.[9,32] The reduction of the palladium was not studied.

5.4. Bis(1-diphenylphosphinoindenyl)iron(II)-*cis*-dichloroplatinum(II) (5.4)

rac-Bis(1-diphenylphosphinoindenyl)iron(II)-*cis*-dichloroplatinum(II) (***rac*-5.4**) was synthesized by the reaction of bis(benzonitrile)dichloroplatinum(II) with ***rac*-5.1** in tetrahydrofuran, as shown in Scheme 5.3. Complex ***rac*-5.4** was isolated in good yield (79%) as a brown powder.

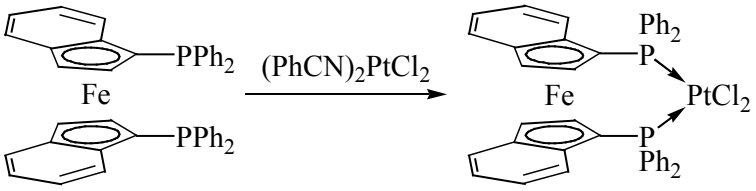

5.4

Scheme 5.3. Synthesis of *rac*-5.4.

The ^1H-NMR spectrum of ***rac*-5.4** consists of an aromatic multiplet centred at 7.33 ppm and doublets at 2.42 and 4.62 ppm corresponding to H2 and H3 respectively. The resonances for H2 and H3 appear in positions comparable to those observed for ***rac*-5.3**, an indication that conformation of the two complexes, in solution, is similar. The $^{13}C\{^1H\}$-NMR spectrum of ***rac*-5.4** is consistent with the formation of the diphosphine-platinum complex. In general, the carbon resonances are

shifted upfield, relative to ***rac*-5.1**, though interestingly, the resonances for C1 and C2 are significantly downfield. The $^{31}P\{^{1}H\}$-NMR spectrum of ***rac*-5.4** consists of a singlet at 12.65 ppm flanked by two satellites due to coupling with the ^{195}Pt nucleus. The magnitude of the coupling, $^{1}J_{PtP}$ = 3818 Hz, is indicative of the phosphine being *trans* to the chlorine (a ligand with a moderate *trans* influence) and is similar in value to that observed for (dppf)$PtCl_2$ (3765 Hz).[29] The value of $^{1}J_{PtP}$ for ***rac*-5.4** is large in comparison with other *cis*-$PtCl_2(PR_3)_2$ complexes and is suggestive of a relatively long Pt-Cl bond.[33]

Crystals suitable for single crystal X-ray structure analysis were obtained from vapour diffusion of diethyl ether into a dichloromethane solution of ***rac*-5.4**. The molecular structure of ***rac*-5.4** is shown in Figure 5.4. Selected bond lengths (Å) and angles (°) are listed in Table 5.4.

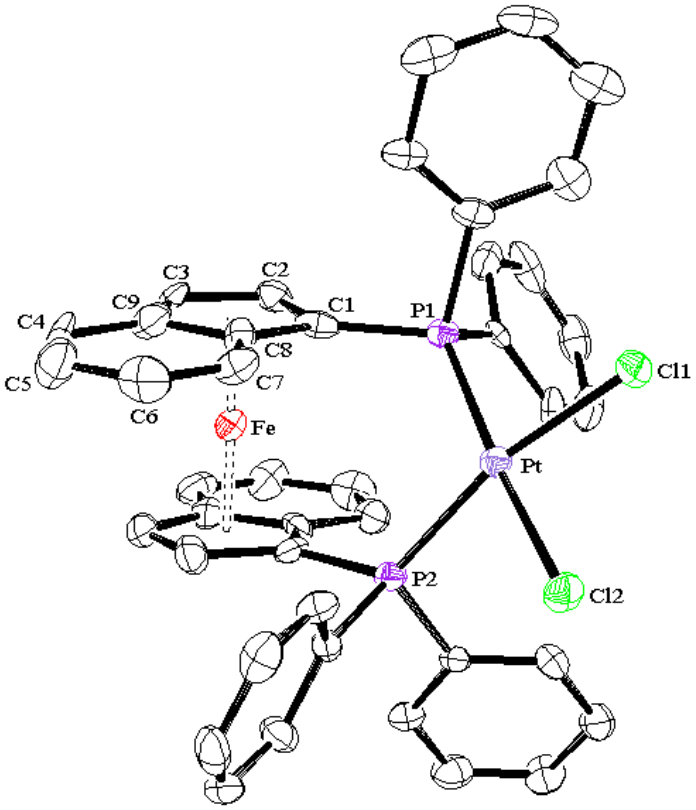

Figure 5.4. ORTEP of *rac*-5.4 indicating the numbering of the atoms. The thermal ellipsoids have been drawn at 50% probability.

Table 5.4. Selected bond lengths [Å] and angles [°] for *rac*-5.4.

Pt-P1	2.2666(19)	P1-Cl1	1.793(7)	P1-C1-Fe	127.9(3)
Pt-P2	2.2791(19)	P2- C12	1.825(7)	P2-C1A-Fe	125.6(3)
Pt-Cl1	2.3491(19)	C1-C2	1.449(9)	C2-C1-C8	106.4(6)
Pt-Cl2	2.3566(18)	C1A-C2A	1.430(9)	C2A-C1A-C8A	107.7(6)
Fe-C1	2.010(7)	C1-C8	1.462(9)	C1-C2-C3	108.6(6)
Fe-C1A	2.012(6)	C1A-C8A	1.461(9)	C1A-C2A-C3A	107.7(7)
Fe-C2	2.033(7)	C2-C3	1.448(9)	C2-C3-C9	107.8(6)
Fe-C2A	2.027(7)	C2A-C3A	1.429(10)	C2A-C3A-C9A	109.4(6)
Fe-C3	2.050(7)	C3-C9	1.411(10)	C1-C8-C9	107.6(6)
Fe-C3A	2.051(7)	C3A-C9A	1.433(10)	C1A-C8A-C9A	107.8(6)
Fe-C8	2.063(7)	C8-C9	1.441(10)	C3-C9-C8	109.4(6)
Fe-C8A	2.094(6)	C8A-C9A	1.437(9)	C3A-C9A-C8A	107.2(6)
Fe-C9	2.069(7)	P1-Pt-P2	100.50(7)		
Fe-C9A	2.105(7)	Cl1-Pt-Cl2	85.16(7)		

Complex ***rac*-5.4** crystallizes in the monoclinic space group $P2_1/n$, with one complete molecule being in the asymmetric unit. The indenyl ligands are coordinated to the iron atom via their five-membered rings in an η^5-fashion. The average Fe-C bond lengths for the indenyl rings of ***rac*-5.4** are 2.045 and 2.058 Å for C1-C9 and C1A-C9A, respectively. As with ***rac*-5.3**, the Fe-C bond lengths for C8A and C9A are, on average, 0.061 Å longer than the remaining eight carbons of the five-membered rings. The unfavorable steric interaction between C7A and C21 observed in ***rac*-5.3** is also present here (C···C distance of 3.254 Å), resulting in the indenyl rings of ***rac*-5.4** not being coplanar (tilted at an angle of 4.4°). The distortion from planarity is reflected by the slip-fold parameters, with values of 0.04 and 0.07 Å for C1-C9 and C1A-C9A, respectively. The iron atom is, on average, 1.646 Å from the centroids of the five-membered rings of the indenyl ligands and forms an angle, with the centroids, of 177.7°.

The diphenylphosphino moieties of ***rac*-5.4** adopt, with respect to each other, a synclinical conformation with a C1-CNT-CNTA-C1A torsion angle of 29.3°. The phosphorus atoms are displaced out of the C_5 ring plane: P1 by 0.022 Å, away from the Fe atom, and P2 by 0.013 Å, towards the Fe atom. The geometry around the

phosphorus atoms is approximately tetrahedral, with average values for C-P-C and C-P-Pt of 103.7 and 115.1°, respectively. The average dihedral angle between the C10-P-C20 and C1-P-Pt planes is 91.2°. The carbon-phosphorus bond lengths are: 1.793, 1.831, 1.824 Å for C1, C10, and C20, respectively; and 1.825, 1.835, 1.830 Å for C1A, C10A, and C20A, respectively. The phenyl rings adopt orientations similar to what is observed in ***rac*-5.3**, with the C_5 ring planes bisecting the planes through: C1-P1-C10 at an angle of 94.3°; C1-P1-C20 at 12.9°; C1A-P2-C10A at 130.8°; and C1A-P2-C20A at 19.2° (Figure 5.5). As with ***rac*-5.3**, P1 and P2 are displaced out of the $PtCl_2$ plane (by 0.06 and 0.29 Å, respectively).

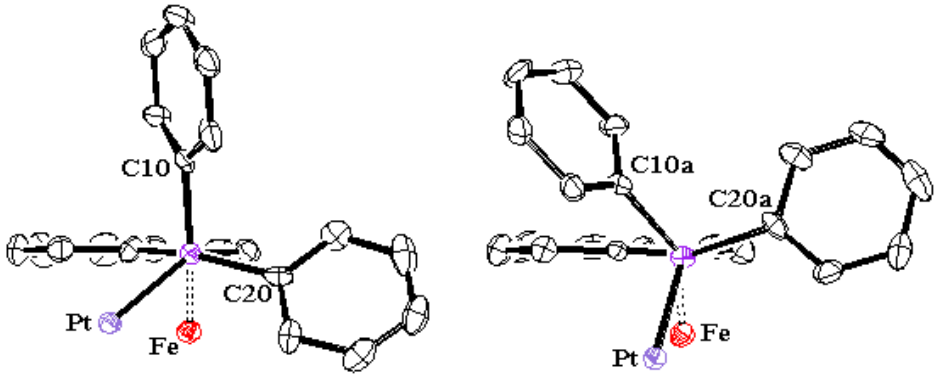

Figure 5.5. Views down P–C1 axes showing orientation of phenyl rings.

The platinum atom in ***rac*-5.4** adopts a distorted square planar geometry, with a dihedral angle between the P-Pt-P and Cl-Pt-Cl planes of 7.3°. The most noticeable feature of the geometry about the Pt is the large P-Pt-P bite angle (100.5°) and small Cl-Pt-Cl angle (85.2°). This is comparable to the geometry observed for (dppf)$PtCl_2$, with P-Pt-P and Cl-Pt-Cl angles of 99.0 and 85.8°, respectively.[26,34] The average Pt-P and Pt-Cl bond distances are 2.273 and 2.353 Å, respectively, slightly longer than the equivalent bond distances in (dppf)$PtCl_2$ (2.260 and 2.342 Å, respectively).

The electrochemistry of ***rac*-5.4** was investigated using cyclic voltammetry. The complex undergoes a reversible one-electron oxidation of the ferrocenyl fragment centred at 248 mV versus Fc/Fc^+. The difference in peak potential (75 mV) is indicative of a fast redox process. The oxidation of the ferrocenyl moiety of **5.4** occurs at a potential 325 mV less positive than (dppf)$PtCl_2$.[9,34]

5.5. [(Cyclooctadiene)(*rac*-bis(1-diphenylphosphinoindenyl)iron(II))rhodium(I)] tetraphenylborate (5.5)

[(Cyclooctadiene)(*rac*-bis(1-diphenylphosphinoindenyl)iron(II))rhodium(I)]tetraphenylborate (**5.5**) was synthesized by the reaction of ***rac*-5.1** with $[Rh(COD)_2]BF_4$ followed by the addition of $NaBPh_4$ (Scheme 5.4). Complex **5.5** was isolated in good yield (84%) as a yellow powder. Although the reaction was attempted with 2 equivalents of ***rac*-5.1**, only a single COD was displaced from the rhodium by the diphosphine. Similarly, Chaloner et al. reported that the addition of 2 equivalents of 1,1'-bis(diisopropylphosphino)ferrocene (disoppf) to $[Rh(NBD)_2]BF_4$ led to the exclusive formation of $[Rh(NBD)(disoppf)]BF_4$.[35] Subsequent treatment of $[Rh(NBD)(disoppf)]BF_4$ with a ten-fold excess of dppf produced, exclusively, $[Rh(NBD)(dppf)]BF_4$. It was suggested that large distortions in the geometry about the rhodium, caused by the bulkiness of the diphosphine ligands, was responsible for the inability of the second diphosphine to displace the remaining NBD ligand.[14,36] It is anticipated that **5.5** will suffer from similar steric demands, making substitution of the second COD ligand more difficult. Interestingly, the homoleptic species $[M(dppf)_2]BF_4$ (M = Rh, Ir) has been prepared via a different synthetic route.[37] It was found that the geometry around the iridium atom was severely distorted from square planar, with a dihedral angle between the planes defined by the two P-Ir-P bite angles of 51°.

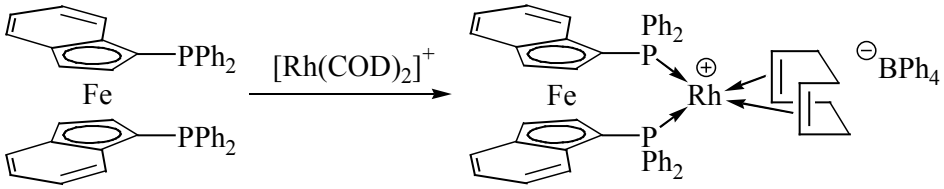

5.5

Scheme 5.4. Synthesis of 5.5.

The NMR spectra of **5.5** are consistent with the displacement of a single cyclooctadiene from the rhodium precursor. The ^{1}H-NMR spectrum consists of an aromatic multiplet centred at 7.31 ppm and two singlets 2.81 and 4.96 ppm for H2 and H3, respectively. The resonances for the CH_2 and CH protons of the cyclooctadiene occur at 2.56 and 4.37 ppm, respectively. The resonances for H2 and H3 are upfield of those for ***rac*-5.1**, similar to what was observed for ***rac*-5.3** and **5.4**. This suggests that

the indenyl ligands in **5.5** are adopting a conformation similar to what was seen for the palladium and platinum complexes, with H2 positioned over the benzo ring. The $^{31}P\{^{1}H\}$-NMR spectrum of **5.5** consists of a doublet at 29.1 ppm, with a rhodium-phosphorus coupling constant of 150 Hz. The values for the chemical shift and coupling constant are similar to those previously seen for analogous rhodium-dppf complexes.[37,38]

5.6. Dichloro(bis(1-diphenylphosphinoindenyl)iron(II))nickel(II) (5.6)

The synthesis of dichloro(bis(1-diphenylphosphinoindenyl)iron(II))nickel(II) (**5.6**) was attempted by the reaction of ***rac*-5.1** with dichloro(bis(triphenyl-phosphine)nickel(II) (or anhydrous nickel chloride) as shown in Scheme 5.5. The reaction mixture immediately changes colour change from dark green to red, consistent with the complex formation. Removal of the solvent produced a red-brown residue. Due to the presence of paramagnetic material, it was not possible to obtain an assignable NMR spectrum of the residue, and mass spectroscopy did not yield any conclusive results. Single crystal X-ray structural analysis identified the complex to be *trans*-dichloro(bis(1-diphenylphosphinoindene))nickel(II) (**5.7**) (see below). It is unclear at what stage **5.7** is produced, but the position of the phosphorus on C1 of the indene suggests that hydrolysis of the indenyl moiety after the formation of **5.6** is the most likely scenario.

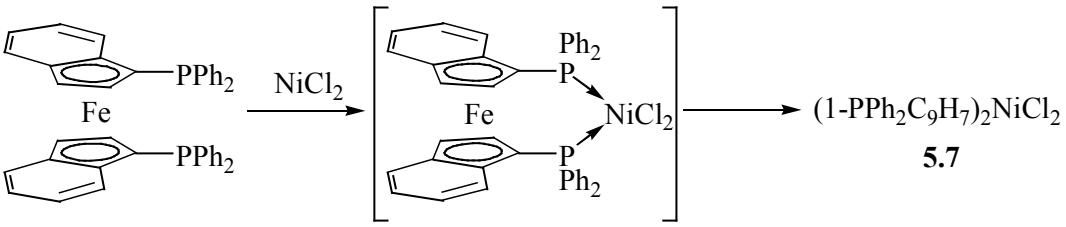

Scheme 5.5. Proposed synthesis of 5.7.

Crystals of **5.7** suitable for single crystal X-ray structure analysis were obtained by vapour diffusion of diethyl ether into a dichloromethane solution. The molecular structure of **5.7** is shown in Figure 5.6. Selected bond lengths (Å) and angles (°) are listed in Table 5.5.

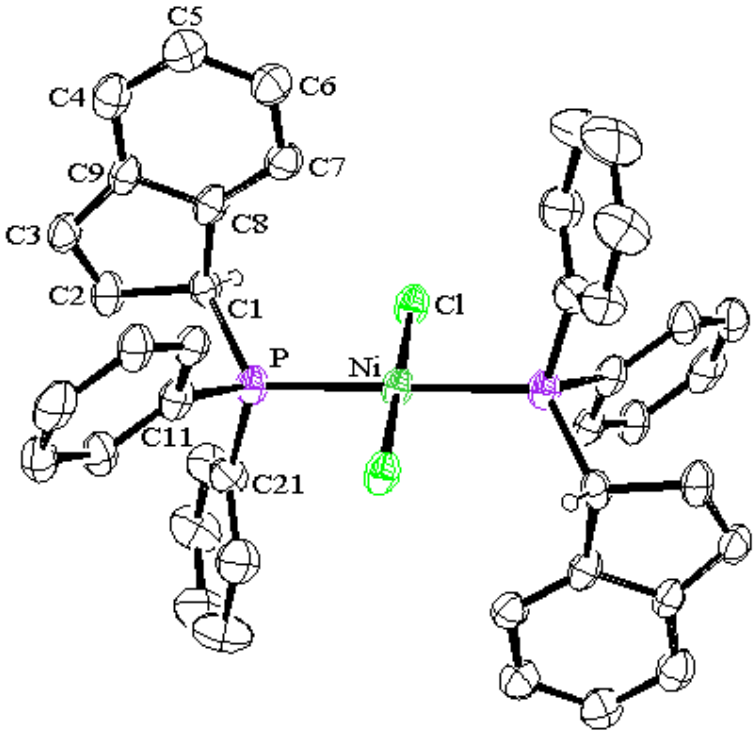

Figure 5.6. ORTEP of 5.7 indicating the numbering of the atoms. The thermal ellipsoids have been drawn at 40% probability.

Table 5.5. Selected bond lengths [Å] and angles [°] for 5.7.

Ni-Cl	2.168(2)	C1-C8	1.527(13)	C2-C1-C8	100.7(7)
Ni-P	2.231(2)	C2-C3	1.316(13)	C1-C2-C3	112.2(9)
P-C1	1.842(9)	C3-C9	1.424(13)	C2-C3-C9	109.4(9)
P-C11	1.847(9)	C8-C9	1.402(12)	C1-C8-C9	107.6(8)
P-C21	1.825(10)	Cl-Ni-P	90.19(9)	C3-C9-C8	110.0(9)
C1-C2	1.518(12)	C1-P-Ni	117.6(3)		

Complex **5.7** crystallizes in the rhombohedral space group R-3, with one half molecule in the asymmetric unit. The remainder of the molecule is generated by inversion through the Ni atom. The Ni atom adopts a square planar geometry, with *trans* chloride and phosphine ligands. The P-Ni-Cl bond angle is 90.2° with the Ni-P and Ni-Cl bond distances being 2.231 and 2.168 Å, respectively. The orientation of

the Ni atom, with respect to the indene, is considerably different than the equivalent orientations found for the oxide, sulfide, and selenide derivatives of 1,3-bis(diphenylphosphino)indene, with X-P-C1-C2 torsion angles of: 179.70° for X = Ni, 57.0° for X = O, 59.9° for X = S, 58.4° for X = Se.[20,39] The structural parameters of the indene ring are consistent with those previously reported for similar compounds. The C2-C3 bond length of 1.316 Å is indicative of a double bond, whereas the C1-C2 and C1-C8 bonds are similar in length at 1.518 and 1.527 Å, respectively. The C2-C1-C8 bond angle is the smallest within the five-membered ring, as expected for an sp^3 carbon. The C-C bond lengths of the six-membered ring are all very similar, with an average length of 1.392 Å. The geometry around the phosphorus atom is approximately tetrahedral, with the dihedral angle between the planes defined by C11-P-C21 and C1-P-Ni being 95.7°. The carbon-phosphorus bond lengths for C1, C11, and C21 are all similar at 1.842, 1.847, and 1.825 Å, respectively. The indene and phenyl rings adopt a propeller conformation (Figure 5.7), with the Ni-P-C bond angles being 106.0, 117.6, and 118.8° for C21, C1, and C11, respectively. The opening up of the Ni-P-C1 and Ni-P-C11 bond angles is due to steric interactions between both C1 and C11 with the chlorine atoms, with the C···Cl distances being 3.270 and 3.229 Å, respectively.

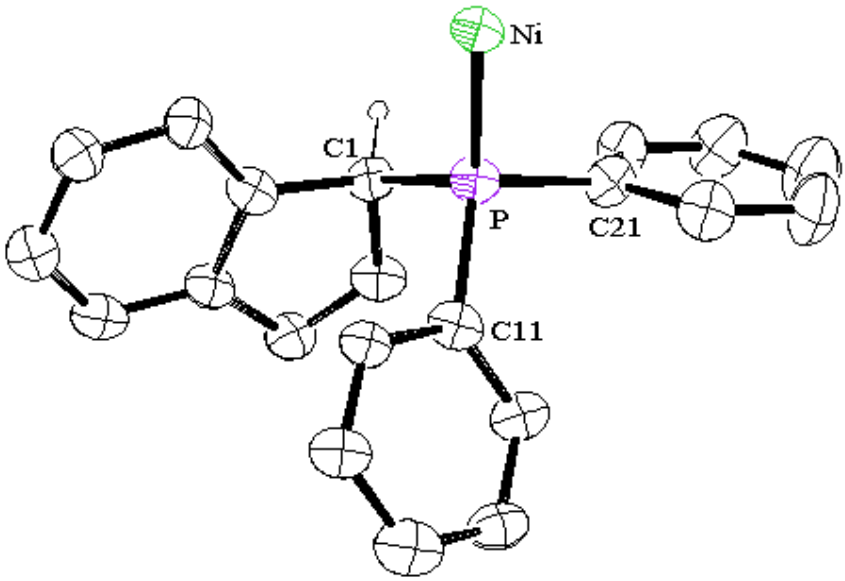

Figure 5.7. Propeller conformation of 5.7.

Complexes of the type P_2NiCl_2 (P = tertiary phosphine) are known to exhibit tetrahedral ↔ square planar equilibrium in both solution and solid-state.[40,41] The position of the equilibrium is dependent on both the steric and electronic properties of the phosphine. Bulky ligands have been shown to favour the tetrahedral geometry whereas strong-field ligands favour the square planar configuration. Thus, dichloronickel(II) complexes of PPh_3 (a weak-field ligand) are tetrahedral in geometry whereas similar complexes containing (alkyl)PPh_2 ligands are typically square planar.[42,43]

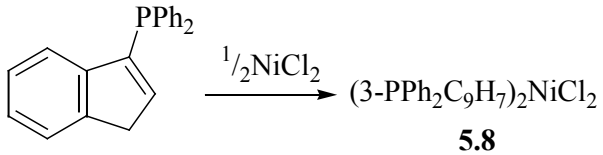

5.8

Scheme 5.6. Synthesis of 5.8.

Bis(3-diphenylphosphinoindene)dichloronickel(II) (**5.8**) was synthesized by the reaction of 3-diphenylphosphinoindene with anhydrous nickel chloride in refluxing tetrahydrofuran (Scheme 5.6). The complex was isolated in good yield (74%) as a red powder. The characterization of **5.8** was hindered by the lack of solubility of the complex in all common solvents. The solid-state magnetic susceptibility of **5.8** was determined using the Gouy method. The room temperature value for μ_{eff} is 3.01 B.M., suggestive of a tetrahedral geometry about the nickel. The geometries observed for **5.7** and **5.8** are consistent with previous complexes containing (alkyl)PPh_2 ligands.

5.7. Palladium Catalyzed Cross-coupling Reactions

Since the reporting of the nickel-phosphine catalyzed cross-coupling of Grignard reagents with aryl halides in 1972,[44,45] a wide variety of similar coupling reactions have been developed and used successfully in organic chemistry.[46] Palladium catalysts have been found to be particularly effective at mediating the cross-coupling of Grignard reagents with aryl halides. However, the introduction of a secondary alkyl group to aryl halides remains problematic due to the isomerization of the alkyl group and/or the reduction of the halide. The catalyst (dppf)$PdCl_2$ was found to be highly

effective at couplings involving secondary alkyl groups, with near perfect *sec*-/*n*-selectivity.[27]

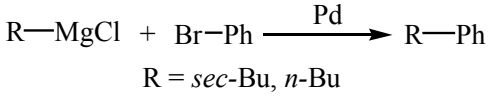

Scheme 5.7. Cross-coupling of bromobenzene and Grignard reagents.

The cross-coupling of *n*- and *sec*-butylmagnesium chloride with bromobenzene was carried out in the presence of complex **5.3** (Scheme 5.7). The results and reaction conditions are summarized in Table 5.6.

Table 5.6. Cross-Coupling of (*n*-/*sec*-)Butylmagnesium Chloride with Bromobenzene in THF.

				Yield, %[a]		
catalyst	conc[b]	chloride	time, h	*sec*-BuPh	*n*-BuPh	other[c]
$(Ph_3P)_2PdCl_2$	1	*n*-BuCl	16	34	49	5
5.3	0.5	*n*-BuCl	18	24	34	24
5.3	1	*n*-BuCl	17	27	45	7
5.3	0.5	*sec*-BuCl	1	11	4	81
5.3	1	*sec*-BuCl	1	18	7	63
5.3	5	*sec*-BuCl	2	48	26	5
5.3	1	*sec*-BuCl	18	47	28	8

[a] Yield determined by GC using an internal standard. [b] Concentration in mol% of Pd. [c] Recovered bromobenzene. When the yields of the coupled products were low compared with consumed bromobenzene, variable amounts of benzene was detected by GC.

Complex **5.3** was found to catalyze the reaction of bromobenzene with *n*-butylmagnesium chloride to give *n*-butylbenzene in a modest yield (45%) at a catalyst loading of 1 mol% of palladium. The reaction, however, was not selective with considerable amounts of *sec*-butylbenzene and benzene also being formed. The ratio of *n*- and *sec*-butylbenzene formed was 63:37. Decreasing the catalyst loading to 0.5 mol% of palladium results in a decrease in both yield and selectivity. The results are similar to those obtained for the equivalent reaction using $(PPh_3)_2PdCl_2$, with a *n*-/*sec*-ratio of 59:41 observed. Hayashi et. al. reported that $(dppf)PdCl_2$ catalyses the

coupling of bromobenzene with *n*-butylmagnesium chloride in excellent yield (92%) and with high selectivity (100%).

In an analogous manner, the cross-coupling of bromobenzene with *sec*-butylmagnesium chloride was accomplished with **5.3** to yield *sec*-butylbenzene (47%) with a *sec*-/*n*- ratio of 63:37, at a catalyst loading of 1 mol% of palladium. Increasing the catalyst loading to 5 mol% of palladium reduces the reaction time, without loss of selectivity. The equivalent reaction with (dppf)$PdCl_2$ produced *sec*-butylbenzene in excellent yield (95%) and with high selectivity (100%).[27]

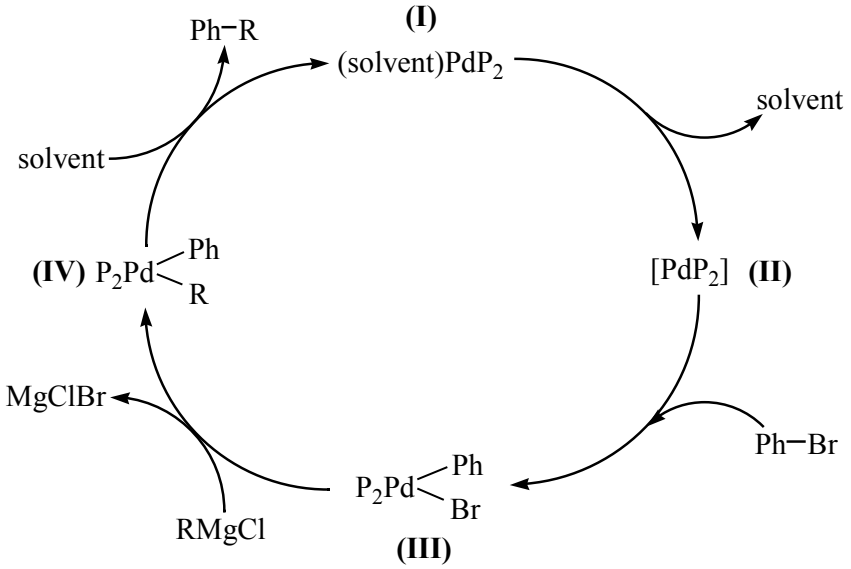

Scheme 5.8. Mechanism for the Pd-catalyzed cross-coupling of bromobenzene and Grignard reagents.

The generally accepted catalytic cycle for the palladium-catalyzed cross-coupling of Grignard reagents with aryl bromides is shown in Scheme 5.8.[47] After the initial oxidative addition of the aryl bromide to the palladium-phosphine complex, transmetallation of the Grignard reagent occurs to yield the σ-alkylmetal intermediate **IV**. Reductive elimination follows to yield the coupled product and the regenerated catalyst. The side products observed during the coupling reaction are believed to arise from a σ-π interconversion of the σ-alkylmetal intermediates **IV** and the hydrido-olefin-metal intermediate **V** (Scheme 5.9).[48] The β-hydride elimination responsible for this interconversion also accounts for the reduction of the aryl bromide to benzene.

The suppression of this β-hydride elimination is essential if the reaction is to proceed with high yield and selectivity. Correlations have previously been made between catalyst activity and the Cl-Pd-Cl bond angle, with small values of the latter proposed to accelerate the reductive elimination of the coupled product.[27] The Cl-Pd-Cl bond angle for ***rac*-5.3** was determined to be 86.8°, smaller than that of (dppf)$PdCl_2$. With this small angle, it was anticipated that coupling reactions catalyzed by complex **5.3** would proceed with high yields and selectivity. The results obtained here suggest that the β-hydride elimination is still competing strongly with the reductive elimination step of the catalytic cycle, despite the small bond angle. One should note, however, that due to solubility problems with **5.3**, the cross-coupling reactions were performed in THF and not diethyl ether as was used in the previous studies. The choice of solvent has been shown to be important for high selectivity, with reduced s*ec*-/*n*-ratios and increased amounts of the reduced aryl halide observed for cross-coupling reactions performed in THF.[49]

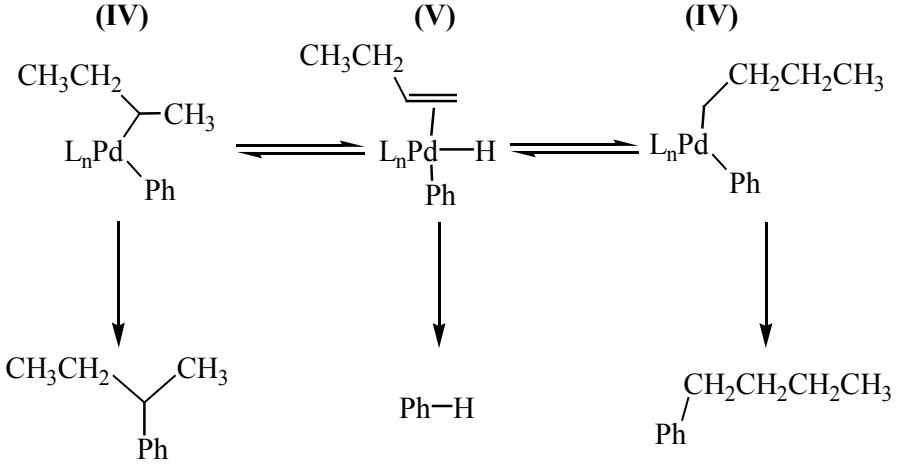

Scheme 5.9. Mechanism for the formation of cross-coupling byproducts.

5.8. Indene-arene coupling reactions

Complexes of group 13 and 14 transition metals have found extensive use as catalysts for many organic transformations, with metallocenes of group IV being particularly effective in the synthesis of highly stereospecific polypropylenes.[50] These metallocenes generally contain cyclopentadienyl-like ligands, but there are examples where arenes have been used in conjunction with cyclopentadienyl ligands to form

mixed-ring metallocenes.[51] Previous work within the Curnow group has seen the preparation of cyclopentadienyl-2,6-diphenylbenzene by the palladium-catalysed Stille coupling of tributyl(cyclopentadienyl)tin and iodo-2,6-diphenylbenzene (Figure 5.8).[52] It was anticipated that the use of a sterically-constrained ligand would force the coordination of both cyclopentadienyl and arene ligands upon metallation. The introduction of an indene to a similarly sterically-constrained arene core is seen as an effective method for introducing planar chirality to the ligand. Palladium catalysed couplings of cyclopentadienylmetal (or indenylmetal) with aryl halides have been the subject of a number of investigations.[53-56]

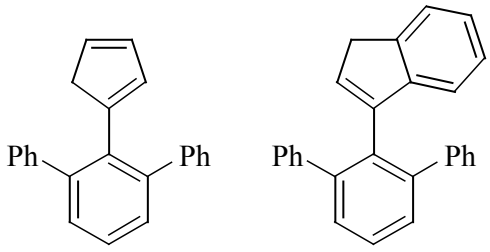

5.9

Figure 5.8. Potential cyclopentadienyl-arene ligands.

The synthesis of indenyl-2,6-diphenylbenzene (**5.9**) was attempted by the palladium-catalysed coupling of an indenyl-zinc chloride complex with iodo-2,6-diphenylbenzene in refluxing tetrahydrofuran (Scheme 5.10), following the method of Haltermann et al..[57] Unfortunately, the reaction was unsuccessful with the ^{1}H-NMR spectrum showing predominantly iodo-2,6-diphenylbenzene, with trace amounts of unidentified products.

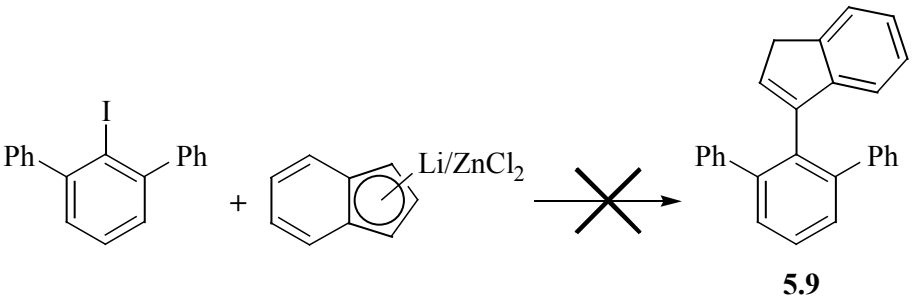

5.9

Scheme 5.10. Attempted synthesis of 5.9 via a Zn mediated reaction.

The synthesis of **5.9** was also attempted by palladium-catalysed Stille coupling of tributyl(indenyl)tin with iodo-2,6-diphenylbenzene in refluxing tetrahydrofuran for 2 days, as shown in Scheme 5.11. The catalyst, temperature and solvent were all varied in an attempt to optimise yields while CuI (co-catalyst) and $AsPh_3$ (soft palladium ligand) were kept constant in all reactions.[58] The catalytic systems investigated were: $(PhCN)_2PdCl_2$/THF, $(PhCN)_2PdCl_2$/DMF, $Pd(PPh_3)_4$/THF, and $Pd(PPh_3)_4$/DMF. In all cases, the reaction proved to be unsuccessful, with the ^{1}H-NMR spectra of the resulting mixtures showing predominantly iodo-2,6-diphenylbenzene. Generally, the reactions were terminated by the precipitation of "palladium black". This termination occurred within a couple of hours at room temperature, and more rapidly at elevated temperatures.

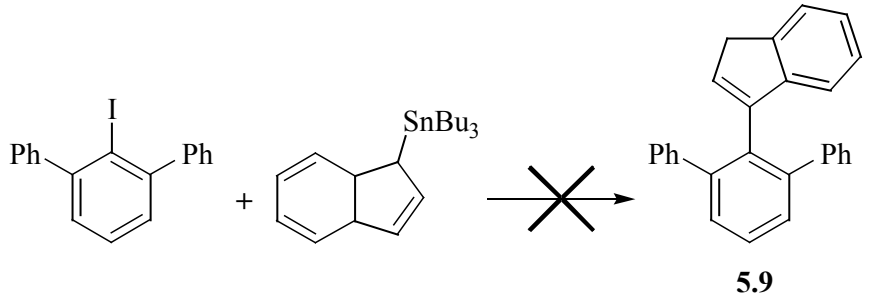

5.9

Scheme 5.11. Attempted synthesis of 5.9 via Stille-coupling reaction.

The effect of steric interactions on the Stille coupling were investigated by the reaction of tributyl(indenyl)tin with both iodobenzene and 2-iodobiphenyl (Scheme 5.12). In both instances, the couplings were successful with phenylindene (**5.10**) and 2-(indenyl)biphenyl (**5.11**) produced in moderate yields (50 and 46%, respectively). The successful coupling of these species strongly suggests that unfavorable steric

interactions may be hindering the transmetallation reaction, resulting in little or no coupling of the bulkier iodo-2,6-diphenylbenzene to tributyl(indenyl)tin.

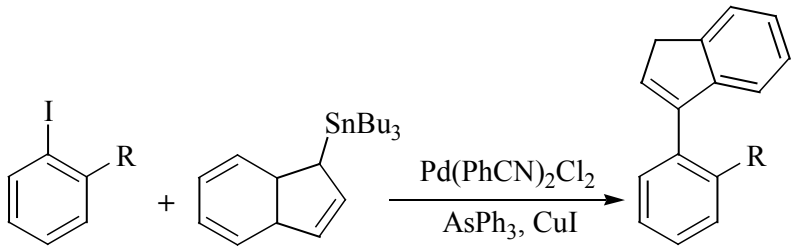

5.10 R = H
5.11 R = Ph

Scheme 5.12. Synthesis of 5.10 and 5.11.

5.9. Conclusions

The ferrocenylphosphine **5.1** has been shown to act as a bidentate ligand to different transition metals, with the formation of bimetallic palladium (**5.3**), platinum (**5.4**), and rhodium complexes (**5.5**). An attempt to prepare a bimetallic nickel complex (**5.6**) led to the formation of the square planar nickel complex *trans*-dichloro(bis(1-diphenylphosphinoindene))nickel(II) (**5.7**). Interestingly, the reaction of 3-diphenylphosphinoindene with nickel dichloride produced the tetrahedral complex **5.8**.

The cross-coupling of Grignard reagents of *n*- and *sec*-butylchloride with bromobenzene was accomplished by the use of **5.3** as a catalyst. However, in all instances the coupling was not selective with considerable amounts of the isomerized product and benzene obtained. The formation of these by-products suggests that β-hydride elimination is competing with the reductive elimination step of the catalytic cycle. Further studies are required on **5.3** to investigate its potential as a catalyst for other organic transformations.

The synthesis of indenyl-2,6-diphenylbenzene by an indene-arene coupling reaction was unsuccessful due to unfavorable steric interactions. The related phenylindene and 2-(indenyl)biphenyl were successfully synthesized.

References

1. (a) Memmler, H.; Walsh, K.; Gade, H.; Lauher, J.W. *Inorg. Chem*. **1995**, *34*, 4062. (b) Proulx, G.; Bergmann, R.G. *J. Amer. Chem. Soc*. **1996**, *118*, 1981. (c) Bakhmutov, V.I.; Visseaux, M.; Baudry, D.; Dormond, A.; Richard, P. *Inorg. Chem*. **1996**, *35*, 7316.
2. (a) Bullock, R.M.; Casey, C.P. *Acc. Chem. Res*. **1987**, *20*, 167. (b) Baranger, A.M.; Bergman, R.G. *J. Amer. Chem. Soc*. **1994**, *116*, 3822. (c) Steffey, B.D.; Vites, J.C.; Cutler, A.R. *Organometallics* **1991**, *10*, 3432.
3. (a) Kauffmann, T.; Bisling, M.; Teuben, J.H.; Konig, R. *Angew. Chem. Int. Ed*. **1980**, *19*, 328. (b) Bosch, B.; Erker, G.; Frohlich, R. *Inorg. Chim. Acta* **1998**, *270*, 446. (c) Graham, T.W.; Llamazares, A.; McDonald, R.; Cowie, M. *Organometallics* **1999**, *18*, 3490.
4. Rudie, A.W.; Lictenberg, D.W.; Katcher, M.L.; Davison, A. *Inorg. Chem*. **1978**, *17*, 2859.
5. Hor, T.S.A.; Phang, L.-T. *J. Organomet. Chem.* **1989**, *373*, 319.
6. Hor, T.S.A.; Phang, L.-T. *Polyhedron* **1990**, *9*, 2305.
7. Hor, T.S.A.; Phang, L.-T. *J. Organomet. Chem*. **1990**, *381*, 121.
8. Bandini, A.L.; Banditelli, G.; Cinellu, M.A.; Sanna, G.; Minghette, G.; Demartin, F.; Mannassero, M. *Inorg. Chem*. **1989**, *28*, 404.
9. Corain, B.; Longato, G.; Favero, G.; Ajo, D.; Pilloni, G.; Russo, U.; Kreissl, F.R. *Inorg. Chim. Acta* **1989**, *157*, 259.
10. Hayashi, T.; Konishi, M.; Kumada, M. *Tetrahedron Lett*. **1979**, 1871.
11. Katayama, T.; Umeno, M. *Chem. Lett*. **1991**, 2073.
12. Pridgen, L.N.; Killmer, L.B. *J. Org. Chem*. **1981**, *46*, 5402.
13. Alcock, N.W.; Brown, J.M.; Rose, M.; Wienand, A. *Tetrahedron: Asymmetry* 1991, *2*, 47.
14. Cullen, W.R.; Kim, T.-J.; Einstein, F.W.B.; Jones, T. *Organometallics* **1985**, *4*, 346.
15. Cullen, W.R.; Han, N.F. *Appl. Organomet. Chem*. **1987**, *1*, 1.
16. Cullen, W.R.; Evans, S.V.; Han, H.F.; Trotter, J. *Inorg. Chem*. **1987**, *26*, 514.
17. Hayashi, T.; Yamamoto, A.; Hojo, M.; Ito, Y. *J. Chem. Soc., Chem. Commun*. **1989**, 495.
18. Hayashi, T.; Kawamura, N.; Ito, Y. *J. Amer. Chem. Soc*. **1987**, *109*, 7876.

19. Togni, A.; Rihs, G.; Blumer, R.E. *Organometallics* **1992**, *11*, 613.
20. Adams, J.J.; Berry, D.E.; Browning, J.; Burth, D.; Curnow, O.J. *J. Organomet. Chem*. **1999**, *580*, 245.
21. Reetz, M.T.; Beuttenmuller, E.W.; Goddard, R.; Pasto, M. *Tetrahedron Lett*. **1999**, *40*, 4977.
22. Donaghy, K.J.; Carroll, P.J.; Sneddon, L.G. *Inorg. Chem*. **1997**, *36*, 547-553.
23. Durand, M.; Jouany, C.; Jugie, G.; Elegant, L.; Gal, J.-F. J. *Chem. Soc., Dalton Trans*. **1977**, 57-60.
24. Gan, K.-S.; Hor, T.S.A. In *Ferrocenes*; Togni, A., Hayashi, T., Eds.; VCH: New York, **1995**; Chapter 1, pp 3-104.
25. Adams, J.J. Masters Thesis, University of Canterbury **1998**.
26. de Lima, G.M.; Filgueiras, C.A.L.; Giotto, M.T.S.; Mascarenhas, Y.P. *Transition Met. Chem*. **1995**, *20*, 380.
27. Hayashi, T.; Konishi, M.; Kobori, Y.; Kumada, M.; Higichi, T.; Hirotsu, K. *J. Amer. Chem. Soc.* **1984**, *106*, 158.
28. Steffen, W.L.; Palenik, G.J. *Inorg. Chem*. **1976**, *15*, 2432.
29. Bandini, A.L.; Banditelli, G.; Cinellu, M.A.; Sanna, G.; Minghetti, G.; Demartin, F.; Manassero, M. *Inorg. Chem*. **1989**, *28*, 404.
30. Goodfellow, R.J. *J. Chem. Soc., Chem. Commun*. **1968**, 114.
31. Brown, R.A.; Houlton, A.; Roberts, R.M.G.; Silver, J. *Polyhedron* **1992**, *11*, 2619.
32. McCulloch, B.; Ward, D.L.; Woolins, J.D.; Brubaker, C.H. *Organometallics* **1985**, *4*, 1425.
33. Appleton, T.G.; Bennett, M.A.; Tomkins, I.B. *J. Chem. Soc., Dalton Trans*. **1976**, 439.
34. Clemente, D.A.; Pilloni, G.; Corain, B.; Longato, B.; Tiripicchio-Camellini, M. *Inorg. Chim. Acta* **1986**, *115*, L9.
35. Avent, A.G.; Bedford, R.B.; Chaloner, P.A.; Dewa, S.Z.; Hitchcock, P.B. *J. Chem. Soc., Dalton Trans*. **1996**, 4633.
36. Cullen, W.R.; Kim, T.-J.; Einstein, F.W.B.; Jones, T. *Organometallics* **1983**, *2*, 714.
37. Casellato, U.; Corain, B.; Graziana, R.; Longato, B.; Pilloni, G. *Inorg. Chem*. **1990**, *29*, 1193.

38. Longato, B.; Pilloni, G.; Graziani, R.; Casellato, U. *J. Organomet. Chem*. **1991**, *407*, 369.
39. Stradiotto, M.; Kozak, C.M.; McGlinchey, M.J. *J. Organomet. Chem*. **1998**, *564*, 101.
40. Pignolet, L.H.; Horrocks, W.; Holm, R.H. *J. Amer. Chem. Soc.* **1970**, *92*, 1855.
41. Hayter, R.G.; Humler, F.S. *Inorg. Chem*. **1965**, *12*, 1701.
42. Stone, P.J.; Dori, Z. *Inorg. Chim. Acta* **1971**, *5*, 434.
43. Allen, E.A.; Wilkinson, W. *Spectrochim. Acta* **1974**, *30A*, 1219.
44. Corriu, R.J.P.; Masse, J.P. *J. Chem. Soc., Chem. Commun*. **1972**, 144.
45. Tamao, K.; Sumitani, K.; Kumada, M. *J. Amer. Chem. Soc.* **1972**, *94*, 4374.
46. Negeshi, E. *Acc. Chem. Res*. **1982**, *15*, 340.
47. Castle, P.L.; Widdowson, D.A. *Tetrahedron Lett*. **1986**, *27*, 6013.
48. Bergstrom, D.E.; Ogawa, M.K. *J. Amer. Chem. Soc.* **1978**, *100*, 4106.
49. Hayashi, T.; Ogasawara, M.; Yoshida, K. *Organometallics* **2000**, *19*, 1567.
50. Togni, A.; Halterman, R.C. (Eds), Metallocenes: Synthesis, Reactivity, Applications, Wiley-VCH, Weinheim, Volumes 1 & 2, **1998**
51. (a) Gillis, D.J.; Tudoret, M-J.; Baird, M.C. *J. Am. Chem. Soc.* **1993**, *115*, 2543. (b) Sabmannshausen, J.; Powell, A.K.; Anson, C.E.; Wocadlo, S.; Bochmann, M. *J. Organomet. Chem*. **1999**, *592*, 84.
52. Curnow, O.J.; Fern, G.M.; Wöll, D. *Inorg. Chem. Comm*. **2003**, *6*, 1201–1204.
53. Katz, T.J.; Gilbert, A.M.; Huttenloch, M.E.; Min-Min, G.; Brintzinger, H.-H. *Tetrahedron Lett*. **1993**, *34*, 3551.
54. Boese, R.; Braunlich, G.; Gotteland, J.-P.; Hwang, J.-T.; Troll, C.; Vollhardt, K.P.C. *Angew. Chem. Int. Ed*. **1996**, *35*, 995.
55. Baker, R.W.; Wallace, B.J. Chem. Commun. 1999, 1405
56. Littke, A.F.; Dai, C.; Fu, G.C. *J. Amer. Chem. Soc.* **2000**, *122*, 4020.
57. Haltermann, R.L.; Tretyakov, A.; Khan, M.A. *J. Organomet. Chem*. **1998**, *568*, 41.
58. Farina, V.; Kapadia, S.; Krishnan, B.; Wang, C.; Liebeskind, L.S. *J. Org. Chem*. **1994**, *59*, 5905.
59. Tebby, J.C., In *Phosphorous-31 NMR Spectroscopy in Stereochemical Analysis: Organic Compounds and Metal Complexes*, Verkade, J.; Quin, L.D. Eds.; VCH: **1987**; Chapter 1, pp 1-60.

60. Bandoli, G.; Dolmella, A. *Coord. Chem. Rev*. **2000**, *209*, 161.

Publications

Publications

1. Curnow, O. J.; Fern, G. M. *Organometallics* **2002**, *21*, 2827–2829.
2. Adams, J. J.; Berry, D. E.; Curnow, O. J.; Fern, G. M.; Hamilton, M. L.; Kitto, H. J.; Pipal, J. R. *Aust. J. Chem*. **2003**, *56*, 1153–1160.
3. Curnow, O. J.; Fern, G. M.; Wöll, D. *Inorg. Chem. Comm*. **2003**, *6*, 1201–1204.
4. Curnow, O. J.; Fern, G. M.; Hamilton, M. L.; Zahl, A.; van Eldik, R. *Organometallics* **2004**, *23*, 906–912.
5. Curnow, O. J.; Fern, G. M.; Klaib, S.; Lang, H. *J. Organomet. Chem*. **2004**, *689*, 1139–1144.
6. Curnow, O. J.; Fern, G. M.; Hamilton, M. L.; Jenkins, E. J. *J. Organomet. Chem*. **2004**, *689*, 1897–1910.
7. Curnow, O. J.; Fern, G. M. *J. Organomet. Chem*. **2005**, *690*, 3018.
8. Curnow, O. J.; Fern, G. M.; Klaib, S.; Böhme, U; Lang, H.; Holze, R. *J. Electroanal. Chem*. **2005**, *585*, 167-171.
9. Curnow, O. J.; Fern, G. M.; Jenkins, E. J. *J. Organomet. Chem*. **2006**, *691*, 643–647.

Appendix

Appendix 1: Crystallography

Tables A1-A9 list the crystal data and X-ray experimental details for the refined crystal structures discussed in this thesis. Throughout the text, selected bond lengths and angles are discussed and listed with the appropriate figures, while the remaining distances and angles are available on request from: the Department of Chemistry, University of Canterbury for ***rac*-5.3**, ***rac*-5.4**, and **5.7**; and the Cambridge Crystallographic Data Centre: CCDC No. 256589 for **3.22**; CCDC No. 256590 for **3.25**; CCDC No. 210352 for **3.31**; CCDC No. 229441 for ***rac*-3.32**; CCDC No. 229345 for ***rac*-3.34**; and CCDC No. 229346 for ***rac*-3.35**.

All Measurements were made with a Siemens CCD area detector using graphite monochromatised Mo Kα (λ = 0.71073 Å) radiation at the temperature indicated in the following tables. The data reduction was performed using SAINT.[1] The intensities were corrected for Lorentz and polarisation effects and for absorption using SADABS.[1] The structures were solved by direct methods using SHELXS[2] and refined on F^2 using all data by full-matrix least-squares procedures using SHELXL-97.[2] All non-hydrogen atoms were refined with anisotropic displacement parameters. Aromatic and aliphatic hydrogen atoms were included in calculated positions with isotropic displacement parameters 1.2 and 1.5 times the isotropic equivalent of their carrier carbon atoms, respectively. The figures throughout the text were generated using ORTEP-3 for Windows.[3]

References

1. SAINT and SADABS, Siemens Analytical, Madison, WI, **1994**.
2. Sheldrick, G.M. SHELXTL ver 5.1, Bruker AXS, Madison, WI, **1998**.
3. Farrugia, L.J. *J. Appl. Cryst*. **1997**, *30*, 565.

Table A1.1. Crystal data and structure refinement for di(2-methylindenyl)iron(II) (3.22).

Empirical formula	$C_{20}H_{18}Fe$	
Formula weight	314.19	
Temperature (K)	168(2)	
Crystal system	Tetragonal	
Space group	$P4_32_12$	
Unit cell dimensions	a = 8.2242(12) Å	α = 90°
	b = 8.2242(12) Å	β = 90°
	c = 43.278(13) Å	γ = 90°
Volume ($Å^3$)	2927.2(10)	
Z	8	
Density (calculated) (Mg/m^3)	1.426	
Absorption coefficient (mm^{-1})	1.020	
F(000)	1312	
Crystal size (mm^3)	0.66 x 0.21 x 0.21	
Theta range for data collection (°)	1.88 to 26.37	
Index ranges	$-10 \le h \le 10$	
	$-10 \le k \le 10$	
	$-54 \le l \le 34$	
Reflections collected	37152	
Independent reflections [R(int)]	2974 [0.0812]	
Completeness to θ	(26.37°) 99.3 %	
Data / restraints / parameters	2974 / 0 / 190	
Goodness-of-fit on F^2	0.869	
R indices [$I>2\sigma(I)$] (R, R_w)	0.0433, 0.0884	
R indices (all data) (R, R_w)	0.0506, 0.0919	
Final maximum/minimum (e $Å^{-3}$)	0.250, –0.334	

Table A1.2. Atomic coordinates (x 10^4) and equivalent isotropic displacement parameters (Å^{2}x 10^3) for 3.22. U(eq) is defined as $^1/_3$ of the trace of the orthogonalized U^{ij} tensor.

	x	y	z	U(eq)		x	y	z	U(eq)
Fe	776(1)	8150(1)	681(1)	20(1)	C1A	-1509(5)	8880(5)	826(1)	26(1)
C1	1610(4)	9790(4)	362(1)	22(1)	C2A	-392(5)	8894(4)	1078(1)	25(1)
C2	2719(5)	9695(4)	613(1)	24(1)	C3A	257(5)	7280(5)	1112(1)	29(1)
C3	3275(4)	8047(5)	639(1)	25(1)	C4A	-361(5)	4543(5)	825(1)	34(1)
C4	2662(5)	5436(5)	310(1)	27(1)	C5A	-1263(6)	3890(5)	595(1)	41(1)
C5	1755(5)	4880(5)	70(1)	32(1)	C6A	-2371(6)	4862(6)	415(1)	40(1)
C6	704(5)	5946(5)	-102(1)	29(1)	C7A	-2538(5)	6491(6)	468(1)	34(1)
C7	598(4)	7561(4)	-34(1)	22(1)	C8A	-1620(5)	7237(5)	711(1)	25(1)
C8	1516(4)	8204(5)	219(1)	21(1)	C9A	-516(5)	6245(5)	892(1)	25(1)
C9	2567(4)	7121(5)	395(1)	23(1)	C10A	-46(6)	10318(5)	1286(1)	40(1)
C10	3291(5)	11103(5)	808(1)	32(1)					

Table A1.3. Anisotropic displacement parameters (Å^{2}x 10^3) for 3.22. The anisotropic displacement factor exponent takes the form: $-2p^2[h^2 a^{*2}U^{11} + ... + 2 h k a^* b^* U^{12}]$.

	U^{11}	U^{22}	U^{33}	U^{23}	U^{13}	U^{12}		U^{11}	U^{22}	U^{33}	U^{23}	U^{13}	U^{12}
Fe	24(1)	21(1)	16(1)	1(1)	2(1)	0(1)	C1A	31(2)	25(2)	24(2)	2(2)	9(2)	5(2)
C1	22(2)	24(2)	22(2)	2(1)	3(2)	-1(2)	C2A	29(2)	25(2)	21(2)	0(2)	8(2)	-2(2)
C2	26(2)	23(2)	23(2)	-1(1)	-1(2)	-6(2)	C3A	32(2)	34(2)	21(2)	2(2)	4(2)	3(2)
C3	22(2)	30(2)	23(2)	3(2)	1(2)	3(2)	C4A	39(2)	23(2)	38(2)	3(2)	15(2)	2(2)
C4	29(2)	28(2)	25(2)	0(2)	2(2)	10(2)	C5A	52(3)	23(2)	47(3)	-8(2)	18(2)	-7(2)
C5	34(2)	23(2)	40(2)	-10(2)	6(2)	4(2)	C6A	43(3)	45(3)	32(2)	-8(2)	5(2)	-17(2)
C6	34(2)	34(2)	18(2)	-10(2)	2(2)	1(2)	C7A	27(2)	44(3)	30(2)	2(2)	1(2)	-8(2)
C7	24(2)	29(2)	13(2)	0(1)	0(1)	2(2)	C8A	22(2)	28(2)	26(2)	2(2)	4(2)	1(2)
C8	21(2)	27(2)	15(2)	0(2)	5(1)	-1(2)	C9A	27(2)	27(2)	21(2)	4(2)	6(2)	-1(2)
C9	21(2)	25(2)	23(2)	1(2)	4(1)	1(2)	C10A	57(3)	34(2)	30(2)	-7(2)	8(2)	-7(2)
C10	34(2)	33(2)	27(2)	-12(2)	-2(2)	-6(2)							

Table A1.4. Hydrogen coordinates (x 10^4) and isotropic displacement parameters (Å^{2}x 10^3) for 3.22.

	x	y	z	U(eq)		x	y	z	U(eq)
H1	1026	10791	291	27	H1A	-2128	9838	746	32
H3	4048	7625	798	30	H3A	1073	6931	1270	35
H4	3352	4717	421	33	H4A	369	3884	940	40
H5	1816	3764	15	39	H5A	-1166	2762	552	49
H6	72	5515	-266	34	H6A	-2994	4361	256	48
H7	-80	8253	-153	26	H7A	-3255	7123	344	40
H10A	4256	11592	713	47	H10D	-829	10327	1457	60
H10B	3563	10714	1015	47	H10E	-143	11330	1168	60
H10C	2425	11919	822	47	H10F	1058	10223	1369	60

Table A2.1. Crystal data and structure refinement for bis(4,7-dimethylindenyl)iron(II) (3.25).

Empirical formula	$C_{22}H_{22}Fe$	
Formula weight	342.25	
Temperature (K)	163(2)	
Crystal system	Orthorhombic	
Space group	Pbca	
Unit cell dimensions	a = 12.380(6) Å	α = 90°
	b = 15.649(8) Å	β = 90°
	c = 25.774(14) Å	γ = 90°
Volume ($Å^3$)	4993(5)	
Z	12	
Density (calculated) (Mg/m^3)	1.366	
Absorption coefficient (mm^{-1})	0.903	
F(000)	2160	
Crystal size (mm^3)	0.54 x 0.27 x 0.05	
Theta range for data collection (°)	2.24 to 26.41	
Index ranges	$-15 \le h \le 7$	
	$-19 \le k \le 19$	
	$-32 \le l \le 31$	
Reflections collected	58884	
Independent reflections [R(int)]	5081 [0.0599]	
Completeness to θ	(26.41°) 99.1 %	
Data / restraints / parameters	5081 / 0 / 414	
Goodness-of-fit on F^2	0.784	
R indices [$I>2\sigma(I)$] (R, R_w)	0.0274, 0.0674	
R indices (all data) (R, R_w)	0.0563, 0.0775	
Final maximum/minimum (e $Å^{-3}$)	0.238, –0.303	

Table A2.2. Atomic coordinates (x 10^4) and equivalent isotropic displacement parameters (Å^{2}x 10^3) for 3.25. U(eq) is defined as $^1/_3$ of the trace of the orthogonalized U^{ij} tensor.

	x	y	z	U(eq)		x	y	z	U(eq)
Fe1	733(1)	1194(1)	6272(1)	21(1)	C11A	-2261(2)	2169(2)	6576(1)	73(1)
Fe2	4363(1)	574(1)	4589(1)	18(1)	C1B	5544(4)	1071(4)	4119(2)	23(1)
C1	1325(2)	2081(1)	6784(1)	27(1)	C2B	4725(3)	653(3)	3818(2)	28(1)
C2	2137(2)	1828(1)	6422(1)	31(1)	C3B	4672(4)	-221(3)	3977(2)	26(1)
C3	2301(2)	930(1)	6467(1)	27(1)	C4B	4186(6)	1101(4)	5349(3)	25(1)
C4	1440(1)	-223(1)	7077(1)	26(1)	C5B	3411(4)	1017(3)	4994(2)	33(1)
C5	652(2)	-308(1)	7442(1)	30(1)	C6B	2886(7)	223(6)	4903(3)	30(2)
C6	35(1)	398(1)	7629(1)	29(1)	C7B	6865(4)	508(5)	4827(2)	27(1)
C7	196(1)	1211(1)	7463(1)	25(1)	C8B	6028(3)	453(3)	4450(2)	21(1)
C8	1001(1)	1339(1)	7067(1)	22(1)	C9B	5486(6)	-368(5)	4362(3)	20(1)
C9	1612(1)	621(1)	6873(1)	21(1)	C10B	4731(3)	1947(2)	5482(2)	37(1)
C10	2147(2)	-946(1)	6899(1)	41(1)	C20B	7438(2)	1389(1)	4869(1)	42(1)
C11	-419(2)	1966(2)	7671(1)	42(1)	C1C	3875(4)	1500(3)	5099(2)	25(1)
C1A	-357(2)	1791(1)	5800(1)	33(1)	C2C	3055(3)	1338(3)	4721(2)	26(1)
C2A	412(2)	1331(1)	5501(1)	34(1)	C3C	2746(7)	457(5)	4747(3)	26(2)
C3A	360(2)	456(1)	5637(1)	31(1)	C4C	6647(5)	774(4)	4632(2)	25(1)
C4A	-870(2)	-372(1)	6291(1)	38(1)	C5C	5926(5)	928(4)	4242(3)	27(1)
C5A	-1657(2)	-235(2)	6650(1)	48(1)	C6C	5211(4)	294(3)	4033(2)	33(1)
C6A	-2096(2)	579(2)	6753(1)	54(1)	C7C	5211(6)	-503(6)	4208(3)	23(2)
C7A	-1771(2)	1298(2)	6496(1)	43(1)	C8C	4070(6)	724(4)	5389(3)	21(1)
C8A	-926(1)	1195(1)	6117(1)	29(1)	C9C	3338(3)	78(3)	5162(2)	19(1)
C9A	-478(1)	361(1)	6019(1)	27(1)	C20C	7438(2)	1389(1)	4869(1)	42(1)
C10A	-424(2)	-1237(1)	6169(1)	56(1)	C11C	4505(3)	-1215(3)	3990(2)	39(1)

Table A2.3. Anisotropic displacement parameters ($Å^2 x\ 10^3$) for 3.25. The anisotropic displacement factor exponent takes the form: $-2p^2[\ h^2\ a^{*2}U^{11} + ... + 2\ h\ k\ a^*\ b^*\ U^{12}\ ]$.

	U^{11}	U^{22}	U^{33}	U^{23}	U^{13}	U^{12}		U^{11}	U^{22}	U^{33}	U^{23}	U^{13}	U^{12}
Fe1	18(1)	24(1)	19(1)	2(1)	0(1)	-1(1)	C11A	50(2)	108(2)	61(2)	-6(2)	-1(1)	46(2)
Fe2	16(1)	21(1)	16(1)	1(1)	1(1)	1(1)	C1B	25(3)	23(3)	21(3)	5(2)	7(2)	5(2)
C1	30(1)	21(1)	31(1)	0(1)	-5(1)	-4(1)	C2B	28(2)	41(2)	14(2)	2(2)	3(2)	4(2)
C2	26(1)	35(1)	32(1)	8(1)	-2(1)	-11(1)	C3B	25(2)	32(2)	21(2)	-6(2)	3(2)	-3(2)
C3	16(1)	38(1)	27(1)	0(1)	0(1)	0(1)	C4B	31(3)	18(3)	25(3)	9(3)	9(2)	17(3)
C4	23(1)	25(1)	29(1)	1(1)	-7(1)	2(1)	C5B	25(2)	43(3)	32(3)	14(2)	6(2)	12(2)
C5	33(1)	28(1)	29(1)	9(1)	-8(1)	-6(1)	C6B	15(3)	50(6)	25(5)	2(3)	-7(3)	5(3)
C6	23(1)	46(1)	19(1)	4(1)	0(1)	-4(1)	C7B	19(3)	36(4)	27(3)	0(3)	2(2)	-3(3)
C7	23(1)	36(1)	18(1)	-5(1)	-1(1)	2(1)	C8B	22(2)	23(2)	18(2)	1(2)	5(2)	5(2)
C8	22(1)	24(1)	21(1)	-2(1)	-4(1)	-2(1)	C9B	15(3)	30(4)	15(4)	-1(3)	1(3)	2(3)
C9	15(1)	27(1)	22(1)	-1(1)	-4(1)	0(1)	C10B	42(2)	20(2)	49(3)	1(2)	17(2)	1(2)
C10	39(1)	30(1)	55(2)	-2(1)	-5(1)	9(1)	C20B	35(1)	40(1)	51(1)	-9(1)	7(1)	-13(1)
C11	42(1)	49(1)	36(1)	-10(1)	9(1)	10(1)	C1C	21(2)	20(2)	33(2)	-4(2)	8(2)	-2(2)
C1A	34(1)	35(1)	32(1)	10(1)	-11(1)	4(1)	C2C	21(2)	28(2)	29(2)	6(2)	3(2)	9(2)
C2A	31(1)	50(1)	22(1)	9(1)	-3(1)	-8(1)	C3C	15(3)	42(5)	21(4)	1(3)	-1(3)	2(3)
C3A	30(1)	40(1)	22(1)	-6(1)	-3(1)	-2(1)	C4C	29(3)	23(3)	23(3)	-1(2)	12(3)	-2(2)
C4A	35(1)	45(1)	35(1)	11(1)	-17(1)	-18(1)	C5C	33(4)	24(3)	24(4)	10(3)	9(3)	13(3)
C5A	33(1)	71(2)	39(1)	20(1)	-10(1)	-26(1)	C6C	28(2)	52(3)	17(2)	4(2)	5(2)	16(3)
C6A	19(1)	110(2)	33(1)	10(1)	1(1)	-10(1)	C7C	16(4)	40(4)	14(4)	0(3)	-3(2)	4(3)
C7A	21(1)	74(2)	35(1)	1(1)	-3(1)	11(1)	C8C	24(3)	18(3)	20(3)	3(3)	6(2)	9(3)
C8A	20(1)	41(1)	26(1)	5(1)	-6(1)	4(1)	C9C	16(2)	23(3)	19(2)	0(2)	5(2)	2(2)
C9A	23(1)	35(1)	23(1)	2(1)	-7(1)	-8(1)	C20C	35(1)	40(1)	51(1)	-9(1)	7(1)	-13(1)
C10A	67(2)	39(1)	62(2)	8(1)	-24(1)	-22(1)	C11C	30(2)	60(3)	28(2)	-11(2)	-6(2)	-10(2)

Table A2.4. Hydrogen coordinates (x 10^4) and isotropic displacement parameters ($Å^2$x 10^3) for 3.25.

	x	y	z	U(eq)		x	y	z	U(eq)
H1A	1044	2674	6836	33	H1B	5751	1687	4094	28
H2A	2524	2216	6176	37	H2B	4266	927	3546	34
H3A	2820	580	6259	33	H3B	4165	-661	3836	31
H5A	506	-861	7577	36	H5B	3204	1502	4795	40
H6A	-511	294	7880	35	H6B	2339	197	4645	36
H10A	1873	-1486	7040	62	H10G	4482	2391	5241	55
H10B	2887	-853	7021	62	H10H	5516	1884	5451	55
H10C	2143	-972	6519	62	H10I	4546	2111	5838	55
H11A	-979	1768	7911	63	H20A	8017	1356	5127	63
H11B	-756	2275	7382	63	H20B	6913	1824	4975	63
H11C	78	2348	7855	63	H20C	7744	1543	4531	63
H1AA	-492	2421	5783	40	H1C	4244	2060	5157	30
H2AA	913	1584	5238	41	H2C	2757	1768	4472	31
H3AA	814	-13	5489	37	H3C	2195	167	4525	31
H5AA	-1924	-710	6840	57	H5C	5898	1488	4100	33
H6AA	-2639	630	7011	65	H6C	4725	448	3764	39
H10D	-744	-1661	6402	84	H20D	8167	1257	4745	63
H10E	362	-1232	6215	84	H20E	7415	1338	5248	63
H10F	-597	-1385	5809	84	H20F	7246	1974	4768	63
H11D	-2713	2163	6888	110	H11G	4054	-987	3710	59
H11E	-2705	2319	6274	110	H11H	4043	-1443	4266	59
H11F	-1684	2592	6617	110	H11I	4965	-1673	3854	59

Table A3.1. Crystal data and structure refinement for bis(1,3-bis(trimethylsilyl)indenyl)iron(II) (3.31).

Empirical formula	$C_{30}H_{46}FeSi_4$	
Formula weight	574.88	
Temperature (K)	168(2)	
Crystal system	Monoclinic	
Space group	$P2_1/c$	
Unit cell dimensions	a = 19.557(13) Å	α = 90°
	b = 10.238(5) Å	β = 118.361(7)°
	c = 18.634(9) Å	γ = 90°
Volume ($Å^3$)	3283(3)	
Z	4	
Density (calculated) (Mg/m^3)	1.163	
Absorption coefficient (mm^{-1})	0.622	
F(000)	1232	
Crystal size (mm^3)	0.43 x 0.30 x 0.03	
Theta range for data collection (°)	2.19 to 26.43	
Index ranges	$-24 \le h \le 24$	
	$-12 \le k \le 12$	
	$-20 \le l \le 23$	
Reflections collected	41643	
Independent reflections [R(int)]	6712 [0.0921]	
Completeness to θ	(26.43°) 99.3 %	
Data / restraints / parameters	6712 / 0 / 316	
Goodness-of-fit on F^2	0.580	
R indices [$I>2\sigma(I)$] (R, R_w)	0.0387, 0.1107	
R indices (all data) (R, R_w)	0.0936, 0.1515	
Final maximum/minimum (e $Å^{-3}$)	0.311, –0.285	

Table A3.2. Atomic coordinates ($x10^4$) and equivalent isotropic displacement parameters ($Å^2x10^3$) for 3.31. U(eq) is defined as $^1/_3$ of the trace of the orthogonalized U^{ij} tensor.

	x	y	z	U(eq)		x	y	z	U(eq)
Fe	2643(1)	6666(1)	4732(1)	21(1)	C21	1186(3)	9855(5)	4749(3)	58(1)
Si1	2291(1)	4399(1)	3054(1)	26(1)	C22	107(2)	7560(5)	3897(3)	49(1)
Si2	858(1)	8681(1)	3892(1)	32(1)	C1A	2533(2)	5764(3)	5669(2)	25(1)
Si1A	1761(1)	4968(1)	5831(1)	32(1)	C2A	2802(2)	7081(3)	5874(2)	26(1)
Si2A	4145(1)	8773(1)	6261(1)	35(1)	C3A	3522(2)	7297(3)	5863(2)	26(1)
C1	2254(2)	5938(3)	3563(2)	22(1)	C4A	4414(2)	5605(4)	5643(2)	32(1)
C2	1620(2)	6335(3)	3697(2)	24(1)	C5A	4492(2)	4330(4)	5524(2)	39(1)
C3	1662(2)	7682(3)	3905(2)	25(1)	C6A	3908(2)	3399(4)	5418(2)	38(1)
C4	2629(2)	9473(4)	3905(2)	32(1)	C7A	3247(2)	3769(4)	5428(2)	31(1)
C5	3222(2)	9688(4)	3734(2)	42(1)	C8A	3144(2)	5100(3)	5568(2)	25(1)
C6	3566(2)	8635(4)	3517(2)	41(1)	C9A	3733(2)	6041(3)	5682(2)	26(1)
C7	3323(2)	7386(4)	3488(2)	32(1)	C10A	1008(2)	4106(4)	4917(2)	45(1)
C8	2688(2)	7124(3)	3640(2)	23(1)	C11A	2261(3)	3734(4)	6650(3)	51(1)
C9	2335(2)	8180(3)	3851(2)	25(1)	C12A	1321(2)	6222(4)	6211(3)	48(1)
C10	1764(2)	4828(4)	1947(2)	35(1)	C20A	4832(3)	8435(5)	7351(3)	69(2)
C11	3303(2)	3865(4)	3322(2)	38(1)	C21A	3522(3)	10198(4)	6187(3)	53(1)
C12	1776(2)	3077(4)	3291(2)	34(1)	C22A	4726(2)	9075(5)	5722(3)	53(1)
C20	428(2)	9626(4)	2915(3)	47(1)					

Table A3.3. Anisotropic displacement parameters ($Å^2 x\ 10^3$) for 3.31. The anisotropic displacement factor exponent takes the form: $-2p^2[\ h^2\ a^{*2}U^{11} + ... + 2\ h\ k\ a^*\ b^*\ U^{12}\ ]$.

	U^{11}	U^{22}	U^{33}	U^{23}	U^{13}	U^{12}		U^{11}	U^{22}	U^{33}	U^{23}	U^{13}	U^{12}
Fe	20(1)	22(1)	18(1)	1(1)	8(1)	-2(1)	C21	58(3)	63(3)	46(3)	-13(2)	18(2)	21(3)
Si1	28(1)	26(1)	22(1)	-2(1)	10(1)	-1(1)	C22	34(2)	60(3)	58(3)	18(2)	25(2)	15(2)
Si2	30(1)	35(1)	28(1)	4(1)	12(1)	9(1)	C1A	28(2)	25(2)	23(2)	3(1)	12(2)	-2(2)
Si1A	34(1)	35(1)	30(1)	3(1)	19(1)	-9(1)	C2A	28(2)	28(2)	18(2)	2(1)	8(2)	0(2)
Si2A	36(1)	39(1)	24(1)	-6(1)	9(1)	-17(1)	C3A	25(2)	32(2)	18(2)	0(2)	8(1)	-4(2)
C1	21(2)	23(2)	20(2)	2(1)	7(1)	-1(1)	C4A	24(2)	48(2)	22(2)	7(2)	10(2)	1(2)
C2	20(2)	25(2)	22(2)	0(1)	7(1)	-2(1)	C5A	28(2)	56(3)	28(2)	11(2)	11(2)	14(2)
C3	25(2)	28(2)	18(2)	4(1)	8(1)	0(2)	C6A	53(2)	32(2)	27(2)	6(2)	18(2)	14(2)
C4	42(2)	23(2)	29(2)	1(2)	14(2)	-3(2)	C7A	38(2)	29(2)	24(2)	6(2)	13(2)	2(2)
C5	47(2)	33(2)	40(2)	6(2)	16(2)	-14(2)	C8A	25(2)	26(2)	19(2)	10(1)	6(1)	2(2)
C6	40(2)	50(3)	40(2)	0(2)	24(2)	-16(2)	C9A	25(2)	32(2)	16(2)	7(2)	6(1)	0(2)
C7	31(2)	37(2)	31(2)	-1(2)	17(2)	-7(2)	C10A	46(2)	51(3)	42(2)	-4(2)	24(2)	-20(2)
C8	24(2)	25(2)	17(2)	2(1)	8(1)	-3(1)	C11A	66(3)	49(3)	42(2)	11(2)	29(2)	-11(2)
C9	26(2)	24(2)	19(2)	3(1)	7(1)	-2(1)	C12A	45(2)	57(3)	55(3)	-5(2)	35(2)	-4(2)
C10	41(2)	34(2)	26(2)	-1(2)	14(2)	0(2)	C20A	63(3)	89(4)	27(2)	-9(2)	-1(2)	-26(3)
C11	35(2)	43(2)	35(2)	-3(2)	15(2)	5(2)	C21A	63(3)	40(3)	57(3)	-14(2)	28(2)	-19(2)
C12	42(2)	26(2)	33(2)	-4(2)	16(2)	-7(2)	C22A	43(2)	68(3)	46(3)	2(2)	20(2)	-25(2)
C20	37(2)	49(3)	48(3)	16(2)	16(2)	11(2)							

Table A3.4. Hydrogen coordinates (x 10^4) and isotropic displacement parameters ($Å^2$x 10^3) for 3.31.

	x	y	z	U(eq)		x	y	z	U(eq)
H2	1207	5728	3668	28	H2A	2511	7778	5993	31
H4	2411	10178	4060	38	H4A	4804	6212	5701	38
H5	3410	10551	3759	50	H5A	4948	4042	5511	46
H6	3974	8813	3391	50	H6A	3984	2505	5338	45
H7	3574	6692	3367	38	H7A	2857	3143	5343	38
H10A	1234	5109	1800	52	H10D	735	4738	4476	67
H10B	1742	4062	1622	52	H10E	636	3683	5054	67
H10C	2038	5538	1838	52	H10F	1258	3444	4739	67
H11A	3568	4569	3195	57	H11D	2664	4164	7138	76
H11B	3279	3086	3005	57	H11E	2499	3067	6462	76
H11C	3590	3661	3905	57	H11F	1882	3322	6783	76
H12A	1249	3367	3149	52	H12D	1732	6652	6693	71
H12B	2060	2872	3874	52	H12E	954	5801	6356	71
H12C	1747	2295	2974	52	H12F	1047	6873	5784	71
H20A	1	10170	2880	70	H20D	4539	8286	7649	103
H20B	230	9018	2453	70	H20E	5179	9185	7588	103
H20C	828	10184	2900	70	H20F	5140	7657	7390	103
H21A	1413	9376	5267	87	H21D	3165	10381	5612	80
H21B	741	10369	4696	87	H21E	3851	10963	6437	80
H21C	1577	10441	4739	87	H21F	3223	9998	6471	80
H22A	330	7069	4410	73	H22D	4374	9264	5146	79
H22B	-65	6950	3438	73	H22E	5035	8298	5764	79
H22C	-337	8072	3845	73	H22F	5072	9822	5972	79

Table A4.1. Crystal data and structure refinement for *rac*-bis(1-diphenylphosphinoindenyl)iron(II) (*rac*-3.32).

Empirical formula	$C_{42}H_{32}FeP_2$	
Formula weight	654.47	
Temperature (K)	168(2)	
Crystal system	Orthorhombic	
Space group	Pbcn	
Unit cell dimensions	a = 12.959(6) Å	α = 90°
	b = 12.396(5) Å	β = 90°
	c = 19.296(8) Å	γ = 90°
Volume ($Å^3$)	3100(2)	
Z	4	
Density (calculated) (Mg/m^3)	1.402	
Absorption coefficient (mm^{-1})	0.621	
F(000)	1360	
Crystal size (mm^3)	0.30 x 0.21 x 0.04	
Theta range for data collection (°)	2.11 to 26.44	
Index ranges	$-16 \le h \le 16$	
	$-15 \le k \le 8$	
	$-23 \le l \le 23$	
Reflections collected	37580	
Independent reflections [R(int)]	3142 [0.1169]	
Completeness to θ	(26.4°) 98.3 %	
Data / restraints / parameters	3142 / 0 / 204	
Goodness-of-fit on F^2	0.966	
R indices [$I>2\sigma(I)$] (R, R_w)	0.0351, 0.0783	
R indices (all data) (R, R_w)	0.0908, 0.1124	
Final maximum/minimum (e $Å^{-3}$)	0.308, –0.427	

Table A4.2. Atomic coordinates (x 10^4) and equivalent isotropic displacement parameters (Å^{2}x 10^3) for *rac*-3.32. U(eq) is defined as $^1/_3$ of the trace of the orthogonalized U^{ij} tensor.

	x	y	z	U(eq)		x	y	z	U(eq)
Fe	0	1725(1)	2500	19(1)	C11	2097(3)	-482(3)	4897(2)	30(1)
P	604(1)	615(1)	4073(1)	22(1)	C12	2994(3)	-559(3)	5284(2)	34(1)
C1	1016(2)	1245(2)	3262(2)	20(1)	C13	3671(3)	306(3)	5322(2)	38(1)
C2	1275(2)	766(2)	2602(2)	23(1)	C14	3439(3)	1246(3)	4970(2)	37(1)
C3	1476(2)	1588(2)	2104(2)	22(1)	C15	2536(3)	1313(3)	4584(2)	31(1)
C4	1499(2)	3691(3)	2220(2)	26(1)	C20	325(2)	-760(2)	3778(2)	22(1)
C5	1335(3)	4502(3)	2681(2)	29(1)	C21	-693(3)	-1114(3)	3812(2)	29(1)
C6	1047(3)	4298(3)	3390(2)	28(1)	C22	-954(3)	-2153(3)	3608(2)	36(1)
C7	919(2)	3285(3)	3629(2)	24(1)	C23	-188(3)	-2846(3)	3379(2)	37(1)
C8	1098(2)	2399(2)	3164(2)	21(1)	C24	828(3)	-2509(3)	3338(2)	34(1)
C9	1387(2)	2605(2)	2452(2)	21(1)	C25	1086(3)	-1467(3)	3537(2)	27(1)
C10	1850(2)	445(2)	4528(2)	24(1)					

Table A4.3. Anisotropic displacement parameters (Å^{2}x 10^3) for *rac*-3.32. The anisotropic displacement factor exponent takes the form: $-2p^2[h^2 a^{*2}U^{11} + ... + 2 h k a^* b^* U^{12}]$.

	U^{11}	U^{22}	U^{33}	U^{23}	U^{13}	U^{12}		U^{11}	U^{22}	U^{33}	U^{23}	U^{13}	U^{12}
Fe	16(1)	17(1)	22(1)	0	-2(1)	0	C11	36(2)	26(2)	29(2)	3(2)	-2(2)	-2(2)
P	22(1)	20(1)	25(1)	1(1)	-1(1)	1(1)	C12	39(2)	37(2)	26(2)	5(2)	-3(2)	15(2)
C1	17(2)	19(2)	25(2)	1(1)	-3(1)	0(1)	C13	29(2)	54(3)	30(2)	-2(2)	-11(2)	8(2)
C2	19(2)	21(2)	28(2)	-3(2)	-3(2)	4(1)	C14	36(2)	37(2)	39(2)	-1(2)	-11(2)	-4(2)
C3	18(2)	25(2)	23(2)	2(2)	2(2)	3(1)	C15	33(2)	27(2)	32(2)	1(2)	-5(2)	2(2)
C4	18(2)	28(2)	32(2)	8(2)	-2(2)	-4(2)	C20	24(2)	20(2)	23(2)	5(1)	-1(2)	-1(1)
C5	22(2)	17(2)	47(2)	4(2)	-7(2)	-2(1)	C21	27(2)	31(2)	28(2)	6(2)	-2(2)	-4(2)
C6	23(2)	23(2)	38(2)	-5(2)	-5(2)	-1(2)	C22	30(2)	35(2)	43(2)	12(2)	-7(2)	-10(2)
C7	20(2)	25(2)	27(2)	-2(2)	-4(2)	0(2)	C23	49(3)	21(2)	41(2)	4(2)	-12(2)	-8(2)
C8	14(2)	19(2)	28(2)	0(1)	-3(1)	0(1)	C24	41(2)	25(2)	35(2)	-2(2)	-5(2)	1(2)
C9	14(2)	22(2)	27(2)	1(2)	-4(2)	0(1)	C25	28(2)	26(2)	28(2)	2(2)	0(2)	-1(2)
C10	26(2)	26(2)	19(2)	-2(1)	-1(2)	4(2)							

Table A4.4. Hydrogen coordinates (x 10^4) and isotropic displacement parameters ($Å^2$x 10^3) for *rac*-3.32.

	x	y	z	U(eq)		x	y	z	U(eq)
H2	1294	-27	2505	27	H13	4287	253	5587	45
H3	1665	1476	1607	26	H14	3895	1845	4992	45
H4	1685	3845	1754	31	H15	2380	1968	4351	37
H5	1412	5228	2531	34	H21	-1215	-640	3977	34
H6	946	4889	3696	34	H22	-1652	-2387	3626	43
H7	715	3159	4095	29	H23	-363	-3562	3249	44
H11	1638	-1079	4884	36	H24	1346	-2988	3174	40
H12	3147	-1208	5524	41	H25	1783	-1233	3509	33

Table A5.1. Crystal data and structure refinement for *rac*-bis(1-diphenylphosphino-3-methylindenyl)iron(II) (*rac*-3.34).

Empirical formula	$C_{44}H_{36}FeP_2$	
Formula weight	682.52	
Temperature (K)	163(2)	
Crystal system	Monoclinic	
Space group	C2/c	
Unit cell dimensions	a = 15.569(16) Å	α = 90°
	b = 13.705(15) Å	β = 110.40(3)°
	c = 17.401(18) Å	γ = 90°
Volume ($Å^3$)	3480(6)	
Z	4	
Density (calculated) (Mg/m^3)	1.303	
Absorption coefficient (mm^{-1})	1.556	
F(000)	1424	
Crystal size (mm^3)	0.40 x 0.24 x 0.19	
Theta range for data collection (°)	2.04 to 26.31	
Index ranges	$-10 \le h \le 19$	
	$-16 \le k \le 17$	
	$-21 \le l \le 11$	
Reflections collected	6664	
Independent reflections [R(int)]	3209 [0.0416]	
Completeness to θ	(26.3°) 90.7 %	
Data / restraints / parameters	3209 / 0 / 213	
Goodness-of-fit on F^2	0.892	
R indices [$I>2\sigma(I)$] (R, R_w)	0.0373, 0.0788	
R indices (all data) (R, R_w)	0.0652, 0.0840	
Final maximum/minimum (e $Å^{-3}$)	0.339, –0.369	

Table A5.2. Atomic coordinates (x 10^4) and equivalent isotropic displacement parameters (Å^{2}x 10^3) for *rac*-3.34. U(eq) is defined as $^1/_3$ of the trace of the orthogonalized U^{ij} tensor.

	x	y	z	U(eq)		x	y	z	U(eq)
Fe	10000	6565(1)	7500	20(1)	C11	7994(2)	5789(2)	8989(1)	26(1)
P	8253(1)	5469(1)	8062(1)	26(1)	C12	8641(2)	6164(2)	9708(2)	29(1)
C1	9343(2)	6112(2)	8283(1)	23(1)	C13	8392(2)	6423(2)	10377(2)	32(1)
C2	10271(2)	5745(2)	8554(1)	24(1)	C14	7493(2)	6303(2)	10339(2)	36(1)
C3	10906(2)	6536(2)	8712(1)	24(1)	C15	6845(2)	5925(2)	9633(2)	38(1)
C4	10634(2)	8435(2)	8656(2)	30(1)	C16	7089(2)	5680(2)	8964(2)	31(1)
C5	9957(2)	9126(2)	8475(2)	38(1)	C21	8652(2)	4190(2)	8278(2)	26(1)
C6	9011(2)	8870(2)	8196(2)	36(1)	C22	8826(2)	3717(2)	9030(2)	33(1)
C7	8732(2)	7921(2)	8105(2)	29(1)	C23	9071(2)	2734(2)	9118(2)	41(1)
C8	9409(2)	7166(2)	8304(1)	22(1)	C24	9140(2)	2207(2)	8459(2)	41(1)
C9	10374(2)	7424(2)	8575(1)	23(1)	C25	8978(2)	2674(2)	7712(2)	45(1)
C10	11938(2)	6475(2)	9024(2)	34(1)	C26	8731(2)	3656(2)	7620(2)	35(1)

Table A5.3. Anisotropic displacement parameters (Å^{2}x 10^3) for *rac*-3.34. The anisotropic displacement factor exponent takes the form: $-2p^2[h^2 a^{*2}U^{11} + ... + 2 h k a^* b^* U^{12}]$.

	U^{11}	U^{22}	U^{33}	U^{23}	U^{13}	U^{12}		U^{11}	U^{22}	U^{33}	U^{23}	U^{13}	U^{12}
Fe	20(1)	20(1)	21(1)	0	8(1)	0	C11	29(1)	23(1)	27(1)	4(1)	11(1)	1(1)
P	25(1)	29(1)	24(1)	0(1)	9(1)	-5(1)	C12	26(1)	31(1)	31(2)	1(1)	10(1)	-1(1)
C1	24(1)	27(1)	21(1)	1(1)	11(1)	-3(1)	C13	40(2)	30(2)	26(1)	2(1)	12(1)	1(1)
C2	29(1)	22(1)	22(1)	3(1)	9(1)	3(1)	C14	48(2)	35(2)	37(2)	3(1)	28(2)	8(1)
C3	24(1)	28(1)	19(1)	-1(1)	7(1)	-2(1)	C15	30(2)	45(2)	47(2)	2(1)	23(2)	2(1)
C4	29(1)	30(1)	32(1)	-7(1)	11(1)	-9(1)	C16	28(2)	33(2)	34(2)	-3(1)	13(1)	-6(1)
C5	47(2)	24(1)	45(2)	-8(1)	20(2)	-5(1)	C21	24(1)	30(1)	26(1)	-5(1)	9(1)	-9(1)
C6	36(2)	27(1)	48(2)	-2(1)	19(2)	8(1)	C22	39(2)	30(2)	31(2)	-3(1)	15(1)	-5(1)
C7	24(1)	31(2)	33(2)	0(1)	14(1)	1(1)	C23	44(2)	34(2)	43(2)	7(1)	14(2)	-5(1)
C8	24(1)	26(1)	20(1)	-3(1)	12(1)	-4(1)	C24	38(2)	27(2)	59(2)	-1(2)	17(2)	2(1)
C9	25(1)	27(1)	19(1)	-2(1)	9(1)	-5(1)	C25	45(2)	41(2)	50(2)	-16(2)	20(2)	-3(2)
C10	23(1)	40(2)	33(2)	-2(1)	4(1)	-2(1)	C26	40(2)	37(2)	31(2)	-6(1)	15(1)	-9(1)

Table A5.4. Hydrogen coordinates (x 10^4) and isotropic displacement parameters (Å^{2}x 10^3) for *rac*-3.34.

	x	y	z	U(eq)		x	y	z	U(eq)
H2	10442	5039	8605	29	H13	8838	6682	10858	38
H4	11261	8620	8831	36	H14	7321	6478	10794	44
H5	10123	9796	8538	45	H15	6231	5834	9608	46
H6	8563	9373	8069	43	H16	6636	5435	8481	38
H7	8098	7763	7913	34	H22	8778	4068	9484	39
H10A	12169	6470	9625	50	H23	9191	2422	9632	49
H10B	12188	7041	8829	50	H24	9297	1534	8519	50
H10C	12128	5875	8821	50	H25	9035	2321	7262	53
H12	9259	6242	9740	35	H26	8615	3966	7106	42

Table A6.1. Crystal data and structure refinement for *rac*-bis(1-diphenylphosphino-2,3-dimethylindenyl)iron(II) (*rac*-3.35).

Empirical formula	$C_{46}H_{40}FeP_2$	
Formula weight	710.57	
Temperature (K)	183(2)	
Crystal system	Triclinic	
Space group	P-1	
Unit cell dimensions	a = 9.397(19) Å	α = 93.93(4)°
	b = 14.16(3)Å	β = 101.65(6)°
	c = 14.23(3) Å	γ = 90.03(6)°
Volume ($Å^3$)	1850(7)	
Z	2	
Density (calculated) (Mg/m^3)	1.276	
Absorption coefficient (mm^{-1})	0.526	
F(000)	744	
Crystal size (mm^3)	0.41 x 0.15 x 0.07	
Theta range for data collection (°)	1.98 to 26.46	
Index ranges	$-11 \le h \le 10$	
	$-17 \le k \le 17$	
	$-17 \le l \le 17$	
Reflections collected	22975	
Independent reflections [R(int)]	7267 [0.0900]	
Completeness to θ	(26.5°) 95.0 %	
Data / restraints / parameters	7267 / 0 / 446	
Goodness-of-fit on F^2	1.053	
R indices [$I>2\sigma(I)$] (R, R_w)	0.1102, 0.3143	
R indices (all data) (R, R_w)	0.2086, 0.3593	
Final maximum/minimum (e $Å^{-3}$)	2.047, –0.415	

Table A6.2. Atomic coordinates (x 10^4) and equivalent isotropic displacement parameters (Å^{2}x 10^3) for *rac*-3.35. U(eq) is defined as $^1/_3$ of the trace of the orthogonalized U^{ij} tensor.

	x	y	z	U(eq)		x	y	z	U(eq)
Fe	2456(2)	2045(1)	6972(1)	50(1)	C36	279(12)	4678(7)	8254(8)	61(3)
P1	2883(2)	4518(2)	7639(2)	35(1)	C1A	2439(10)	1762(5)	8387(5)	37(2)
P2	2807(3)	2531(2)	9504(2)	38(1)	C2A	973(13)	1721(6)	7816(6)	60(3)
C1	2770(10)	3457(5)	6789(6)	41(2)	C3A	886(16)	1035(8)	7035(8)	76(4)
C2	4101(12)	2964(6)	6759(6)	50(3)	C4A	2690(20)	-174(8)	6523(9)	99(5)
C3	3792(13)	2225(7)	5988(7)	60(3)	C5A	3941(18)	-498(10)	6787(9)	93(5)
C4	1521(17)	1813(7)	4660(7)	74(4)	C6A	4971(16)	-66(9)	7635(10)	101(5)
C5	122(16)	2031(8)	4330(8)	76(4)	C7A	4679(16)	706(7)	8199(7)	78(4)
C6	-575(13)	2775(8)	4844(8)	71(3)	C8A	3252(12)	1039(6)	7959(6)	54(3)
C7	195(12)	3261(7)	5662(7)	60(3)	C9A	2194(16)	600(6)	7117(7)	69(4)
C8	1664(12)	3084(6)	6009(6)	48(2)	C10A	-351(11)	2250(8)	8025(8)	72(3)
C9	2365(12)	2303(6)	5491(6)	54(3)	C11A	-609(15)	804(8)	6302(7)	96(5)
C10	5575(11)	3154(7)	7362(8)	62(3)	C21A	2191(9)	1758(7)	10327(6)	43(2)
C11	4952(15)	1529(8)	5734(8)	82(4)	C22A	1990(12)	770(8)	10174(8)	70(3)
C21	3579(9)	5402(6)	6957(6)	37(2)	C23A	1446(15)	264(12)	10860(12)	114(6)
C22	3661(13)	5290(7)	5993(7)	64(3)	C24A	1112(17)	728(17)	11666(12)	121(7)
C23	4314(14)	6016(8)	5576(8)	70(3)	C25A	1311(15)	1690(15)	11820(10)	107(6)
C24	4872(11)	6814(8)	6111(10)	74(4)	C26A	1843(11)	2197(9)	11172(8)	68(3)
C25	4804(11)	6926(8)	7087(9)	66(3)	C31A	4776(9)	2532(6)	9968(6)	40(2)
C26	4199(10)	6231(6)	7498(7)	49(2)	C32A	5523(11)	1823(7)	10501(6)	55(3)
C31	1019(9)	4917(6)	7557(6)	39(2)	C33A	7049(13)	1939(10)	10858(9)	79(4)
C32	254(10)	5457(6)	6795(7)	49(2)	C34A	7783(13)	2708(13)	10664(10)	97(5)
C33	-1162(12)	5720(7)	6799(10)	74(3)	C35A	7056(17)	3420(14)	10170(9)	112(6)
C34	-1845(14)	5471(10)	7534(12)	94(4)	C36A	5549(11)	3337(9)	9825(7)	65(3)
C35	-1118(15)	4931(10)	8267(11)	96(5)					

Table A6.3. Anisotropic displacement parameters ($Å^2 x\ 10^3$) for *rac*-3.35. The anisotropic displacement factor exponent takes the form: $-2p^2[\ h^2\ a^{*2}U^{11} + ... + 2\ h\ k\ a^*\ b^*\ U^{12}\ ]$.

	U^{11}	U^{22}	U^{33}	U^{23}	U^{13}	U^{12}		U^{11}	U^{22}	U^{33}	U^{23}	U^{13}	U^{12}
Fe	90(1)	30(1)	29(1)	6(1)	7(1)	-1(1)	C36	60(7)	61(6)	69(7)	11(5)	26(6)	-1(5)
P1	41(1)	31(1)	35(1)	8(1)	11(1)	-1(1)	C1A	64(6)	26(4)	21(4)	8(3)	3(4)	-7(4)
P2	43(1)	39(1)	29(1)	4(1)	4(1)	0(1)	C2A	98(9)	40(5)	33(5)	15(4)	-13(5)	-25(6)
C1	66(6)	27(4)	31(4)	8(3)	11(4)	8(4)	C3A	123(11)	50(6)	46(6)	20(5)	-12(7)	-32(7)
C2	86(8)	35(5)	37(5)	14(4)	29(5)	16(5)	C4A	188(17)	39(6)	57(8)	4(5)	-11(9)	9(8)
C3	87(8)	56(6)	45(6)	17(5)	26(6)	10(6)	C5A	153(14)	80(9)	49(7)	-9(7)	29(8)	34(9)
C4	142(13)	43(6)	44(6)	18(5)	29(7)	-2(7)	C6A	121(12)	90(10)	95(11)	17(8)	23(9)	59(9)
C5	105(10)	61(7)	55(7)	4(6)	0(7)	-21(7)	C7A	148(12)	46(6)	45(6)	15(5)	27(7)	47(7)
C6	83(8)	71(7)	50(6)	23(6)	-12(6)	-19(6)	C8A	99(8)	27(4)	34(5)	13(4)	7(5)	10(5)
C7	72(8)	47(6)	57(6)	13(5)	2(6)	-3(5)	C9A	149(12)	20(5)	35(5)	-1(4)	10(6)	-6(6)
C8	83(8)	34(5)	27(4)	9(4)	8(5)	1(5)	C10A	57(7)	70(7)	79(8)	30(6)	-22(6)	-19(6)
C9	93(8)	40(5)	33(5)	2(4)	22(5)	1(5)	C11A	166(13)	68(7)	29(5)	17(5)	-41(7)	-69(8)
C10	56(7)	64(7)	68(7)	18(5)	10(6)	15(5)	C21A	24(5)	73(6)	32(5)	22(4)	-1(4)	-1(4)
C11	145(12)	62(7)	56(7)	15(5)	58(7)	46(7)	C22A	68(8)	85(8)	53(6)	23(6)	-5(5)	-33(6)
C21	31(5)	35(4)	49(5)	14(4)	16(4)	11(4)	C23A	80(9)	139(13)	111(12)	89(11)	-36(9)	-65(9)
C22	108(9)	51(6)	48(6)	15(5)	46(6)	8(6)	C24A	84(11)	220(20)	74(11)	96(14)	10(8)	-18(13)
C23	113(10)	59(7)	55(6)	22(5)	53(7)	12(7)	C25A	72(9)	202(18)	66(9)	67(11)	42(7)	38(11)
C24	51(7)	55(7)	134(12)	44(7)	50(7)	6(5)	C26A	57(7)	99(8)	61(7)	29(6)	34(6)	15(6)
C25	57(7)	61(7)	85(9)	23(6)	22(6)	2(5)	C31A	36(5)	48(5)	35(5)	4(4)	6(4)	-6(4)
C26	54(6)	41(5)	53(6)	18(4)	6(5)	-4(4)	C32A	56(7)	68(7)	37(5)	-4(5)	1(5)	2(5)
C31	33(5)	36(4)	52(5)	9(4)	19(4)	-1(4)	C33A	53(7)	113(10)	66(8)	0(7)	1(6)	6(7)
C32	40(6)	41(5)	73(7)	21(5)	21(5)	12(4)	C34A	35(7)	166(15)	88(10)	21(10)	6(7)	-14(8)
C33	49(7)	52(6)	122(11)	26(7)	13(7)	14(5)	C35A	95(11)	194(17)	48(7)	28(9)	14(7)	-67(11)
C34	54(8)	103(10)	139(13)	21(10)	51(9)	10(7)	C36A	50(7)	103(9)	43(6)	18(6)	4(5)	-15(6)
C35	83(10)	102(10)	128(13)	38(9)	70(10)	4(8)							

Table A6.4. Hydrogen coordinates (x 10^4) and isotropic displacement parameters (Å^{2}x 10^3) for *rac*-3.35.

	x	y	z	U(eq)		x	y	z	U(eq)
H4	1952	1320	4330	89	H4A	2073	-425	5947	119
H5	-416	1704	3764	91	H5A	4233	-1032	6434	112
H6	-1564	2922	4610	85	H6A	5901	-343	7801	121
H7	-282	3726	5995	71	H7A	5387	993	8712	94
H10A	6262	3273	6948	93	H10D	-814	1891	8449	109
H10B	5889	2604	7730	93	H10E	-1043	2323	7420	109
H10C	5545	3711	7807	93	H10F	-48	2875	8339	109
H11A	5655	1871	5455	123	H11D	-463	303	5822	143
H11B	4478	1026	5268	123	H11E	-953	1375	5978	143
H11C	5457	1249	6319	123	H11F	-1333	593	6654	143
H22	3284	4732	5616	77	H22A	2216	444	9618	84
H23	4361	5944	4914	84	H23A	1312	-403	10760	136
H24	5307	7294	5824	89	H24A	743	383	12116	145
H25	5178	7487	7460	79	H25A	1081	2008	12379	128
H26	4193	6303	8165	59	H26A	1979	2862	11296	82
H32	717	5631	6296	59	H32A	5022	1276	10623	66
H33	-1675	6073	6297	89	H33A	7561	1472	11236	95
H34	-2809	5670	7536	112	H34A	8809	2751	10872	116
H35	-1585	4746	8760	116	H35A	7570	3967	10062	134
H36	772	4316	8754	73	H36A	5047	3835	9489	78

Table A7.1. Crystal data and structure refinement for *rac*-bis(1-diphenylphosphinoindenyl)iron(II)-*cis*-dichloropalladium(II) (5.3).

Empirical formula	$C_{42}H_{32}Cl_2FeP_2Pd$	
Formula weight	831.77	
Temperature (K)	293(2)	
Crystal system	Monoclinic	
Space group	$P2_1/n$	
Unit cell dimensions	a = 12.694(3) Å	α = 90°
	b = 16.070(3) Å	β = 98.77(3)°
	c = 16.736(3) Å	γ = 90°
Volume ($Å^3$)	3374.1(12)	
Z	4	
Density (calculated) (Mg/m^3)	1.637	
Absorption coefficient (mm^{-1})	1.248	
F(000)	1680	
Crystal size (mm^3)	0.45 x 0.20 x 0.09	
Theta range for data collection (°)	1.88 to 26.50	
Index ranges	$-15 \le h \le 14$	
	$-19 \le k \le 20$	
	$-20 \le l \le 20$	
Reflections collected	41499	
Independent reflections [R(int)]	6957 [0.0734]	
Completeness to θ	(26.50°) 99.4 %	
Data / restraints / parameters	6957 / 0 / 433	
Goodness-of-fit on F^2	1.356	
R indices [$I>2\sigma(I)$] (R, R_w)	0.1360, 0.3168	
R indices (all data) (R, R_w)	0.1844, 0.3679	
Final maximum/minimum (e $Å^{-3}$)	8.605, –1.522	

Table A7.2. Atomic coordinates (x 10^4) and equivalent isotropic displacement parameters (Å^{2}x 10^3) for 5.3. U(eq) is defined as $^1/_3$ of the trace of the orthogonalized U^{ij} tensor.

	x	y	z	U(eq)		x	y	z	U(eq)
Pd	8294(1)	2028(1)	-864(1)	46(1)	C19	6174(8)	659(7)	-1266(6)	49(2)
Fe	6403(1)	2434(1)	1036(1)	48(1)	C20	5108(9)	939(8)	-1508(6)	57(3)
P1	8617(2)	2898(2)	223(2)	46(1)	C21	4444(11)	517(8)	-2126(7)	66(3)
P2	7022(2)	1193(2)	-467(2)	46(1)	C22	4848(11)	-170(8)	-2465(7)	65(3)
Cl2	8365(2)	1146(2)	-1950(2)	56(1)	C23	5884(12)	-447(8)	-2248(7)	72(4)
Cl1	9551(2)	2844(2)	-1378(2)	53(1)	C24	6534(10)	-26(7)	-1648(6)	61(3)
C1	6094(8)	1655(7)	81(6)	48(2)	C25	7627(9)	342(7)	133(6)	52(2)
C2	5641(8)	1331(7)	766(7)	54(3)	C26	7054(9)	-314(7)	375(7)	53(3)
C3	4939(8)	1928(7)	995(6)	49(3)	C27	7560(12)	-951(8)	838(7)	67(3)
C4	4289(9)	3353(8)	442(8)	62(3)	C28	8661(11)	-910(8)	1081(7)	61(3)
C5	4429(10)	3928(8)	-125(7)	66(3)	C29	9214(10)	-272(8)	834(7)	63(3)
C6	5094(10)	3770(8)	-701(7)	63(3)	C30	8724(10)	345(8)	353(6)	57(3)
C7	5643(8)	3047(7)	-713(7)	55(3)	C31	8507(8)	3979(6)	-80(5)	42(2)
C8	5569(9)	2455(7)	-100(6)	50(3)	C32	7993(9)	4196(9)	-819(6)	59(3)
C9	4877(9)	2607(8)	493(7)	55(3)	C33	7815(11)	5028(8)	-1008(7)	66(3)
C10	7866(8)	2904(6)	1063(6)	43(2)	C34	8242(9)	5637(7)	-474(8)	59(3)
C11	7146(9)	3546(7)	1232(7)	58(3)	C35	8805(9)	5431(8)	242(7)	58(3)
C12	6710(8)	3310(8)	1929(6)	52(3)	C36	8958(9)	4589(7)	461(6)	55(3)
C13	7040(8)	2045(8)	2895(6)	54(3)	C37	9942(8)	2696(7)	763(6)	48(2)
C14	7607(9)	1336(9)	3008(7)	64(3)	C38	10251(9)	2985(6)	1533(6)	47(2)
C15	8351(9)	1087(8)	2501(7)	62(3)	C39	10673(9)	2187(7)	437(7)	52(3)
C16	8488(9)	1544(7)	1864(6)	55(3)	C40	11636(8)	2018(7)	875(6)	54(3)
C17	7916(8)	2296(7)	1686(7)	51(3)	C41	11903(10)	2341(8)	1646(7)	58(3)
C18	7160(9)	2549(8)	2224(7)	56(3)	C42	11189(10)	2828(7)	1967(7)	59(3)

Table A7.3. Anisotropic displacement parameters ($Å^2$x 10^3) for 5.3. The anisotropic displacement factor exponent takes the form: $-2p^2[h^2 a^{*2}U^{11} + ... + 2 h k a^* b^* U^{12}]$.

	U^{11}	U^{22}	U^{33}	U^{23}	U^{13}	U^{12}		U^{11}	U^{22}	U^{33}	U^{23}	U^{13}	U^{12}
Pd	44(1)	50(1)	45(1)	0(1)	7(1)	2(1)	C19	49(6)	58(6)	42(5)	-3(5)	13(4)	-8(5)
Fe	42(1)	55(1)	49(1)	1(1)	9(1)	0(1)	C20	59(7)	64(7)	45(6)	0(5)	0(5)	-18(6)
P1	42(1)	49(2)	46(1)	3(1)	7(1)	-1(1)	C21	70(8)	60(7)	67(7)	0(6)	1(6)	-22(6)
P2	45(1)	46(2)	48(2)	2(1)	8(1)	-1(1)	C22	75(8)	74(8)	44(6)	11(6)	5(6)	-25(7)
Cl2	55(2)	62(2)	50(1)	-7(1)	9(1)	1(1)	C23	90(10)	63(8)	58(7)	-5(6)	-3(7)	-4(7)
Cl1	51(2)	58(2)	52(2)	0(1)	13(1)	-2(1)	C24	72(8)	63(7)	46(6)	-1(5)	5(5)	-8(6)
C1	38(5)	57(6)	45(5)	-6(5)	-3(4)	-8(5)	C25	57(6)	47(6)	53(6)	-6(5)	13(5)	5(5)
C2	45(6)	56(6)	62(7)	8(5)	8(5)	-9(5)	C26	43(6)	53(6)	64(7)	-3(5)	16(5)	6(5)
C3	41(5)	60(7)	49(6)	-12(5)	13(4)	-5(5)	C27	98(10)	50(7)	55(7)	10(5)	17(6)	6(7)
C4	43(6)	69(8)	74(8)	0(6)	11(5)	-2(6)	C28	76(8)	55(7)	52(6)	2(5)	11(6)	18(6)
C5	61(7)	66(8)	64(7)	-2(6)	-10(6)	4(6)	C29	55(7)	62(7)	71(8)	-10(6)	8(6)	23(6)
C6	64(7)	64(8)	61(7)	8(6)	13(6)	7(6)	C30	67(7)	66(7)	38(5)	2(5)	7(5)	0(6)
C7	38(6)	70(8)	55(6)	-2(5)	6(5)	-5(5)	C31	43(5)	48(6)	39(5)	9(4)	18(4)	6(4)
C8	57(6)	49(6)	40(5)	8(4)	-4(5)	-1(5)	C32	57(6)	92(9)	29(5)	6(5)	7(4)	-31(7)
C9	46(6)	64(7)	58(7)	-13(6)	14(5)	-1(6)	C33	74(8)	67(8)	56(7)	8(6)	12(6)	2(7)
C10	36(5)	53(6)	39(5)	-8(4)	8(4)	1(4)	C34	47(6)	42(6)	90(9)	1(6)	21(6)	4(5)
C11	58(7)	47(6)	67(7)	5(5)	6(6)	-8(5)	C35	49(6)	60(7)	72(7)	-1(6)	29(6)	2(5)
C12	41(5)	68(7)	44(6)	-1(5)	0(4)	-12(5)	C36	59(7)	62(7)	47(6)	4(5)	13(5)	1(6)
C13	33(5)	90(9)	40(6)	5(5)	6(4)	-8(6)	C37	37(5)	62(6)	45(6)	-8(5)	12(4)	-13(5)
C14	56(7)	86(9)	51(6)	12(6)	14(5)	-6(7)	C38	51(6)	45(6)	45(5)	-10(4)	7(5)	-1(5)
C15	57(7)	65(7)	59(7)	8(6)	-4(5)	3(6)	C39	62(7)	47(6)	45(6)	-5(5)	7(5)	1(5)
C16	51(6)	69(7)	45(6)	0(5)	8(5)	13(6)	C40	43(6)	60(7)	61(7)	-5(5)	12(5)	1(5)
C17	31(5)	68(7)	53(6)	-7(5)	1(4)	5(5)	C41	56(7)	76(8)	43(6)	4(5)	8(5)	4(6)
C18	50(6)	71(8)	49(6)	-5(5)	13(5)	-15(6)	C42	60(7)	62(7)	53(6)	-7(5)	5(5)	-3(6)

Table A7.4. Hydrogen coordinates (x 10^4) and isotropic displacement parameters ($Å^2$x 10^3) for 5.3.

	x	y	z	U(eq)		x	y	z	U(eq)
H2	5791	816	1011	65	H24	7232	-206	-1495	73
H3	4566	1871	1429	59	H26	6318	-329	224	63
H4	3806	3452	796	74	H27	7172	-1402	986	81
H5	4077	4436	-131	79	H28	9009	-1322	1413	73
H6	5162	4173	-1088	75	H29	9948	-249	994	75
H7	6058	2945	-1115	66	H30	9128	768	171	68
H11	6993	4033	936	69	H32	7760	3788	-1198	71
H12	6204	3611	2156	62	H33	7405	5176	-1496	79
H13	6579	2199	3251	65	H34	8138	6195	-612	71
H14	7508	994	3438	76	H35	9097	5846	596	70
H15	8744	601	2615	74	H36	9351	4442	955	66
H16	8966	1368	1530	66	H38	9772	3311	1764	56
H20	4853	1399	-1259	68	H39	10494	1967	-79	62
H21	3750	696	-2301	80	H40	12119	1684	657	65
H22	4402	-463	-2861	78	H41	12566	2227	1945	70
H23	6134	-906	-2501	86	H42	11362	3046	2485	70

Table A8.1. Crystal data and structure refinement for *rac*-bis(1-diphenylphosphinoindenyl)iron(II)-*cis*-dichloroplatinum(II) (5.4).

Empirical formula	$C_{42}H_{32}Cl_2FeP_2Pt$	
Formula weight	920.46	
Temperature (K)	168(2)	
Crystal system	Monoclinic	
Space group	$P2_1/n$	
Unit cell dimensions	a = 12.822(5) Å	α = 90°
	b = 16.199(6) Å	β = 98.669(7)°
	c = 16.964(7) Å	γ = 90°
Volume ($Å^3$)	3483(2)	
Z	4	
Density (calculated) (Mg/m^3)	1.755	
Absorption coefficient (mm^{-1})	4.705	
F(000)	1808	
Crystal size (mm^3)	0.16 x 0.09 x 0.02	
Theta range for data collection (°)	1.75 to 26.39	
Index ranges	$-7 \le h \le 15$	
	$-20 \le k \le 17$	
	$-21 \le l \le 21$	
Reflections collected	25108	
Independent reflections [R(int)]	7104 [0.0865]	
Completeness to θ	(26.39°) 99.5 %	
Data / restraints / parameters	7104 / 0 / 433	
Goodness-of-fit on F^2	0.897	
R indices [$I>2\sigma(I)$] (R, R_w)	0.0393, 0.0750	
R indices (all data) (R, R_w)	0.0825, 0.0967	
Final maximum/minimum (e $Å^{-3}$)	1.441, –0.772	

Table A8.2. Atomic coordinates (x 10^4) and equivalent isotropic displacement parameters (Å^{2}x 10^3) for 5.4. U(eq) is defined as $^1/_3$ of the trace of the orthogonalized U^{ij} tensor.

	x	y	z	U(eq)		x	y	z	U(eq)
Pt	6714(1)	2026(1)	10853(1)	19(1)	C19	6392(7)	-952(5)	8906(5)	39(2)
Fe	8607(1)	2422(1)	8974(1)	23(1)	C20	5793(6)	-319(5)	9142(4)	35(2)
P1	7957(1)	1189(1)	10461(1)	21(1)	C21	6259(5)	326(5)	9624(4)	28(2)
P2	6395(1)	2887(1)	9781(1)	20(1)	C1A	7149(5)	2890(4)	8951(4)	22(2)
Cl1	6650(1)	1174(1)	11965(1)	29(1)	C2A	7864(5)	3526(4)	8793(4)	28(2)
Cl2	5456(1)	2837(1)	11377(1)	28(1)	C3A	8292(6)	3295(5)	8094(5)	32(2)
C1	8895(5)	1662(4)	9918(4)	23(2)	C4A	7974(6)	2028(5)	7135(4)	38(2)
C2	9330(5)	1320(4)	9248(4)	25(2)	C5A	7408(6)	1326(6)	6985(5)	43(2)
C3	10073(5)	1906(5)	9005(5)	31(2)	C6A	6681(6)	1070(5)	7494(5)	36(2)
C4	10723(5)	3353(5)	9570(5)	41(2)	C7A	6509(5)	1537(4)	8134(4)	25(2)
C5	10599(6)	3902(5)	10136(5)	43(2)	C8A	7102(5)	2280(4)	8312(4)	21(2)
C6	9931(6)	3762(5)	10708(5)	39(2)	C9A	7832(5)	2530(4)	7793(4)	25(2)
C7	9358(6)	3049(5)	10709(5)	33(2)	C10A	6489(5)	3979(4)	10061(4)	22(2)
C8	9440(5)	2446(4)	10114(4)	24(2)	C11A	6064(6)	4595(4)	9539(5)	28(2)
C9	10140(5)	2581(5)	9537(5)	32(2)	C12A	6190(6)	5414(5)	9739(5)	34(2)
C10	8811(5)	655(4)	11265(4)	24(2)	C13A	6752(6)	5626(5)	10453(5)	37(2)
C11	9838(6)	917(5)	11512(4)	31(2)	C14A	7187(6)	5035(5)	10999(5)	35(2)
C12	10489(6)	492(5)	12134(5)	37(2)	C15A	7064(5)	4209(5)	10798(4)	28(2)
C13	10099(7)	-186(5)	12493(5)	43(2)	C16A	5072(5)	2681(4)	9238(4)	20(2)
C14	9069(7)	-446(5)	12252(5)	41(2)	C17A	4799(5)	2982(4)	8460(4)	27(2)
C15	8428(6)	-28(4)	11631(4)	33(2)	C18A	3823(6)	2816(4)	8037(5)	33(2)
C16	7365(5)	334(4)	9852(4)	21(2)	C19A	3098(6)	2342(5)	8349(5)	34(2)
C17	7963(6)	-329(4)	9630(4)	30(2)	C20A	3357(5)	2029(4)	9110(4)	30(2)
C18	7466(7)	-957(5)	9154(5)	40(2)	C21A	4347(5)	2203(4)	9557(4)	26(2)

Table A8.3. Anisotropic displacement parameters ($Å^2 x\ 10^3$) for 5.4. The anisotropic displacement factor exponent takes the form: $-2p^2[\ h^2\ a^{*2}U^{11} + ... + 2\ h\ k\ a^*\ b^*\ U^{12}\ ]$.

	U^{11}	U^{22}	U^{33}	U^{23}	U^{13}	U^{12}		U^{11}	U^{22}	U^{33}	U^{23}	U^{13}	U^{12}
Pt	19(1)	21(1)	19(1)	-1(1)	2(1)	0(1)	C19	63(6)	31(5)	26(5)	-7(4)	14(4)	-18(4)
Fe	18(1)	27(1)	23(1)	0(1)	3(1)	-1(1)	C20	36(4)	42(5)	28(5)	-3(4)	4(4)	-15(4)
P1	20(1)	21(1)	20(1)	0(1)	2(1)	0(1)	C21	32(4)	31(4)	24(5)	-4(4)	12(3)	-6(3)
P2	18(1)	23(1)	20(1)	1(1)	4(1)	2(1)	C1A	10(3)	34(4)	21(4)	4(4)	-3(3)	3(3)
Cl1	28(1)	34(1)	25(1)	7(1)	3(1)	-1(1)	C2A	25(4)	28(4)	30(5)	2(4)	7(3)	1(3)
Cl2	27(1)	29(1)	32(1)	-4(1)	12(1)	3(1)	C3A	32(4)	34(4)	31(5)	11(4)	9(4)	3(4)
C1	18(3)	25(4)	25(5)	-4(3)	0(3)	8(3)	C4A	30(4)	61(6)	22(5)	7(5)	9(3)	7(4)
C2	23(4)	21(4)	33(5)	2(3)	4(3)	5(3)	C5A	35(5)	63(6)	29(5)	-15(5)	2(4)	-2(4)
C3	15(3)	44(5)	36(5)	8(4)	10(3)	7(3)	C6A	38(5)	41(5)	28(5)	-9(4)	-1(4)	-4(4)
C4	18(4)	50(5)	56(6)	4(5)	11(4)	-11(4)	C7A	20(4)	29(4)	26(5)	1(4)	1(3)	-4(3)
C5	33(5)	35(5)	60(7)	-9(5)	8(4)	-9(4)	C8A	17(3)	26(4)	19(4)	3(3)	0(3)	3(3)
C6	40(5)	30(5)	45(6)	-13(4)	0(4)	-2(4)	C9A	22(4)	32(4)	20(4)	0(4)	3(3)	2(3)
C7	27(4)	40(5)	29(5)	-4(4)	-1(3)	-1(4)	C10A	25(4)	19(4)	25(5)	2(3)	11(3)	0(3)
C8	19(4)	29(4)	24(5)	-1(4)	-2(3)	-5(3)	C11A	37(4)	23(4)	25(5)	3(3)	5(3)	3(3)
C9	17(4)	37(5)	42(6)	-2(4)	2(3)	3(3)	C12A	32(4)	28(5)	45(6)	11(4)	11(4)	6(4)
C10	30(4)	22(4)	21(4)	-4(3)	5(3)	9(3)	C13A	35(5)	23(4)	59(6)	-5(4)	25(4)	-1(4)
C11	32(4)	36(5)	23(5)	1(4)	1(3)	8(4)	C14A	31(4)	35(5)	38(5)	-9(4)	6(4)	-9(4)
C12	33(4)	51(6)	24(5)	-15(4)	-1(4)	16(4)	C15A	25(4)	30(4)	28(5)	-1(4)	0(3)	4(3)
C13	56(6)	41(5)	31(5)	-4(4)	-2(4)	27(5)	C16A	18(3)	23(4)	18(4)	4(3)	5(3)	2(3)
C14	63(6)	30(5)	31(5)	-2(4)	13(4)	18(4)	C17A	16(3)	37(4)	27(4)	8(4)	3(3)	-5(3)
C15	41(5)	27(4)	31(5)	-5(4)	6(4)	6(4)	C18A	32(4)	43(5)	23(5)	2(4)	2(3)	4(4)
C16	27(4)	22(4)	14(4)	6(3)	2(3)	0(3)	C19A	27(4)	44(5)	28(5)	-3(4)	-5(3)	-8(4)
C17	29(4)	31(4)	31(5)	3(4)	10(3)	-4(3)	C20A	27(4)	26(4)	35(5)	6(4)	4(3)	-6(4)
C18	69(6)	24(4)	31(5)	-3(4)	19(5)	-6(4)	C21A	25(4)	27(4)	26(5)	5(3)	3(3)	1(3)

Table A8.4. Hydrogen coordinates (x 10^4) and isotropic displacement parameters (Å^{2}x 10^3) for 5.4.

	x	y	z	U(eq)		x	y	z	U(eq)
H2	9124	781	8981	31	H2A	8035	4038	9115	33
H3	10466	1845	8543	37	H3A	8834	3615	7856	38
H4	11185	3465	9195	49	H4A	8467	2185	6798	45
H5	10978	4408	10154	51	H5A	7497	1000	6535	52
H6	9876	4171	11101	47	H6A	6308	566	7387	43
H7	8914	2960	11102	39	H7A	6001	1371	8456	30
H11	10107	1381	11265	37	H11A	5678	4446	9036	33
H12	11192	672	12303	44	H12A	5887	5828	9379	41
H13	10537	-473	12906	52	H13A	6851	6194	10583	45
H14	8798	-905	12504	49	H14A	7563	5195	11502	42
H15	7727	-213	11460	40	H15A	7369	3797	11160	33
H17	8703	-349	9803	36	H17A	5291	3303	8226	32
H18	7876	-1398	8996	48	H18A	3645	3034	7514	39
H19	6067	-1382	8575	47	H19A	2428	2230	8046	41
H20	5052	-319	8977	42	H20A	2865	1696	9333	35
H21	5836	753	9794	34	H21A	4518	1991	10083	32

Table A9.1. Crystal data and structure refinement for *trans*-dichloro(bis(1-diphenylphosphinoindene))nickel(II) (5.7).

Empirical formula	$C_{42}H_{32}Cl_2P_2Ni$	
Formula weight	730.24	
Temperature (K)	168(2)	
Crystal system	Rhombohedral	
Space group	R-3	
Unit cell dimensions	a = 34.565(8) Å	α = 90°
	b = 34.565(8) Å	β = 90°
	c = 9.814(4) Å	γ = 120°
Volume ($Å^3$)	10155(6)	
Z	9	
Density (calculated) (Mg/m^3)	1.433	
Absorption coefficient (mm^{-1})	0.857	
F(000)	3618	
Crystal size (mm^3)	0.25 x 0.10 x 0.10	
Theta range for data collection (°)	2.18 to 26.52	
Index ranges	$-43 \le h \le 42$	
	$-43 \le k \le 43$	
	$-12 \le l \le 7$	
Reflections collected	39184	
Independent reflections [R(int)]	4601 [0.2940]	
Completeness to θ	(26.52°) 98.1 %	
Data / restraints / parameters	4601 / 0 / 214	
Goodness-of-fit on F^2	0.976	
R indices [$I>2\sigma(I)$] (R, R_w)	0.1046, 0.2915	
R indices (all data) (R, R_w)	0.2320, 0.3534	
Final maximum/minimum (e $Å^{-3}$)	1.386, –0.560	

Table A9.2. Atomic coordinates (x 10^4) and equivalent isotropic displacement parameters (Å^{2}x 10^3) for 5.7. U(eq) is defined as $^1/_3$ of the trace of the orthogonalized U^{ij} tensor.

	x	y	z	U(eq)		x	y	z	U(eq)
Ni	0	5000	5000	48(1)	C11	479(3)	4428(3)	6597(8)	54(2)
P	310(1)	4854(1)	6776(2)	51(1)	C12	172(3)	4024(3)	6022(8)	51(2)
Cl	362(1)	4806(1)	3616(2)	57(1)	C13	263(4)	3687(4)	5902(8)	60(3)
C1	-13(3)	4673(3)	8372(8)	50(2)	C14	675(4)	3750(4)	6404(9)	76(3)
C2	230(4)	4587(4)	9515(8)	58(3)	C15	987(4)	4157(4)	7005(10)	67(3)
C3	20(3)	4166(4)	9904(9)	60(3)	C16	885(3)	4492(4)	7102(8)	60(3)
C4	-734(4)	3478(4)	9241(10)	66(3)	C21	821(3)	5376(3)	7159(9)	59(3)
C5	-1098(4)	3323(4)	8370(10)	67(3)	C22	864(4)	5648(3)	8318(11)	69(3)
C6	-1129(4)	3614(4)	7448(10)	65(3)	C23	1238(4)	6037(4)	8552(13)	88(4)
C7	-795(3)	4060(3)	7375(9)	57(2)	C24	1593(5)	6185(5)	7640(15)	106(5)
C8	-428(3)	4212(3)	8233(8)	54(2)	C25	1577(4)	5944(4)	6465(14)	99(4)
C9	-390(3)	3928(3)	9174(8)	53(2)	C26	1176(4)	5526(4)	6228(11)	78(3)

Table A9.3. Anisotropic displacement parameters (Å^{2}x 10^3) for 5.7. The anisotropic displacement factor exponent takes the form: $-2p^2[h^2 a^{*2}U^{11} + ... + 2 h k a^* b^* U^{12}]$.

	U^{11}	U^{22}	U^{33}	U^{23}	U^{13}	U^{12}		U^{11}	U^{22}	U^{33}	U^{23}	U^{13}	U^{12}
Ni	67(1)	57(1)	26(1)	-2(1)	-4(1)	36(1)	C11	82(7)	65(6)	23(4)	-4(4)	1(4)	44(5)
P	66(2)	63(2)	29(1)	-4(1)	-5(1)	36(1)	C12	69(6)	61(6)	29(5)	1(4)	2(4)	37(5)
Cl	81(2)	70(2)	31(1)	-1(1)	0(1)	46(1)	C13	89(8)	81(7)	25(5)	-4(4)	-4(5)	53(6)
C1	57(6)	61(6)	32(5)	-6(4)	-10(4)	30(5)	C14	119(10)	104(9)	28(5)	8(5)	20(6)	72(8)
C2	80(7)	78(7)	27(5)	-9(5)	-11(4)	47(6)	C15	84(7)	96(8)	41(5)	3(6)	-1(5)	61(7)
C3	72(7)	85(8)	32(5)	10(5)	4(5)	45(6)	C16	77(7)	91(7)	29(5)	-3(5)	-2(4)	54(6)
C4	91(8)	80(8)	45(6)	4(5)	3(5)	56(7)	C21	61(6)	76(7)	42(5)	-6(5)	-2(5)	35(5)
C5	82(8)	69(7)	50(6)	-4(5)	4(5)	36(6)	C22	70(7)	63(7)	64(7)	-14(5)	-6(5)	27(6)
C6	71(7)	70(7)	54(6)	-3(5)	0(5)	34(6)	C23	82(9)	89(9)	82(9)	-39(7)	-12(7)	35(7)
C7	62(6)	68(7)	39(5)	2(5)	2(4)	31(5)	C24	75(9)	99(9)	105(9)	-43(9)	-22(8)	16(8)
C8	78(7)	64(6)	26(5)	2(4)	4(4)	40(5)	C25	64(8)	96(9)	109(9)	-25(8)	6(7)	19(7)
C9	76(7)	63(6)	28(5)	7(4)	5(4)	40(6)	C26	85(8)	88(8)	59(7)	-6(6)	-3(6)	41(7)

Table A9.4. Hydrogen coordinates (x 10^4) and isotropic displacement parameters (Å^{2}x 10^3) for 5.7.

	x	y	z	U(eq)		x	y	z	U(eq)
H1	-99	4897	8666	60	H14	741	3515	6332	92
H2	503	4811	9904	70	H15	1263	4199	7339	80
H3	125	4041	10568	72	H16	1091	4769	7514	72
H4	-717	3281	9883	79	H22	620	5550	8933	82
H5	-1326	3018	8400	80	H23	1262	6209	9333	105
H6	-1381	3506	6864	78	H24	1857	6461	7818	128
H7	-817	4257	6747	68	H25	1823	6053	5853	118
H12	-106	3982	5707	61	H26	1151	5352	5447	94
H13	53	3412	5488	72					